Development and Characterisation of Polymeric Matrix Materials used for Applications in Two-Photon Patterning of Optical Waveguides

Dissertation
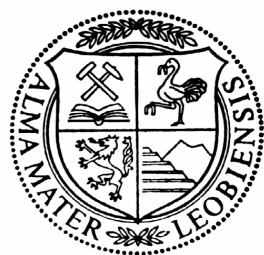
of

Rachel Woods M.Sc

Submitted to

Chair of Chemistry of Polymeric Materials

Montanuniversität Leoben

In Cooperation with

Polymer Competence Center Leoben GmbH

Supervisor: Univ. Prof. Wolfgang Kern

Second Examiner / Referee: Univ. Prof. Ernst Lankmayr

For My Grandfather David Woods

"Science knows no country, because knowledge belongs to humanity, and is the torch which illuminates the world."

(Louis Pasteur)

Declaration

This thesis was performed at the Chair of Chemistry of Polymeric Materials, Montanuniversität Leoben, between May 2008 and July 2011.

Acknowledgement

First and foremost I would like to thank my supervisor Wolfgang Kern, who, along with the whole research group, supported me throughout my three years at Leoben, staying positive during tough times and always coming up with new ideas, giving me the enthusiasm to learn and gain successful results in a new and challenging area of research.

Thank you to past and present researchers working in Prof. Kern's group, who helped me in so many ways, supporting me in finding my way around the labs, helping out with experiments and generally making my time working in Leoben an enjoyable one. Special thanks goes to Sandra Schlögl, Dietmar Lenko, Jörg Schauberger, Simone Radl, Mattias Edler, Thomas Grießer and Manuela Belzik, who all helped me through difficult times, giving me advice during various stages of my project and creating a great working atmosphere. I am grateful to have spent time travelling to some incredible locations to attend conferences with a number of you. Cocktails in Cancun, getting lost in the Souks in Marrakech and so many great experiences we shared that will never be forgotten.

I would also like to give special thanks Sonja Feldbacher, who worked closely with me on this project, being thrown in at the deep end during a period when nothing seemed to be working, to helping in the development of our "magic polymer". It was your experience and knowledge in this research field which led to the success of our material in the last year. It was a pleasure to work with you. Thank you also to David Zidar for bringing new and fresh ideas to the project, and always trying new experiments, even when you knew they weren't going to work!

A number of people collaborated with me on this project from Graz University of Technology. Thank you to Josefine Hobisch for performing NMR and STA measurements and later further measurements coupled with MS. Thank you to Karin Bartl, who spent hours trying to fix the GC and aiding with the analysis. It was possible to perform headspace GC with the help of Prof. Lankmayr and Xinghua Guo, who helped to come up with the best way to analyse difficult samples.

For cut back experiments, Dr. Nicole Galler from the Institute of Physics, Karl-Franzens-University of Graz spent a significant amount of time working on earlier developed materials which were difficult to analyse. Thank you for persevering and achieving great results.

I would like to thank Prof. Robert Liska and members of his research group from the Institute of applied Synthetic Chemistry, including Niklas Pucher and Zhiquan Li, who developed and provided us with the photoinitiator N-DPD, along with a number of other two-photon photoinitiators to experiment with. With these we were able to produce functional waveguide structures.

I am most grateful to a number of colleagues from Joanneum Research, NMP in Weiz. Thank you to Valentin Satzinger, who painstakingly set up the laser system for our

requirements, and with his expertise and patience, managed to produce outstanding structuring results with all materials investigated, despite the constant distractions from us with our questions and laughs when the boredom set in after long, unsuccessful days in the "grey room". Thank you for always staying positive. Thank you to Volker Schmidt and also Georg Jakopic, who performed Ellipsometric measurements on challenging samples, as well as NIR Spectroscopy.

I also wish to thank Gerhard Schmid and Prof. W. Leeb, from the Institute of Telecommunications, Vienna University of Technology, for performing a number of time consuming data transmission and photocurrent measurements on our opto-electronic boards. Clear and concise reporting of the results made analysis of complicated data less of a daunting task.

During the project I worked closely with a number of people at AT&S, Leoben, who also contributed financially. Thank you to Gregor Langer for leading the project, always sharing new ideas and always fighting to keep the project alive. Thanks to Ronnie Frosch and Szabolcs Veress for performing STA and FT-IR microscopy measurements.

Lastly I would like to thank my family and friends for their love and encouragement. My parents always supported me along every path I chose to take, and their constant encouragement gave me the strength to achieve my goals. Special thanks to my twin sister Laura, who always believed in me and taught me to chase my dreams.

Abstract

Different polymeric materials were investigated for their suitability as novel inert matrix materials, used for two-photon patterning of three dimensional optical waveguides. By investigating different PDMS based materials containing photo-polymerisable monomers, waveguides were able to be inscribed into the material using two-photon photopolymerisation. To produce the optical waveguides, an ultra fast femto second laser was used to induce a photopolymerisation of functional monomers, either added to the polymeric material, or directly attached to the polymer backbone. This enabled the production of true three dimensional waveguide structures to be embedded into the material in a single step. Cross-linked materials based on a hydride terminated polysiloxane containing high refractive index methacrylate monomers, an epoxy propoxy terminated polysiloxane cross-linked with a diamine, containing acrylate monomers, and a silanol terminated polysiloxane, containing acrylate functional groups attached to the polymer backbone were fully characterised and investigated for their suitability as optical materials used for waveguide applications. Each matrix material was characterised by FT-IR, STA and near-infrared spectroscopy as well as ellipsometry to determine the refractive index difference between the waveguide core and cladding material. Optical and phase contrast microscopy were used to observe the waveguide core, with cut back measurements and RNF measurements carried out on the more successful waveguides. Successful matrix materials were used in the development of demonstrators, by accurately inscribing optical waveguides between laser and photo diodes on specially designed printed circuit boards. The demonstrators were then used to monitor the long term stability of the polymeric material as well as the optical waveguides, by detecting the photocurrents.

Table of Contents

1   General Introduction

Within the ever increasing technology of optical processing, more functions and faster speeds are needed in this competitive industry and effective integration of components is required[1]. Polymers are being increasingly investigated due to their low cost and excellent optical properties. Waveguides fabricated from polymers are being investigated extensively due to their potential applications in telecommunication and data communication. This particular research is focused on the design of integrated optical interconnections for signal transmission. The optical waveguides are formed via a two-photon polymerisation process using selected monomers in an inert silicone matrix.

This study focuses on the photopolymerisation of a selection of methacrylate or acrylate monomers in an inert silicone matrix, or functional groups attached directly to the backbone of a polymeric material. The photopolymerisation is carried out using a femto-second laser, leading to polymerisation of the monomers or functional groups in the matrix by induced by TPA. This process causes a highly localised polymerisation inside the matrix material, enabling the fabrication of waveguide structures, drawn precisely into the optical material, or on a printed circuit board containing mounted diodes. The waveguides can then be used in the design of integrated optical interconnections for signal transmission. The first part of this introduction details the principles of photopolymerisation, photoinitiators and two-photon processes. A second part of the introduction focuses on recent studies and up to date research being carried out in this field.

1.1   Photopolymerisation

Photopolymerisation is the reaction of monomers or macromers to produce polymeric structures by light-induced initiation via the excitation of a photoinitiator to produce polymers. Over the last few decades the practical applications have evolved significantly and better understanding of the reaction mechanisms has led to a number of industrial and medical applications. To generalise the process, the concept of photopolymerisation is to conjugate and solidify fluid reactants into a stable structure using light[2]. This procedure is usually irreversible. Complex patterns can be produced by photopolymerisation to print integrated circuits, wiring boards, or microfabricated biomaterial structures. The rate of photopolymerisation depends on the light source intensity, the concentration of photoinitiator and presence of oxygen, the quantum yield of the radical generation and the initiation efficiency of the

generated radicals. The rate is usually increased with the incident light intensity, but not with initiator concentration. If an initiator has a high extinction coefficient, a high concentration of initiator can lead to inefficient energy transfer. Different concentrations of initiators can also lead to different molecular weight distributions resulting in final polymers with adjustable mechanical properties.

1.2   Two-Photon Absorption

Two-photon absorption (TPA) is process similar to single photon absorption, but instead an electron absorbs two photons at approximately the same time. This achieves an excited state that corresponds to the sum of the energy of the incident photons[3]. There does not have to be an intermediate state for the atom to reach before arriving at the final excited state, the atom is excited instead to a "virtual state" which does not need to correspond to any electric or vibrational energy state. A normal single-photon polymerisation (1PP) process consists of the steps shown in equation 1 below:

$$hv \text{ UV} + \text{initiator} \rightarrow R^{\cdot} \text{ or } R^{+}$$
$$R^{\cdot} \text{ or } R^{+} + \text{monomers} \rightarrow \text{free radical or cationic polymerisation (1)}$$
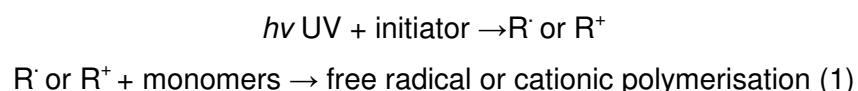
In 1PP processes, the initiator only absorbs one UV photon with a short wavelength through linear absorption. For a two-photon polymerisation process (2PP), the first step of the reaction is different to a 1PP process, shown below in equation (2)

$$2hv \text{ NIR} + \text{initiator} \rightarrow R^{\cdot} \text{ or } R^{+} \text{ (2)}$$

The initiator absorbs two near infrared photons with a long wavelength through non-linear absorption. The two photons are absorbed simultaneously by a PI molecule, and the cross section for 2PP is orders of magnitude lower than that of 1PP, so the excitation beam intensities should be in the order of TW/cm^2 to generate a high enough density of initiating species. With TPA high energy levels can be populated that are not reachable by single photon transitions from the ground state. Once electrons have absorbed two photons and are at a high enough energy level, it will take only the absorption of another photon to release the electron and ionise the atom. An energy level diagram of TPA is shown in Figure 1. An intense, monochromatic photon source, such as a high energy laser can be used to excite

atoms through TPA, which assures there are enough photons to continue the excitation process and ionise the electron before it radiates back to a lower energy level. For TPA, the material has to be transparent to the laser wavelength used, and the absorption occurs via a virtual intermediate state, which has a very short lifetime. As already stated the process is non linear and a high intensity laser is needed due to the short lifetime of the intermediate state. The TPA threshold is generally lower for shorter wavelengths which can lead to the risk of single photon monomer bond cleavage, which is an undesirable process during TPA. An advantage of TPA is that the majority of resins that polymerise upon UV irradiation can also polymerise upon simultaneous absorption of two photons of double wavelength as long as there is a strong enough laser power. The fundamentals behind TPA are described in Figure 2. The fabrication window and voxel size during TPA structuring is strongly dependant on the laser pulse energy above the threshold, and laser writing using TPA is a true 3D technique, carried out in transparent media, producing structures with µm and sub µm resolution. The process is shown diagrammatically in Figure 3.
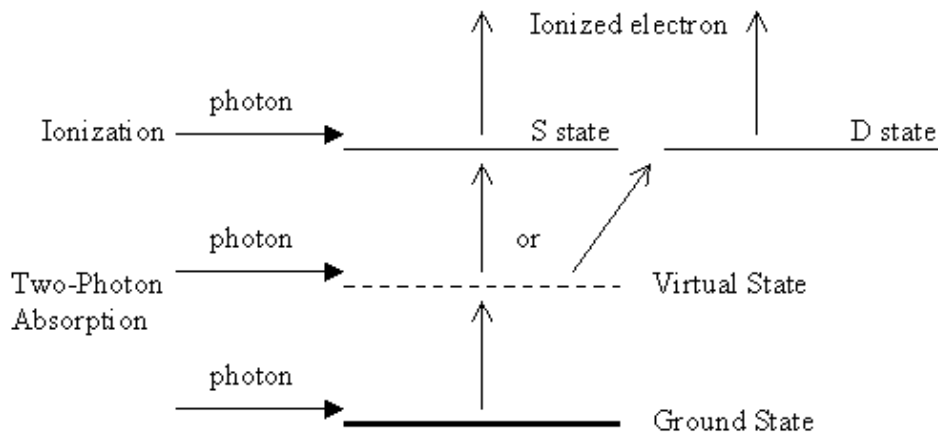
Figure 1: Energy level diagram of Two-Photon Absorption and ionization

Dependency of I^2 along laser beam axis
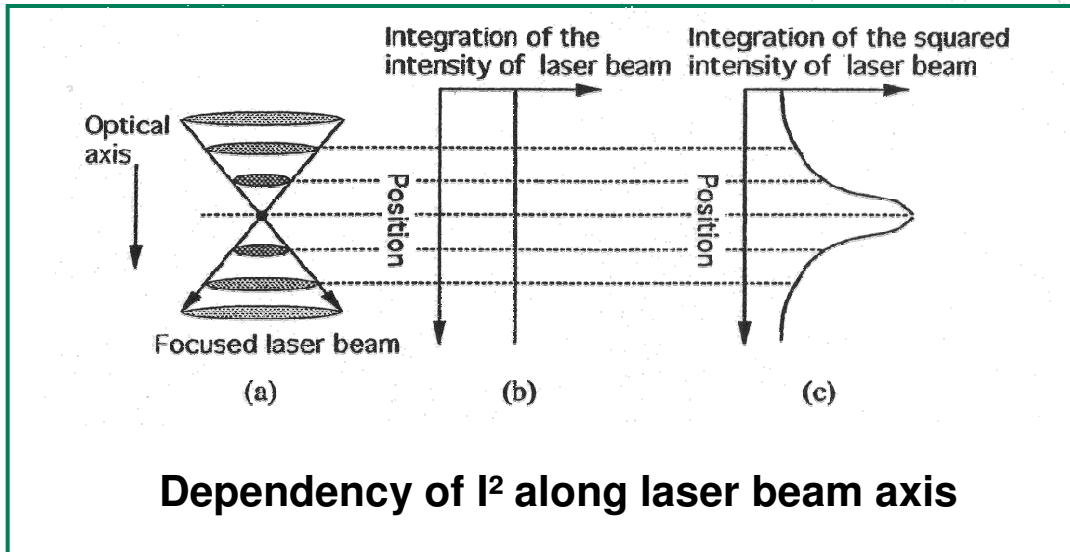
Figure 2: Fundamentals of TPA: The net excitation per transversal plane is constant for 1PA, however for TPA it is localised near the focal plane

In Figure 2:, the diagram shows a), the focused laser beam, b), total one photon absorption per transversal plane-integration of the intensity over the plane, and c), total two-photon absorption per transversal plane-integration of squared intensity over plane[4].
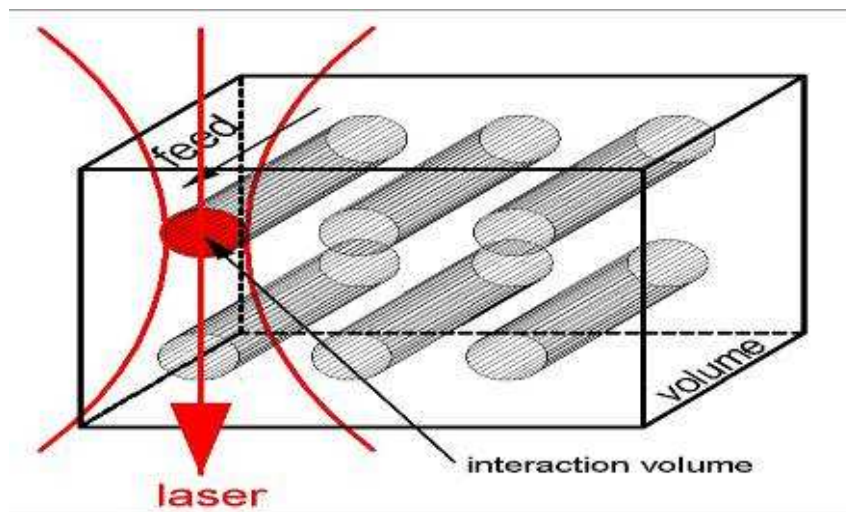
Figure 3: Illustration of the area in which interaction with the laser occurs

1.3 Two-Photon Photopolymerisation

Photopolymerisation is a process commonly fabricated via TPA. Fabrication is performed in a viscous liquid pre-polymer resin containing a photoinitiator. TPA by the photoinitiator leads to the generation of radicals that induce a polymerisation chain-reaction, which hardens the resin locally. The initiator absorbs visible or IR photons in a two-photon polymerisation process, and are then absorbed simultaneously by the photoinitiator molecule, which in its excited state becomes a radical that interacts with the surrounding monomers and triggers a polymerisation chain reaction. The reaction stops as soon as the various oligomers generated in the process link to form the final polymer. Once the fabrication is complete, the unexposed resin can be washed away with solvent, leaving behind a 2D structure. Most commonly used materials are acrylate resins, as they generally have high rates of polymerisation and a number of varieties are available[5]. The physical and chemical properties can also be easily tailored to the specific application. Two-photon photopolymerisation technologies can be applied to 3D fabrication of microstructures in polymer materials and the method could replace the traditional optical devices fabrication methods of lithography and etching processes on silicon substrates which include many time consuming steps. The fabrication method can be simplified into a single step by laser-induced photopolymerisation.

1.4 Photoinitiators

Photoinitiators are compounds, which upon the exposure of UV light, will decompose to form free radicals. Following the absorption of UV radiation, an unstable excited species is produced. In photo-induced polymerisation, formation of a free radical by rearrangement, fragmentation or energy transfer, followed by the attack on a monomer, leads to polymerisation. A simple scheme is presented below.

$I + h\nu \rightarrow I^*$ (excited state)
$I^* + M \rightarrow I + M^* \rightarrow M\bullet$ (initiation)
$M\bullet + nM \rightarrow (M)nM\bullet$ (propagation)
$(M)nM\bullet + \bullet R \rightarrow (M)nMR$ (chain transfer and termination)
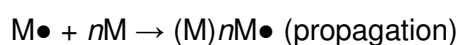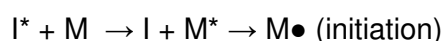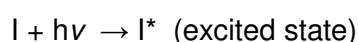
Type I photoinitiators undergo a unimolecular bond cleavage when irradiated, giving free radicals. In contrast, type II photoinitiators undergo a bimolecular reaction, where the excited state interacts with a second molecule, such as a coinitiator, which then generates free radicals. As we require the effective polymerisation of methacrylate monomers in this research, a photoinitiator was chosen due to its suitability, solubility in the polymeric material and correct absorption in the UV spectrum.

Photoinitiators play a key role in UV curable systems by generating reactive species or ions which initiate the polymerisation of multifunctional monomers and oligomers[6]. Commercial photoinitiators for UV curing systems can absorb photons from the incident radiation. Light absorption from the photoinitiator requires that the emission line from the light source overlaps with an absorption band of the photoinitiator The energy of the photon is transferred to the electronic structure of the photoinitiator, which converts the light energy into chemical energy in the form of reactive intermediates such as free radicals, which will then initiate polymerisation of monomers and oligomers. When exposed to UV light or two-photon NIR light, the photoinitiator is photolysed to produce free radicals via molecular bond cleavage. The bond must have a dissociation energy lower than the excitation energy of the reactive excited state. After absorbing the energy, the initiator transfers from the ground state to an excited singlet or triplet state and part of the absorbed energy can be lost through internal conversion from the excited state to the ground state. Some reactive intermediates can also be quenched by oxygen, or recombination of intermediates. Some initiators abstract hydrogen from hydrogen donors and undergo a photo-induced electron transfer process to produce reactive intermediates. A model initiator should have a number of desirable attributes, including a high molar absorption coefficient and a well-adapted spectral absorption range. It should be able to produce intermediates with good reactivity and photolysis by-products with low-toxicity. It should also be compatible with the monomers and oligomers and disperse in the monomer uniformly before photopolymerisation.

Two-photon technology has great potential in the application of 3D microfabrication and optical data storage areas, so it is desirable to design and synthesise highly active organic two-photon chromophores. Understanding the relationship of the molecular structure and properties with varied structural parameters and reproducing characterisation of two-photon properties is still a challenge for researchers. One common design concept is based on the relationship between the molecular two-photon cross-section and the components of the third order nonlinear susceptibility. A common structure used in the two-photon initiator is the π-conjugation bridge chromophore with high planarity substitutes of electron donor or acceptor. A Type I

structure is symmetrical, such as D-π-D, D-π-A-π-D and A-π-D-π-A molecules. Type II structures are asymmetrical, such as D-π-A molecules[7]. Some strategies have been investigated to increase the cross-section of the molecules, such as extending the π-conjugation length, increasing the planarity of the chromophore and increasing the strength of the donors and acceptors[8]. The initiator molecules should have a large two-photon absorption cross-section, and also have a high efficiency to produce reactive intermediate radicals or cations. When a two-photon initiator is used the photo-sensitivity of the whole system is increased.

1.5   Optical Waveguides

Planar lightwave circuits (PLCs) which are based on layers of glass, polymers or other materials, are relatively cheap, and have a high integration density by using well-established fabrication methods from the silicon industry. Processing of these circuits enables automation, integration of multiple functions and customisation to requirements[9]. The fundamental components in PLC's are optical waveguides. These components act as photonic analogues of copper circuits, serving as interconnects among different components on a chip. Optical waveguides confine and direct optical signals in a region of higher refractive index than its surrounding material. The optical energy is confined in the substrate, and the superstrate has the highest refractive index, so provides a guiding region. The refractive index is achieved from the waveguide fabrication process. Simple waveguide structures can be produced, but complex optical circuits can also be fabricated. The waveguides contain different structures and shapes that form various functions and can be classified into two categories. Passive devices exhibit static characteristics for optical waves and functional devices for optical wave control. Polymer optical devices are becoming increasingly popular within the applications of optical networks, due to their optical functions, and their ease of production at low costs. Polymers have the desirable property of having a very large negative thermo-optic coefficient, which is the gradient of refractive index, (*dn/dT),* around ten to forty times larger than other conventional optical materials. Polymers have a wide range of refractive indices closely matched to that of silica fibre, so it is possible to optimise the material for a number of different applications in all transmission windows of silica fibre. A number of different polymers are being used in integrated optics, including polyacrylates, polyamides, polycarbonates and polyolefins.

21

1.6   TPA Fabrication of Waveguides

Two-photon absorption processes can be used to perform selective polymerisation for the fabrication of basic elements needed in optical circuits in photopolymerisable resins. Organics are desirable materials to use in this field, as their optical properties can be controlled. The refractive index of polymeric materials can be modulated by the rate of polymerisation induced by the illumination. Polymeric integrated optics has applications in fibre interconnections, made in triacrylate monomers by making use of light induced self-written waveguides (LISW)[10,11]. LISW has the limitation however, in that it only allows straight waveguides, and so the fabrication of complex optical integrated circuits is not possible. For these structures you need a 3D control of the photopolymerisation process. TPA polymerisation enables the inscription of random designs in a resin.

A number of 3D microstructures have been reported, such as the inscription of a structure in a mixture of two polymers[12], and successful sub-wavelength structures have been made on photonic crystals and in arbitrary shapes[13]. In a recent paper the fabrication of some basic elements used in optical circuits, such as bends and Y-splitters in a photopolymerisable resin have been studied. A single monomer was used and the refractive index was controlled by a pre-polymerisation step. This application of TPA led to promising results and research continues into using polymeric materials for integrated optics. The same research group used laser scanning to convert pre-designed computer aided design (CAD) patterns to a structure in the resin. Two modes for direct scanning were used: raster-scan mode and vector scan mode. The raster scan mode works by all voxels in the cubic volume that contain the micro structure being scanned by the laser focal point. In the vector mode, the laser directly traces the profile to be defined, requiring a smaller number of voxels. Using the two different modes, the same object was fabricated. The "micro-bull", shown in Figure 4 was produced by Kawata et al. using layer by layer raster scanning schemes, so all voxels consisting of the bull were exposed point-by-point, line-by-line and layer-by-layer using the two-photon process, taking 3 hours to complete. The same structure was then fabricated using the vector scan method, and only took 13 minutes to complete.
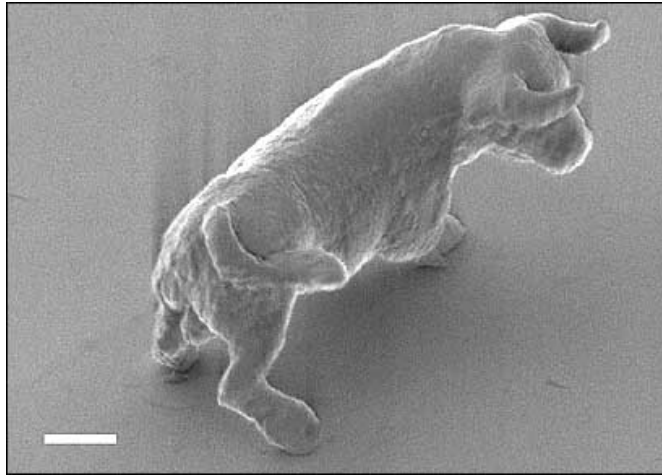
Figure 4: SEM image of a "microbull" structure produced by raster scanning (10 μm long and 7 μm high)

2 Introduction - Current Research

2.1   Two-Photon Photopolymerisation for Microfabrication

The fields of two-photon photopolymerisation and the development of waveguide structures formed from polymeric materials are still relatively new, and most recent reviews focus on the investigation into new photoinitiators, the use of two-photon absorption for the fabrication of 3D microstructures, and the writing of optical waveguides in a number of different polymeric materials. The following sections highlight current research being carried out in the field of two-photon photopolymerisation, three dimensional waveguide fabrication and a number of state of the art microfabrication techniques.

Microfabrication is increasing in importance as practical advances in micro-electromechanical systems and nanotechnology are being adapted and extended. Polymers are being chosen more and more due to their inexpensiveness, ease of use, special optical properties and ease of processing. Polymeric materials can be flexible and easy to modify into composites to achieve desirable chemical and physical functionality. The resins used to fabricate such microstructures are multi-functional monomers and oligomers. A chosen photoinitiator (PI) suitable for the specific use of the polymer can be added to the resin through a solvent-mixing process, to initiate the polymerisation process and produce desired structures.

Efforts are being made into the synthesis and photochemical studies of new TPA photoinitiators that have more desirable properties. This is due to the fact that conventional photoinitiators often have small TPA cross-sections (δ) in the near-IR wavelength range, where femto-second lasers are used for TPA induced polymerisation. Previously reported δ values for a few conventional photoinitiators are of the order of less than 10 Göppert Mayer (GM) units, where 1 GM = 10^{-50}cm^{4}s per photon [14]. In spite of the low δ values, the general use of a variety of conventional photoinitiators for TPA polymerisation of acrylates, epoxides, vinyl ethers and thiol-ene monomers have been reported[15,16]. Because commercially available photoinitiators generally have low δ values, research has been carried out on the preparation of new photoinitiators that have higher TPA cross-sections, with the hope that greater δ values will mean the use of lower laser power and a shorter irradiation time. This would mean minimum optical damage to the polymer materials. Photoinitiators with higher δ could also allow the use of cheaper micro-lasers but with the same polymerisation speed from that obtained by the conventional femtosecond-

lasers and commercial UV resins[17]. It is a challenge to produce new photoinitiators with improved photosensitivity to the near-IR radiation for TPA polymerisation, and many synthetic procedures are needed. It would however have a great impact on the success of 3D photopolymerisation if better TPA initiators were developed. TPA-induced polymerisations used for micro and optical-component fabrication often use conventional, commercially available UV-visible photoinitiators.

The mechanism of two-photon polymerisation has been studied extensively by numerous authors. Lu et al. have carried out studies with the emphasis on the types of photoinitiators containing three different two-photon chromophores[18]. Lu et al. reported the synthesis of the three types of chromophores; D-π-D-π-D, D-π-D and D-π-a-π-D, where D is the strong donor terminal group, π is a π-conjugated core, and D and A are the electron-accepting side group linked with the π-conjugated core. Their use as two-photon initiators was fully investigated in earlier works[19]. The sensitivity of two-photon polymerisation was found not to be related to the enhanced two-photon absorption, but is based on the fact that the sensitivity of TPA is dependent on TPA and the electron transfer from the lowest singlet state of the chromophore to the monomer. Electron charge transfer from the excited initiator molecule to the monomer was through intra-exciplex. The rate of the TPIP was determined by equilibrium of electron transfer and back electron transfer between the initiator and monomer.

The TPA properties of a number of common, commercially available photoinitiators were reported by Schafer et al., using two non-linear transmission spectroscopic methods[20]. Many of the photoinitiators undergo Norrish type I α-cleavage reactions involved in the radical generation. The photoinitiators studied were α-hydroxyketones, α-aminoketones, acylphosphine oxides, a metallocene, an iodium salt photoacid generator (PAG), an aryl ketone initiator isopropylthioxanthone (ITX) and two newer materials. A white-light continuum pump-probe technique and a Z-scan technique were used to measure the TPA properties of the photoinitiators. In the Z-scan technique, the transmittance of a focused beam is monitored after passage through the sample. The sample is translated along the axis of a focused beam and passes through the middle of the beam where the irradiance is at a maximum and provided the sample exhibits TPA, the transmittance of the beam should be at a minimum. Fitting this transmittance versus the sample position led to the δ being determined. Diphenylaminobenzothiazolylfluorene (DPABz), a strong

two-photon absorption compound, exhibited high TPA and was found to be as efficient as a two-photon free radical photoinitiator.

A number of researchers have been working with different photoinitiators and materials to create 3D micro-structures by two-photon photopolymerisation. Smaller structures are being fabricated, and at faster rates with more detailed shapes and forms. This enables the fabricated structures to be integrated into complicated devices. Wu et al. reported on the recent developments and improvements of TPA technology for micro-fabrication, along with their current research on the topic[21]. When concerning TPA photopolymerisation, two types of photoinitiators are generally reported: UV-visible photoinitiators [22], and electron-rich molecules optimised for TPA in the desired wavelength range. Greater values of TPA cross sections in the second class of molecules allows for lower powers and shorter times of exposure, leading to cheaper production costs[23]. A number of lasers are available at shorter wavelengths in the visible range, such as the Ar-ion laser or the frequency doubled Nd-YAG laser, which can lead to better polymerisation resolution and smaller 3D structures being realised. Research is still in the early stages of manufacturing TPA initiators in the visible range. One such study is the investigation into two symmetric *N, N'*-bis-(4-methoxyphenyl)-*N,N'*-diphenyldiamino derivatives[23]. These molecules have a D-π-D structure and are known to be well suited to photopolymerisation[24]. The molecules used in this research were biphenyl or fluorene derivatives, and the moderate conjugation in the molecules showed a shift the TPA properties in the visible range. The TPA cross sections were characterised as well as the ground state oxidation potentials and threshold energies for the polymerisation of triacrylate monomers. The molecules were found to be efficient TPA initiators in the 500-600 nm spectral range. The molecules were successfully used for acrylate photopolymerisation without any coinitiator. Polymerisation thresholds can be understood in terms of the idea that a resin is polymerised as soon as the density of the radicals $\rho = \rho$ (*r, z, t,*), exceeds a certain minimum concentration (ρ_{th}). These were determined by the analysis of polymer lines produced at variable exposure dose.

New research is currently being carried out on novel chromophores for photoinitiators containing double and triple bonds. A number of new applications are being developed in the field of thin films, so formulations have to be adapted to give the optimum performance for the particular uses. The type of resin chosen influences the characteristics such as mechanical and physical performance, properties such as hardness, toughness and oxygen permeability. Photoinitiators, as already discussed,

are the key component in these formulations. By modifying the photoinitiators, there can be significant manipulation on the curing performance, such as the rate of polymerisation (R_p), double bond conversion, and the final properties such as the gel content or colour. Many radical generating photoinitiators are based on benzoyl chromophores and are classified into the cleavable Type I or hydrogen abstracting Type II systems. Initiators can be modified by adding suitable substituents to give desirable properties, such as better solubility. The conjugation can also be extended which leads to absorption shifting to the visible range of the spectrum. This is important in a number of current applications. Another way to shift the absorption would be to introduce hetero-substituents such as OR, SR, or NR_2[25]. In the case of NR_2, decreased photoactivity is sometimes observed due to charge-transfer interactions with the carbonyl group and so lowers the quantum yield for $n-\pi^*$ transitions. The benzoyl chromophore is a structure widely used in photoinitiators, as it is cheap, universally applicable and has good reactivity. Usually however, coinitiators such as tertiary amines are used which can give rise to odours and discolouration. One-component systems based on thioxanthone have recently been described.[26].

Seidl et al. are carrying out continuing research into new chromophores for photoinitiators. Recently, a series of double and triple bond containing photoinitiators based on benzophenone, thioxanthone, benzyl, benzyl dimethyl ketal, and hydroxyalkylphenone were investigated[25]. It has previously been shown from differential scanning photocalorimetry (photo-DSC) experiments using monomers with abstractable hydrogens, that 1,5-diphenylpenta-1,4-diyn-3-one (DPD) gives high activity for double bond conversion and polymerisation at low photoinitiator concentrations of 0.0025 M, and without the use of a coinitiator. UV-Vis spectroscopy shows a strong absorption up to 350 nm which may be explained by a cross-conjugation effect. Photoinitiators based on donor substituted DPD have been found to be suitable for two-photon initiated photopolymerisation. Because of these findings Seidl et al. extended their research into other types of photoinitiators based on DPD. To evaluate the new initiators, UV-Vis spectroscopy was used, as it was expected to see significant red-shift compared to other compounds. The rate of decomposition (R_d) was determined by steady state photolysis in combination with HPLC. Photoreactivity was also determined by photo-DSC. UV-spectroscopy revealed that the absorption shifted up to 50 nm to the visible region of the spectrum, and with the steady-state photolysis experiments, the R_d was determined. These rates were almost identical to commercially available reference photoinitiators. Quenching reactions with 2,2,6-tetramethylpiperidine-1-oxyl (TEMPO) identified α-cleavage for

27

Type-I initiators. All the compounds synthesised were found to be suitable to use as photoinitiators for longer wavelengths. For optimum stability, the photoinitiator concentration should be selected carefully to achieve optimum reactivity.

2.2   TPA Sensitising Systems

A number of research groups are working on TPA compounds and exploiting efficient photoinitiators and sensitisers to achieve better microfabricated structures and greater TPA cross sections. The Nanophotonic Materials Laboratory at Hannam University, Korea, has recently been working on the development of highly efficient TPA photosensitisers and matrix materials, as well as novel mechanical approaches and optical setups. By employing TPA active dyes and computer aided design systems (CAD) the research group successfully increased the spatial resolution of microfabrication to below 100 nm[27]. Lee et al. have also recently introduced a method for fabricating 3D nano and microstructures in a single step using a multi-layered stamp via two-photon polymerisation. Lee et al. have also carried out a number of different studies on the synthesis of efficient two-photon absorbing materials. The main types of materials are based on phenylene vinylene, phenylene ethynlene, and fluorene and dithienothiophene moieties as TPP sensitisers. Organic TPA materials received very little attention until 3D data storage was demonstrated in 1989 by Rentzepis. Since then, various chromophores have been investigated for the use as TPA photosensitisers. Reinhardt et al. studied a series of TPA dyes based on π-conjugated benzenoid structures.[28]. The study consisted of the characterisation of the TPA activities as a function of the change of the chemical structures and design, to increase the TPA efficiency. This included the extension of conjugation length, the increase of planarity, of the π-conjugation and the increase of pendant chain length. Leading on from this Kannan et al. synthesised a number of fluorene derivatives in which a donor was fixed with diphenylamine at one end, a π-centre with fluorene and acceptors. The pendant alkyl group was changed to investigate the TPA activity. It was shown that 2-benzoylthiazolyl and benzoyl groups were more efficient acceptors than pyridine moieties. Owing to improved laser and optics technology, lasers can cover from 500 to 1200 nm and sometimes up to 2400 nm. This means it is now possible to characterise diverse nonlinear optical properties of materials. Strehmel et al. studied the effect of conjugation length of a series of molecules containing strong acceptors such as fluorinated phenyl moieties[29]. As expected the longest conjugated system showed the highest TPA activity of 500 GM at the longest wavelength of 850 nm. Marder et al. synthesized and investigated a series of dipolar chromophores with

pyrrole auxiliary donors and thiazole acceptors[30]. These compounds exhibited very high TPA-cross sections of around 1500 GM. The most extensively studied TPA dyes are those of centrosymmetric quadrupolar structures, D-π-D, and A-π-A, shown in Figure 5. Efforts have been made to establish TPA activity-structure relationships for these dyes through experimental studies. Marder et al. investigated, through mechanistic and theoretical studies, the nature of TPA on bis(styryl)benzene derivatives. The study showed that for linear centrosymmetric quadrupolar TPA molecules the intramolecular charge transfer (ICT) character of the TPA molecule is important in enhancing the TPA activity. From the study, the results revealed that the extension of the π-conjugation, introduction of acceptors on the centre ring, increase of donor strength and reversal of the direction of charge transfer from D-π-D to A-π-A enhance TPA activity[31]. Other structural designs have been considered for TPA molecules. Another research group investigated the effects of double and triple bond containing molecules, and the effects of their TPA activity. The work concluded that double bonds have a greater effect than triple bonds in enhancing TPA efficiency. Comparing the TPA efficiency of longer π-conjugated molecules containing triple bonds to ones with only double bonds they showed the coplanarity of the molecule is a critical element for enhancing the TPA activity due to efficient π-electron conjugation.
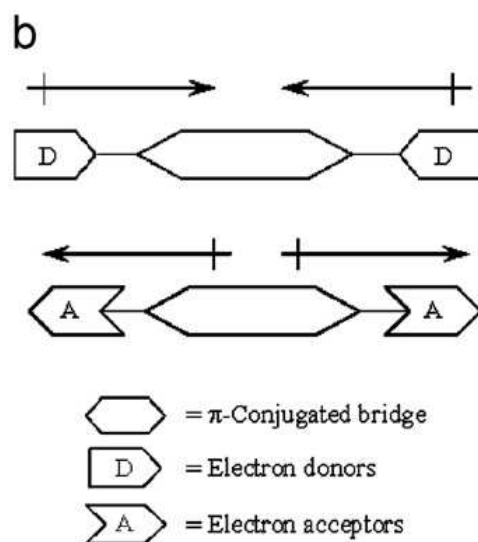
Figure 5: Symbolic representation of D-π-D, and A-π-A

2.3   Cationic Two-Photon Induced Photopolymerisation

Cationic two-photon induced photopolymerisation was first reported in 2000[32]. TPIP of an epoxy resin sensitised by isopropylthioxanthone and diarylidonium salt was also reported in 2001, where the study concerned the dependence of the polymerisation due to light intensity and the value dependence on the concentration of the initiator[33]. It was shown that cationic TPIP with a low threshold and a high dynamic range could be achieved using the initiating system of isopropylthioxanthone/diarylidonium salt, for the cationic polymerisation of di-epoxide. The material could be polymerised at intensities more than 100 times the threshold level without damage.

2.4   Organic Resins

Many types of materials are commonly used for two-photon photopolymerisation and the group of materials routinely used and have already been discussed are acrylate resins. Baldacchini et al. have reported on the development of a new acrylate resin for the use in multi-photon polymerisation that has improved physical and chemical properties[34]. The report included the characterisation of the multi-photon initiator properties and also structures that exhibit low shrinkage and high mechanical strength and hardness. The resin formulation contained three components. Ethoxylated trimethylolpropane triacrylate, which was used to help reduce shrinkage during polymerisation, tris(2-hydroxyethyl)isocyanurate triacrylate, which promoted hardness of the polymer, and Lucirin TPO-L, which is an acylphosphine oxide radical photoinitiator. It has already shown to be an efficient initiation of photopolymerisation by TPA. This demonstrates that it has a considerable TPA cross section for light with a wavelength near 800 nm. In single-photon polymerisation, it is necessary for the absorption path length to be comparable or larger than the thickness of the object to be polymerised so the absorption does not prevent the polymerisation of the portion of the object furthest away from the light source. This means there is a limit to the concentration of photoinitiator that can be used. With multiphoton absorption, the sample is transparent at the laser wavelength and occurs only at the focal region. This means it is possible to use a higher concentration of photoinitiator. In this work, the optimum concentration of Lucirin TPO-L was determined by preparing samples of equal amounts of the starting materials and various weights of the photoinitiator. A laser beam was focused in the middle of the sample. Different spots in the sample were exposed for 5 s each at various powers, and the damage threshold ($P_{th,dam}$) (defined as the minimum power at which uncontrolled polymerisation took place after

the exposure time) was determined. It was shown that $P_{th,dam}$ decreased as the concentration of photoinitiator increased up to around 1.5 wt%. Following this, only a small decrease was seen. To determine the polymerisation action spectrum, $P_{th, fab}$ was measured as a function of excitation wavelength. From this, it was concluded that Lucirin TPO-L initiated best near a wavelength of 725 nm. The authors created a number of 3D microstructures fabricated using multiphoton absorption. The structures showed no sagging or distortion, which indicated the polymer had excellent mechanical properties, and the straightness of the edges near the base of the structures showed that the resin did not shrink significantly during the polymerisation. The novel resin consisted of readily available components and was prepared in a simple process. The fabrication of 3D structures with high structural rigidity, using low amount of output power of a Ti-sapphire oscillator was found to be possible.

2.5   3D Structures – Hybrid Materials

The interaction of lasers with polymer surfaces and bulk samples is becoming increasingly important from a technological perspective. Adapting polymers to laser beam characteristics is a challenge, and as the method of TPA using femtosecond lasers has been successful and a considerable amount of work has gone into optimising the process. Structures already fabricated are for example, photonic crystals and some mechanical devices. Inorganic-organic hybrid polymers have attracted much attention as a material suitable for optical or microelectronic devices. The physical properties of the hybrids can be tailored, such as the refractive index, or the compounds can be mixed to achieve desirable properties. A slow writing speed, low energy and multiple exposures were needed to obtain well-defined lines. From these studies, it was found that by substituting an organo-alkoxysilane with a Ti alkoxide, the refractive index could be increased by around 7 %. High refractive indices were achieved without thermal treatment and for samples with a low degree of cross linking.

2.6   Photonic Crystals

3D photonic crystals are becoming interesting in the field of two-photon polymerisation. Photonic crystals are periodic dielectric microstructures, which can be fabricated at lattice parameters small enough to observe their unusual optical properties in the NIR or visible spectral regions. A number of functional defects are able to be introduced into photonic crystal structures, which makes them good candidates for device fabrication. A recent paper has been written on the development of a single-monomer acrylate based resin and how it can be used to fabricate 3D photonic crystals using TPA[35]. Structures with isolated or weakly linked structural elements such as photonic crystals featuring rods with diameters in the order of 200 nm are difficult to construct with TPA. The choice of material is therefore crucial. The structures need to be mechanically stable and free from distortions related to shrinkage during the polymerisation process. Sample post processing should leave the fabricated structure unharmed, and the resin must be homogenous and transparent at the fabrication wavelength. When used for optical microstructures, the polymerised material must be transparent at the operational wavelength such as telecommunication wavelengths in the NIR spectral region. When using commercially supplied resins; the minimum structural element size of structures varies between 5 and 1 µm. The commercially available polysiloxane polymer inorganic glass hybrid materials (IPG, RPO Inc) produced minimal sizes of isolated structures of elements of around 350 nm, however the quality of the photonic crystals was degraded quite considerably from shrinkage. Due to the shortcomings of commercially available resins, pure acrylate-base polymers, as well as inorganic-organic hybrid polymers have been developed. Using these materials, isolated polymerised voxels with diameters of 120 nm have been fabricated. Wu et al. used the single monomer acrylate resin with an aromatic ketone photoinitiator to produce photonic crystal structures by TPA. The resin was easily prepared and the monomer was found to generate an insoluble cross-linked network by free radical polymerisation. The polymerised material was thermally stable up to 300 °C and its refractive index increases from 1.54 to 1.59 after polymerisation. Photonic crystals were fabricated in a "woodpile" structure at a layer spacing of 500 nm. The structures with sub-micrometer resolution of the structural elements by TPP were fabricated, and featured bandgaps in the NIR spectral region.

2.7   Organically Modified Silicon Alkoxides

Over the past ten years, organically modified silicon alkoxides have been utilised for the formation of hybrid organic-inorganic materials. When one of the organic groups can be polymerised, the addition of a photoinitiator will make the material UV photopolymerisable. UV irradiation of thin films made from the hybrid material results in the formation of a stable cross linked network of hybrid molecular chains. When the UV irradiation is selective, what can be formed is planar channel waveguides. These planar channel waveguides are similar to optical fibres, which are essentially a material with a high refractive index core surrounded by a low refractive index cladding. Planar waveguides differ from this, as they are formed in thin coatings and do not have circular cross-sections, but square. Fabrication of these structures can be achieved by precise UV exposure techniques, such as mask photolithography or direct laser writing. Hybrid materials have been used in recent years for many applications, and one of interest is the application in planar lightwave circuits (PLCs) for photonics applications in the area of telecommunications and sensing. The performance of waveguides is linked strongly to the exact properties of the hybrid material, and the propagation of light is affected by scattering and absorption processes. This has led to recent research focused on developing novel photopolymerisable sol-gel materials with high transparency at the telecommunication wavelengths. R. Copperwhite et al., have recently carried out extensive research on understanding the photopolymerisation processes involved during waveguide formation[36]. There is little research on the behaviour of different photoinitiators in sols and their effect on the structure of the resulting waveguides. The type of photoinitiator and the molar concentration used relative to the photosensitive groups in the sol has an influential role in the resulting waveguide shape and its optical performance. The effect of the chelating agent also, and its ratio to the other precursors in the sol, have been investigated.

2.8   Polydimethylsiloxane (PDMS) Materials for Microfabrication

Of interest to us is the potential applicability of waveguide writing in 3D by two-photon photopolymerisation. Much research has been carried out recently on this topic, including the use of polysiloxanes. Extensive research has recently been carried out on two-photon 3D lithography and selective single-photon photopolymerisation in a prefabricated polydimethylsiloxane matrix[37]. The potential applicability of these processes lies in waveguide writing in 3D by two-photon polymerisation. TPP allows the fabrication of sub-micron structures from a photopolymerisable resin. By using

low-energy near-infrared lasers, it is possible to produce 3D structures with a spatial fabrication resolution down to 120 nm. The technique can be used to inscribe waveguides into materials that are otherwise not accessible. New photoinitiators for 3D structuring by TPP have been reported; along with an approach to writing waveguides by selective one-photon polymerisation in a preformed polydimethylsiloxane (PDMS) matrix. Recent efforts have been concentrated on the preparation of novel photoinitiators that possess higher TPA activity. For waveguide applications, TPP has to induce a refractive index change in the range of $\Delta n/n \sim 0.1$-1%[38]. Inscription of waveguides in 3D requires materials and methods suitable for a selective refractive change in a preformed material block. Literature reports a number of approaches, such as selective curing of a component in a resin mixture[39] or by direct writing into various glasses[40]. To achieve suitable refractive index changes for waveguides, Infuehr et al. used the approach based on selective photopolymerisation of monomers within a preformed flexible PDMS matrix. Polysiloxane waveguides are routinely fabricated from thermosetting siloxanes by lithographic methods combined with reactive ion etching or by using moulds. In this study, PDMS specimens were swollen by photoreactive monomer formulations containing acrylates or vinyl compounds with higher refractive indices than PDMS. The monomer was then photopolymerised and the remaining monomer removed by evaporation. When considering the characteristics of monomers for structuring optical waveguides, it has to form a polymer that has a higher refractive index than the matrix so that total internal reflection inside the waveguide occurs. With specially tailored cross-conjugated photoinitiators, feature resolutions in the range of 300 nm with only 0.025 wt. % of initiator in the photosensitive resin were achieved.

The effects of branched structures using phenylene-ethylene derivatives have also examined. The majority of work carried out on two-photon 3D microfabrication has been performed using radical initiated polymerisation of acrylates. PDMS-based microfabrication uses a thermal initiation and platinum-catalysed hydrosilylation to cure the viscous liquid composed of dimethyl-vinyl-terminated PDMS, poly(methylhydrosiloxane-co-dimethylsiloxane) and dimethylvinylated silica into an elastomeric solid. The active component is usually a platinum compound, which decomposes on exposure to UV irradiation to give an active hydrosilylation catalyst, and a heterogeneous platinum colloid [41].

2.9   Waveguide Materials

Modified silicon alkoxides, as already discussed are widely used in the preparation of hybrid organic-inorganic materials. One research group has carried out extensive studies on these materials, and their use in the development of channel waveguides[42]. At the telecommunication wavelengths absorption processes are caused by the presence of OH and C-H groups inherent to the hydrolytic sol-gel route and to the hybrid precursors. The role of OH groups in the attenuation at 1550 nm has been considered, absorption by C-H aliphatic groups induce a stronger attenuation at this wavelength. Aromatic and vinylic C-H groups also do not contribute to any absorption at 1550 nm[43]. Due to these discoveries, the research was focused on preparing photosensitive materials containing the minimal amount of C-H aliphatic groups. To achieve this, the introduction of aromatic or vinylic alkoxysilanes within a photosensitive alkoxysilane was investigated, by means of a three-step sol-gel technique. Four new organo-siloxanes were synthesised and their refractive indices determined. The compounds were applicable to the fabrication of photo-patternable channel waveguides. The photosensitive part of the materials came from the incorporation of methacryloxpropyltrimethoxysilane (MAPTMS), which possesses a methacrylate group which allows polymerisation when irradiated with UV light. When additional aromatic precursors were introduced, it was found to increase the refractive index, and the incorporation of a vinylic precursor produce the opposite effect to the aromatic species, and cause a decrease in the refractive index with increasing concentration. To improve the structural homogeneity and decrease the concentration of aliphatic groups further, vinyltriethoxysilane (VTES) was replaced with phenyltriethoxysilane (PHTES), which is similar in structure but only contains one aromatic group. This means there is less steric hindrance and the condensation between the aliphatic and aromatic oligomers is improved.

Currently technologies based on inorganic glasses and crystalline semiconductor materials are often used for optical processing and optical waveguide applications. These materials need, however, complex manufacturing processes and are unlikely to be used for more sensitive processes. Polymers however, can be utilised for performing integrated circuits at a low cost, and etching processes to fabricate polymer waveguides that can perform large integration scale optical circuits, with standard photolithography technology. There is always the need to improve the materials used, and to maximise their efficiencies in their specific functions, as technology adapts, and smaller, more defined structures are needed. A recent study

35

by Bosc et al. involved the strengthening of some polymer materials so that they can endure the process for standard integrated optical circuits[44]. Polymethacrylate materials are commonly used to fabricate integrated optical circuits (IOC), because they have good optical properties and are easy to form films with. A problem with these materials is that they have to pass thermal treatments without defects occurring in the surface. Polymethylmethacrylate (PMMA) cannot be used without modifications as the surface undergoes "worm-like" defects, during the thermal treatment. Bosc's report attempts to overcome this problem by strengthening the material using modified structures such as imidized PMMA. For the material to be used effectively, the elastic modulus and the glass transition temperature have to be high enough to avoid failure of the material.

2.10 Further Technologies used in Waveguide Fabrication

The field of integrated optics is developing into the field of optical communication and optical sensing. Integrated optics are analogous to integrated electronics, but the difference is integrated optics and circuits provide the functional information signals imposed on optical wavelengths, usually in the visible spectrum or near infrared. Communications and sensing can be improved using integrated optics due to its high bandwidth and resistibility to electromagnetic interference. Waveguide devices have been investigated for fabricating optical integrated circuits that could play an important role in electro-optic devices. Polymers are being developed for electro-optic devices for a number of reasons, one being their flexibility[45]. Polymers can be used as spun-on layers which are compatible with many substrate materials and can be tailored for specific applications. The refractive index profile in waveguide cross sections is important, and defines the properties of the waveguide as an informational system element and so sets the performance of the whole planar device.

Common techniques used for polymeric waveguide fabrication are ion implantation, which is a process whereby ions of a material are implanted into another solid, thus changing the physical properties. Also used is photolithography, which is a process that selectively removes parts of a thin film or the bulk of a substrate. Light is used to transfer a geometric pattern from a photomask to a light sensitive chemical (photoresist) on the substrate. A series of chemical treatments then engraves the exposure pattern into the material under the photoresist. Reactive ion etching is also used, which is a technique which uses chemically reactive plasma to remove material

deposited on wafers. The plasma is generated under a low pressure vacuum by an electromagnetic field. High-energy ions then attack the wafer surface and react with it. Methods such as these, although well established, involve many processing steps, or lengthy fabrication times. Watt et al. have developed the new technique of proton beam writing, which has the advantage of being maskless, which allows rapid and inexpensive prototyping. Comparing the application to electron beam lithography, there is the advantage that, unlike electron beam exposures, where the electron trajectories are erratic due to multiple large angle collisions, protons have a straight trajectory and a well defined range in a photoresist. The use of this technique to fabricate low-loss, passive polymer waveguide structures such as symmetric y-branching waveguides in SU-8 (a viscous polymer commonly used as a negative photoresist) have been reported.[46]. Proton beam writing is a direct-write micromachining technique which can produce 3D micro-structures with straight and smooth sidewalls. A focused sub-micron beam of 2.0 MeV protons is used to directly write onto suitable polymers. The protons are focused using magnetic quadrapole lenses. Sub-micron beam resolution is important for proton beam writing as it is essential to direct-write the optical pathways accurately to realise the optimal design and minimise optical losses. The research included spin-coating SU-8 on a glass substrate, and measuring the transmission spectra and refractive index of the polymer when it was proton beam cross-linked. The new technique was applied to fabricate symmetric y-branching waveguides, and it is believed that the proton beam writing technique gives flexibility, to create waveguides of arbitrary patterns, and could also be applied to rapid prototyping of optical circuits.

The first waveguide grating was reported in 1970 and since then, research has moved into the area of integrated optics. Inexpensive and reliable waveguide gratings are in demand, and so polymers are being investigated in great detail as the material of choice. Polymeric waveguide gratings are fabricated by a number of methods, such as UV-photobleaching, laser ablation and photoisomerisation. Their optical properties such as optical switches, photonic band-gap and resonant grating-waveguide structure have also been comprehensively characterised. The most common methods used to form gratings in polymeric materials are by physical means. This means there are no chemical changes in the polymeric waveguides during the process. It has been reported that a grating with electronically switchable properties has been fabricated with electronically switchable properties by using TPP[47]. Yu et al. recently described a fabrication method of coupling gratings by TPP[48]. Compared to the physical methods, TPP is convenient, flexible, is relatively cheap and is automated. TPP was demonstrated for the fabrication of the coupling

grating in a thin polymeric waveguide film. The results showed that when the incident laser with wavelengths of 514 and 632 nm reached the coupling grating in the waveguide at an appropriate angle, the laser was coupled into the film and propagated to the other side of the film.

The thermo-optic coefficient of polymers is important in determining waveguide device performance. A large thermo-optic coefficient means a reduction of power and consumption for devices such as thermal optical switches (TOS) and variable optical attenuators (VOA) because it corresponds to small temperature changes and so a small power input for causing the change in the refractive index of polymer waveguides required for optical switching or optical attenuation. Studies were carried out on a polymer/silica hybrid VOA, and showed that when the coefficient of the cladding polymer was changed from -1×10^{-4} to -6×10^{-4} ($°C^{-1}$), the power consumption of the devise was reduced by 80 %[49]. Only when power consumption is reduced significantly will the fabrication of high channel counting TOS and VOA and the integration of devices with arrayed waveguide grating (AWG) on one chip become practical. A large thermo-optic coefficient is not desirable for AWG, because its wavelength shifts when the refractive index of the waveguide is changed and the wavelength shift is sensitive to temperature variation, so minimising the coefficient is necessary for fabricating AWG using polymers. The thermo-optic coefficient of polymers is important for controlling device performance, and has to be properly selected for different types of devices. Zhang et al. have developed an empirical equation for estimating the thermo-optic coefficient of a polymer using its coefficient of thermal expansion which is easily measured using routine polymer testing equipment such as a TMA and dilatometer, and is available for many commercial polymers[50].

2.11   Multiphoton Lithography

There is much interest in the potential for the application of producing 3D structures with nanoscale resolution using multiphoton lithography (MPL). In depth studies have been carried out on the fabrication of nanoscale polymeric features with a width of 65 nm using 520 nm femtosecond pulse excitation[51]. A photosensitive resin used for the MPL consisted of a 50:50 wt% blend of triacrylate monomers and 0.1 wt% photoinitiator consisting of 4,4'bis(di-*n*-butylamino)biphenyl (DABP) or *E,E*-1,4-bis[4-(di-*n*-butylamino)styryl]-2,5-dimethoxybenzene (DABSB). Lines were written between supports, at various powers and scan speeds in order to establish the threshold for multiphoton writing of polymeric lines and the minimum feature sizes that could be

obtained with laser wavelengths of 730 and 520 nm for the resin systems. It was shown that the line widths initially grow and then approach a constant value with increasing exposure time for a given power. The laser-induced polymerisation using a photoinitiator with a large cross-section in the visible wavelength region allowed for the multiphoton 3D lithography with nanoscale lateral feature resolution. Line widths of 80 nm and 65 nm in "woodpile" photonic crystal structures were able to be fabricated, and the formation of such nanoscale structures using MPL is seen to have an impact on the fabrication of photonic and electronic devices in the future.

2.12 Experimental Methods for the Characterisation of Two-Photon Absorption

TPA can be measured by a number of techniques, including two-photon excited fluorescence (TPEF) and nonlinear transmission (NLT). Pulsed lasers are routinely used to study TPA, as it is a third order nonlinear optical process, and so is most efficient at high intensities. The process is described as nonlinear, due to the fact that the strength of the interaction increases faster than linearly with the electric field of the light. In ideal conditions the rate of TPA is proportional to the square of the field intensity. To study TPA phenomena, lasers are necessary due to the high light intensity required. In addition, to understand the TPA spectrum, monochromatic light is needed to measure the TPA cross section at different wavelengths, so the choice of excitation is a tuneable pulsed laser, such as frequency-doubled Nd-YAG-pumped optical parametric oscillators (OPO's).

A number of research groups have carried out studies on the measurements of TPA cross-sections and the mechanisms of TPIP. Optimisation of the sensitivity of TPIP using a number of different photoinitiators has been reported. The use of bis(diphenylamino)-diphenylhexatriene, used to induce the polymerisation of a highly functional free radical polymerisable monomer dipentaerythritol pentaacrylate has been studied, and the efficient two-photon absorbers based on bis-(stryl)-benzene structures bearing electron donating moieties were synthesised and found to undergo a two-photon induced electron transfer to the functional triacrylate monomer[52,53].

3 Development and Characterisation of Matrix Materials - Requirements of the Optical Material

When considering a matrix material suitable for the use in applications in waveguide fabrication, such a material has to fulfil a number of requirements. For this study, the material is to be used on printed circuit boards, which have to undergo harsh processing steps. The chosen material, as well as the inscribed waveguide, has to therefore withstand these processing steps, which include temperatures of over 220 °C, high pressures and chemical exposure. The developed material therefore has to be thermally stable above 220 °C and be chemically inert. Long term stability is also important and processing steps kept to a minimum. The material must also be free from toxic or hazardous components including halides, and be fully flexible, to enable the use of the optical waveguides on flexible printed circuit boards. Polymer optical waveguides need to have low optical losses, and for our purposes, the telecom (1310 and 1550 nm) and datacom (840 nm) wavelengths, losses need to be kept to a minimum. The chemical structure of the polymer has to therefore contain mostly functional groups, which do not absorb light in the telecom and datacom regions. OH and C-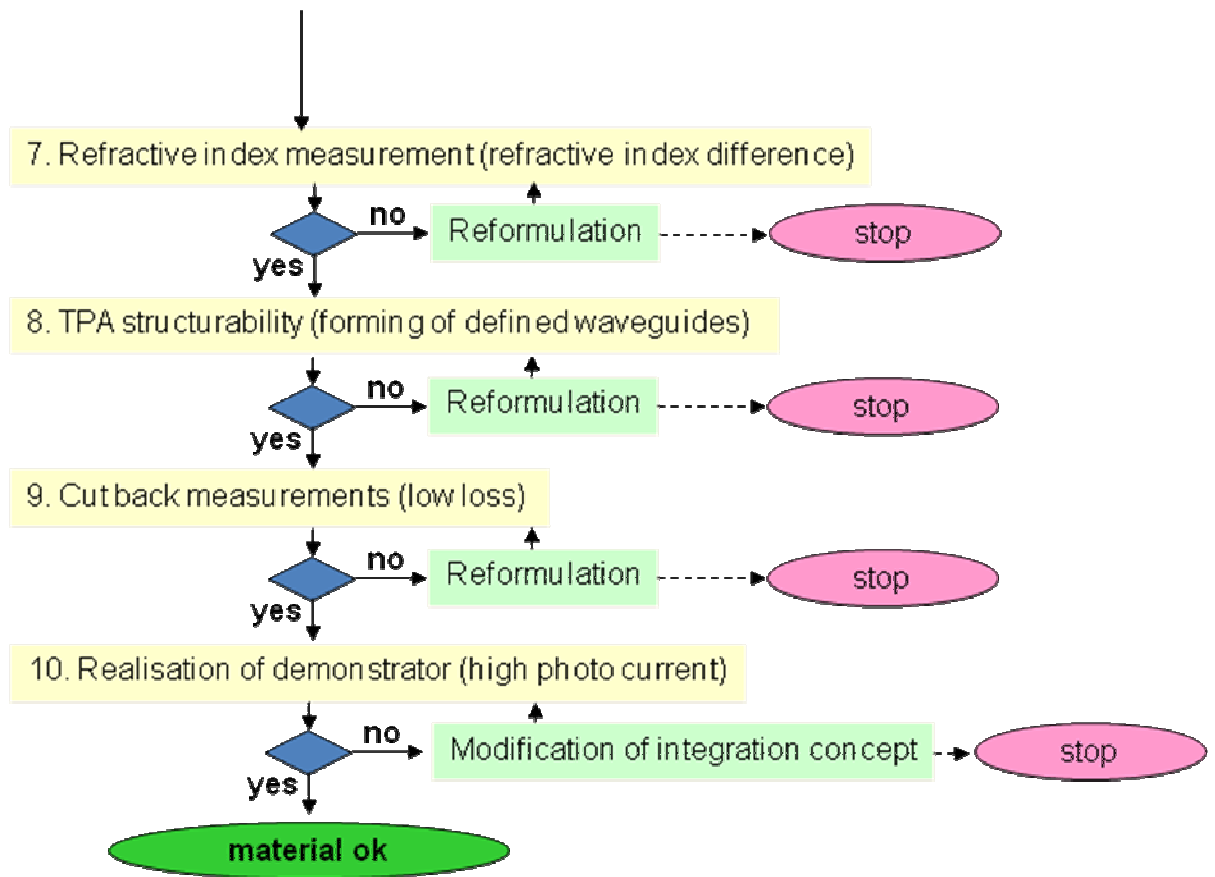H functional groups are known to absorb in the telecommunication wavelengths, so replacing C-H groups with phenyl groups for example, can not only reduce optical losses, but also increase the flexibility of the polymer. Electronic absorptions in polymers are unlikely to contribute notably to optical losses in the 1300 and 1550 nm region, unless they are highly coloured. Near-infrared spectroscopy (NIRS) is one way of determining the optical losses at specific wavelengths. However one must also consider losses can occur through scattering, Polarisation-dependent loss (PDL) and insertion loss. PDL is the maximum difference of attenuation between any two polarization states. For waveguides, PDL is defined as the maximum difference of loss between the elliptical polarization states, but varies with different optical devices. Insertion loss can be defined as -10 $\log_{10}$ (P_{out}/P_{in}) with P_{out} and P_{in} defined as the output and input power from the optical devises. Waveguide geometry and the design of the device means the polymer used as the waveguide core has the have a refractive index higher than the cladding material. In this study, high refractive index monomers are added to the material, and the poly(meth)acrylate, which forms the waveguide core, must have a higher refractive index to that of the polymeric cladding material. The packing density, the polarisability and the difference between the optical wavelengths used all influence the refractive index of the material, so it is important to determine the refractive index

of the cladding and waveguide core, especially at the telecommunication wavelengths. The refractive index of the cladding material can be tuned depending on the concentration of high refractive index monomers present, as well as functional groups attached to the polymeric chain. For this study, it is desirable to have a refractive index difference (Δ n) of between 0.003 and 0.1, so the refractive indices of the poly(meth)acrylate core and the cladding material, with and without the monomers need to be determined. The cladding material needs to be fully stable, so full removal of any remaining free monomers needs to be carried out following the fabrication of the optical waveguides, which will also lead to a larger difference of the refractive index. Temperature also leads to a variation in the refractive index of polymers, with the refractive index decreasing with temperature at a rate of 10^{-4}/°C.

When considering a polymeric material used for the fabrication, all of these characteristics need to be considered, along with other material requirements, including having a suitable viscosity, speed of cure and the ability to form thin films. A summary of the evaluation steps of the material during development is presented in Figure 6. Once the material has been developed, each step, shown in the processing flow diagram is evaluated. Three materials were developed during this study, and each evaluated using such processing steps, leading to the polymeric matrix materials being utilised on suitably designed PBCs containing laser and photo diodes to form fully operational optical interconnects. The next sections will describe the development and characterisation of three different materials, based on polysiloxanes, containing acrylate or methacrylate monomers, which undergo photopolymerisation by TPA, to form the optical waveguide core.

X. [action] [(requirement)]

[decision] ◆ ⟶ [reaction] ┄┄┄▶ [result]

1. Solubility of components (no phase separation)

◆ —no→ Changing of mixing ratio, new component

yes ↓

2. UV-reaction and temperature curing reaction (curing of material)

◆ —no→ Reformulation, changing of conditions

yes ↓

3. Check of thermal stability of the materia (no mass loss for T > 250°C)

◆ —no→ stop ⟶ new material search

yes ↓

4. Optical check (no yellowing effect, low transmission in VIS-range)

◆ —no→ Reformulation ┄┄┄▶ stop

yes ↓

5. Viscosity check of system (application of thick films ~ 300 μm)

◆ —no→ Reformulation ┄┄┄▶ stop

yes ↓

6. Mechanical check (flexibility, no cracks, adhesion to substrate)

◆ —no→ Reformulation, surface treatment ┄▶ stop

yes ↓

7. Refractive index measurement (refractive index difference)
  no → Reformulation - - - - - → stop
  yes ↓

8. TPA structurability (forming of defined waveguides)
  no → Reformulation - - - - - → stop
  yes ↓

9. Cutback measurements (low loss)
  no → Reformulation - - - - - → stop
  yes ↓

10. Realisation of demonstrator (high photo current)
  no → Modification of integration concept - → stop
  yes ↓

material ok

Reformulation = modifications of the ratio of ingredients, no chemical modifications

Figure 6: Evaluation process carried out on each newly developed optical material, resulting in the continuation or modification of properties

The present PhD thesis contains three sections, with three materials investigated for the use as matrix materials for TPA patterning of optical waveguides. Each material is characterised, and the optical properties are detailed, including the fabrication of fully operational optical interconnects. The three developed materials denoted System A, System B and System C, were characterised fully and investigated for their optical properties and suitability in being used as matrix materials for the fabrication of optical waveguides.

Development and Characterisation of Optical Matrix Materials – System A

4 Characterisation of an Optical Material Developed from Vinyl and Hydride Terminated Polysiloxanes (System A)

4.1 Introduction

Taking into consideration the characteristics needed for a material used for a matrix material used to produce optical waveguides, a material was developed based on a hydride terminated polysiloxane cross linked with a vinyl terminated polysiloxane. The hydrosilylation reaction is a Pt catalysed reaction, involving the addition of an Si-H bond across an unsaturated bond, with alkenes leading to alkyl and vinyl silanes. The reaction is important in the preparation of organosilicon compounds. Vinyl functional polymers and hydride functional polymers can undergo addition curing at low temperatures, with no by-products being formed. The hydrosilylation reaction is one of the most important methods for producing silicon-carbon bonds and cross linked silicon polymers. Mild conditions are used, with the Pt catalyst often a chloroplatinic acid in alcohol or Pt(0) complexes with phosphines[54] Hydrosilylation curing can be performed at relatively low temperatures, depending on the catalyst utilised. A typical system generally consists of a methylhydrosiloxane-dimethylsiloxane, and a Pt catalyst. Preparation is carried out in two parts, with one part containing 5-10 ppm Pt catalyst, and the other part containing the hydride functional siloxane. It is possible to modify the hardness of the resulting materials, by controlling the cross linking, and length of the polymer chains. Polymers with vinyl pendant on the chain can alter the hardness, rather than being on the chain end. For this study, it was desirable to develop a material, which could be processed in a minimum amount of steps, and at relatively low temperatures. The Pt catalyst usually controls the curing temperature, with Pt in vinyldisiloxanes making curing possible at room temperature. When deciding on the type of vinyl terminated polysiloxane for this work, it was important to consider also the optical properties and vinyl polymers with phenyl groups can alter the refractive index of the resulting cross linked material, along with the mechanical properties. The hydride functional siloxanes, such as methylhydrosiloxane-dimethylsiloxane copolymers have controlled reactivity and result in stronger polymers. The reaction with vinyl functional siloxanes was performed using a 1:1 stoichiometry and it was possible to employ phenyl substituted hydrosiloxanes, due to their greater solubility and optical properties, along with the phenyl substituted vinyl terminated polysiloxanes.

Taking into account the characteristics required for such an optical material, a polymeric system was developed using the Pt catalysed hydrosilylation reaction, between a vinyl terminated polydiphenyl dimethyl siloxane, cross linked with a hydride terminated methylhydroxy-phenylmethylsiloxane copolymer. The development and

characterisation of the material is described elsewhere [55,56,57], however the next sections will summarise the material in brief, focusing on further alterations to the final product and including optical characterisation; leading to the development of fully working optical waveguides on specially designed printed circuit boards (PCB) to form optical interconnects.
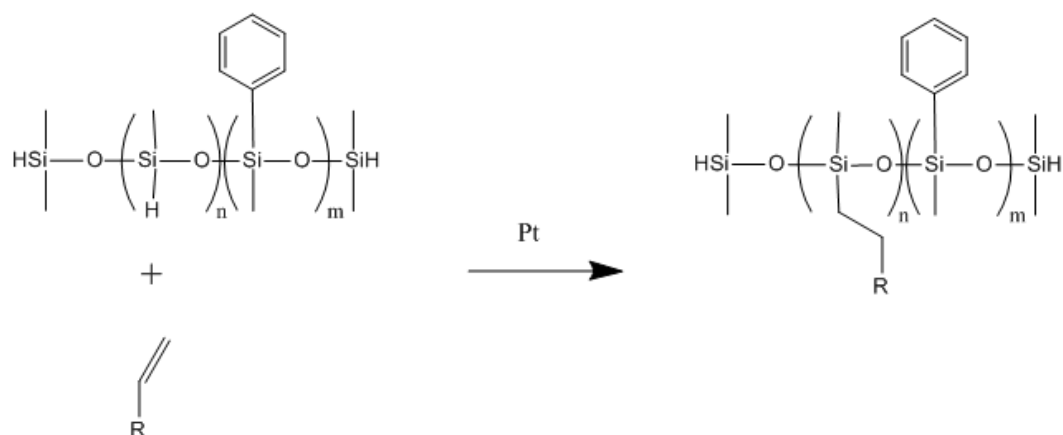

Figure 7: General mechanism of the platinum catalysed hydrosilylation reaction

4.2 Development of System A

A polysiloxane matrix material was previously designed for this project, consisting of a vinyl terminated diphenylsiloxane-dimethylsiloxane copolymer (PDV 1635) and hydride terminated methylhydrosiloxane-phenylmethylsiloxane copolymer (HPM 502). The materials including the Pt catalyst, platinum carbonyl cyclovinylmethyl siloxane complex were obtained from ABCR GmbH (Germany), and used without further treatment. The three methacrylate monomers used; phenyl methacrylate (PMA), benzyl methacrylate (BMA) and ethylene glycol dimethacrylate (EGDMA) were purchased from Sigma Aldrich. These monomers were chosen as they have relatively high refractive indices, can be dissolved adequately in the silicone resin and have a low enough volatility to enable the removal of the unpolymerised monomers after laser exposure by means of a thermal treatment using a vacuum process. Irgacure 379, purchased from Ciba, was used as photoinitiator. This photoinitiator is already known for its performance in TPA experiments [58,59] To form the cross linked material, HPM 502, PDV 1635 and either 8 or 10 wt.% in total of the methacrylate monomers in a ratio 1:1:1 (PMA:BMA:EGDMA) were gently mixed together, including 1.8 wt.% Irgacure 379, using the monomers to dissolve the photoinitiator. In a separate container PDV 1635 and 10 ppm Pt catalyst were mixed together, to avoid pre-curing during the first stage. The two mixtures were then added together and filtered using a 0.45 µm PTFE syringe filter. Following further mixing, the material was applied onto selected substrates, with layer thicknesses of between

300 and 500 µm. Each component and the cross linking mechanism via the hydrosilylation reaction are presented below. To cure the material, a thermal step of 80 °C for 25 minutes was performed, producing a partially cross linked and flexible thin polymeric film.
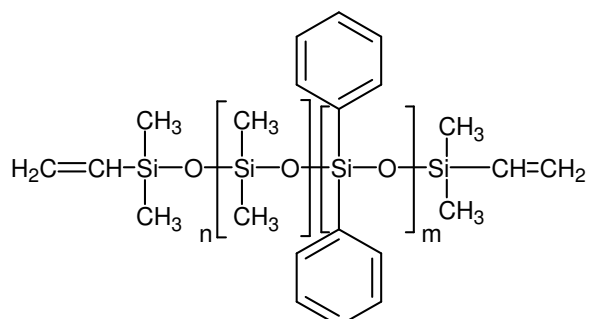

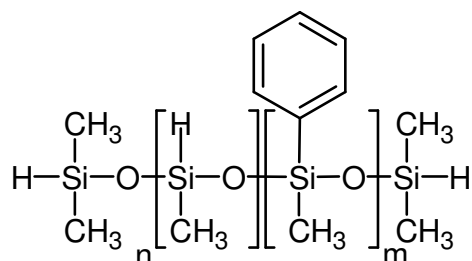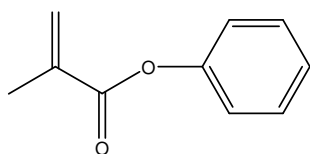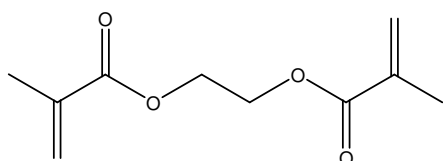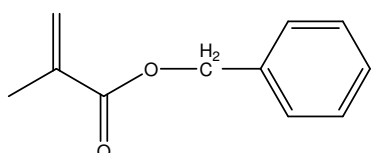**Figure 8: Vinyl terminated diphenylsiloxane dimethyl siloxane copolymer**

Figure 9: Methylhydrosiloxane – phenylmethylsiloxane copolymer, hydride terminated

Phenyl methycrylate (PMA)

Ethylene glycol dimethacrylate (EGDMA)

Benzyl methacryate (BMA)

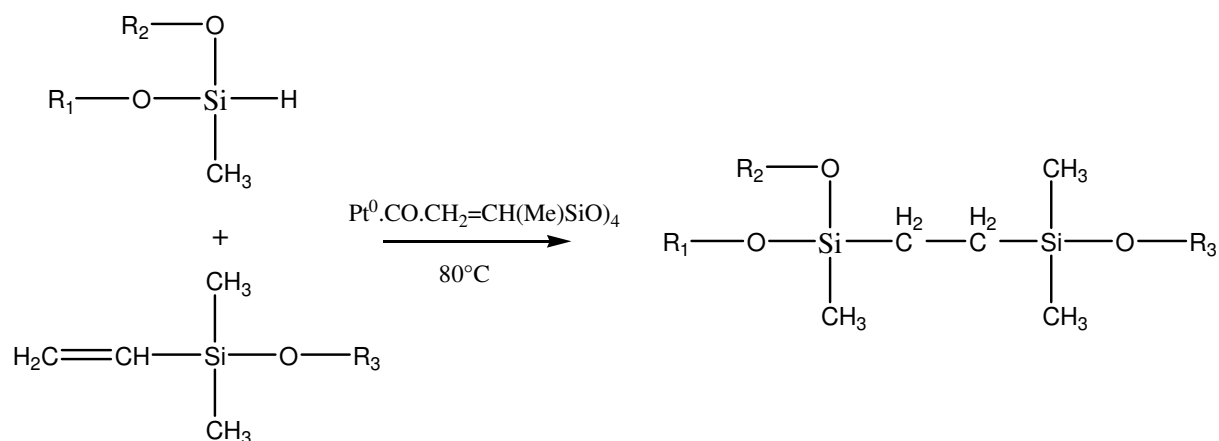**Figure 10: Chemical structure of methacrylate monomers**

Figure 11: Cross linking of the vinyl terminated and the hydride terminated copolymer via hydrosilylation

4.2.1   Characterisation of components in System A

The components used in the formation of the silicone matrix were characterised by FT-IR-spectroscopy. The materials used in the silicone matrix; PDV 1635, HPM 502 PMA, BMA and EGDMA were used to collect FT-IR data, with which the data could then be used to optimise the monomer concentration, determine the correct conditions with which to remove the monomers from the matrix and the correct concentration of photoinitiator required to achieve the optimum polymerisation of the methacrylate monomers. Each component was dissolved in CH_2Cl_2 and sandwiched between two CaF_2 slides. The characteristic peaks were noted along with any peaks which altered during the curing process and polymerisation of the acrylate monomers. FT-IR was then used to monitor the photo-induced polymerisation and determine the degree of conversion. The FT-IR spectrum of PDV 1635 is presented in Figure 12, which could then be used to monitor changes of the uncured and cured material, as well as determining whether peaks corresponding to the methacrylate monomers could be discerned in the spectra. Figure 13 displays the FT-IR spectrum of the second component. HPM 502. Each important band was identified and included in Table 1 and Table 2.

49

Figure 12: FT-IR spectrum of PDV 1635

Table 1: Wavenumbers of the characteristic vibrations in PDV 1635

Wavenumber / cm^{-1}	Responsible vibration
3072	C-H str, Si-Ph
1593	Si-Ph
1410	Si-CH=CH$_2$, CH$_2$ in plane
1124	Si-Ph
1087	Si-O stretch, Si-O-Si
1019	Si-O stretch (two bands of almost equal intensity) Si-O-Si Si-Ph
842	Si-CH$_3$ rocking –Si(CH$_3$)$_2$

Figure 13: FT-IR spectrum of HPM 502

Table 2: Wavenumbers of the characteristic vibrations in HPM 502

Wavenumber / cm^{-1}	Responsible vibration
3072	C-H str, Si-Ph
3052	Si-Ph
3005	Si-CH=CH$_2$, CH$_2$, in plane
2964	C-H str.
2161	Si-O stretch, Si-O-Si
1593	Si-O stretch (two bands of almost equal intensity) Si-O-Si Si-Ph
1429	Si-CH$_3$ rocking –Si(CH$_3$)$_2$
1261	Si-CH$_3$
1124	Si-Ph
1039	Si-O
906	Si-H

Figure 14, Figure 15 and Figure 16 display the FT-IR spectra taken of the three methacrylate monomers BMA, PMA and EGDMA. In order to determine the double bond conversion of the monomers separately, along with how well the monomers polymerised while present in the matrix material, the peaks corresponding to C=C stretching vibrations were identified, along with all characteristic peaks present in the monomers. It was possible to calculate the double bond conversion using reference peaks and monitoring the decrease in the C=C peaks after illumination of samples. The characteristic peaks present in the FT-IR spectra of the monomers are included in Table 3, Table 4 and Table 5.
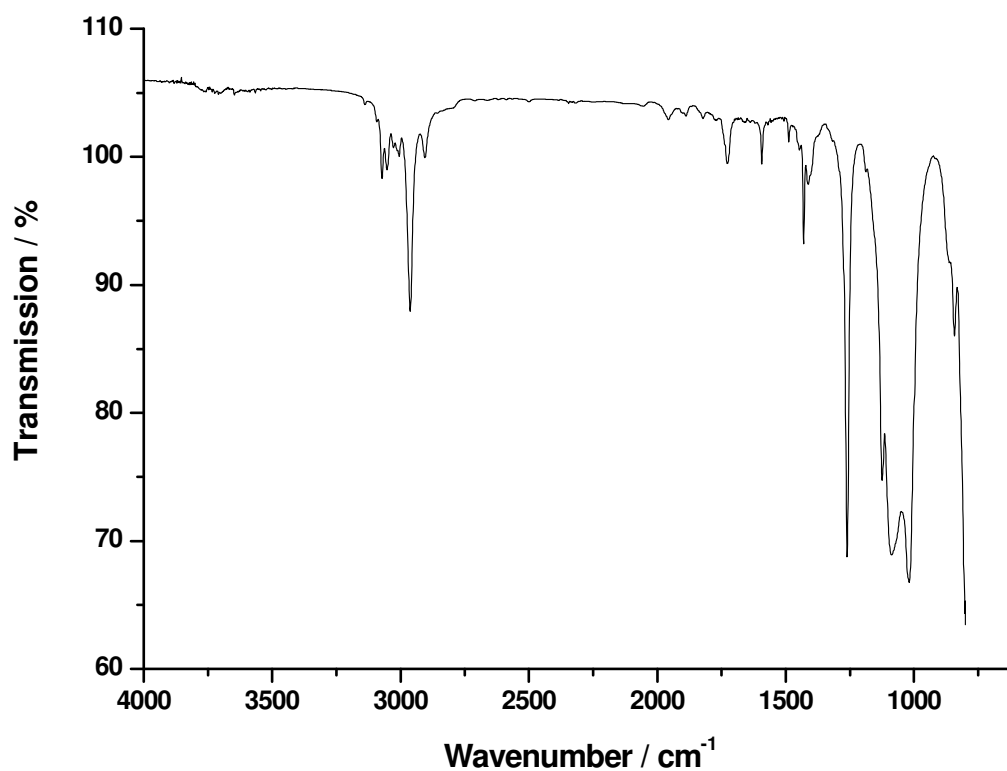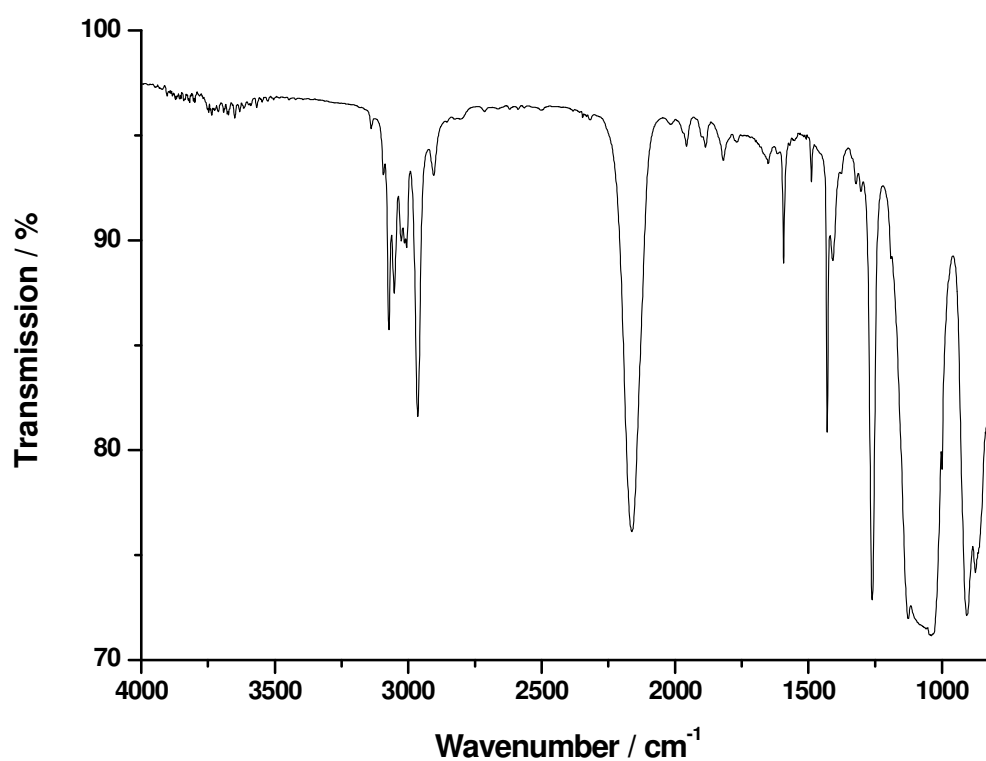

Figure 14: FT-IR spectrum of BMA

Table 3: Wavenumbers of the characteristic vibrations in BMA

Wavenumber cm^{-1}	Responsible vibration
3066	C-H stretching (aromatic)
3034	C-H stretching (aromatic)
2958	C-H stretching
1717	C=O stretching (ester)
1637	C=C stretching (methacrylate)
	C=C stretching (aromatic)
1498	C=C stretching (aromatic)
1454	C=C stretching (aromatic)
1403	=CH$_2$ def (methacrylate)
1321	=CH rocking (methacrylate)
1318	C-O-C stretching
1159	C-O-C stretching
970	Wagging =CH$_2$ (methacrylate)
814	Twisting =CH$_2$ (methacrylate)

Figure 15: FT-IR Spectrum of PMA

Table 4: Wavenumbers of the characteristic vibrations in PMA

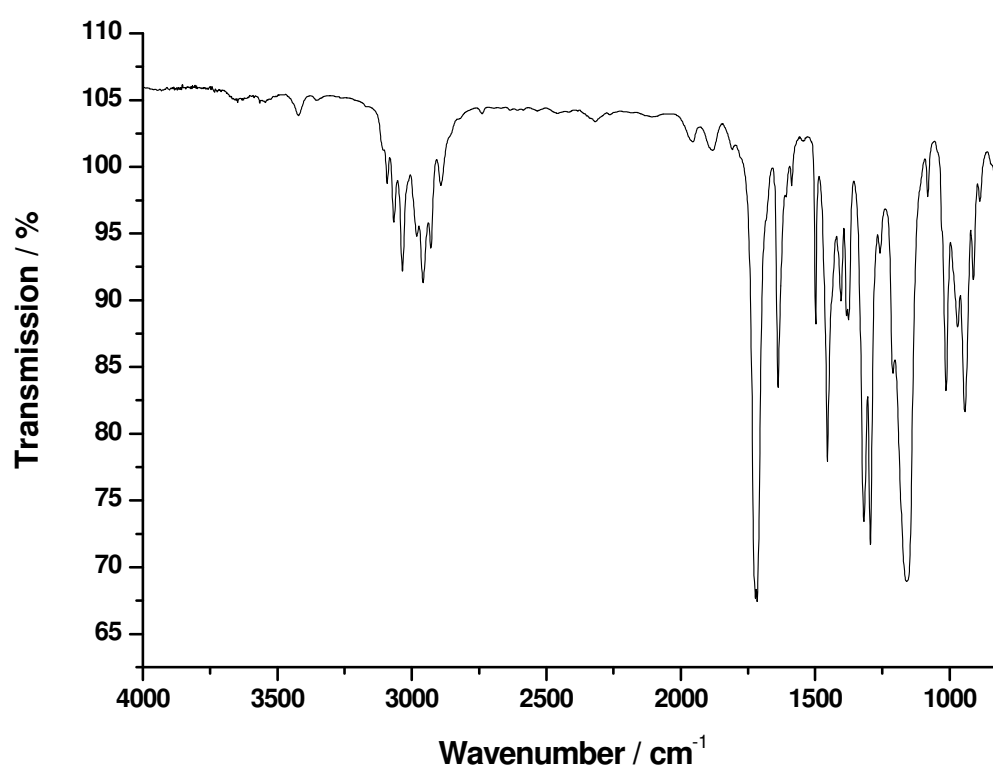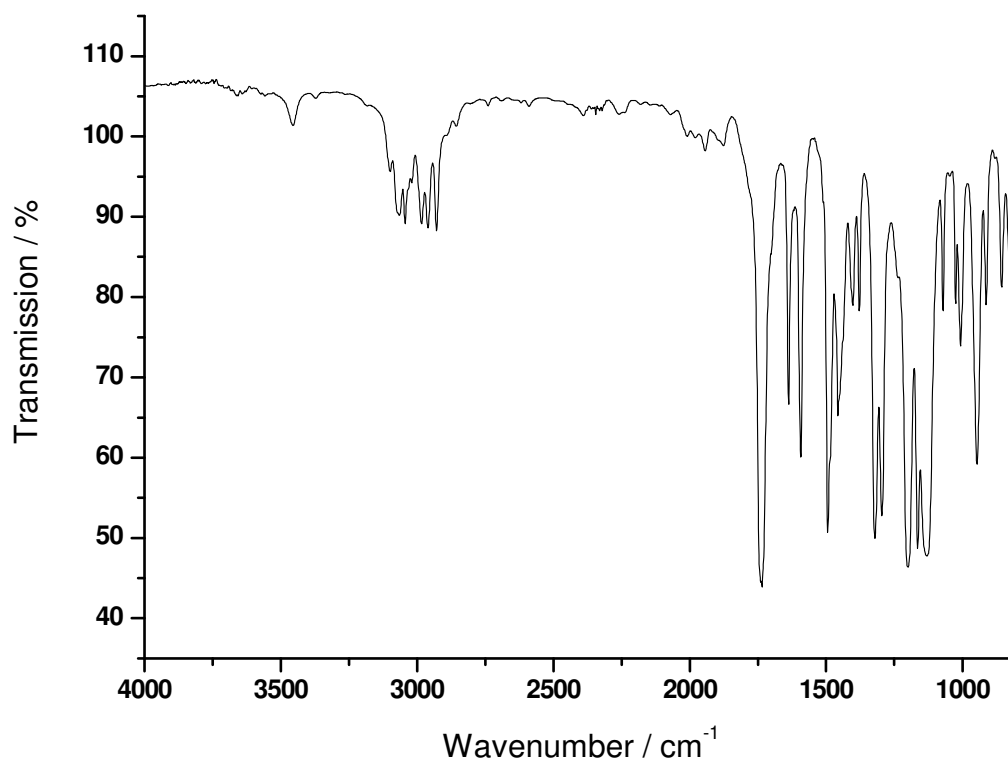| Wavenumber / cm^{-1}	Responsible vibration
3065	C-H stretching (aromatic)
3044	C-H stretching (aromatic)
2960	C-H stretching (CH_3)
2928	C-H stretching (CH_3)
1735	C=O stretching
1637	C=C stretching (methacrylate)
1592	C=C stretching
1402	=CH_2 def (methacrylate)
1310-1071	C-O-R (ester)
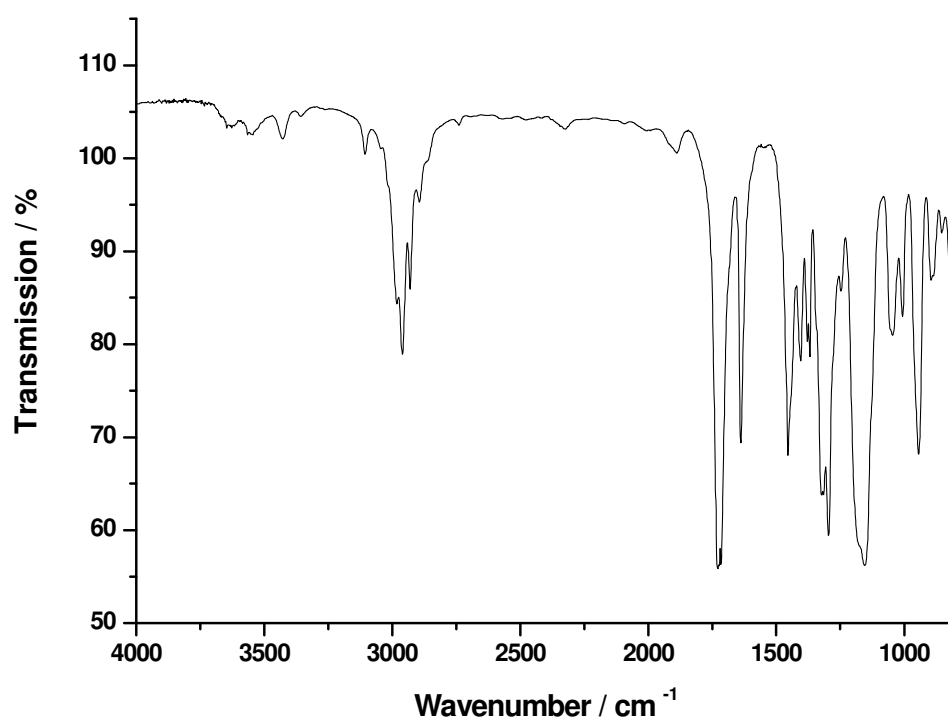
Figure 16: FT-IR Spectrum of EGDMA

Table 5: Wavenumbers of the characteristic vibrations in EGDMA

Wavenumber /cm^{-1}	Responsible Vibration
3544.81	C=O (overtone)
2930.21	C-H stretching (CH$_3$)
2960.59	C-H stretching (CH$_3$)
1728.04	C=O stretching
1638.70	C=O stretching
1154.81	C-O (ester)
1045.42	C-O (ester)

Following the characterisation of all components, samples were prepared containing the whole matrix (System A), in order to carry out investigations into the double bond conversion of the methacrylate monomers inside the matrix, and to monitor the stability of the monomers during the thermal curing step. Figure 17 and Table 6 include the FT-IR spectrum of System A, revealing the small but discernable peaks corresponding to the C=C bonds of the methacrylate monomers.

Figure 17: FT-IR spectrum of System A: - cross-linked and containing 10 wt-% monomers (1:1:1, BMA:PMA:EGDMA)

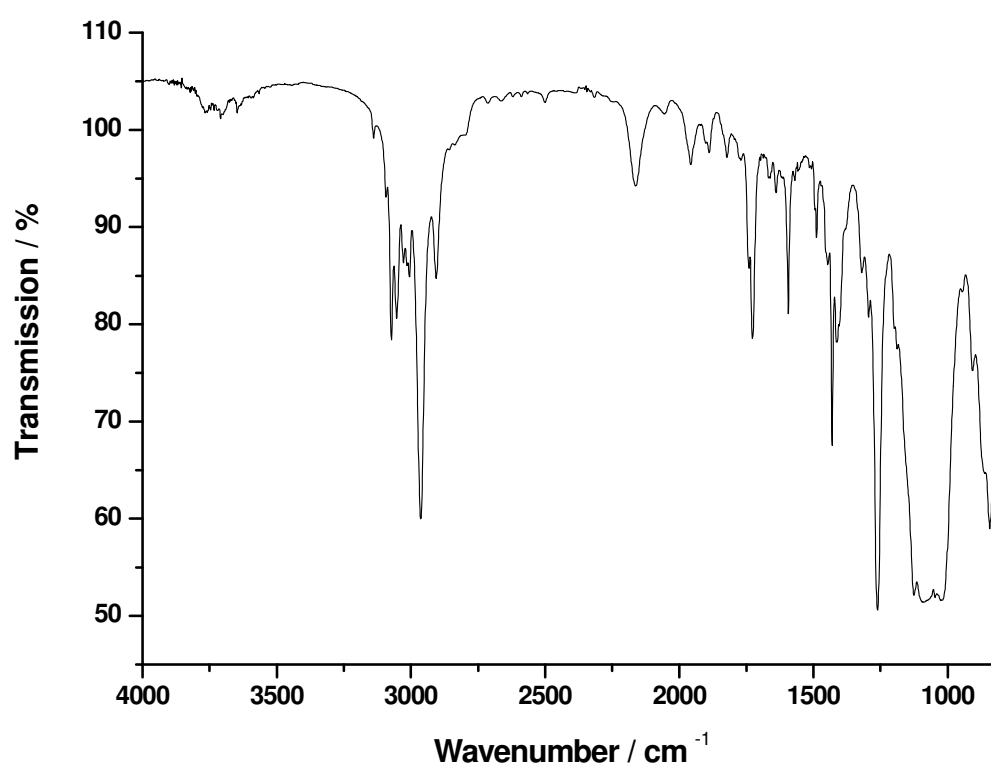**Table 6: Wavenumbers of the characteristic vibrations in the polysiloxane matrix containing 10 wt % methacrylate monomers**

Wavenumber / cm^{-1}	Responsible vibration
3072.38	C-H (aromatic)
3052.35	C=C-H stretching
2161.83	Si-H stretch
1429.63	C=C stretching (aromatic) (Si-Ph)
1261.22	Si-CH$_3$ stretching
1039.16	Si-O stretch (siloxane chain)

4.2.2 Choice of Photoinitiator

In this study, the photoinitiator Irgacure 379 was chosen to be used in the polysiloxane matrix, due to its already well known efficiency as a two-photon photoinitiator[60] and due to its solubility in the methacrylate monomers as well as the hydride and vinyl terminated polysiloxane. Irgacure 379 is a highly efficient one-photon photoinitiator, and is designed for uses in the photopolymerisation of unsaturated pre-polymers, and has a higher solubility compared to other photoinitiators, making it possible to incorporate into the polysiloxane resin, with only a slight yellowing being observed. 1:8 wt % of Irgacure 379 was added to the material, with any remaining undissolved photoinitiator removed during filtering. The structure of Irgacure 379, as well as α-cleavage of the molecule is presented in Figure 18.
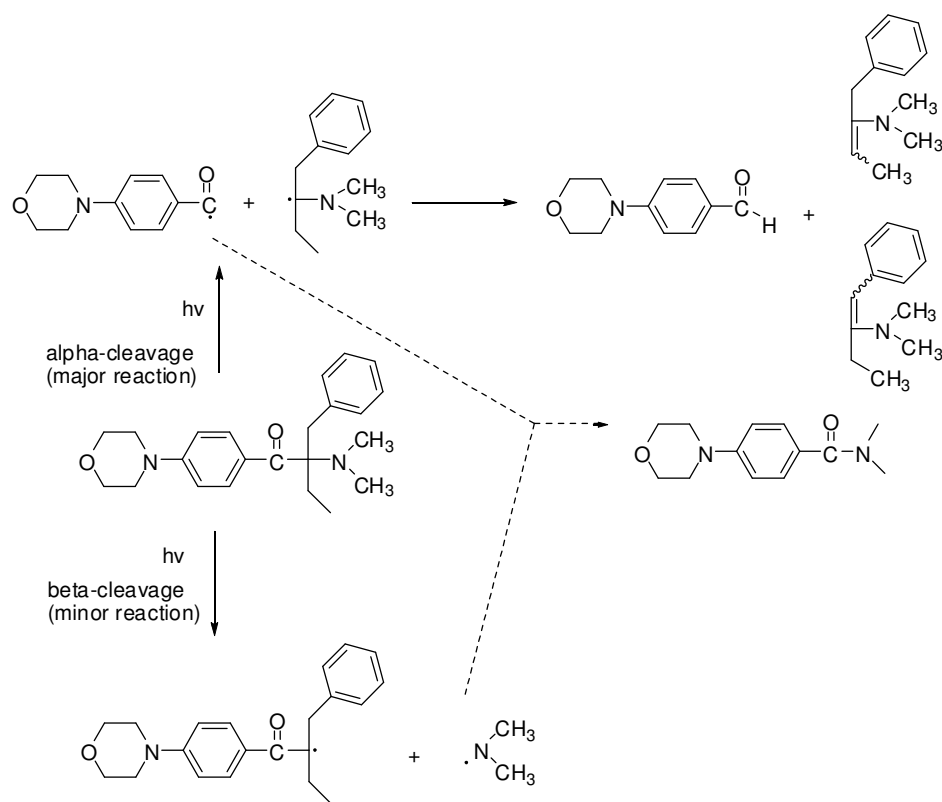
Figure 18: Photoinitiated Norrish Type 1 cleavage (α-cleavage) of the photoinitiator Irgacure 379[61]

4.2.3 Monitoring of the Photo-induced Photopolymerisation using Different Concentrations of Photoinitiator – FT-IR Spectroscopy

This study was carried out to determine the efficiency of the photoinitiator Irgacure 379. To determine the optimum concentration of photoinitiator to be used in the polysiloxane material, FT-IR was carried out on samples containing different concentrations of Irgacure 379. The standard silicone matrix was made up using 10 wt % methacrylate monomers, with a ratio1:1:1(BMA:PMA:EGDMA). The three silicone mixtures contained 0.5, 1 and 1.5 wt % photoinitiator. The samples were diluted in CH_2Cl_2 and drop cast onto CaF_2 plates. The silicone matrix was sandwiched between two plates to avoid oxygen getting to the material during the photopolymerisation. An initial FT-IR measurement was carried out on all the samples. Each sample was then irradiated using a spot cure lamp (Novacure) for five minutes. A second FT-IR measurement was then carried out on the samples and the spectra was evaluated to determine the difference in peak areas of the peak responsible for the C=C double bond. The percentage of conversion or polymerisation could then be determined from comparing the area with a reference peak. A reference peak at 1591 cm^{-1} was chosen, which corresponds to the Si-Ar stretching mode, and is unaffected by the polymerisation process, so no reduction of this peak is observed. The results including the FT-IR spectra are presented in Figure 19,Figure 20 and Table 7.

With increasing amount of photoinitiator; the percentage of conversion increases, with almost 100 % conversion with 1.5 wt %. Between 1.5 and 1.8 wt % Irgacure 379 is added to the formulation for TPA structuring, which was found to result in good waveguide structures, and no recrystallisation occurred. Results of structuring experiments using this matrix material and photoinitiator are included in section 7.

Table 7*: **Results of double bond conversion of methacrylate monomers using different concentrations of Irgacure 379**

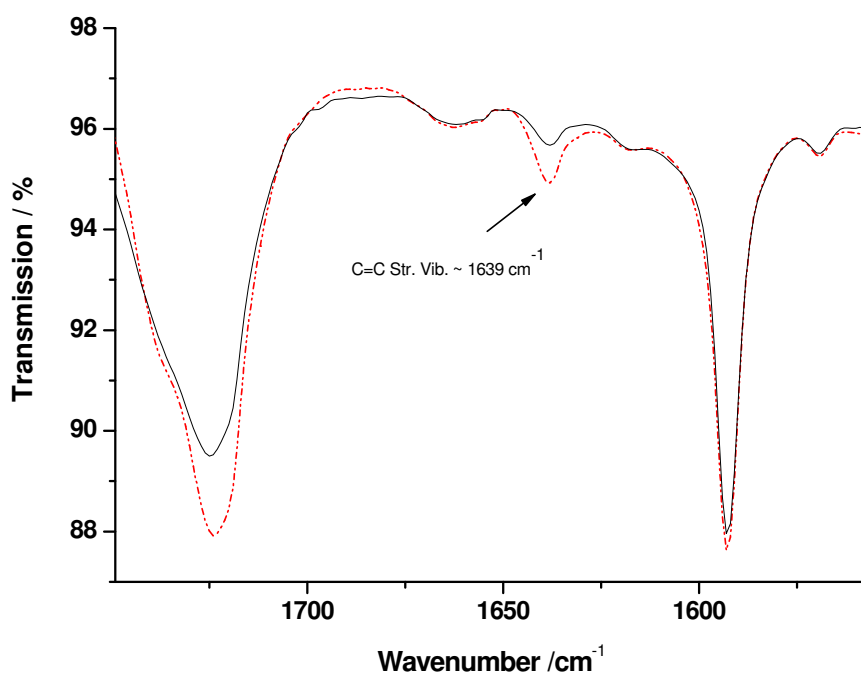| Wt. % Photoinitiator	Time of irradiation [s]	Conversion [%]
0.5	300	58
1.0	300	83
1.5	300	99

Figure 19*:* FT-IR spectra of polysiloxane matrix containing 0.5% photoinitiator-pre (dashed line) and post UV irradiation (solid line)
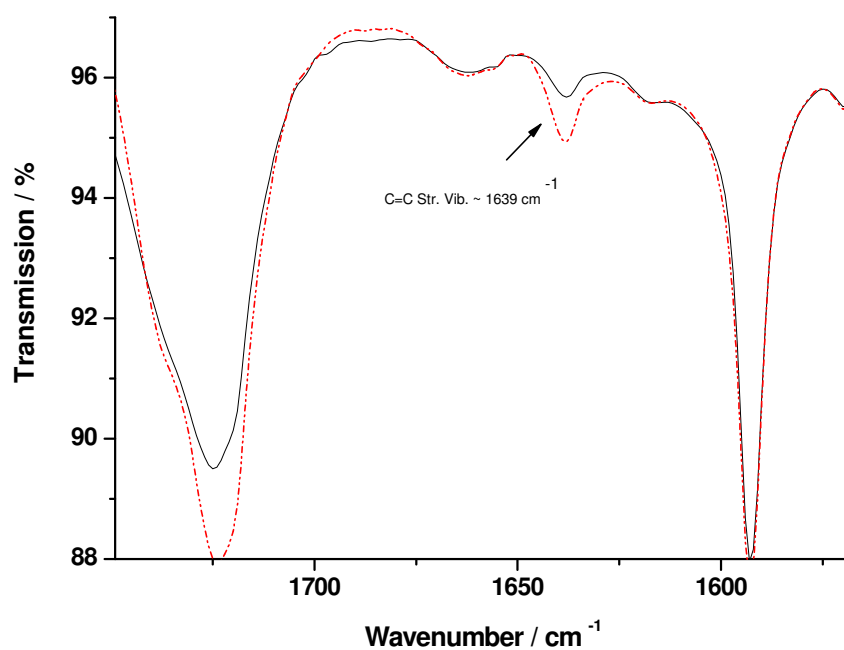

Figure 20: FT-IR spectra of polysiloxane matrix containing 1% photoinitiator-pre (dashed line) and post irradiation (solid line)
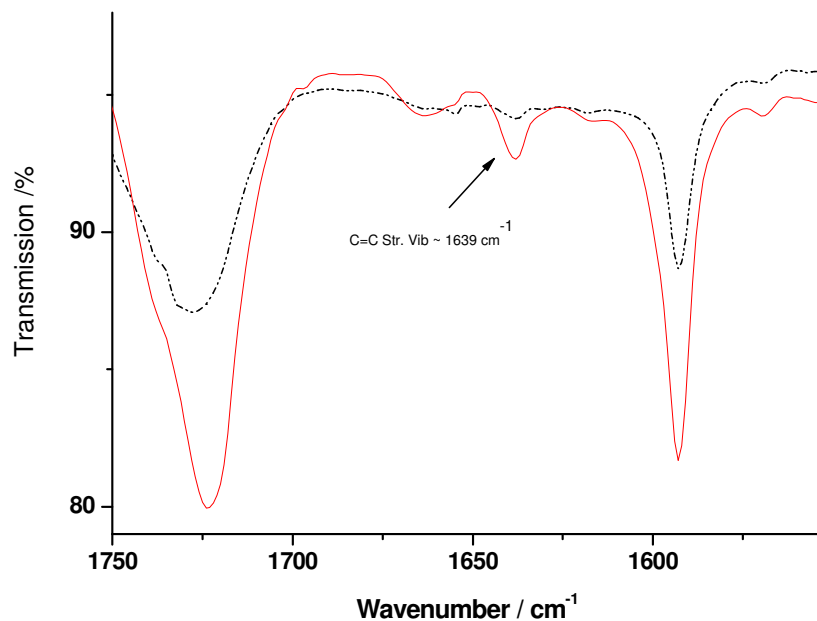
Figure 21: FT-IR spectra of polysiloxane matrix containing 1.5% photoinitiator pre (solid line) and post UV irradiation (dashed line)

4.2.4 FT-IR Measurements to Determine the Volatility of Monomers during Thermal Treatments

An important part of the optical matrix material is the selection and control of the methacrylate monomers, added to the material and which undergo photoinduced TPA polymerisation to form the waveguide core. The selection and concentration of methacrylate monomers used in this study have been previously investigated. However, it needed to be determined what concentration of monomer remained in the material during the thermal pre curing, as well as what concentration of monomers remaining following the post thermal treatment of 100 °C for 24 hours, 40 mbar. This step was performed on the material and all samples following the TPA fabrication, to essentially stabilise the matrix material and further increase the refractive index difference between the waveguide core and cladding material. FT-IR spectroscopy was utilised to calculate the concentration of methacrylate monomer removal during the thermal pre-treatment, as well then the thermal finishing treatment. The silicon matrix, including 0.5 wt % photoinitiator, and 10 wt % of the three monomers, PMA, BMA and EGDMA was prepared and initial measurements were conducted on CaF_2 plates with the depth of the layer on the plate measured at 300 μm. This was chosen as TPA material testing is carried out on film thicknesses in this region. Initial measurements were taken, and the slides were placed in the oven for 25 minutes at 80 °C. FT-IR spectra were then taken, and the samples were placed in the oven at 100 °C for 20 hours under vacuum. Using a reference peak, the peak areas were calculated to determine the decrease in

monomer content. The results are displayed in Table 8. To monitor the hydrosilylation reaction, the peak corresponding to the Si-H stretching was also examined, to monitor the cross linking occurring in the matrix material.

Table 8: Content of monomers removed from the polysiloxane material, following thermal pre and post treatments

Altered peaks following thermal pre-treatment (cm-1)	Reduction following thermal pre-treatment	Reduction following thermal post-treatment
1639 (C=C str.)	10	68
2159 Si-str.	50	75

During the thermal pre-treatment only around 10 % of the total monomers were removed, which suggests that a high enough concentration remained in the matrix for the two-photon photopolymerisation of the optical waveguides. The hydrosilylation reaction could also be determined using FT-IR, due to the decrease of the peak arising at 2159 cm^{-1}, corresponding to the Si-H bond. Using a suitable reference, a 50 % decrease in the peak was observed following the pre thermal step, and a 75 % decrease occurred during the post thermal treatment.

4.2.5 High performance liquid chromatography (HPLC) – Determination of the Amount of Photoinitiator Remaining Following Thermal Treatments

The photoinitiator Irgacure 379 when present in the matrix material, can lead to clusters or so called "out blooming". This effect is shown in Figure 22. Upon exposure to UV light longer than one week, the small clusters became visible, and inevitably lead to instabilities in the material as well as affecting the functioning of the waveguides. To confirm the clusters were formed from the photo induced reaction of Irgacure 379, FT-IR microscopy was performed. Examples of the spectra are shown in Figure 23. A comparison was made with spectra collected from the surrounding cladding material, and an obvious peak arising at 1700 cm^{-1} is observed in the spectra corresponding to the clusters. This peak is due to a photo-cleavage of Irgacure 379 following illumination. A sample of Irgacure 379 was examined by FT-IR, pre and post UV illumination, with a peak arising at ~ 1700 cm^{-1} in the illuminated sample. Following a longer period of illumination, the peak increased in size, confirming the presence of the peak corresponding to the photo-cleavage product of the photoinitiator. The photocleavage products of irgacure 379 is shown in Figure 18. The peak in the illuminated sample of Irgacure 379 is believed to arise from the α-cleavage of the α-aminoalkylphenone,

with the peak arising from the aryl aldehyde, a product originating from the photoreaction of the photoinitiator. Due to this phenomenon, an attempt at removing the remaining photoinitiator and to avoid the formation of clusters was carried out. HPLC coupled with MS was performed on extracted samples of the matrix material containing Irgacure 379, to determine which temperatures and conditions were needed to remove any remaining photoinitiator post TPA structuring. A description of the procedure is included in section 10.1. The results, presented in Table 9, suggest that the thermal treatments usually carried out on the polysiloxane matrix material did not remove the photoinitiator; however, a much higher thermal step removes over 95 %. This was also shown by samples which were thermally treated at over 170 °C for over 18 hours, forming no visible clusters following prolonged exposure to sunlight.
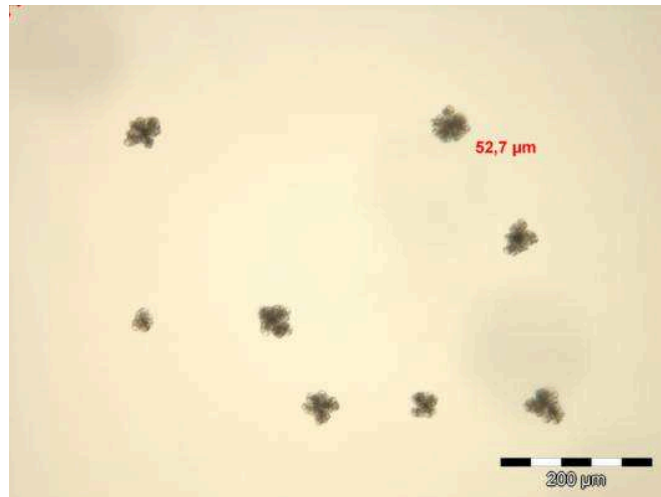
Figure 22: Microscope image of clusters or "out blooming" occurring in the polysiloxane matrix material following exposure to light
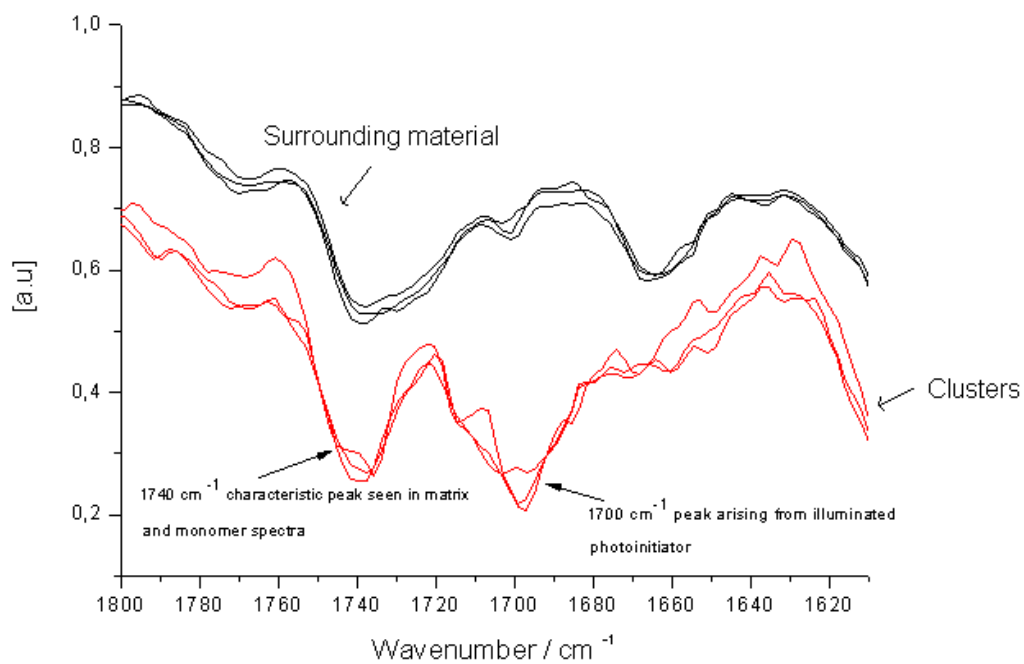
Figure 23: FT-IR microscopy spectra of polysiloxane material (System A) – a comparison of clusters formed following exposure to light and surrounding cladding material

C=O str. vib arising
from illuminated PI
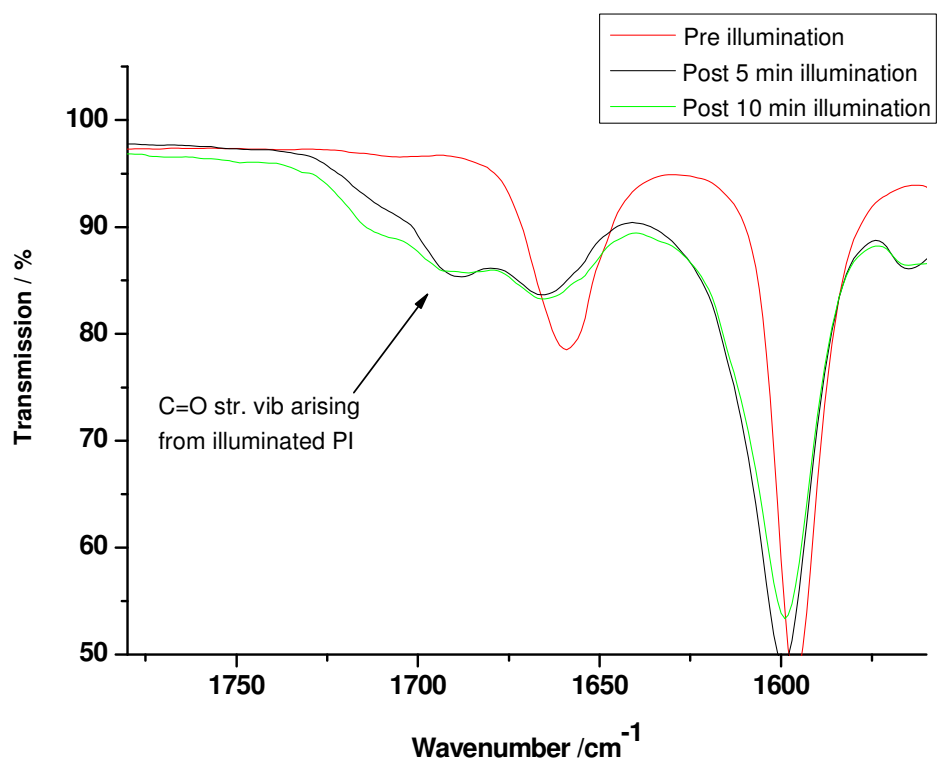
Figure 24: FT-IR spectra of Irgacure 379 before and after UV illumination

Table 9: Results of HPLC analysis of extracted samples of the polysiloxane matrix, containing Irgacure 379, following thermal treatments

Treatment of sample	Irgacure extracted [mg]	% Irgacure detected in extract
80 °C, 25 minutes	2.3	86.8
100 °C, 20 hours	2.2	74
170 °C 18 hours	0.13	5

4.3   Characterisation of Material Properties

4.3.1   Thermal Stability of System A – STA

A requirement of the optical matrix material is high thermal stability, due to the processing steps performed on PBCs. The material needs to be stable at temperatures of over 220 °C, with no decomposition or discolouration occurring. The matrix material must also be stable, and remaining methacrylate monomers in the material need to be removed. The removal of the monomers also leads to an increase in the difference in refractive index between the waveguide core and cladding. Samples analysed included the silicone matrix containing 10 wt. % of the acrylate monomers with a weight 1:1:1 ratio BMA:PMA:EGDMA. Samples were prepared in the same way as described in section 4.2 and were measured from 20-300 °C and heated at 10 K per minute. The results of the analyses can be seen in Figure 25, Figure 26 and Figure 27. The first image displays the results of the analysis carried out on a sample of the three methacrylate monomers, in a ratio 1:1:1. The results show that by 150 °C nearly all monomers are removed, however a thermal step of 100 °C may not remove all remaining monomers from the matrix material. The evaporation of the monomers is a two step process, with the evaporation of the more volatile monomer PMA first. Figure 26 displays the analysis of the silicon matrix only. System A remains stable to 200 °C, with only around 8 % weight loss at 270 °C, suggesting the material will not undergo decomposition during PCB processing. Figure 27 displays the results for System A, including 10 wt. % monomers included in the matrix material. At around 60 °C the weight loss began, due to the removal of the monomers. The largest fraction of the weight loss arose from the evaporation of the monomers. At 100 °C there was a 2 % weight loss, suggesting approximately one third of the monomers were removed at this stage. At around 200 °C approximately a 10 % weight loss was recorded. At 270 °C only a weight loss of 13 % was observed from the whole polysiloxane matrix. We assume 10 % of this arose from the monomers, giving a 3 % weight loss from the material. These results show the matrix system is stable up to the required temperatures. Observing the DSC signal, the exothermic peak seen in Figure 26 corresponds to the cross linking hydrosilylation process, beginning at around 20 °C. In Figure 25 the DSC signal peaks are observed as the monomers began to evaporate. In Figure 27 the DSC signal observed showed a peak at 88 °C, corresponding to the hydrosilylation reaction. This is known to be the initiating temperature of the cross linking reaction. As can be observed in Figure 26, the cross linking hydrosilylation reaction is a two step process, and two endothermic peaks were observed. No exothermic peaks were observed in the analysis of the polysiloxane matrix; giving a good indication the material is stable.
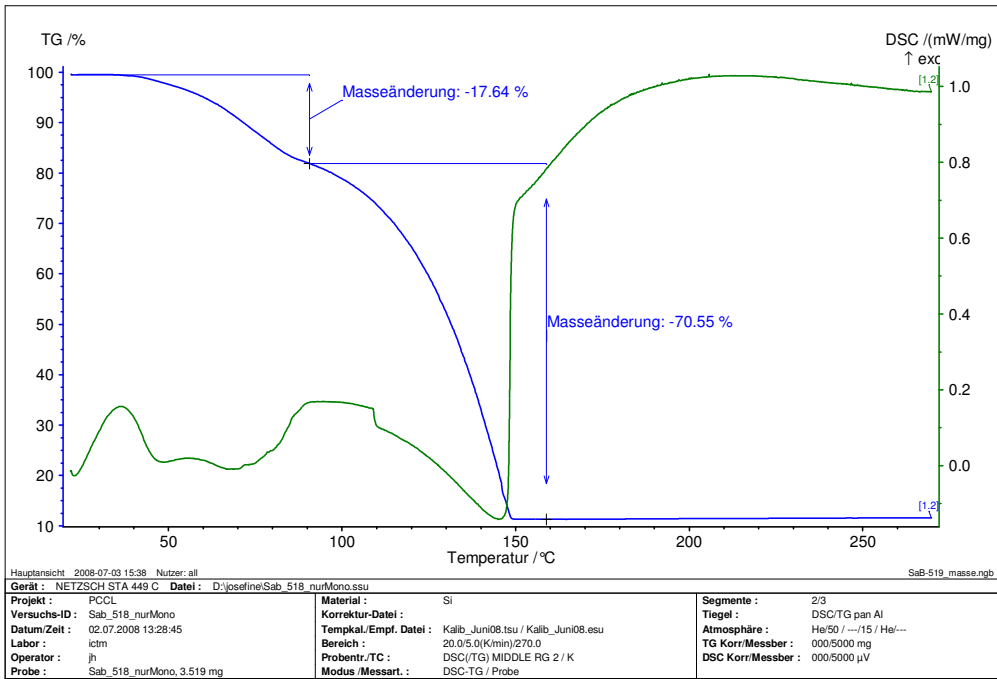
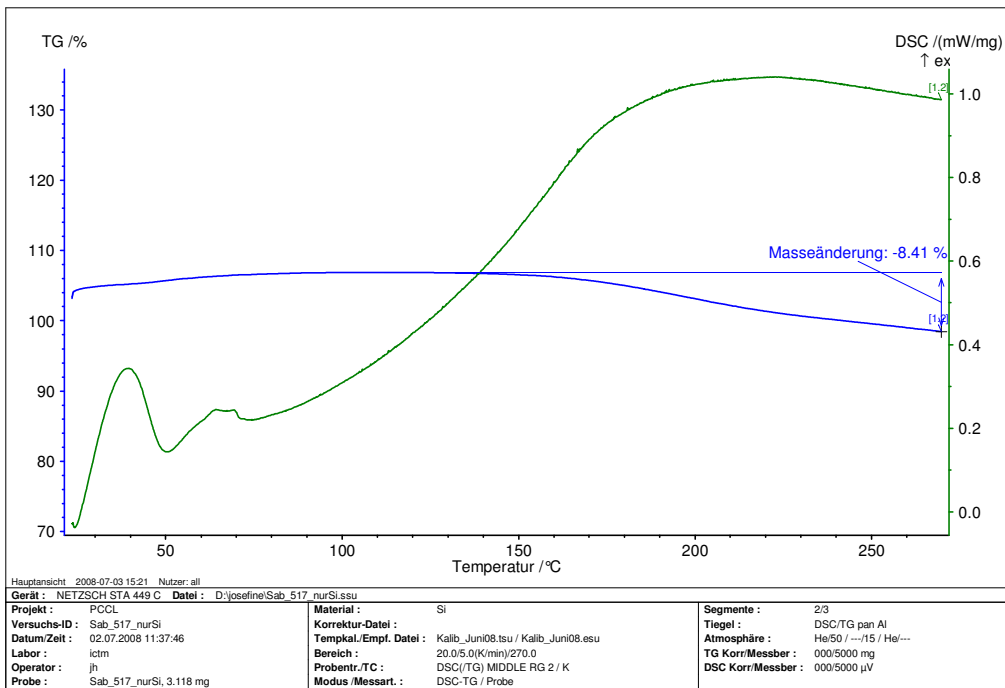**Figure 25: STA analysis of monomers only – BMA:PMA:EGDMA = 1:1:1 (by weight)**

Figure 26: STA analysis of hydride / vinyl terminated polysiloxane matrix only
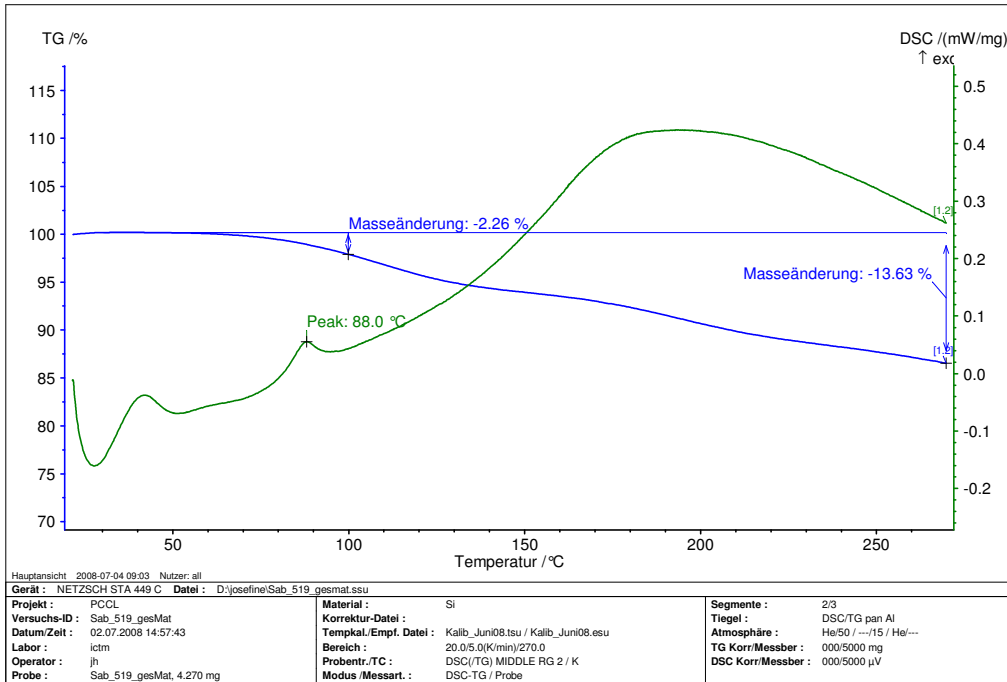
Figure 27: STA analysis of polysiloxane matrix containing 10 wt % monomers (1:1:1)

4.4 Removal of Monomers from System A – Gas Chromatography

To improve the stability of the polysiloxane matrix material, the remaining methacrylate monomers need to be removed following TPA structuring of the waveguides. To determine the weight percent of monomers remaining after the thermal treatments performed, gas chromatography was carried out. A detailed description of experimental details is presented in section 10.

The retention times of the three monomers using the run time of 20 minutes were found to be 9.4 for PMA, 11.7 for EGDMA and 12.2 for BMA. The results can be found in table 10. PMA, with the highest volatility, was most easily removed during the thermal pre treatment, followed by EGDMA and BMA. This result was also comparative to the boiling points of the monomers, with BMA having the highest boiling point of 98 °C. Approximately 33 % of the monomers remained in System A following the pre thermal treatment. The external calibration was carried out by using the peak areas against the concentration, and the internal method was determined by using the peak height ratio against the internal standard heptane, (normalised peak area = S/IS)

67

Table 10: Weight percentage of each monomer remaining in matrix following pre thermal treatment of 80 ℃ for 25 minutes

| Method	%PMA* remaining	% EGDMA* remaining	%BMA* remaining
External Calibration	21	34.8	40.8
Internal Calibration	23.7	37.8	47.1

* With respect to the initial weight concentration in the silicone matrix (%BMA, %EGDMA, %PMA = 100%)

After two injections of the post thermal treatment sample, no monomers were detected, showing that the fraction of monomers remaining was less than the detection limit of the gas chromatograph, and also suggesting that the thermal finishing treatment is an efficient way to remove all the monomers, and improve the stability of System A. Around 33 % of the monomers remained following the thermal pre-treatment, a sufficient amount for the two-photon induced polymerisation to be carried out.

4.5 Improvement of Monomer Performance - Incorporation of Naphthyl Methacrylate Derivatives

In order to investigate the use of different monomers in the polysiloxane matrix material, two new monomers, 2-naphthyl methacrylate, and 2 methyl -1 naphthyl methacrylate were investigated. Naphthyl methacrylate derivatives are commercially available and can be synthesised in a simple process displayed in scheme 1. Derivatives can be synthesised in the same way by using derivatives of naphthol and the acid chlorides. Naphthyl monomers have higher refractive indices than the phenyl and benzyl methacrylates, and so using them in combination with such monomers it was hoped the refractive index difference between the cladding and waveguide core could be increased, thus improving the light guiding. The monomer 2-naphthyl methacrylate was purchased from Sigma Aldrich, and was used to test the suitability of such monomers in the siloxane material. The monomer dissolved in the polysiloxane matrix material when a higher percentage of the cross linker EGDMA was used, as well as BMA and PMA. The material was homogenous and the naphthyl monomer did not affect the colour or the curing of the polysiloxane material. The second naphthyl derivative, 2

methyl -1 naphthyl methacrylate was synthesised and also investigated for its suitability in this matrix material. Details of the synthesis can be found in section 10.

ß - naphthol   methacryloyl chloride   ß-naphthyl - methacrylate
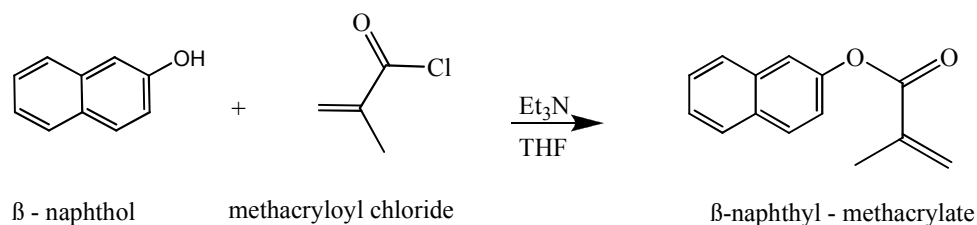
Scheme 1: Synthesis of 2 – naphthyl methacrylate

4.5.1   Reactivity of 2 – Naphthyl Methacrylate

To establish the reactivity of 2- naphthyl methacrylate, a sample of the monomer was diluted in CH_2Cl_2 and FT-IR spectroscopy was carried out to determine the percentage of conversion by evaluating the peak in the spectrum at 1639 cm^{-1}, corresponding to the C=C stretching vibration of the methacrylate, before and after illumination for 5 minutes. The conversion was found to be ~ 39 %. This was then compared to PMA, which was treated in the same way, as this monomer was found to be the most reactive of the methacrylates used. The conversion of the C=C double bond was found to be ~ 89 % with this monomer, so the reactivity of the naphthyl derivative was rather lower in comparison. Figure 28 and Figure 29 display the FT-IR spectra of naphthyl methacrylate and PMA before and after UV illumination.
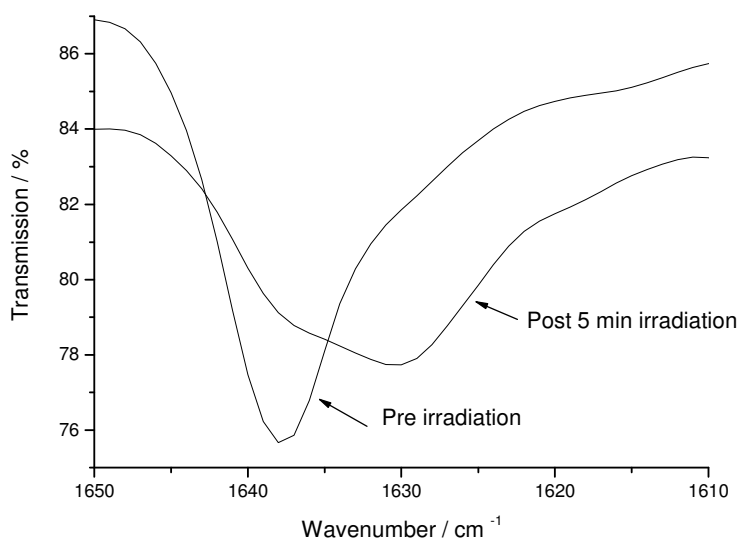
Figure 28: FT-IR Spectra of NMA pre and post irradiation
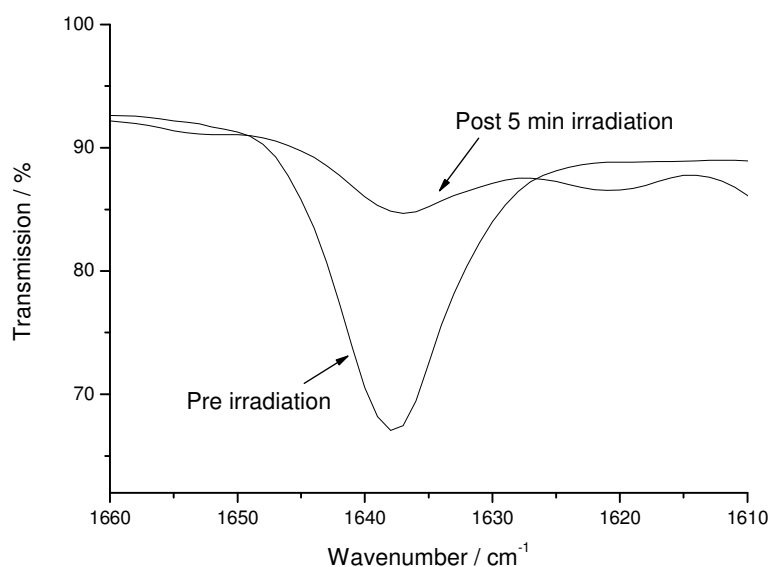
Figure 29: FT-IR spectra of PMA pre and post UV irradiation

4.5.2   Thermal Stability of 2- Naphthyl Methacrylate

The monomers in the ratio 40 mg BMA, 100 mg PMA, 60 mg EGDMA and 40 mg NMA were diluted in 2 g CH_2Cl_2 and drop cast onto a CaF_2 plate. A second plate was placed over the sample to avoid evaporation of the monomers. An initial FT-IR spectrum was recorded The sample was then placed in the oven at a temperature of 80 °C for 3 minutes, (as a comparison to the thermal pre-treatment of baking the samples at 80 °C for 20 minutes to cure the matrix system). A shorted time was chosen due to the thin layer thickness of the monomer sample. A second FT-IR spectrum was then recorded, following the thermal

70

treatment. The results can be seen in Figure 30. It can be seen that there was no change to the peak corresponding to the C=C stretching vibration at 1639 cm^{-1}, suggesting that the new monomer was stable and no polymerisation occurred during the thermal pre treatment.
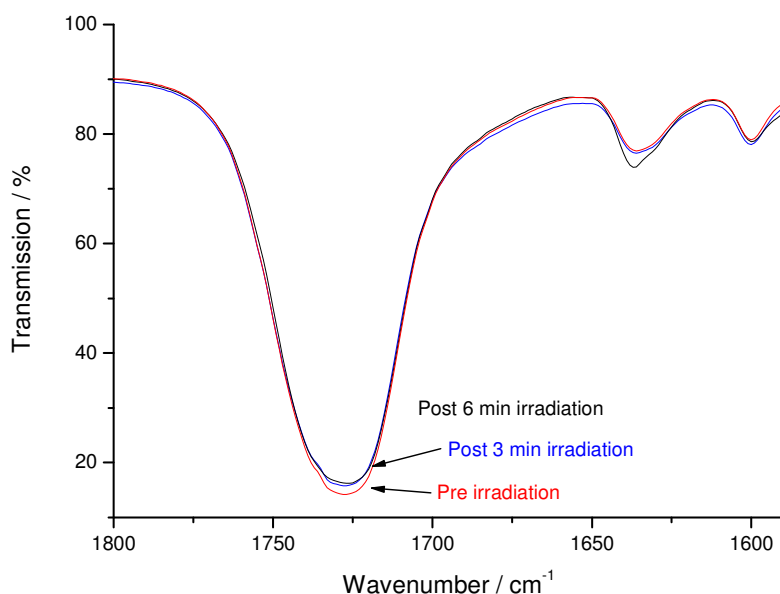
Figure 30: FT-IR spectra of all monomers in System A following 3 and 6 minutes baking (80°C)

The new monomer was incorporated into System A, along with the ethylene glycol dimethacrylate cross linker monomer (EGDMA), to establish primarily, the suitability of the compound. The light pink solid compound did not dissolve well in System A without a larger amount of cross linker. At a ratio of 3:1 with the cross linker, a homogenous mixture was achieved. Three mixtures were prepared, which consisted of 1:1, 2:1 and 3:1 ratio of the cross linker with the new naphthyl derivative. The samples were then diluted in CH_2Cl_2 and drop cast onto CaF_2 plates. An initial FT-IR spectrum was recorded of each slide. The samples were then illuminated using a Novocure spot lamp for 5 minutes, at 1 minute at a time. Between each irradiation an FT-IR spectrum was recorded. The polymerisation of the monomers could then be determined by interpreting the peak responsible for the C=C vibration at 1639 cm^{-1}. Figure 31 below shows an example of the spectra obtained for the monomer ratio 1:2 NMA:EGDMA.

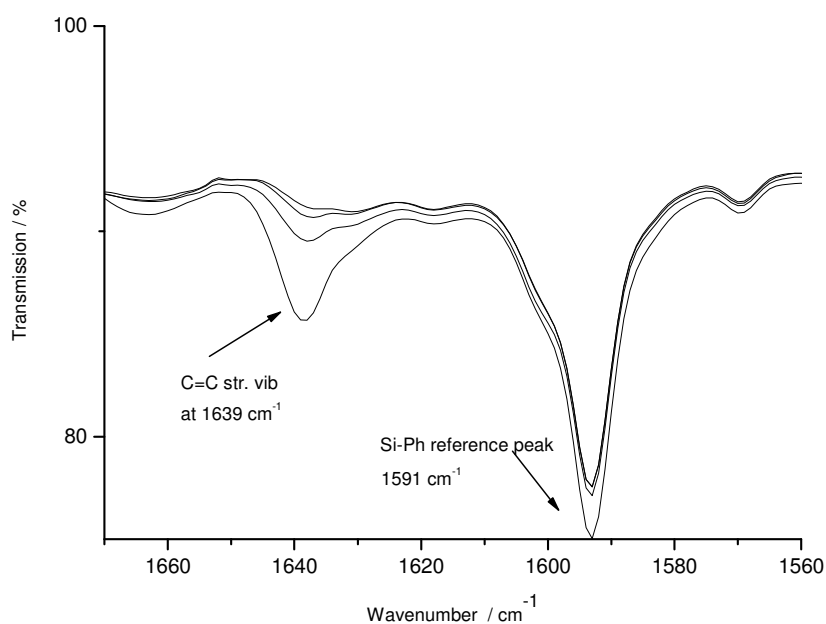**Figure 31: FT-IR spectra of illuminated matrix sample with NMA and EGDMA only (irradiated at 1 minute intervals)**

The monomer 2-naphthyl methacrylate required a higher amount of the cross-linker molecule EGDMA to effectively dissolve in the silicon matrix system, however a ratio of 2:1 EGDMA:NMA showed the highest rate of polymerisation, when monitored by FT-IR spectroscopy.

A second set of experiments were carried out, in which only the monomers were investigated, in differing ratios. To establish whether the new naphthyl monomer was compatible with the existing phenyl monomers, ratios of 1:2:2 = NMA:BMA:EGDMA, 1:2:2 = NMA:PMA:EGDMA and 1:2:2:2 NMA:BMA:PMA:EGDMA were prepared and dissolved in CH_2Cl_2. FT-IR spectroscopy was then carried out on each of the samples before and after irradiation using a spot cure lamp. The conversion of polymerisation was then determined using the peak observed at 1639 cm^{-1} corresponding to the C=C stretching vibration arising from the methacrylates.

4.5.3   Determination of Optimum Monomer Ratio

To determine the ratio of monomers most suited to incorporate into the existing matrix system and the phenyl substituted methacrylates, the monomers only were dissolved in Ch_2Cl_2 in the amounts 40 mg BMA, 100 mg PMA, 60 mg EGDMA and 40 mg NMA. The amount of the phenyl substituted monomers and the cross linker has to be enough to dissolve the naphthyl methacrylate sufficiently, whilst the amount of PMA and NMA have to

be high enough to increase the refractive index change between the core and cladding material. The monomers were then drop cast and sandwiched between CaF_2 slides and initial FT-IR spectrum was taken. The samples were then irradiated for 5 minutes using a spot cure lamp, and a second FT-IR spectrum was recorded. The results are shown in Figure 32. Using the peak in the spectrum at 1591 cm^{-1}, there was found to be ~ 75 % conversion when using the decrease in the C=C stretching vibration peak at 1639 cm^{-1}.
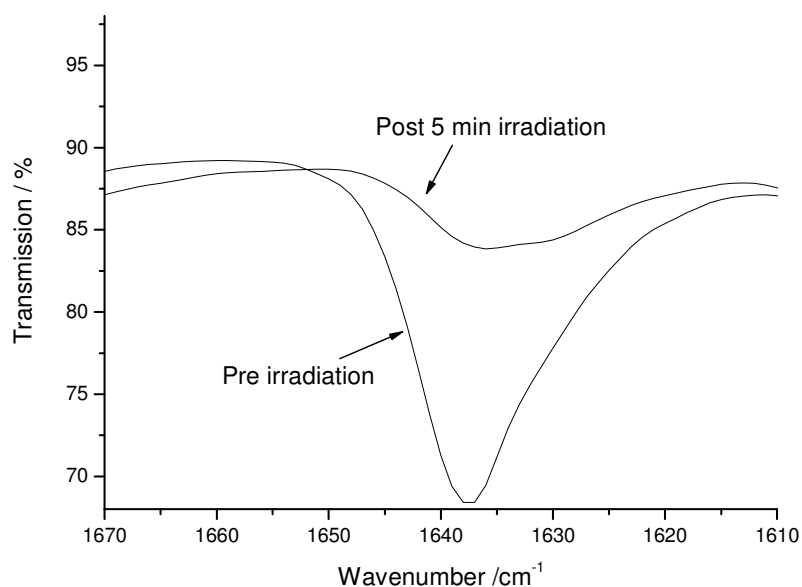
Figure 32: FT-IR Spectra of monomers only pre and post irradiation

A second set of experiments, the same as the last set using only the monomers was carried out with a higher ratio of NMA to determine whether the rate of polymerisation was affected. A higher ratio of NMA was used with a slightly lower ratio of EGDMA being used as this monomer has the lowest refractive index. The amounts used were 40 mg BMA, 100 mg PMA, 50 mg EGDMA and 50 mg NMA. The sample was treated in the same way as previously stated and the results can be seen in Figure 33. Using the same standard peak method as before, a 53 % conversion of the C=C double bond was observed, a slightly lower amount than with the previous ratio of monomers used. The next set of experiments were carried out with a higher ratio of NMA again, to establish if a higher amount of NMA would hinder the polymerisation.

Figure 33: FT-IR Spectra of monomers only pre and post irradiation, displaying peak corresponding to C=C stretching vibration

A sample was made up containing 30 mg BMA, 100 mg PMA, 40 mg EGDMA, and 70 mg NMA. The sample was treated in the same way, and the spectra are displayed below pre and post irradiation. The conversion was found to be ~ 55 % suggesting there was no hindrance of the polymerisation due to a higher amount of NMA present.

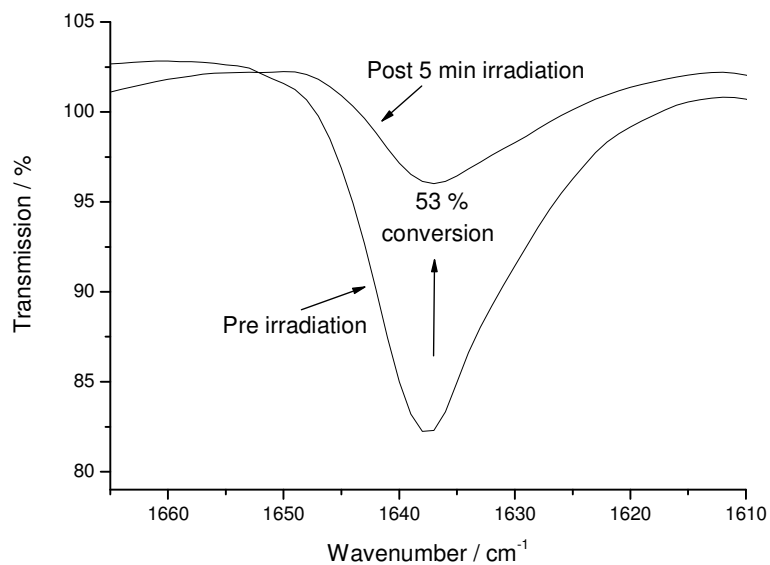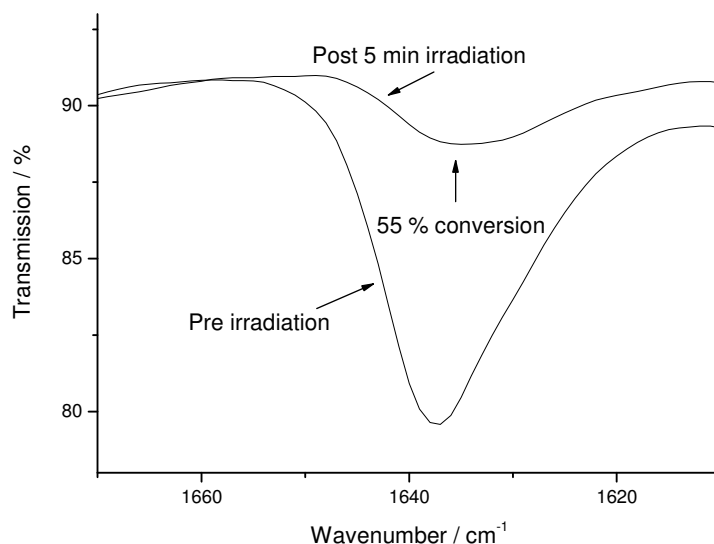**Figure 34: FT-IR Spectra of monomers only pre and post irradiation, displaying peak corresponding to C=C stretching vibration**

4.5.4 Incorporation of 2-Naphthyl Methacrylate into System A

It is predicted that when the monomers are incorporated into the polysiloxane matrix system, an inhibiting effect of the polymerisation of the monomers can occur, so it needed to be established whether sufficient polymerisation occurs when the monomers are added to the matrix. Two experiments were carried out to determine the polymerisation of the monomers, by using either 8 or 10 wt. % of the monomers in different ratios. For the first study, 10 wt. % monomers were used in the amounts 40 mg BMA, 100 mg PMA, 60 mg EGDMA and 40 mg NMA. The matrix system was made containing 1.8 wt % of the photoinitiator Irgacure 379. The sample was then diluted in CH_2Cl_2 and sandwiched between two CaF_2 plates. An FT-IR spectrum was taken before and after 5 minutes irradiation with a Novacure spot cure lamp. The results showed that after 5 minutes irradiation, no visible peak was observed at 1639 cm^{-1}, showing that a high double bond conversion had taken place. Due to these findings a second sample was made containing 8 wt. % monomers in the same ratio as before but using only 1 wt. % of the photoinitiator. These experiments also showed a high level of conversion, with no visible peak observed at 1639 cm$^{-1.}$

Further investigations were then carried out with a higher amount of the naphthyl monomer already investigated using the monomers only. 10 wt. % monomers in the amounts 40 mg BMA, 100 mg PMA, 60 mg EGDMA and 70 mg NMA were included in the polysiloxane matrix system, with 1.8 wt. % photoinitiator Irgacure 379. The material was dissolved in CH_2Cl_2 and FT-IR was carried out before and after 5 minute irradiation. The double bond conversion was found to be ~ 83 %. The results can be seen in Figure 35.
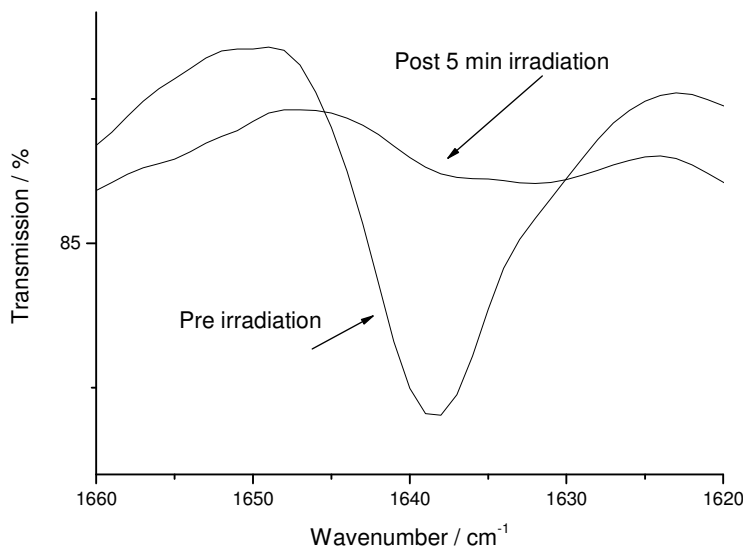
Figure 35: FT-IR spectra of System A containing 10 wt: % monomers (higher ratio NMA) pre and post 5 minute irradiation

4.6 Synthesis of 2 Methyl -1 Naphthyl-Methacrylate

A second naphthyl methacrylate monomer, 2-methyl-1naphthyl-methacrylate was synthesised. The monomer was incorporated into the matrix material, to determine whether it is possible to increase the refractive index contrast between the cladding and waveguide core. The newly synthesised monomer, along with 2-naphthyl methacrylate, was added to the matrix material, along with benzyl and phenyl methacrylate, and various photopolymerisation experiments were carried out, in order to improve the quality of the waveguides. A detailed description of the synthesis is described in section 10.3.

The naphthyl derivative was dissolvable in System A, and was compatible with other naphthyl monomers, as well as phenyl and benzyl methacrylate. Further experiments were not performed due to the development of System B, described in section 5, which performed better during structuring experiments.

4.7 Conclusion

In this chapter the development and characterisation of a polysiloxane material, consisting of hydride and vinyl terminated dimethyl diphenyl polysiloxanes, cured via the hydrosilyation reaction, in the presence of a Pt catalyst was presented. This material was developed in earlier studies, but was fully characterised and optimised here, in order to be able to be used as an optical matrix material, with which to fabricate three dimensional optical waveguides via TPA. The thermal stability, chemical inertness, and compatibility with high refractive index methacrylate monomers as well as the photoinitiator Irgacure 379, deem the material

suitable for this purpose. The material processing is quick with the refractive index of the cladding material and polymethacrylate waveguide core being sufficient to produce optical waveguides. Details of refractive index measurements can be found elsewhere.[70] Naphthyl acrylate monomers were also incorporated into the material, yielding good results in polymerisation experiments; however the lower volatility deemed such monomers unsuitable due to the difficulties in removing the remaining monomers. The newly developed matrix material used in two-photon experiments, including material testing and eventual development of optical interconnects consisting of specially designed printed circuit boards. The results are presented in Section 7.

Development and Characterisation of Optical Matrix Materials – System B

5 Characterisation of an Optical Material Developed from Epoxy Terminated Polysiloxane Cross linked with a Diamine (System B)

5.1 Introduction

As part of the investigation towards a new optically transparent, flexible matrix material, a number of epoxy functional silicones were investigated for their application in this field. Optimum performances of epoxy resins are obtained by cross linking the epoxy with the curing agents being either catalytic or co-reactive. Catalytic curing agents function as an initiator for epoxy resin homo-polymerisation. With co-reactive curing agents, the agent acts as a co-monomer in the polymerisation process. The curing agent reacts with the epoxy and pendant hydroxyl groups on the resin backbone, by either an anionic or cationic mechanism.

Epoxy resins are characterised by the three membered ring known as the epoxy, epoxide, oxirane or ethoxyline group. Epoxy resins generally contain aliphatic, cycloaliphatic or aromatic backbones, and can react with a variety of substrates. Attractive properties of epoxy resins include high chemical and corrosion resistance, good mechanical and thermal properties, good adhesion, low shrinkage upon curing, flexibility, good electrical properties, and ability to be able to be processed under a variety of conditions[62]. Epoxy functional silicones undergo cross linking reactions with amines, producing cured coatings with variable properties, depending on the epoxy content, degree of substitution and the ring opening of the epoxy group to form diols.

Epoxies are known to undergo cross linking reactions with amines, which are the most diverse group of epoxy curing agents. The resulting properties of the final cross-linked material are dependent on the type of crosslinker, substitution of the polymer backbone and ratio of epoxy to amine compound. A number of epoxy materials and diamine compounds have been investigated to form polymeric networks for optical waveguide applications[63,64], however the use of such materials for the applications in TPIP have not yet been reported in detail. Epoxy functional silicones are used in various curing systems, and exhibit good flexibility and high temperature resistance. The epoxy-alkyl functionality reacts with amine functional groups, without the need of catalysts, to give materials which exhibit good thermal and mechanical properties.
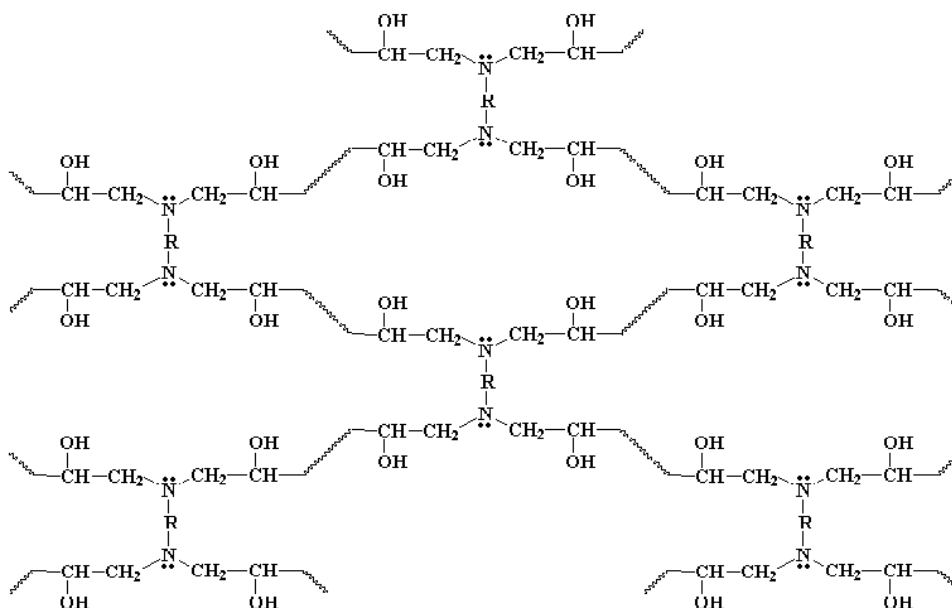
Figure 36: An example of an epoxy polymer cross-linked with a diamine compound

As already discussed, the material has to withstand high temperatures, be compatible with existing PCB materials and processes, as well as form thin films with good adhesion. Epoxy resins are known for their high thermal stability and durability, so a number of epoxy terminated polysiloxanes were investigated for their suitability. The developed matrix material needed to be compatible with a selection of high refractive index acrylate monomers, which were dissolved in the matrix material, along with a specific two-photon photoinitiator. The next sections describe in detail the acrylate monomers and photoinitiators used. An epoxy-propoxy terminated poly(dimethyldiphenyl siloxane) was chosen due to its optical properties and speed of curing with an aminopropyl disiloxane as a matrix material. The aminopropyl disiloxane crosslinker was chosen due to the length of the chain giving the final cross-linked network flexibility. Once a suitable curing method had been developed, three different high refractive index acrylate monomers were dissolved in the polymeric material.

5.2 Choice of Amine Crosslinker

The curing process of epoxies involves the formation of a rigid insoluble and infusible three dimensional network. The properties of the final product are important, and can be modified by changing the quantity and type of crosslinker. The epoxy equivalent weight (EEW) is one of the most important features of epoxy resins, and by knowing this value, the correct amount of the cross linking agent can be calculated. EEW is defined as the weight of resin in grams, which contains 1 g of the equivalent. When the amine hydrogen equivalent weight (AHEW) is

also known, the amount can be calculated using a simple equation. Taking an amine compound with a molecular weight of 146, shown in Figure 37, and a hydrogen functionality of 6, then the AHEW is:

146/6 = 24 g/ eq

The amine content = 1000/24 = 42 eq/ kg

Using the equation below, which gives you the amount of hardener needed: (for 100 g of epoxy resin)

100 × AHEW

EEW

Shown as an example, to cure 100 g of an epoxy resin, with an EEW of 200 g/ eq, one would need:

24 × 100

  200   = 12g
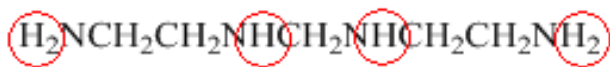
$$H_2NCH_2CH_2NHCH_2NHCH_2CH_2NH_2$$

Figure 37: Diamine compound showing its functionality of 6

5.3   Acrylate Monomers

The monomers used in combination with the developed matrix material must not be too volatile during the handling, so a sufficient amount remains in the material for TPA fabrication of waveguides to be performed; but must however have a certain degree of volatility to be able to be removed following exposure. Three acrylate monomers were investigated and chosen due to their high refractive indices, their high rates of polymerisation, and the volatility of the monomers enabled them to be removed from the material following TPA. The three monomers used were phenyl acrylate (PA), benzyl acrylate (BA) and 1,3 butanediol diacrylate (BDA). PA and BA were chosen due to their high refractive indices of > 1.5, and high volatilities. As with the previous material investigated, BDA was chosen as a cross linking component, in order to form an effective interlinking network of the polymerised acrylates in the waveguide core. The three monomers are displayed in Figure 38. The monomer ethylene glycol phenyl ether acrylate was also used in some experiments instead

of phenyl acrylate; however the lower volatility made this monomer more difficult to remove from the matrix material following TPA structuring, so for waveguide fabrication experiments, PA was the preferred monomer.
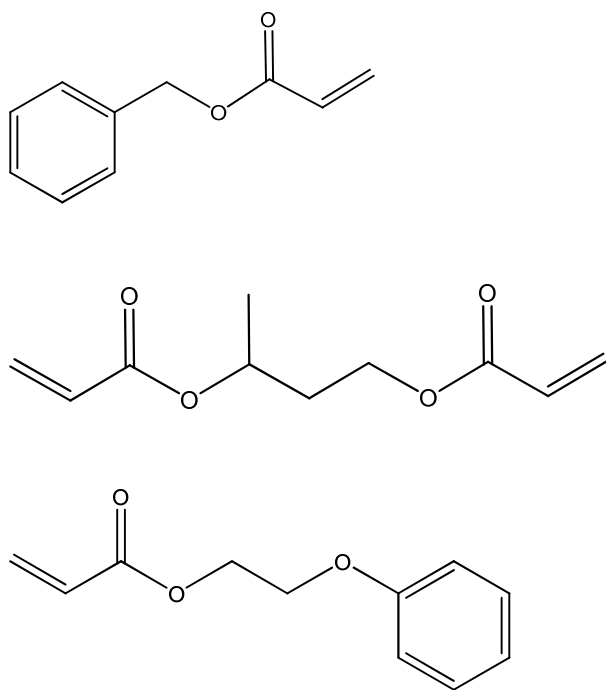
Figure 38: Structures of benzyl acrylate (BA), 1,3 butane dioldiacrylate (BDA) and ethylene glycol phenyl ether acrylate (used in some experiments as a substitute for phenyl acrylate)

5.4 Two-Photon Photoinitiator

Due to the nature of the curing of the hydrosilylation reaction, used in System A it was not possible to use a specific two-photon photoinitiator like N-DPD, developed and synthesised at the Technical University of Vienna, in the research group of Prof. R. Liska[6566] . The triple bond present in the photoinitiator proved to be more unstable than the double bond of the vinyl terminated siloxane in the presence of the Pt catalyst, will react with the vinyl group, leading to a breakdown of the chromophore. However, the epoxy diamine curing mechanism does not affect the photoinitiator in any way, so N-DPD was chosen to be used in this study, due to its extremely good two photoinitiating properties in TPA experiments.[67] N-DPD also functions well in the photopolymerisation of acrylate monomers, with the butyl derivative of the photoinitiator aiding the solubility in polysiloxanes. N-DPD has exceptional properties based on its conjugated π-electron system amplified by the dimethylamine groups resulting in the absorption maximum (λ_{max} = 435 nm) at a wavelength suitable for two-photon applications. For our structuring investigations, the non-modified and the butyl derivative

were used, with both photoinitiators performing well. It was found however, that the butyl derivative gave the matrix material an orange appearance, leading to concerns about the optical losses of the waveguides in the region of 840 nm.
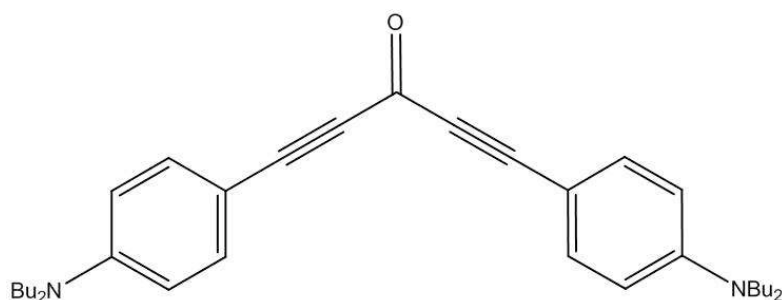

Figure 39: Two-photon photoinitiator N-DPD (butyl derivative)

5.5   Development of System B

To develop System B, an epoxypropoxypropyl terminated siloxane was cross-linked with a suitable diamine compound. Epoxypropoxypropyl terminated poly(phenylmethyl siloxane) and 1,3-bis(3-aminopropyl)tetramethyldisiloxane were both obtained from ABCR GmbH (Germany), and used without further treatment (Figure 40). Benzyl acrylate (BA), purchased from Alfa Aesar, and phenyl acrylate (PA) purchased from Polysciences were used as monomers, due to their high refractive indices of 1.52 and high volatility, which enabled removal following the TPA process. A third acrylate monomer, 1,3 butanediol diacrylate (BDA), obtained from Sigma Aldrich, was used as a cross linking monomer and formed a polymerised network following the photo-induced polymerisation. The resin was prepared by adding the amine to the epoxy, mechanical mixing for 20 minutes, and then heating the mixture at 80 ℃ for 1.5 hours, so a workable consistency was achieved. Following a 1.5 hour pre curing phase the acrylates could be added to the resin, which could then be spread onto substrates and a final curing could be applied. This is carried out at 50 ℃ for ~ 10 hours. All components were characterised by FT-IR spectroscopy.

The specific two-photon photoinitiator 1,5-bis(4-(dimethylamino)phenyl penta-1,4-diyn-3-one (N-DPD), was utilised for all TPA experiments, and was developed and synthesised externally[4] . In all experiments, material mixtures based on the correct epoxy equivalent weight and number of active hydrogen equivalent weight were prepared. 10 wt. % acrylate monomers (in total) were added to the epoxy / diamine matrix material with a ratio 1:1:1 by weight. In order to obtain homogeneous and dust free layers, the components were mixed thoroughly and filtered using a 0.45 μm PTFE syringe filter. Following the sample

preparation, thin films were prepared by scraping the material onto substrates to give film thicknesses of between 300 and 500 µm.
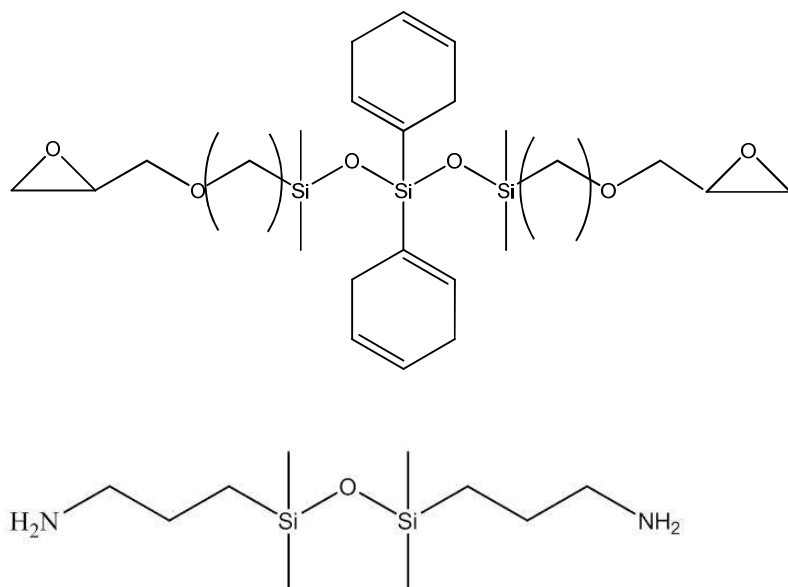

Figure 40: Structures of epoxypropoxypropyl terminated poly(phenylmethyl siloxane) and 1,3-bis(3-aminopropyl)tetramethyldisiloxane

5.6 Characterisation of Components in System B

5.6.1 Epoxy / Diamine Curing – FT-IR Spectroscopy

Each component used in the development of System B was characterised by FT-IR spectroscopy, in order to follow the curing and polymerisation of the selected acrylate monomers. To follow the curing, the samples were drop cast onto CaF_2 plates and an FT-IR spectrum was recorded before, and at regular intervals for 72 hours, at ambient temperature. The matrix material was developed using polyphenylmethyl siloxane, epoxypropoxy propyl terminated (Epoxy –Eq/kg = 3.6-4.0, MW = 500-600) cross-linked with 1,3-bis(3-aminopropyl) tetramethyl-disiloxane (amine hydrogen equivalent weight = 62.13 (MW = 248.52). The components cured to a clear solid resin and the FT-IR showed the formation of a large, broad peak forming at ~ 3400 cm^{-1} corresponding to the OH stretching vibration, which is formed after the opening of the epoxy ring. The increasing broad stretching vibration observed at ~ 3420 cm^{-1}, arising from the formation of the alcohol functional group following ring opening was observed, and can be seen in Figure 41. Table 11 includes a description of the characteristic peaks present in the spectra.
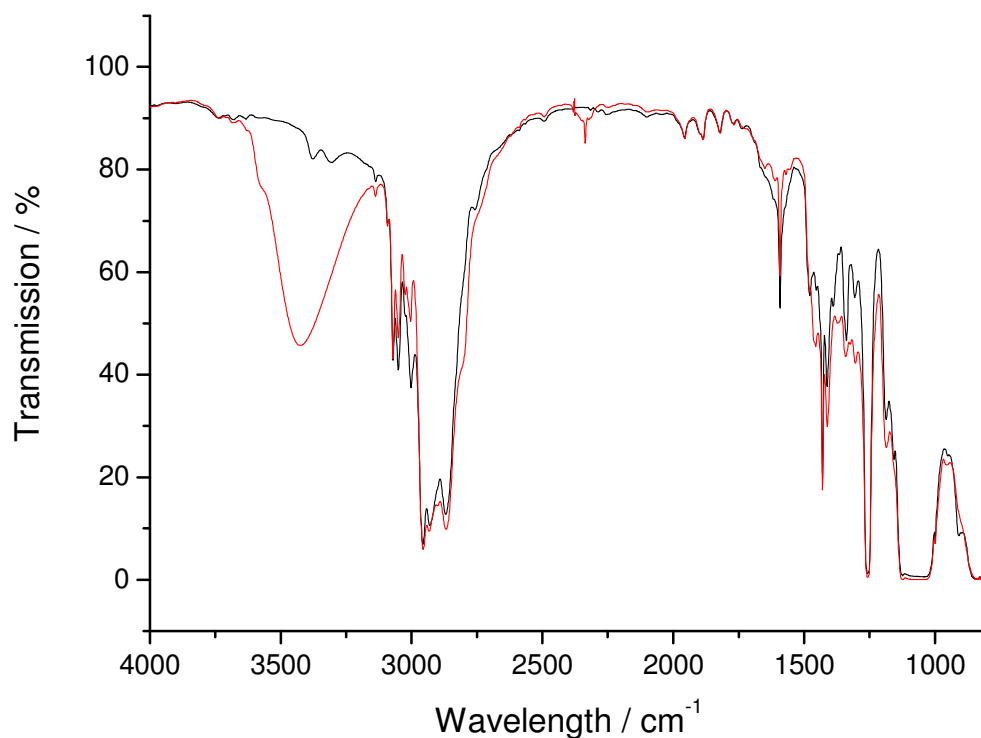
Figure 41: FT-IR spectra of epoxy/diamine matrix material pre and post curing

Table 11: Characteristic bands observed in FT-IR spectra of epoxy-diamine matrix material

Characteristic bands (cm^{-1})	Responsible vibration
1023	(Si-O-Si)$_n$
1095	(Si-O-Si)$_n$
1596	N-H deformation
1095	C-N stretching
1261	Epoxide C-O str
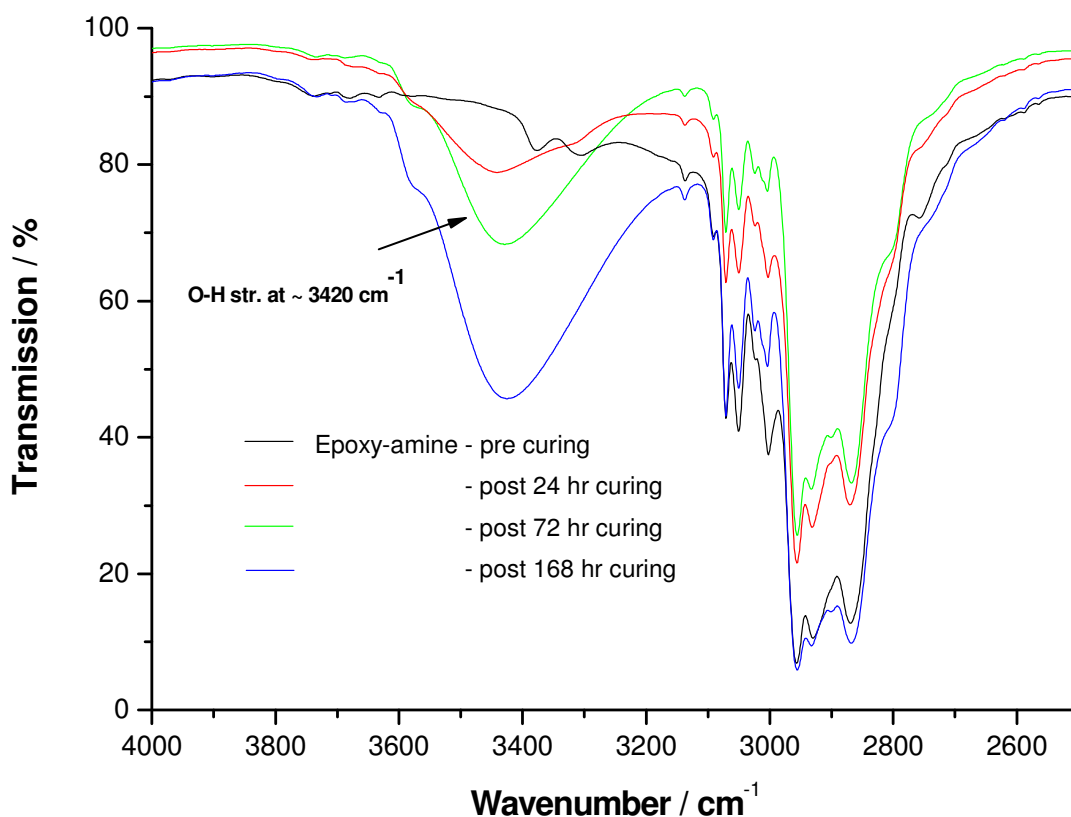
Figure 42: FT-IR spectra following the increase in the broad OH str. at ~3420 cm^{-1} formed following ring opening

5.6.2   FT-IR Spectroscopy of Components Present in System B

Following the development of an epoxy / diamine matrix material, curing was optimised by investigating different temperatures for different periods of time, in order to achieve a gel like consistency and then a flexible material. In the next sections the FT-IR spectra of each of the components is displayed, along with tables to display the characteristic peaks present. The spectra of the acrylate monomers were used to monitor the removal during thermal steps, as well as the stability and rate of polymerisation. Figure 43 and Table 12 display the spectrum and description of the characteristic peaks from 1,3 bis-(aminopropyl) tetramethyldisiloxane, which were used to monitor the cross linking.

1,3 bis- (aminopropyl) tetramethyldisiloxane

A number of amine cross linkers were investigated and used to cure the epoxy polymer, however due to the toxicity of such compounds, a number of them were unsuitable. 1,3 bis-(aminopropyl) tetramethyldisiloxane was chosen as it is a low toxicity liquid, and formed flexible films when used as cross linker. It was not possible to observe the decrease of the peak in the FT-IR spectrum of the NH bond, due to the peak corresponding to OH groups forming.
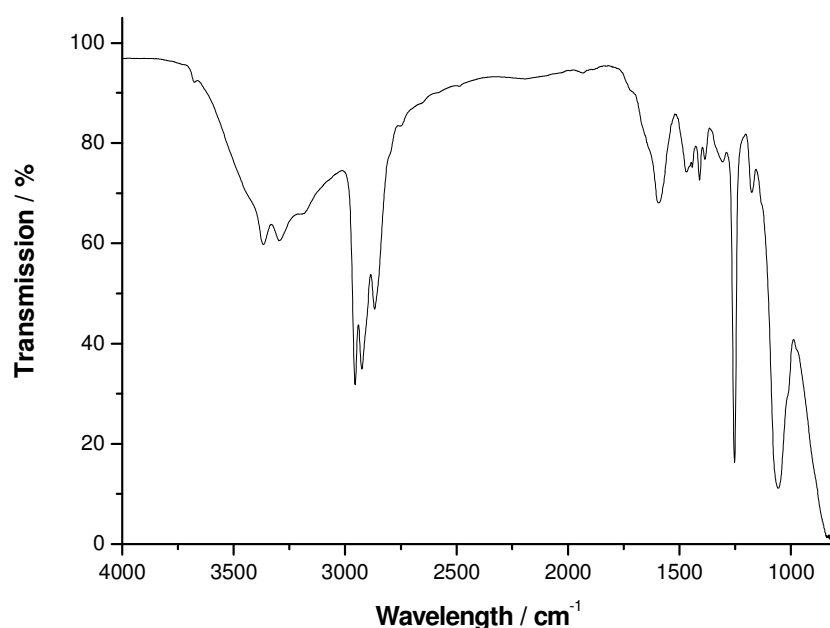
Figure 43: FT-IR spectrum of 1,3-bis (aminopropyl) tetramethyl disiloxane

Table 12: Characteristic peaks present in the FT-IR spectrum of 1,3-bis (aminopropyl) tetramethyl disiloxane

Characteristic bands (cm^{-1})	Responsible vibration
1056	(Si-O-Si)
1253	Si-CH$_3$
3366, 3294	N-H stretching
1594	N-H deformation
1056	C-N stretching
1467	C-H deformation
1175	C-C deformation
2955, 2924, 2867	C-H stretching

Epoxypropoxypropyl siloxane

The epoxy functional silicone has a viscosity of 15-30, a molecular weight of 500-600, and a molar % (epoxy equivalent weight, eq/kg) of 3.6-4.0. An FT-IR spectrum was recorded to characterise the major functional groups in the silicone. The important functional group peaks and FT-IR spectrum are recorded in Figure 44 and Table 13.
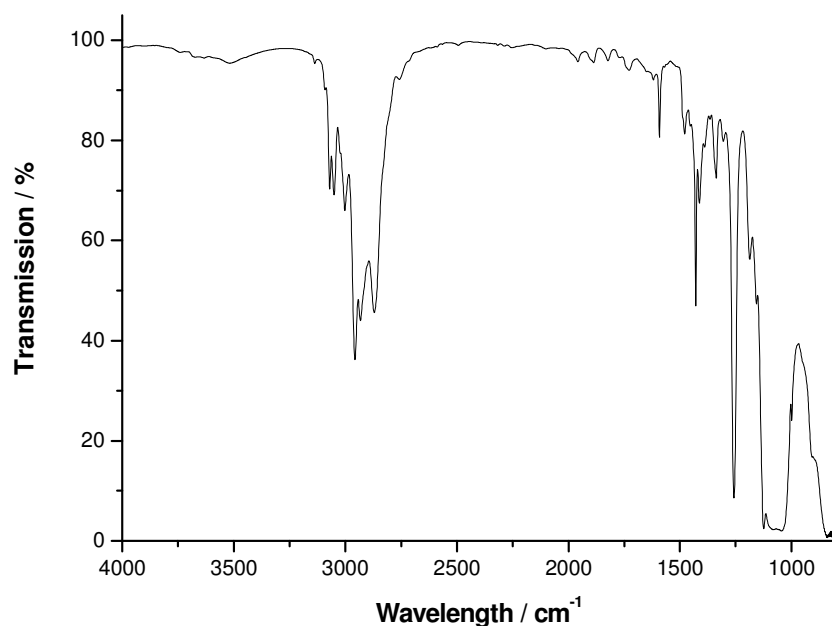
Figure 44: FT-IR spectrum of epoxypropoxypropyl siloxane

Table 13: Characteristic peaks present in the FT-IR spectrum of ,3-bis (aminopropyl) tetramethyl disiloxane

Characteristic bands (cm^{-1})	Responsible vibration
1043, 1123	(Si-O-Si)
1258	Si-CH$_3$, symmetric deformation
1258	C-O stretch (epoxy)
3002	CH$_2$ stretching (epoxy)
3050	CH stretching (epoxy)
1479	C-H deformation
1187	C-C deformation
3070, 3050	CH aryl bonds, stretching
1618, 1592	C-C stretching (aryl)
2957, 2982, 2870	C-H stretching

Benzyl 2-ethyl acrylate
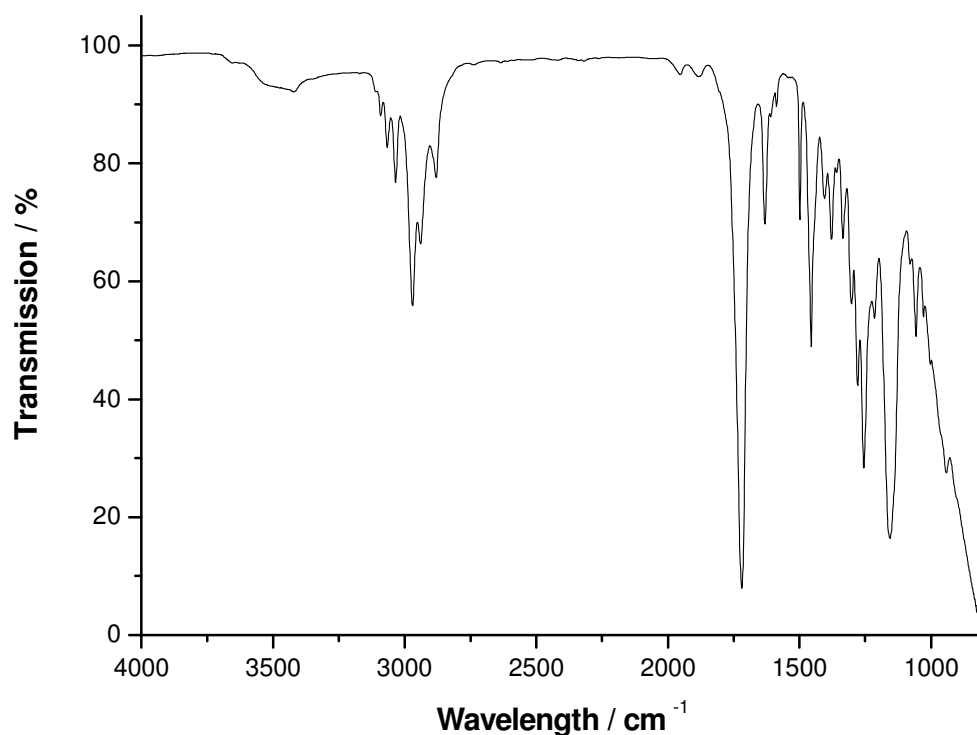
Figure 45: FT-IR spectrum of benzyl 2-ethyl acrylate

Table 14: Characteristic peaks present in the FT-IR spectrum of benzyl acrylate

Characteristic bands (cm^{-1})	Responsible vibration
1631	C=C stretching
1718	C=O stretching
1155	C-C deformation
3091, 3066, 3034	CH ring bonds, stretching
1631	C-C stretching (aryl)
2969, 2939, 2880	C-H stretching (aliphatic)

Ethylene glycol phenyl ether acrylate
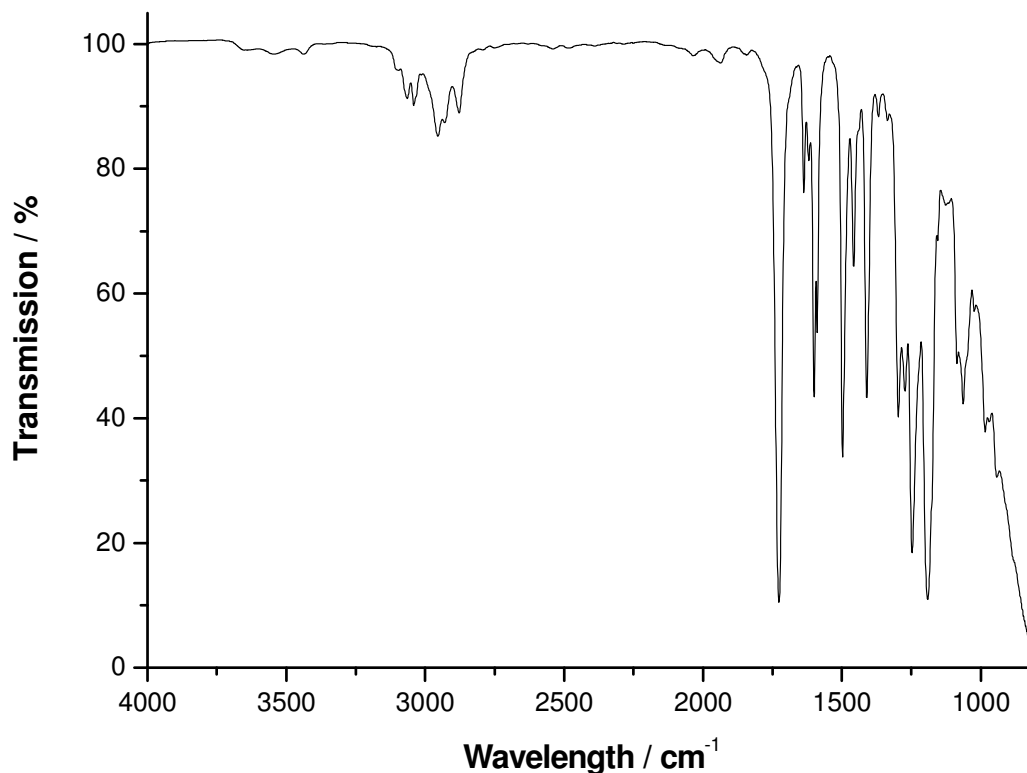
Figure 46: FT-IR spectrum of ethylene glycol phenyl ether acrylate

Table 15: Characteristic peaks present in the FT-IR spectrum of ethylene glycol phenyl ether acrylate

Characteristic bands (cm^{-1})	Responsible vibration
1636, 1619	C=C stretching
1726	C=O stretching
1154	C-C deformation
3064, 3041	CH ring bonds, stretching
1636	C-C stretching (aryl)
2929, 2954, 2878	C-H stretching (aliphatic)

1,3-butanediol diacrylate

This acrylate monomer has a slightly lower refractive index of 1.45, but is to be used as the cross linking monomer and forms a well structured cross linked network, forming the waveguide core. As can be seen with all the spectra of the acrylate monomers, the peak corresponding to the C=C stretching vibration is clearly visible, aiding the monitoring of the double bond conversion under UV irradiation.
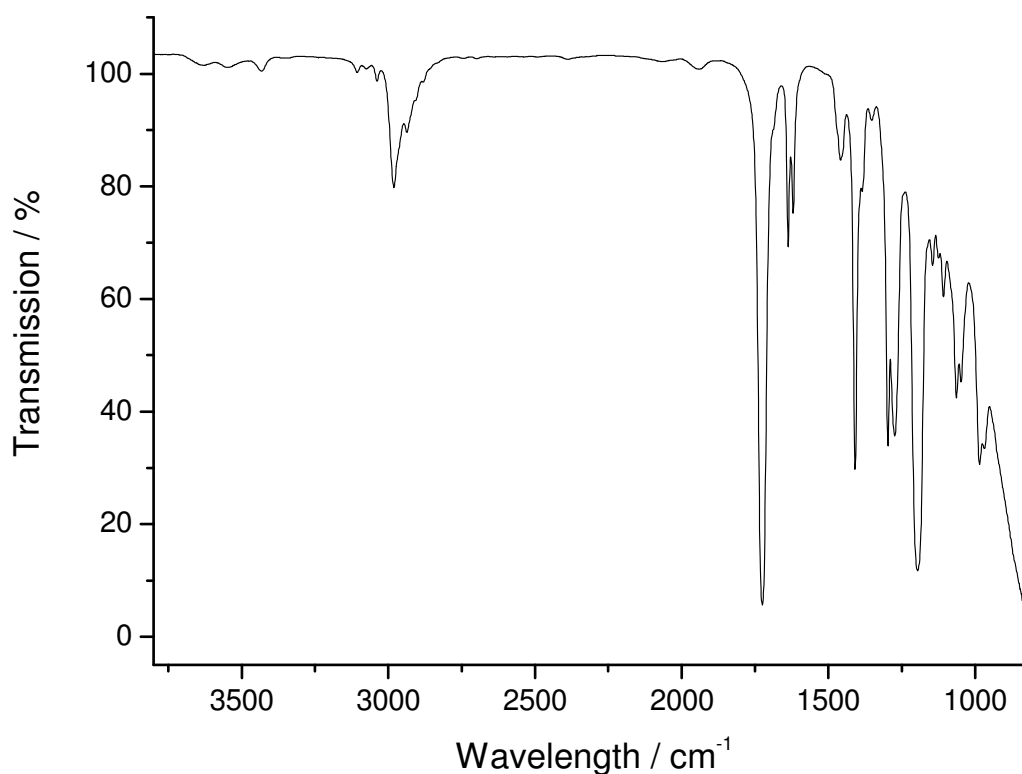

Figure 47: FT-IR spectrum of 1,3 butanediol diacrylate

Table 16: Characteristic peaks present in the FT-IR spectrum of 1,3 butanediol diacrylate

Characteristic bands (cm^{-1})	Responsible vibration
1637, 1620	C=C stretching
1725	C=O stretching
1154	C-C deformation
1274	C-O-C asymmetric stretching
2937, 2981,	C-H stretching (aliphatic)
1296	-CH=CH$_2$ (CH stretch of CH$_2$)

5.6.3   Investigation into the Incorporation of Acrylate Monomers into System B

Once the epoxy silicone material had been cured and a workable consistency had been achieved, the three acrylates previously mentioned, were incorporated into the material after the "pre-gelation" phase. To determine the best ratio of the three monomers to be used in system B, FT-IR spectroscopy was carried out. The monomers, in different ratios were stirred, drop cast and sandwiched between CaF$_2$ plates. An initial FT-IR spectrum was taken, followed by a 2 minute irradiation using a Novacure spot cure lamp. Polymerisation was determined by observing the decrease in the C=C stretching vibration in the spectra, seen at ~ 1639 cm^{-1}. The results of the total double bond conversion, using different ratios of monomers is presented in Table 17.

Table 17: Results of % polymerisation using different acrylate monomer ratios

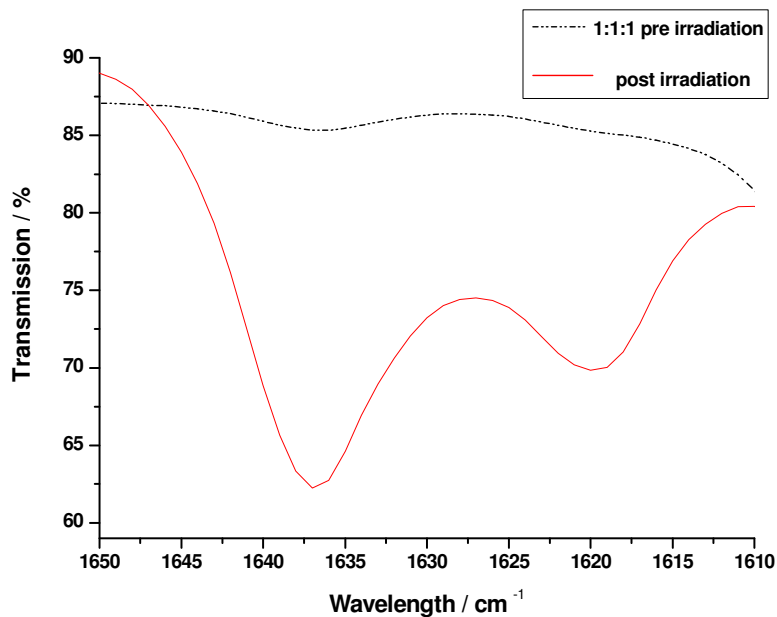| Ratio of monomers (BA:PA:BDA)	Double bond conversion [%]
1:1:1	95
1:1:2	96
1:2:3	97
2:2:1	~100 % (no peak observed)

Figure 48: FT-IR analysis of monomer ratio; analysis of C=C bond pre and post irradiation

The results of the FT-IR investigations suggest that a higher proportion of the benzyl and phenyl acrylate monomers lead to a higher rate of polymerisation, however all ratios resulted in over a 95 % polymerisation. For the preliminary structuring investigations, a ratio of 1:1:1 acrylate monomers were added to the epoxy silicone system.

5.6.4   Investigation into the Stability of Acrylate Monomers in System B

To determine the stability of the acrylates during the curing stage and whether polymerisation occurred at slightly elevated temperatures or during the storage of the material, FT-IR spectroscopy was carried out. The acrylate monomers, in a ratio 1:1:1 (1,3 butanediol diacrylate: ethylene glycol phenyl ether acrylate: benzyl -2-ethyl acrylate) were mixed together in a glass vile, and drop cast and sandwiched between two CaF_2 plates. An initial FT-IR spectrum was recorded and the samples were then placed in the oven at 70 °C for three hours. A second FT-IR spectrum was recorded, and the peak observed at ~ 1636 cm^{-1} was monitored, to determine whether any polymerisation had taken place. The sample was then stored at room temperature for one week in the dark, to determine whether the monomers are stable under these conditions. The results are displayed in and reveal, even after calculating the difference in the size of the peak corresponding to the C=C bond at 1637

cm $^{-1}$, that no polymerisation of the monomers occurred, however some of the monomers evaporate from the material during the thermal treatments.
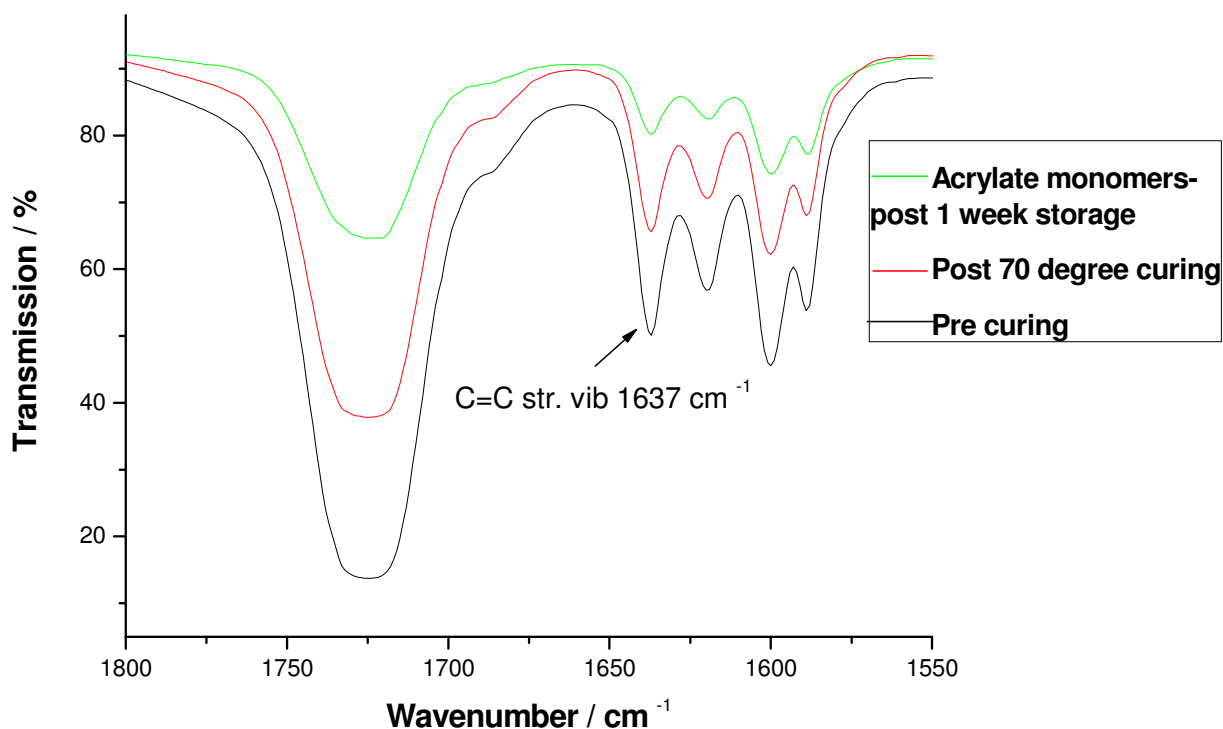
Figure 49: FT-IR spectra of acrylate monomers (PA:BA:BDA) during thermal treatment and storage for 3 days

5.6.5   Investigation into the Polymerisation of Acrylate Monomers in System B – FT-IR Spectroscopy

The acrylate monomers, once included into the epoxy silicone resin, were analysed by FT-IR spectroscopy in order to determine whether the rate of polymerisation was hindered. The silicone matrix was mixed together in a glass vial along with a 1:1:1 ratio of monomers and 0.01 wt. % of the photoinitiator N-butyl NDBD. It should be noted here that N-DPD is not an efficient one-photon photoinitiator, and it was therefore expected that the double bond conversion would be lower than when the photoinitiator Irgacure 379 was utilized. The sample was protected from the light, mechanically stirred and drop cast and then sandwiched between two CaF$_2$ plates. Initial spectra were recorded and are displayed in Figure 50. The sample was then irradiated in two minute intervals with a spot cure lamp. The

results of the double bond conversion are displayed in Table 18. It appeared, that although the conversion of the C=C double bond was found to be less when the acrylate monomers were included in the epoxy silicone material, after four minutes of irradiation, a 70 % conversion was achieved.

Table 18: Results of % polymerisation of acrylates incorporated into epoxy silicone resin

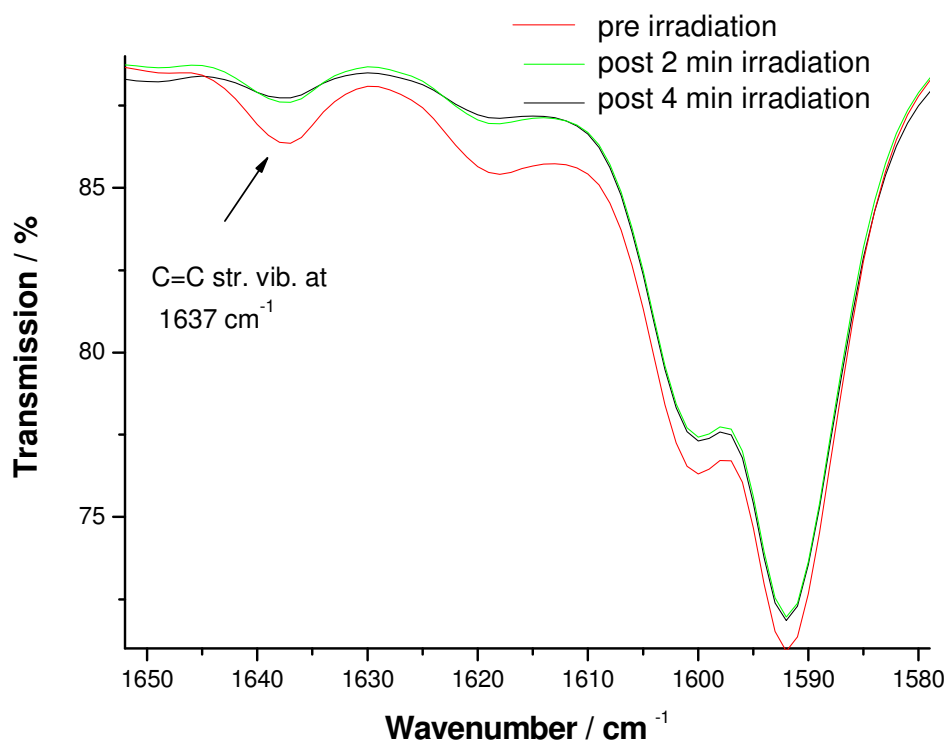| Polymer ratio	Time of irradiation [s]	Conversion [%]
1:1:1	120	44
1:1:1	240	70

Figure 50: FT-IR spectra of acrylate monomer double bond conversion, using N-DPD as photoinitiator

5.7 Rheology Measurements – Determination of Epoxy / Diamine Curing

5.7.1 Introduction

In order to study the curing characteristics of System A, a number of rheological measurements were performed. The instrument utilised was an Anton Paar Physica cone-plate rheometer which allows thermostatted operation. The material could therefore be monitored from starting state to the fully cured resin, measuring the storage and loss modulus as well as the complex viscosity.

Rheology measurements can be carried out to perform material characterisation, due to the fact that flow behaviour is responsive to properties such as molecular weight and molecular weight distribution. In this case, the measurements were used to follow the course of the curing reaction during the thermal treatment. The cone-plate geometry used allowed an absolute viscosity measurement with a precise shear rate and shear stress information. Only a very small sample volume was required, and the temperature was accurately controlled. A detailed description of the principles of rheology is found in Section 10.

5.7.2 Results

All samples were made directly before the analysis took place, and were carried out with the same parameters. The measurements were performed to determine the speed of cross linking between the epoxy polymer and the diamine compound. The time and temperature dependence measurements were carried out over a period of 200 minutes, heating the sample from 20 °C up to 80 °C, with the sample being held at 80 °C after 80 minutes. During this measurement, the storage modulus, which reflects the elastic behaviour, and the loss modulus, which reflects the viscous behaviour of the system, was measured. The point in which the storage and loss modulus cross, is the gelation point and from Figure 51, it is clear this point is reached around 40 minutes from when the acrylate monomers are incorporated into the system. In Figure 51 G` is the storage modulus and G`` is the loss modulus. The final consistency of the material is not overly affected by the addition of the acrylate monomers, however the sample including the acrylates appears to have a more gel like consistency.
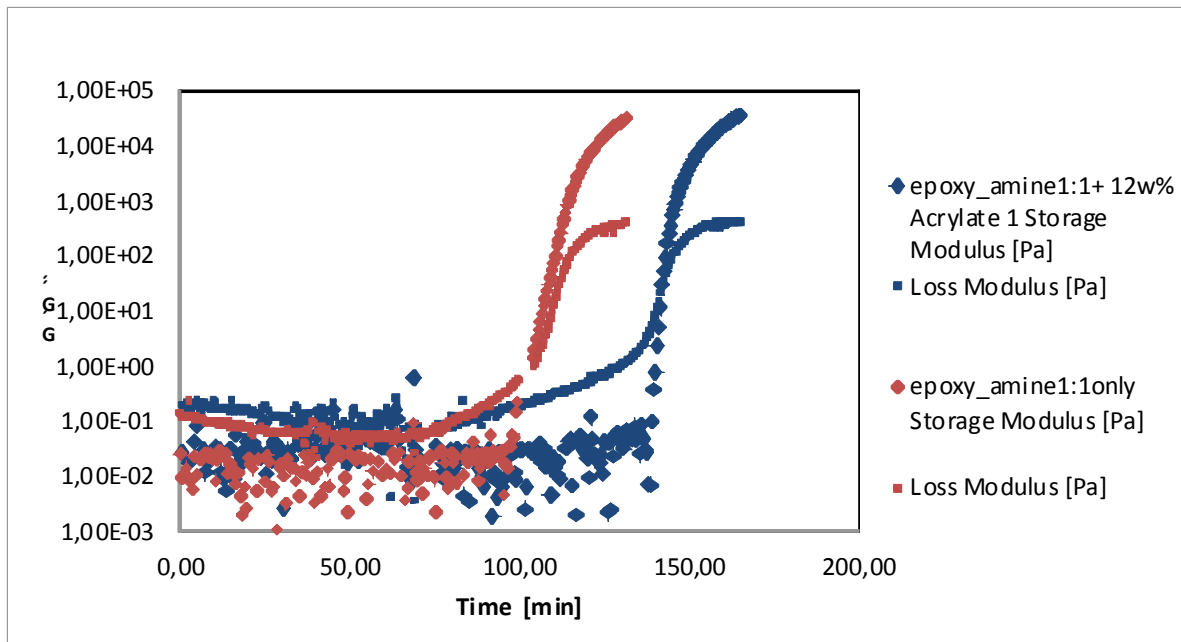
Figure 51: Time dependence plot depicting the difference in curing times of the pure epoxy siloxane matrix compared to the sample containing 12 wt.% acrylate monomers
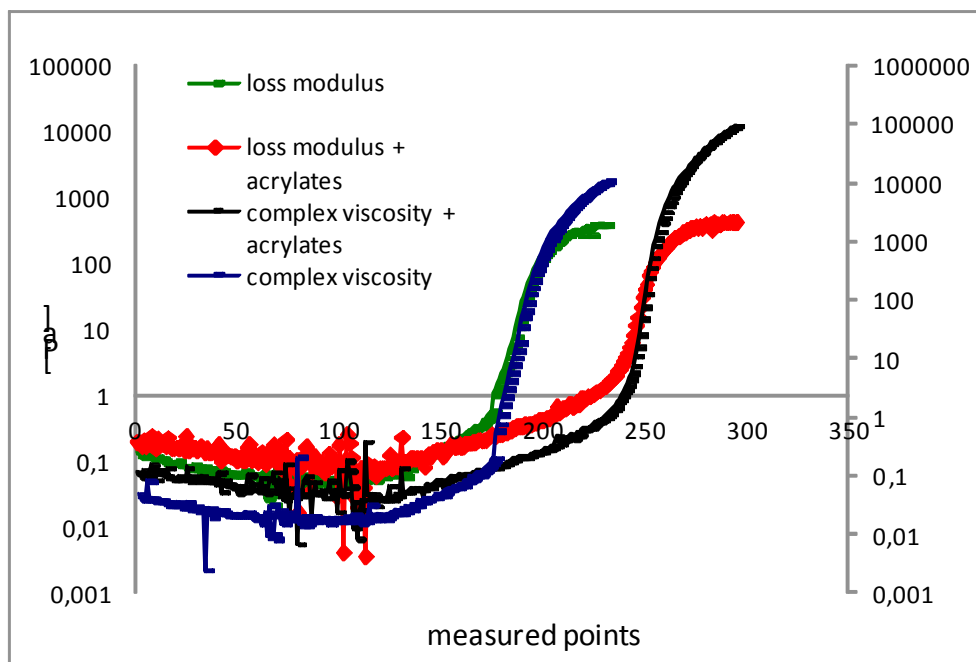

Figure 52: Temperature dependence plot including complex viscosity and loss modulus of pure epoxy siloxane matrix and matrix including acrylate monomers

5.8 Investigation of the Stability of System B by Simultaneous Thermal Analysis (STA)

5.8.1 Introduction

To determine the thermal stability of the epoxy resin, with and without the acrylate monomers present, STA was carried out on the fully cured resin. Samples of the resin were made up and fully cured including and omitting the acrylate monomers. STA measurements were applied to investigate the thermal stability of System B, along with establishing how easily the acrylate monomers can be removed from the cured material following TPA structuring. Three samples based on the epoxypropoxypropyl terminated polyphenylmethyl siloxane and 1,3-bis(3-aminopropyl)tetramethyl-disiloxane polydimethylsiloxane in a molar ratio of 1:1 were prepared. Whereas one sample was made without any additional monomers, the other samples contained 10 wt.% of the acrylate monomers 1,3 butanediol diacrylate, benzyl acrylate and phenyl acrylate, in a ratio of 1:1:1. The curing of the samples was performed at 50 °C for 20 hours. A final curing at elevated temperature and under vacuum (80 °C/20 h / 40 mbar) was carried out on one sample. The measurements were performed using a heating rate of either 10 K/min or 2 K/min.

The test conditions were identical for the TG and DSC signals, (same atmosphere, flow rate and heating rate) so the analysis of the signals is improved as the information concerning the sample behaviour is simultaneously available. The differentiation between phase transformation and decomposition can be simultaneously monitored.

5.8.2 STA of Cured System B

First samples included the epoxypropoxypropyl terminated polyphenylmethyl siloxane and 1,3-bis (3-aminopropyl) tetramethyl-disiloxane polydimethylsiloxane in a molar ratio of 1:1. One sample was prepared without adding any monomer or photoinitiator, and the second sample included 10 wt. % of phenyl acrylate and 1 wt. % of the photoinitiator Irgacure 379. STA measurements were performed within a temperature range of 20 °C to 300 °C. Thermal stability of the silicone matrix was observed up to 300 °C. In case of the sample which included the monomer and the photoinitiator the evaporation of the incorporated phenyl acrylate starting at 130 °C was observed, displayed by the decrease of the corresponding TGA signal. The overall weight loss of the sample at 300 °C was 8 wt. %, which is attributed to the removal of the monomer phenyl acrylate by the thermal treatment, shown in Figure 53.
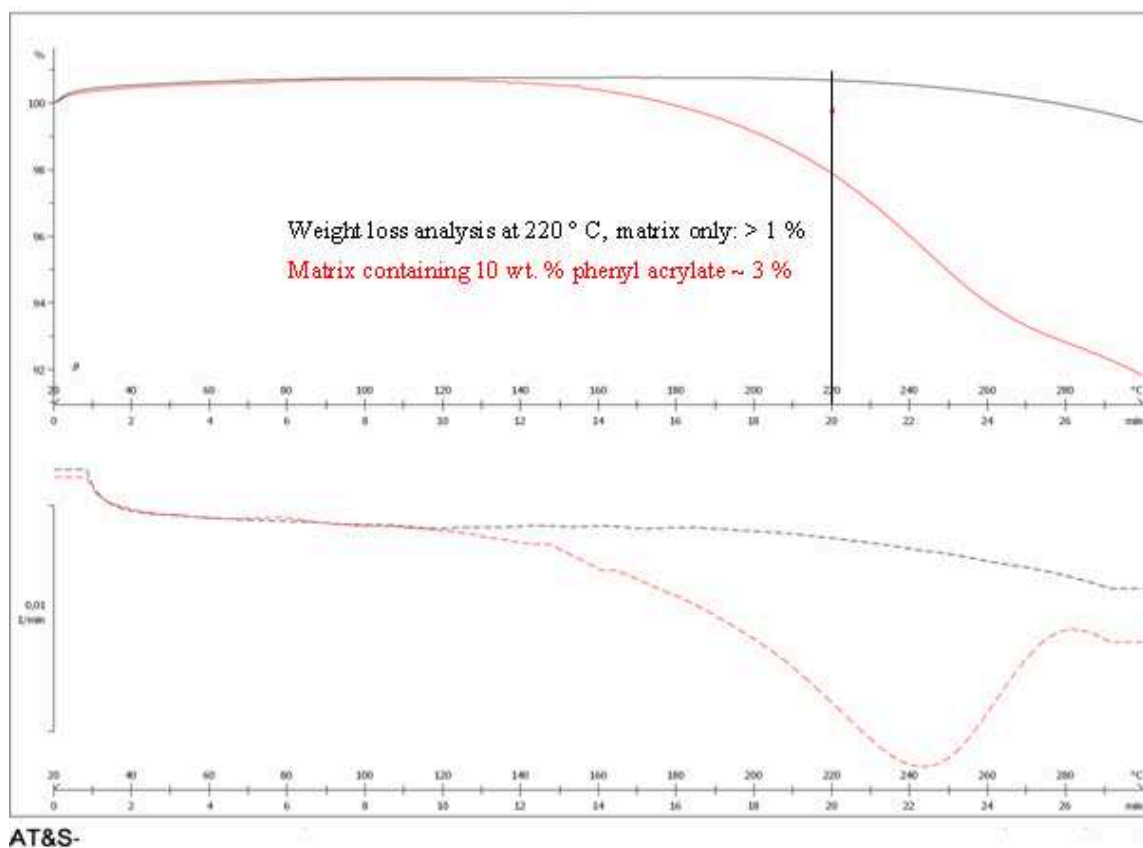
Figure 53: TGA and DSC Signals of the performed STA measurements showing the epoxy siloxane matrix only (black line) and epoxy siloxane matrix containing 10 wt. % acrylate monomer and 1 wt. % photoinitiator Irgacure 379

5.8.3 STA of System B - Comparison of Different Heating Rates

A second set of experiments were performed which included 10 wt. % of the chosen monomers ethylene glycol phenyl ether acrylate, benzyl acrylate and 1,3 butanediol diacrylate. These measurements were carried out at the same conditions as the previous, as well as a slower heating rate of 2 K per minute as a comparison. The results showed that at 300 °C there was a weight loss of 9 % with the sample which was heated at a faster rate of 10 K per min, and 12 % loss was seen with the sample heated at a slower rate of 2 K per min. The results of these measurements are displayed in Figure 54. The matrix once again showed good thermal stability, with only a small weight loss arising from the matrix seen in the slower heated sample.

Weight loss analysis at 220 ° C, matrix including 10 wt. % acrylates
(heating rate 10 K per min)~4 %
Heating rate of 2 K per min ~ 7 %

220 ° C

AT&S-R&D-CCLaboratory: METTLER

Figure 54: TGA signal of the performed STA measurement showing the epoxy siloxane matrix containing 10 wt.% acrylate monomers with a slower heating rate of 2 K / min, (black line) and the same sample heated at a faster rate of 10 K / min (red line)

5.8.4 STA of System B - Comparison of Illuminated and Non-Illuminated Material

Further measurements were carried out on the epoxy siloxane matrix, with 10 wt. % acrylate monomers and 1 wt. % photoinitiator Irgacure 379, following irradiation. The results are displayed in Figure 55. The epoxy matrix, after being applied to optical glass slides and cured, was irradiated using a spot cure lamp. One sample was irradiated for 5 minutes and a second sample for 10 minutes. The samples, along with a third non-irradiated sample were measured under the same parameters as previous experiments, and showed that the irradiated samples displayed only a 10 % weight loss, whereas the non-irradiated sample showed a weight loss of 17 % after heating to 300 °C.

weight loss @100°C   weight loss @150°C   weight loss @200°C   weight loss @300°C

Stufe -0,8602 %   Stufe -4,9718 %   Stufe -9,4474 %   Stufe -17.4830 %

1. derivative

Probe: TGA_sample 03, 7,4750 mg

Probe: TGA_sample 01, 20,6390 mg
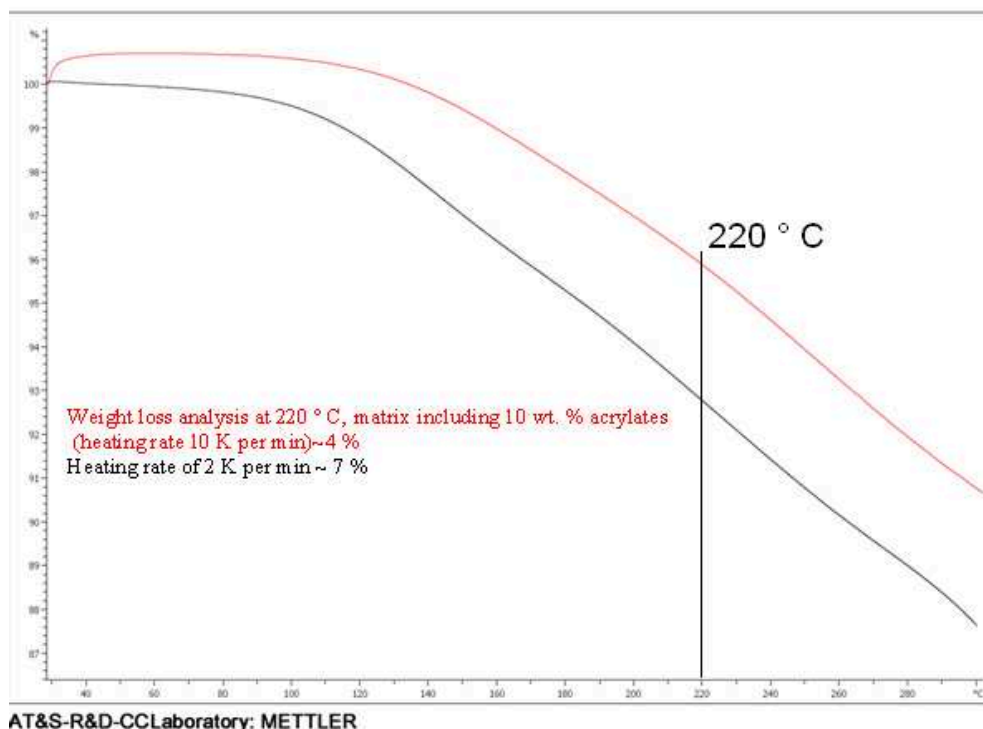
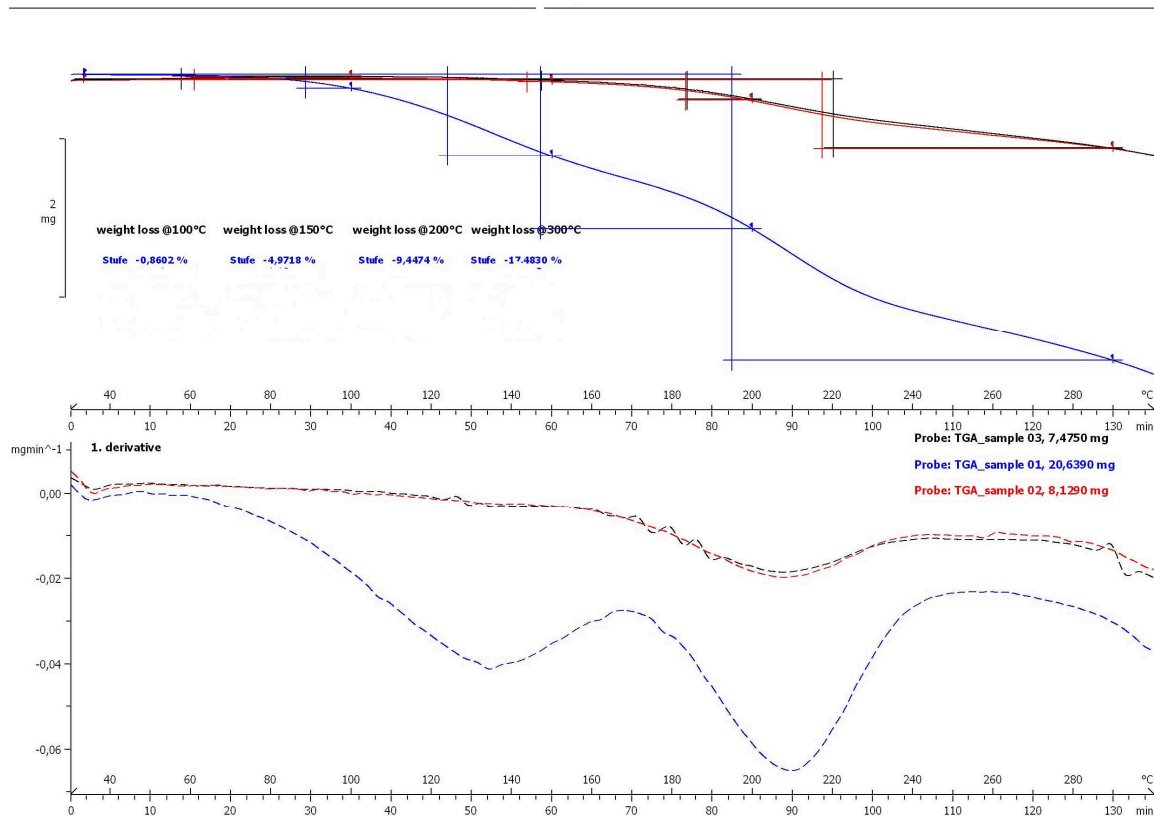Probe: TGA_sample 02, 8,1290 mg

Figure 55: TGA and DSC signals of the performed STA measurements showing the epoxy siloxane matrix containing 10 wt. % acrylate monomers with a heating rate of 10 K / min Black line represents the sample irradiated for 10 minutes; red line represents samples irradiated for 5 minutes, and blue line represents the non-irradiated sample

5.8.5 STA of System A - Comparison of Thermal Finishing Treatments

A final set of STA measurements was carried out to compare different heating rates, and also to compare the pure matrix, and matrix containing acrylate monomers. The results are displayed in Figure 56. A summary of each result is described below. The samples labelled 1-4 represent the following:

1)   (black line) epoxy and amine only, 50 °C for 20 hours (normal curing of sample)

The sample showed a loss of only ~3 % up to 300 °C and a loss of 5 % when analysed at a slower heating rate of 2 ° C per minute. The small weight loss was seen after a temperature of 200 °C in both cases.

2)   (red line) epoxy amine system including 10 wt. % acrylate monomers. 50 ° C for 20 hours (normal curing of sample)

The sample showed a 10 % loss at 300 °C, corresponding to the loss of the acrylate monomers, and in comparison with the sample containing no acrylates, and at a faster heating rate, the sample showed a weight loss of around 12 %, which is comparable to sample containing no acrylates. The DSC signal showed an endothermic peak only in the fast heating rate analysis, observed at around 70 °C, attributed to the loss of the acrylate monomers.

3)   (blue line) Epoxy amine system including 10 wt. % acrylate monomers (50 °C for 20 hours (normal curing of sample) plus a 20 hour post thermal treatment in an open system).

This sample showed the same behaviour as the sample which had not undergone the post thermal treatment, with a loss of around 12 % up to 300 °C, and the sample heated at a slower rate of 2 °C per minute, showed the biggest weight loss of all the samples, of 15 %. The weight loss from this sample also started slightly earlier, at around 120 °C, which can be attributed to the acrylate monomer loss.

4)   (green line) epoxy amine system only (50 °C for 20 hours (normal curing of sample) plus a 20 hour post thermal treatment in an open system).

This sample showed only a loss of 2 % at a temperature of 300 °C when heated at a faster rate. When heated at 2 °C per minute, the sample showed a weight loss of around 5 %.
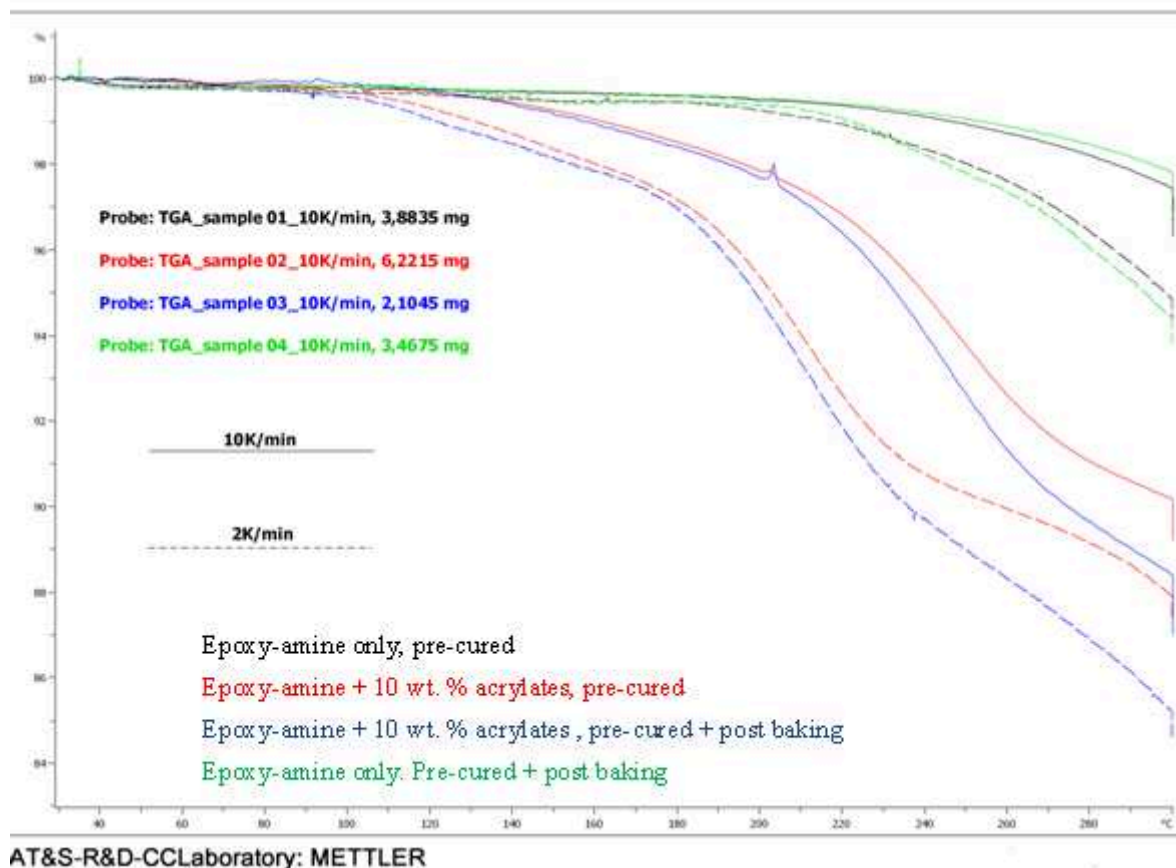
AT&S-R&D-CCLaboratory: METTLER

Figure 56: TGA signal of the performed STA measurements showing the epoxy siloxane matrix only, (black and green lines) and containing 10 wt. % acrylate monomers (red and blue lines)

The results showed that the matrix was stable up to 220 °C, including after the post thermal treatment, of 80 °C for 20 hours. The sample containing 10 wt. % acrylates however, still

showed a 10 % loss, suggesting that a higher temperature is needed to remove the remaining monomers from the matrix.

5.9 Determination of Monomer Loss During Thermal Treatments – Headspace Gas Chromatography

5.9.1 Introduction

Headspace gas chromatography is an analytical technique used to analyse volatile components in solids, liquids and gases. The method was chosen to determine the amount of acrylate monomers present in System B. There has to be a high enough concentration present in the matrix material for the TPA structuring to occur successfully. However following the patterning, the remaining acrylate monomers need to be removed from the surrounding cladding material for an effective refractive index difference between the waveguide core and surrounding cladding, and also to stabilise the material itself. The aim of these sets of experiments was to establish the concentration of each of the three chosen monomers present in the matrix following different stages of curing, as well as thermal treatments to drive out the remaining monomers following TPA structuring. The headspace is the gas space in the chromatography vile above the sample, and so can be used to analyse the components in a gas, such as volatile components in solid samples. A common application includes the analysis of monomers in polymers, hence why this analysis was chosen for this application. Headspace GC works best using light volatiles that can be efficiently partitioned into the headspace gas volume from the solid matrix sample. This method can therefore detect the amount of remaining acrylate monomers in the epoxy-amine cured thin films. An advantage of this method, is that the thin films can be placed directly into vials, and analysed, avoiding too many steps during preparation and extraction, leading to loss of the monomers. Experimental details are described in section 10.

5.9.2 Results

Sample 1: 50 ℃ curing, 20 hours: stored for 1 week at ambient conditions

Benzyl acrylate

For the analysis, all samples contained 3.3 wt. % of each monomer in the epoxy-amine matrix, therefore when 3.3 % of the monomer remains in the material, it can be said that 100 % of the original amount of monomer still remains in the matrix. The final column in the table states the overall percentage removed, as this is the information most beneficial to this investigation.

The first sample, cured at only 50 ℃ for 20 hours under closed conditions, showed a very high concentration of benzyl acrylate was still present. A value above the 5 wt. % calibration curve, indicating this pre curing step removes only a small amount of the monomer. From extrapolating the calibration, the percentage of the monomer remaining in the matrix was found to be 2.8 %

1, 3 butanediol diacrylate

In the case of 1, 3 butanediol diacrylate, a smaller peak area was observed, but still above the amount detectable by the calibration. From extrapolation, the result showed that the weight percentage of monomer remaining in the matrix was found to be 3.3, indicating no monomer is removed during the mild curing process and stored in at ambient conditions for a prolonged period.

Ethylene glycol phenyl ether acrylate

The amount of ethylene glycol phenyl ether acrylate was only slightly above the calibration measurements, the results show 1.8 wt. % of this monomer was still present in the matrix. This amount seems to be slightly misleading, as this acrylate monomer has the highest boiling point of all the monomers, so it should be seen that more of this monomer remains, the calibration may therefore have to include the decomposition compound phenoxyethanol.

Sample 2: 80 ° C, 40 mbar, and 20 hours:

Benzyl acrylate

After a thermal treatment of 20 hours, at 80 ℃, 40 mbar, a high percentage of benzyl acrylate is removed from the epoxy matrix. The calibration reveals that only 0.2 wt. % of the monomer remains, suggesting that ~ 95 % of the original amount of monomer is removed at this temperature.

1, 3 butanediol diacrylate

This monomer, being a larger acrylate, is difficult to remove from the epoxy-amine material, with 34 % of the original amount of added monomer still remaining after the thermal step.

Ethylene glycol phenyl ether acrylate

The phenyl acrylate monomer appears to be removed more easily than the other two acrylate monomers, however it should be noted that this result can be due to the fact, that even during the 2.5 hour heating step of the samples, it is possible that not all of the monomer was volatised, which would give a lower calibration level than would be expected. This is likely as the boiling point of this monomer is the highest of the three acrylates used, so it is possible a higher proportion remains than is calculated.

Sample 3: 100 °C, 40 mbar, and 20 hours:

Benzyl acrylate

Following a baking step of 100 °C, 40 mbar for 20 hours; the matrix was found to contain less than 5 % of the original benzyl acrylate concentration. A more accurate concentration was unable to be determined as the calibration of such a small percentage could not be determined.

1, 3 butanediol diacrylate

After this thermal step, around 9 % of the original percentage of 1, 3 butanediol diacrylate still remained in the matrix. This monomer appears to be the most difficult to remove. There was however no breakdown product observed, suggesting the monomer is more stable then the phenyl and benzyl monomers, but could cause problems concerning the stability of the matrix.

Ethylene glycol phenyl ether acrylate

Ethylene glycol phenyl ether acrylate appeared to be most easily removed from the matrix system, with the smallest percentage remaining after the 100 °C thermal step. Less than 5 % remained in the matrix; once again an accurate measurement could not be performed as the concentration was well below the calibration limits.

5.9.3 Calibration of Ethylene Glycol Phenyl Ether Acrylate - Addition of Phenoxyethanol

To determine whether the degradation product of ethylene glycol phenyl ether acrylate affects the results of the calibration, a calibration curve was constructed which included the area peak of phenoxyethanol. The results from this show a relationship between the decomposition product and the acrylate monomer, and the results from the calibration give the same results as without the phenoxyethanol peak, further confirming that the phenoxy ethanol is a decomposition product from the monomer. The degradation product benzyl alcohol, also detected by the GC-MS, gave the same results, when the peak area of that monomer was included in the calibration.
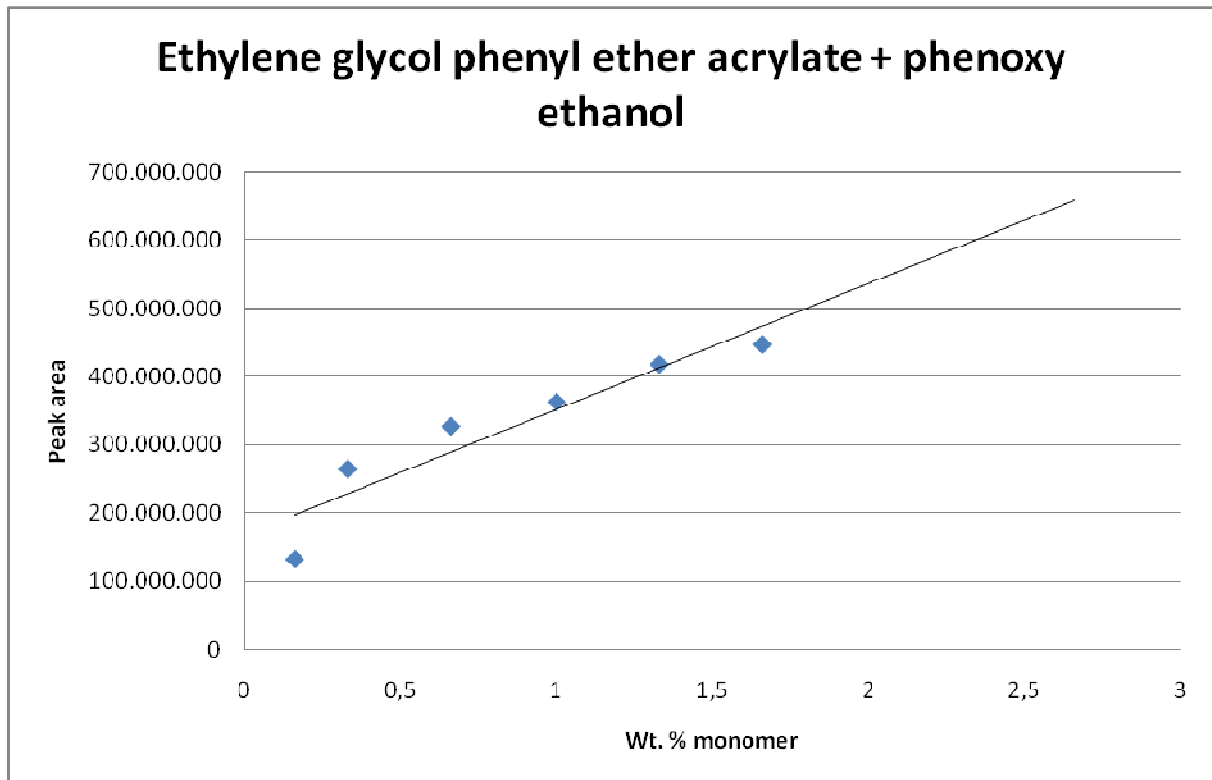
Figure 57: Calibration curve, ethylene glycol phenyl ether acrylate including phenoxy ethanol area peak, average of two analysed sample films

5.10   Conclusion

To summarise, it is clear that the three chosen acrylate monomers are stable in System B during the 50 °C curing step, and storage at ambient temperatures, (open system) the samples were also stable when not stored in an acrylate saturated atmosphere. Only ethylene glycol phenyl ether acrylate showed a loss of around 46 % during this time. The 100 °C step for 20 hours, 40 mbar, appears to remove around 90 % of 1, 3 butanediol diacrylate, and more than 95 % of the phenyl and benzyl acrylate monomers. The results suggest that even higher temperatures may be required if all traces of the acrylate monomers need to be removed, which may lead to damage of the written waveguides in the matrix material. The material is easily processed, with quick curing times, is compatible with acrylate monomers as well as N-DPD, can be used to produce fully flexible thin films. Optical characterisation and the development of optical interconnects using this material are described in Section 8.

Development and Characterisation of Optical Matrix Materials – System C

6 Characterisation of an Optical Material Developed from a Silanol Terminated Polysiloxane Cross linked with an Acryloxy Functional Silane (System C)

6.1 Introduction

Having developed and characterised two previous polymeric optical materials, a third optical matrix material was investigated using a silanol terminated polysiloxane. Polydimethylsiloxane (PDMS) polymers offer a combination of properties including a low glass transition temperature (T_g) and high temperature, chemical and oxidation resistance[68]. To take full advantage of these properties the polymer needs to be cross linked into a network. An important class of reactions used to cross link siloxanes is the condensation of silanol groups to form siloxane bonds, from silanol terminated PDMS. The condensation of silanol groups to form siloxane bonds is one of the most important classes of reactions used to crosslink siloxanes in commercial applications[69]. Room temperature vulcaniseable materials can cure rapidly, and boast properties such as strength, flexibility and transparency. Terminal silanol groups present on silanol terminated PDMS polymers are the main components in one and two part sealant systems, used in combination with small amounts of metal soap catalysts such as dibutyl tin dilaurate. Upon curing, the PDMS system can produce cross linked silicone films, as well as flexible silicone elastomers. With the introduction of a tri or tetra functional molecule, a 3D network can be produced. Trialkoxysilanes (R`Si(OR``)$_3$) when used as cross linkers, enable moisture curing upon exposure to air, with the alkoxy functionality hydrolysing to form silanol and the corresponding alcohol. The silanol then condenses with the Si-OH-terminated polymer, producing a cross linked network. Such chemistry is utilised in silicone sealants, with atmospheric moisture diffusing into the polymer once the sealant is extruded, hydrolysing the reactive groups on the cross linker. Fast curing speeds, and the ability to modify the properties of the final polymer by using functional alkoxy silanes, deems this class of material an appropriate medium for the fabrication of optical waveguides. The unstable silanol end groups, (-SiOH) on the cross linking molecules condense with the silanol end groups on the silicone chain, forming stable siloxane bonds (-Si-O-Si-) in the cured sealant. One part curing systems usually cure within one hour, depending on the temperature, thickness of the sealant and humidity. High modulus silicone sealants usually contain 80 to 85 parts silanol polymer, 5 parts crosslinker, and 0.01 wt. % tin catalyst.[70] After mixing the components, the sealant cures as shown in the scheme below, with the formation of ethanol as by product.

The developed material needed to contain to contain an acrylate functionality either added as monomers or by attaching acrylate functional groups to the polymer backbone. A silanol

terminated dimethyl diphenyl siloxane was chosen, due to its optical properties and speed of curing at room temperature with acryloxymethyl trimethoxy silane. Using this trifunctional cross linker, it was possible to produce an optically transparent, flexible material, which contained high refractive index functional groups attached to the polymer back bone. In the presence of a tin catalyst, the material is fully cross linked in under an hour at room temperature. The acrylate functional groups, in the presence of a two-photon photoinitiator, are polymerised by two-photon excitation. The material is also compatible with the specific two-photon photoinitiator, N-DPD.
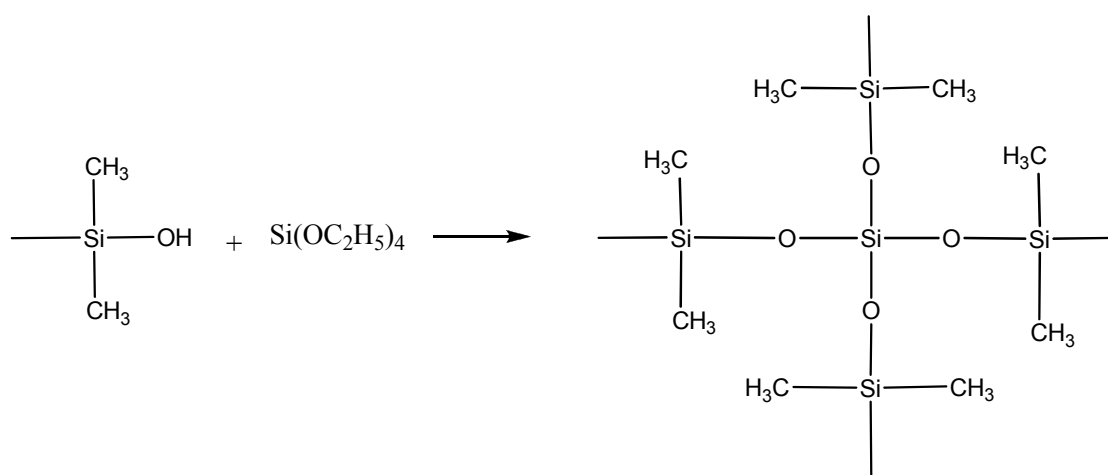

Figure 58: Example of silanol cross linking with a tetra-functional silane

6.2   Development of System C

The work carried out on System C was performed in cooperation with D. Zidar (Montan University, Leoben, Chair of Chemistry of Polymeric Materials, and some of the results in the following section can be found in the Bachelor Thesis[71].
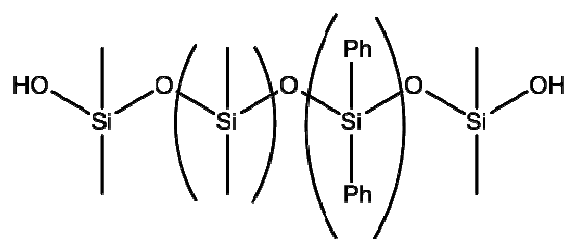
Silanol terminated diphenyl dimethyl polysiloxane (% OH 0.7-1.3, mole % diphenylsiloxane 2.5-3.5), acryloxymethyl trimethoxy silane and dioctyldilauryltin were purchased from ABCR GmbH (Germany), and used without further treatment. Irgacure 379 was supplied by CIBA Specialities (Basal, Switzerland).The specific two-photon photoinitiator 1,5-bis(4-(dimethylamino)phenyl penta-1,4-diyn-3-one (N-DPD), was utilised for all TPA experiments, and was developed and synthesised externally[72]. A description of the photoinitiator can be found in section 4.2.2.

The silanol terminated polysiloxane was cross linked with 20 wt. % acryloxymethyl trimethoxy silane, with the structures of all components displayed in Figure 59. The material can tolerate up to 30 wt. % cross linker, however the curing time has to be extended along with a higher

concentration of Sn catalyst. It was found that using the Sn catalyst dioctyldilauryltin in small concentrations speeded up the curing rate rapidly to less than one hour. This catalyst is different from a previous catalyst used, and has been chosen due to its lower toxicity In order to obtain homogeneous and dust free layers, the components were mixed thoroughly and filtered using a 0.45 µm PTFE syringe filter. 0.025 wt. % N-DPD was dissolved in the cross linker by ultrasonification, and the polymer, cross linker and 1 wt. % Sn catalyst were stirred for one hour during which a pre curing occurs, increasing the viscosity of the material. When all the components are mixed together, the viscosity is too low to form thin films, and when the material cures, due to the nature of condensation curing, the films do not have smooth surfaces, and when for example, mounted chips need to be fully covered on mounted substrates, problems arise when the layer is not flat over the diodes. The best way to achieve a homogeneous thin film is to scrape the material across the surface of the substrates. This can only be achieved when the material has a high enough viscosity, and with a material which cures fast enough not to flow and form films which are too thin. When the material is left to cure at room temperature, it cures from the top down through the material, meaning in the bulk, only the top layer cures, making it impossible to increase the viscosity. A pre curing step is therefore carried out whilst the material is stirred, at slightly elevated temperatures in a water bath, enabling sufficient moisture for the curing.

The specific two-photon photoinitiator N-DPD is compatible with this matrix material, with the crystals dissolving in the cross linker and no recrystallisation being observed. The commercial one-photon photoinitiator Irgacure 379; following long term exposure to ambient light conditions, "out blooms" in this material, with visible crystal-like structures appearing within two weeks. Following the sample preparation, thin films were prepared by scraping the material onto substrates to give film thicknesses of between 300 and 500 µm. Possible cross linking mechanisms occurring during the curing steps are presented in Figure 60. The material was then applied to substrates and cured at room temperature for one hour.
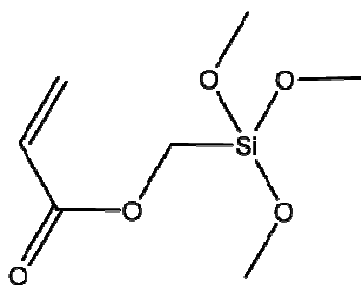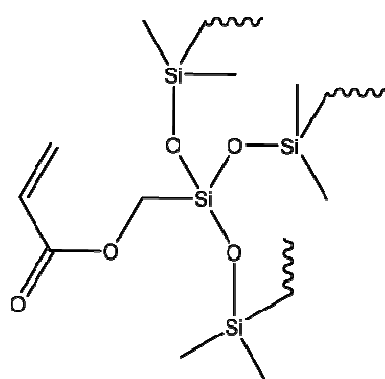
Figure 59: Structures of silanol terminated diphenyl dimethyl polysiloxane (a), acryloxymethyl trimethoxy silane (b), and the subsequent cross linked network (c)
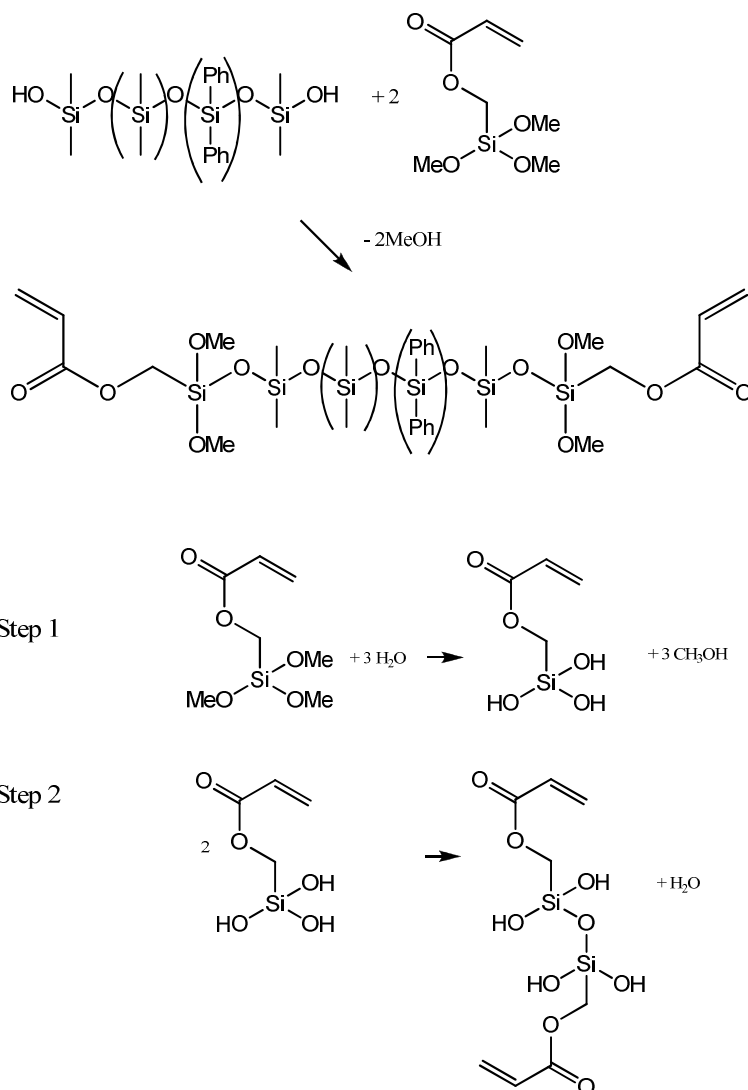
Figure 60: Possible cross linking reactions of silanol terminated polymer and acryloxy cross linker

6.3 Characterisation of Components Present in System C – FT-IR spectroscopy

Each component, used in the silanol matrix material, was characterised by FT-IR spectroscopy, by drop casting suitably diluted solutions onto CaF_2 plates. The characteristic peaks of the functional groups were identified, to aid the monitoring of the curing, as well as the polymerisation of the acrylate functional group attached to the polymer backbone. The next section includes the FT-IR spectra along with tables to identify the characteristic peaks.

Silanol terminated diphenyl dimethyl polysiloxane

The band corresponding to the OH vibration is relatively small in the spectrum, however the decrease is observed during the curing with the acryloxy cross linker.
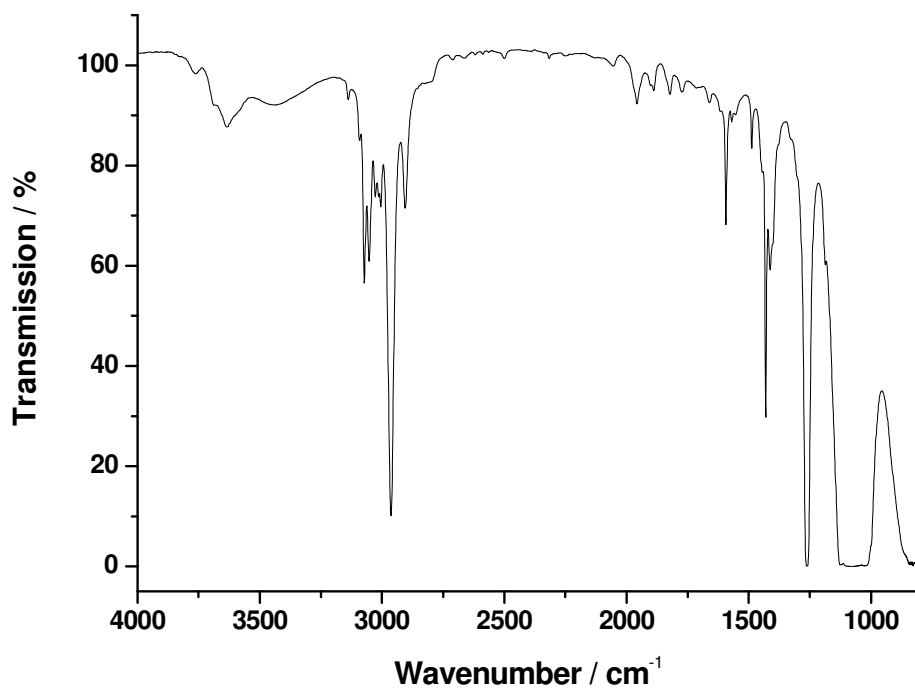

Figure 61: FT-IR spectrum of silanol terminated diphenyl dimethyl siloxane

Table 19: Characteristic bands observed in FT-IR spectra of silanol terminated diphenyl dimethyl siloxane

Characteristic bands (cm^{-1})	Responsible vibration
2948	O-CH$_3$ Stretching
1619, 1635	C=C Stretching
1731	C=O stretching
968,985	=CH$_2$ wagging
1258	Si-C vib

Acryloxy methyl trimethoxy silane

The spectrum of the acryloxy cross linker was used to monitor the double bond conversion of the acrylate functionality during UV polymerisation and is presented in Figure 62.
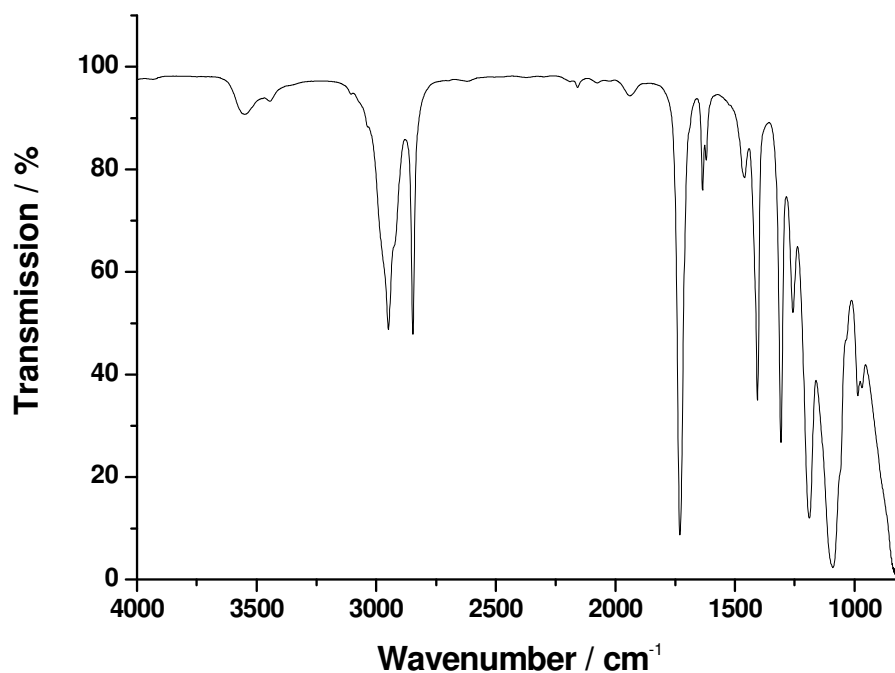

Figure 62: FT-IR spectrum of acryloxy methyl trimethoxy silane

Table 20: Characteristic bands observed in FT-IR spectra of acryloxy methyl trimethoxy silane

Characteristic bands (cm^{-1})	Responsible vibration
1262	Si-CH$_3$ Symmetric deformation
3634	O-H stretching
3071, 3052	C-H stretching (aromatic)
1592	C=C Stretching (aromatic)
1430	Ph-Si ring vibration
1070	Si-O-Si stretching vibration

6.4 Determination of the Conversion of Acrylate Functionality using Irgacure 379 and N-DPD – Time-based FT-IR

6.4.1 Sample Preparation

To determine if the acrylate functional group attached to the crosslinker acryloxymethyl trimethoxy silane polymerises under UV conditions and whether polymerisation occurs in the fully cross-linked material, time-based FT-IR spectroscopy was performed. FT-IR spectroscopy was carried out with samples containing Irgacure 379 as photoinitiator. Silanol terminated diphenyl dimethyl siloxane was cross-linked with 20 wt. % acryloxymethyl trimethoxy silane in the presence of dioctyldilauryltin as catalyst. Samples either contained 1 wt. % Irgacure 379, 0.025 wt. % N-DPD or no photoinitiator. The samples were spin coated onto gold plates to form thin films, and reflectance mode time-based FT-IR spectroscopy was carried out. The samples were placed in a reflectance cell which was purged with nitrogen, to avoid oxidation of the samples during irradiation. Time based software enabled spectra to be collected continuously while each sample was being illuminated. The samples were irradiated using an Omnicure spot cure lamp. In order to follow the rate of polymerisation closely, and then samples were irradiated with a higher light intensity. Following the collection of data, the spectra were used to calculate the double bond conversion, by calculating the peak area corresponding to the C=C double bond, calculating- the ratio against a reference peak. The results were then compared with samples containing N-DPD, Irgacure 379 and the samples containing no photoinitiator. Two sets of time based measurements were carried out, the first carried out using a very low light intensity of 0.1 W/cm^2. The samples prepared with Irgacure 379 and N-DPD were analysed in the same way

6.4.2 Results

Preliminary FT-IR spectra were recorded of samples containing the acryloxy crosslinker, to determine whether the bands were quantifiable. After a 10 second illumination time using a UV spot cure lamp, the peak observed at 1635 cm^{-1} decreased considerably with the sample containing Irgacure 379. The double bond conversion was found to be over 90 %. The samples containing the photoinitiator N-DPD, showed a very low double bond conversion, and even after one minute of UV exposure, the peak corresponding to the C=C in the FT-IR spectrum only decreased slightly, suggesting that the photoinitiator is very inefficient under one-photon conditions. Detailed spectra of the acryloxy cross linker pre and post 1 minute UV exposure are displayed in Figure 63. These results also suggest that the cladding material surrounding the waveguides should not polymerise under UV exposure when N-DPD is used as a photoinitiator in this matrix material. The results show that even at such a

low light intensity, samples containing 1 wt. % Irgacure 379 show a double bond conversion of nearly 50 % after around 6 minutes. In comparison, the sample containing N-DPD, showed a double bond conversion of less than 20 %. This suggests that under normal light conditions, the acrylate functional groups attached to the back bone of the polymer are unlikely to polymerise significantly, and that N-DPD will remain stable in the matrix. The graph also shows, as a comparison, a sample containing Irgacure 379, which was illuminated with a light intensity of 0.7 W/cm^2. After the same time period, a double bond conversion of nearly 90 % was achieved, with the highest conversion occurring in the first minute of light exposure. To continue with the time based experiments, a more realistic light intensity was used to illuminate the thin films, containing N-DPD and Irgacure 379. A sample, containing no photoinitiator was also treated in the same way, in order to determine if any polymerisation occurs, from the light intensity alone, or if oxidation occurs in the thin films, leading to a decrease in the C=C peak at 1635 cm^{-1}. A light intensity of 0.7 W/cm^2 was used on all three samples, which were illuminated for 15 minutes. A plot of the calculated double bond conversion for each sample is displayed in Figure 65. As was expected, the sample containing Irgacure 379, reached a double bond conversion of over 80 % after less than 5 minutes, with a rapid polymerisation occurring in the first minute. Comparing the samples containing no photoinitiator and N-DPD, the results were very similar, with both samples showing a very slow rate of polymerisation. The sample containing no photoinitiator showed a higher rate of polymerisation than expected, however after 12 minutes of illumination, a double bond conversion of less than 70 % was calculated. Using the photoinitiator N-DPD, a conversion of 80 % was achieved, however polymerisation occurred at a much slower rate than with Irgacure 379. All results suggest that although there is some activity using N-DPD as photoinitiator, under normal one-photon conditions, the efficiency is comparable to having no photoinitiator; therefore polymerisation should not occur in the cladding material.
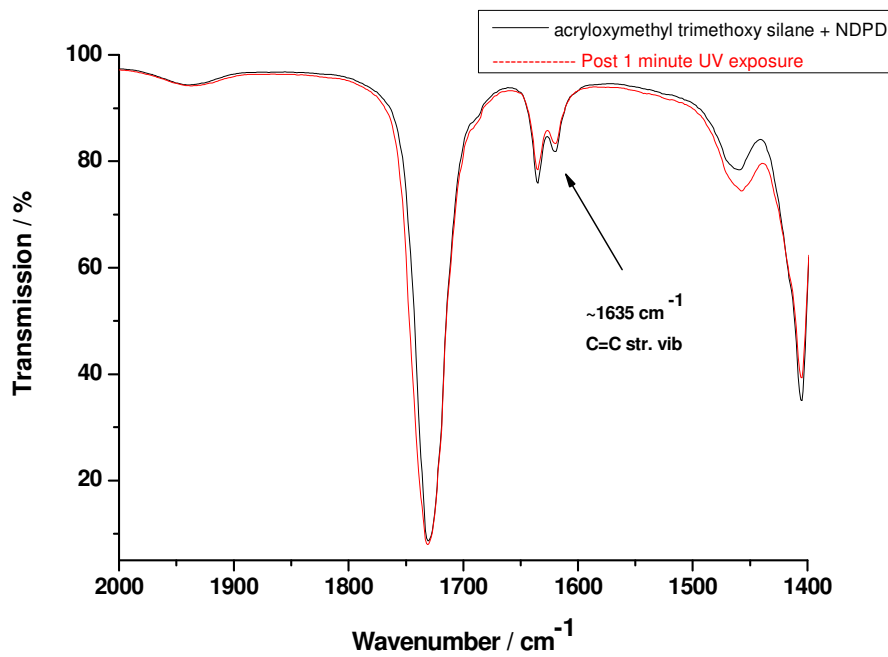
Figure 63: FT-IR spectra of acryloxymethyl trimethoxy silane including 0.025 wt. % N-DPD; pre and post 1 minute UV illumination
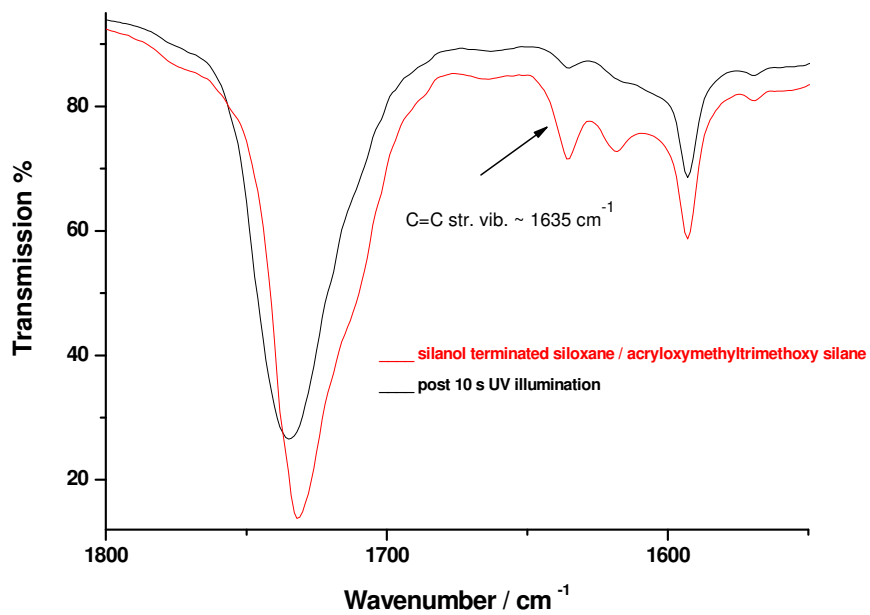

Figure 64: FT-IR spectra of low viscosity silanol terminated polydimethyl diphenyl siloxane cross-linked with acryloxymethyl trimethoxy silane including 1 wt. % Irgacure 379; pre and post 10 s UV illumination
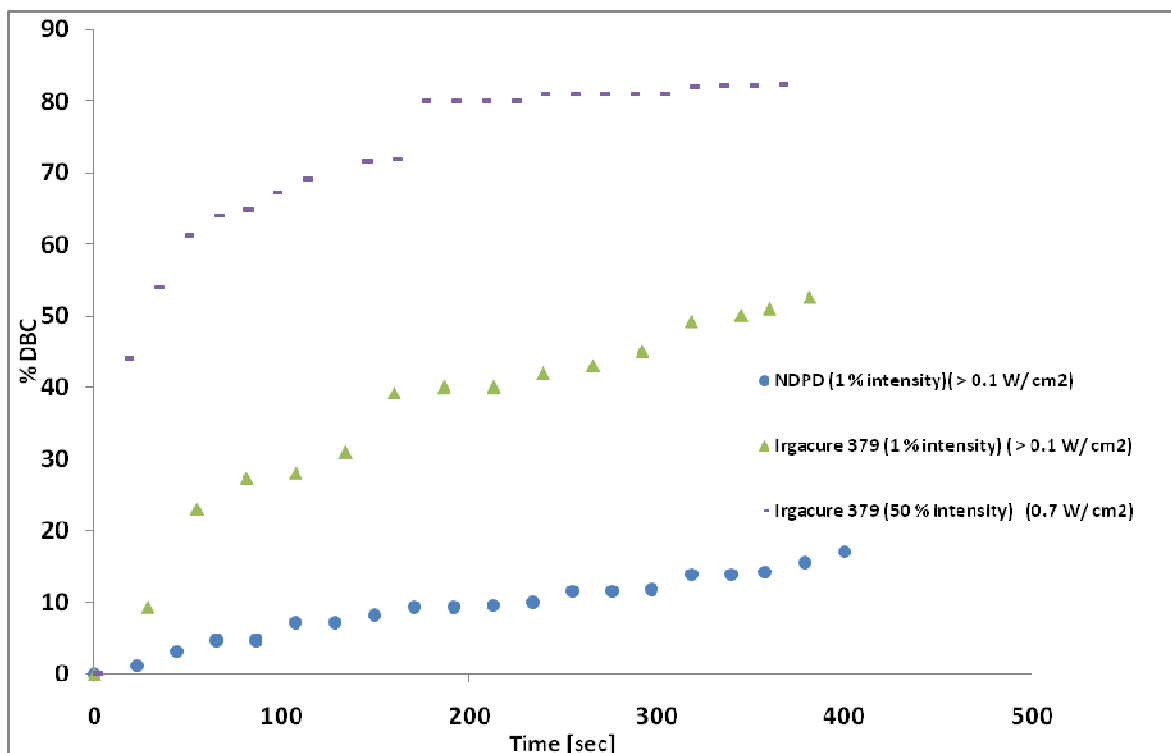
118

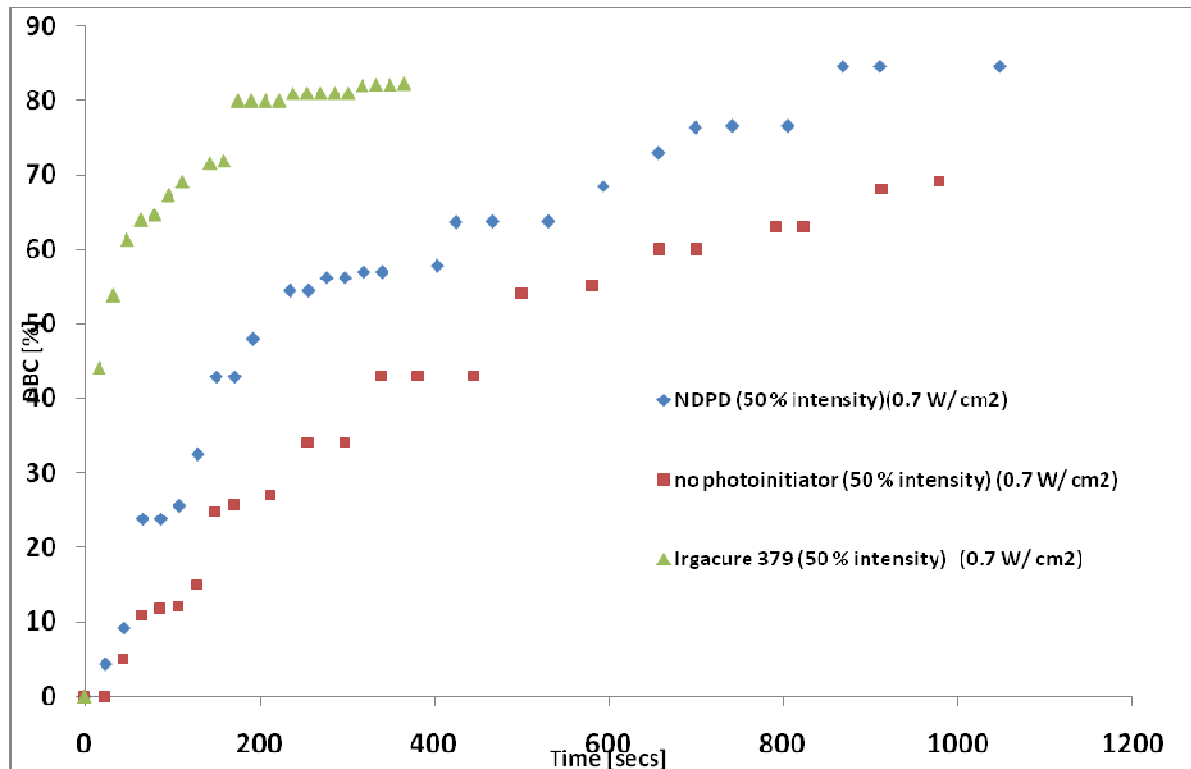**Figure 65: Double bond conversion upon UV irradiation using N-DPD and Irgacure 379 at different light intensities**

Figure 66: Double bond conversion upon UV irradiation using N-DPD, Irgacure 379 and no photoinitiator at a light intensity of 0.7 W/cm^{-1}

6.5 Determination of the Thermal Stability of System C – Simultaneous Thermal Analysis (STA)

6.5.1 Sample Preparation

To perform these measurements, an STA instrument coupled with Mass Spectrometry was used, making it possible to detect which molecules and components present in the matrix material were being lost upon heating. Three samples were analysed, to determine how the material is affected during thermal treatments. Samples were prepared in the same way as described in section 6.2. A thermal treatment of 150 ºC for 1 hour was then carried out on two samples, and then one of these samples was further heated at a temperature of 200 ºC for 10 minutes. Samples were measured from 20 to 300 ºC, with a heating rate of 10 ºC per minute. A comparison was made as to which components were removed during the thermal treatment.

A second set of investigations were carried out to compare the stability of illuminated and non illuminated matrix material. This essentially represented the core and cladding of the optical waveguides. Samples were prepared in the same way as the previous samples, but three samples were illuminated with a UV spot cure lamp, under nitrogen atmosphere, for 1 minute. Due to the fact that N-DPD is ineffective under normal one-photon conditions; 1 wt. % Irgacure 379 was added to the samples for these experiments. The non illuminated sample and one illuminated sample were then given no further treatment, whilst the two further samples were given a thermal treatment of 150 ºC for 1 hour. One of these samples was then further heated at 200 ºC for 10 minutes. Samples were analysed from 20 to 300 ºC, with a heating rate of 10 ºC per minute.

6.5.2 Results

The results of the first sample, which received no thermal treatment, are displayed in Figure 67 At 200 ºC the sample showed a weight loss of 5 %, with the MS data confirming that methanol and water were removed from the sample. It has been calculated that up to 6 wt. % of methanol could be produced through the curing process, so it is likely that this is responsible for some of the weight loss, along with water. Comparing this sample with the two samples which were thermally treated (Figure 68 and Figure 69), a weight loss of only 2 % was detected. This confirms that thermally treating the silanol matrix material removes only the methanol and water, produced from the condensation curing. At 300 ºC a weight loss of only 2 wt. % indicates the cross-linked matrix is stable, with no breakdown of the material occurring. These results are confirmed when the results are compared with the third

sample, which was thermally treated at 150 ºC for 1 hour, followed by 200 ºC for 10 minutes. The results of these two samples are almost identical, signifying a thermal treatment of 150 ºC is capable of removing remaining methanol and water, but also the material is able to withstand processing steps of 200 ºC without breaking down. The DSC trace was similar for all three samples, with one peak observed at around 300 ºC in the trace, corresponding to the sample which was not thermally treated. This is likely to represent a breakdown of the material, due to the sample being held at 300 ºC for 10 minutes. The material was not fully cured, leading to a lower thermal stability. No peaks of troughs were observed in the DSC traces for the thermally treated samples, suggesting no oxidation or decomposition occurred in the material.

Four more samples, prepared in the same way, were analysed to investigate the stability of illuminated and non illuminated material. The results of the STA analyses are presented in Table 21. Each of the four samples analysed was compared to the previous samples, to determine whether the illuminated material (waveguide core) is thermally stable. Each TGA trace was used to measure the weight loss at 200 °C. The results showed that illuminated material appeared to be slightly less stable, however the weight loss varied by less than 1 %. The MS data corresponding to the materials which were not thermally treated showed ion peaks with m/z values of 18 and 32, corresponding to water and methanol. These components would be removed from the matrix during a 150 °C thermal treatment. The results demonstrate the silanol terminated polysiloxane is a stable material, able to withstand processing temperatures.
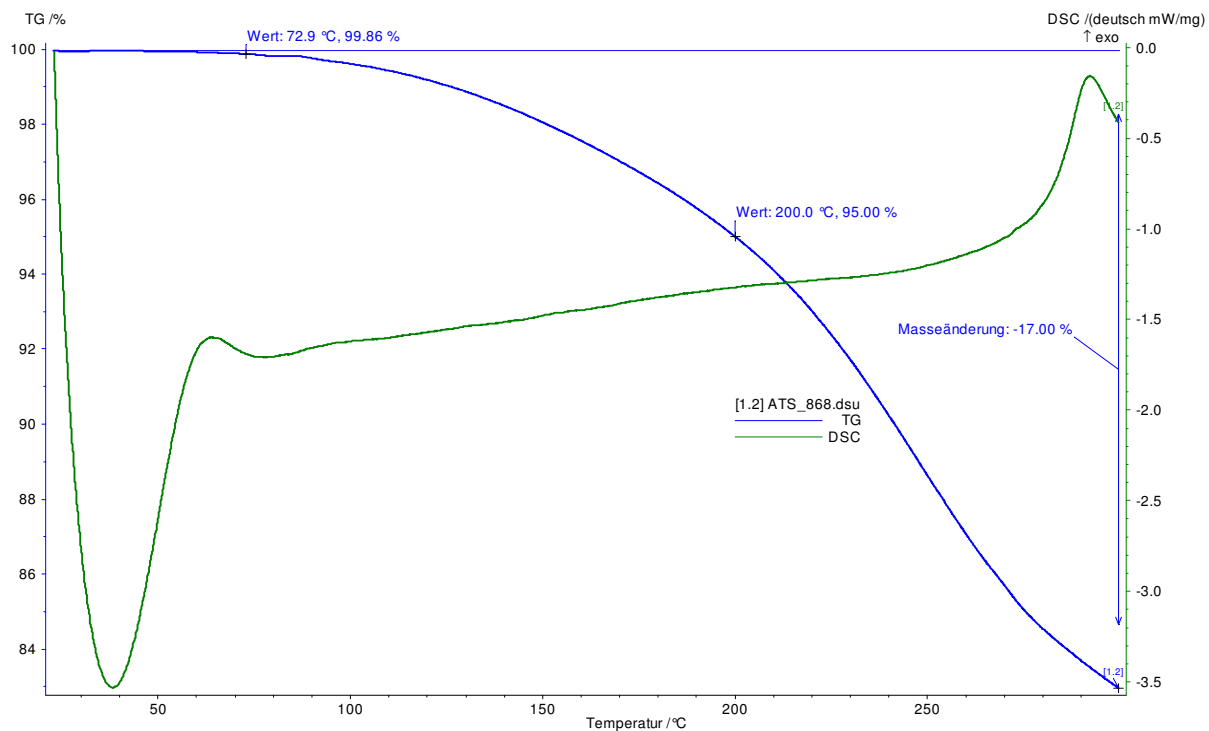
Figure 67: Silanol terminated polysiloxane cross-linked with 20 wt. % acryloxymethyl trimethoxy silane (no thermal treatment)
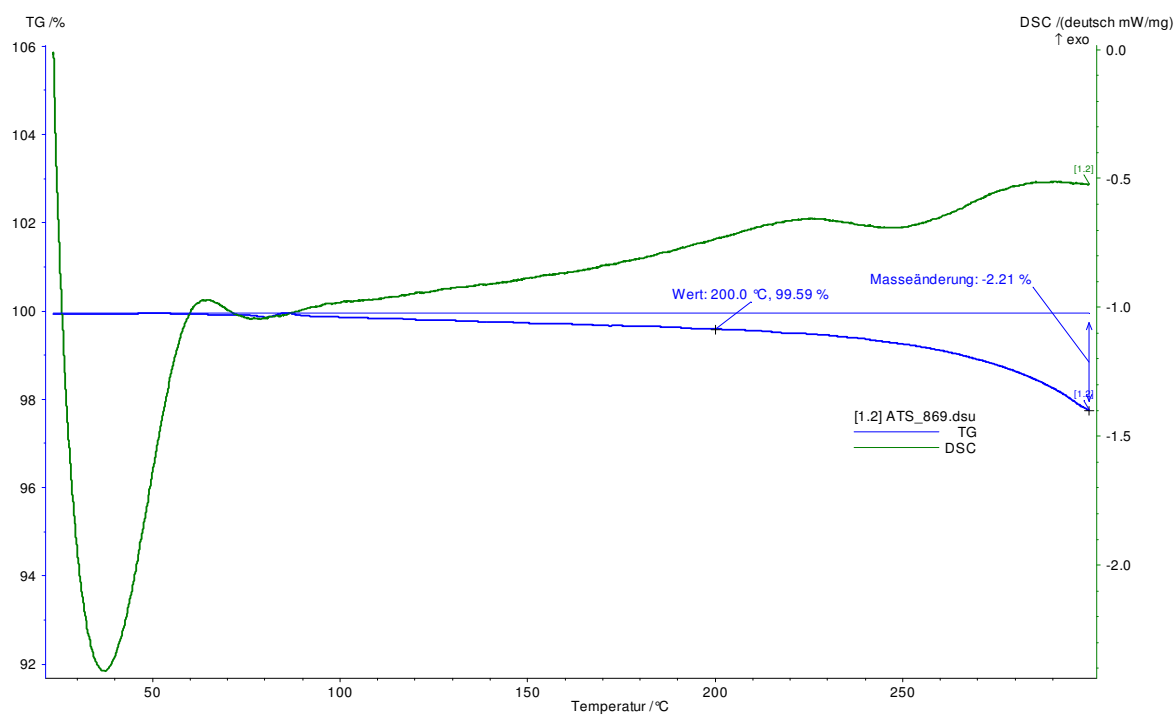

Figure 68: Silanol terminated polysiloxane cross-linked with 20 wt. % acryloxymethyl trimethoxy silane (thermally treated – 150 ºC, 1 hour)
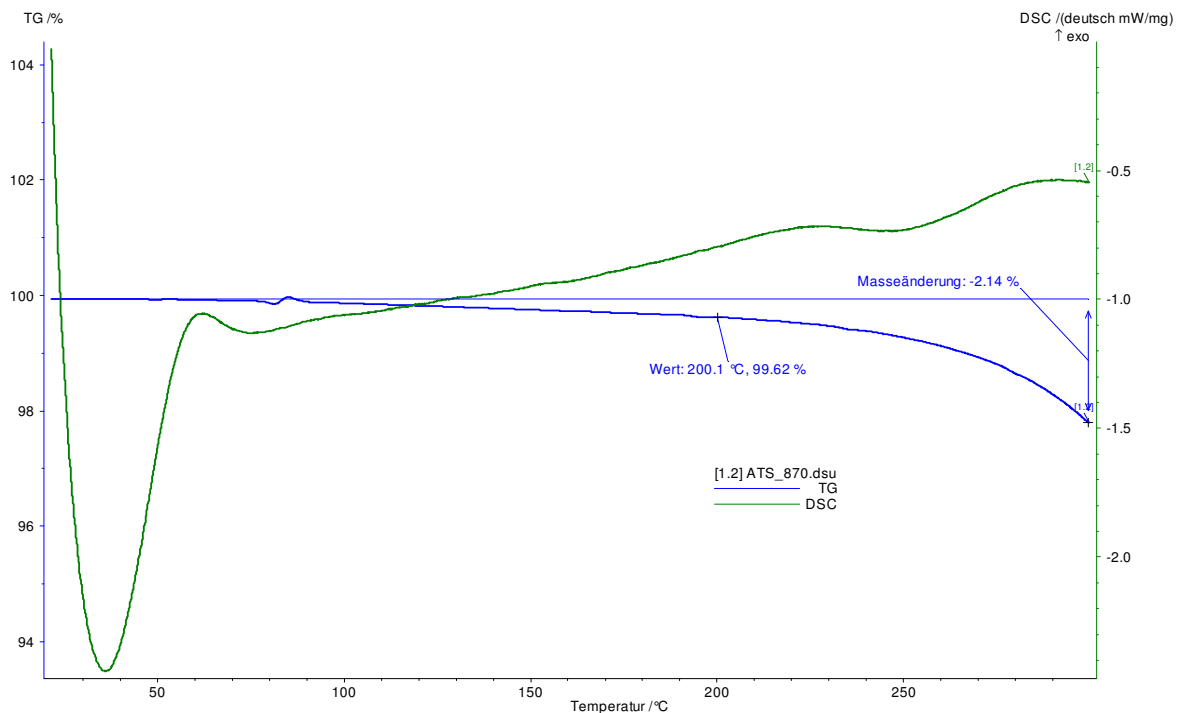
Figure 69: Silanol terminated polysiloxane cross-linked with 20 wt. % acryloxymethyl trimethoxy silane (thermally treated – 150 º C, 1 hour plus 200 ºC 10 min)

Table 21: STA results of all samples, comparing the weight loss at 200 ℃

Sample Description	Wt. loss at 200 ℃ (%)
No thermal treatment / non illuminated (N-DPD)	5
150 ℃ / non illuminated	0.41
150 ℃ / 200 ℃ non illuminated	0.38
No thermal treatment / non illuminated (Irgacure 379)	4.9
No thermal treatment / illuminated	5.5
150 ℃ / illuminated	0.82
150 ℃ / 200 ℃ illuminated	0.7

6.6   Conclusion

A material consisting of a silanol terminated polysiloxane cross linked with acryloxymethyl trimethoxy silane has been characterised and investigated for its suitability as a material used to produce optical interconnects. Previous materials, described in sections 4 and 5, incorporated high volatile, high refractive index methacrylate or acrylate monomers, which needed to be removed following the structuring of waveguides by two-photon polymerisation. Using this material means curing can be carried out rapidly at room temperature, leading to decreased processing times and the absence of high curing temperatures. Condensation curing of a silanol terminated polymer, with moisture sensitive functional silanes, produces a fully cross-linked, yet flexible and transparent matrix material in under an hour at room temperature. The non-hydrolyseable substituent on the silane cross linkers influence how long the curing takes place, with vinyl and methyl groups being utilised for fastest curing speeds. The optical material is flexible, transparent and rapid curing, and can be used in conjunction with the two-photon specific photoinitiator N-DPD. Following the development of this optical material, optical characterisation was performed, along with the production of optical waveguides on PCB`s via two-photon photopolymerisation, the results of which can be found in section 9.

Optical Characterisation

System A

7 Optical Characterisation of a Material Developed from Vinyl and Hydride Terminated Polysiloxanes (System A)

7.1 Introduction

System A, after being fully characterised, was investigated for its optical properties. This section summarises results of optical experiments performed on System A, which are described in detail elsewhere[73]. Based on the properties of waveguides, the material must fulfil a number of requirements. The following section explains each method used to characterise the optical material, continuing to the production of optical interconnects. The material and subsequent optical waveguides, structured by two-photon polymerisation, were characterised by ellipsometry, to determine the refractive index difference between the waveguide and core. Cut back measurements were performed on the written waveguides to determine the optical losses, and phase contrast and optical microscopy were performed to examine the 3D optical waveguides.

7.2 Ellipsometry

7.2.1 Introduction

Based on waveguide geometry, the waveguide core must have a higher refractive index than the surrounding cladding material. The two-photon polymerisation of the methacrylate monomers leads to an interpenetrating network inside the siloxane material, leading to an increase in refractive index.

The refractive index of the UV illuminated and non illuminated thin films were measured by spectroscopic ellipsometry. From ellipsometric data the dispersion of the refractive index (Cauchy fit) could be measured. For our work, we were interested in the index of refraction at the telecom wavelengths of 1310 and 1550 nm, as well as the datacom wavelength of 840 nm. For the sample preparation, the epoxy diamine matrix material was spin cast onto silicon wafers. The samples were then given a pre curing step at 80 °C. Half of the samples were then illuminated using a spot cure lamp. All samples were then given a thermal finishing treatment of 100 °C.

7.2.1 Results

The results of four samples analysed are described. Two samples contained 8 wt. % methacrylate monomers, and two samples contained 10 wt. %. All samples contained 1.8 wt. % Irgacure 379 as photoinitiator. Only two samples were given a thermal pre treatment, in order to determine how the refractive index is affected by illumination performed on the cured

and non cured material. The results are summarised in Table 22, with the results included for the telecom and datacom wavelengths. A Cauchy fit of the refractive index difference achieved for the sample containing 8 wt. % methacrylate monomers is presented in Figure 70. An illumination time was chosen so that the maximum photoinduced polymerisation was achieved. For all samples at the wavelengths of interest, a difference in the index of refraction of $\Delta n = {\sim}0.02$ was obtained. There appeared to be only minor differences in using 8 or 10 wt. % monomers in the samples, as well as performing a thermal pre treatment. Using 8 wt. % methacrylate monomers in the polymer mixture appears to lead to a slightly higher difference in the refractive index, however the thin films used for TPA structuring have a lower flexibility.

Table 22: Ellipsometry results comparing samples containing 8 and 10 wt.% monomers, and including and omitting the pre thermal treatment

Sample	Wavelength [nm]	n (non illuminated)	n (illuminated)	Δn
8 wt. % monomers	850	1.468	1.489	**0.022**
	1310	1.464	1.482	**0.018**
	1550	1.464	1.481	**0.017**
10 wt. % monomers	850	1.469	1.486	**0.017**
	1310	1.464	1.479	**0.015**
	1550	1.463	1.478	**0.014**
8 wt.% no pre treatment	850	1.470	1.490	**0.021**
	1310	1.468	1.484	**0.016**
	1550	1.467	1.483	**0.015**
10 wt.% no pre treatment	850	1.470	1.487	**0.018**
	1310	1.465	1.482	**0.019**
	1550	1.465	1.481	**0.017**

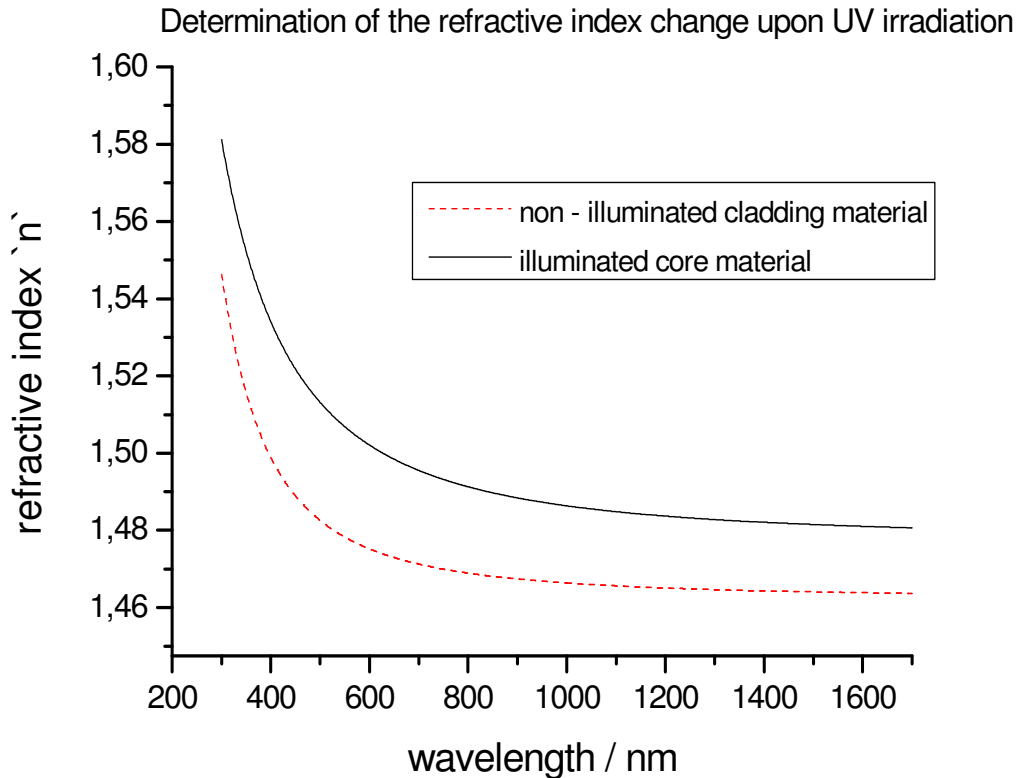Determination of the refractive index change upon UV irradiation

Figure 70: Cauchy fit of the refractive index of illuminated and non illuminated regions at different wavelengths, with a sample containing 8 wt% monomers

7.3 TPA Structuring

7.3.1 Introduction

TPA material testing was performed on our material, to determine whether optical waveguides could be structured successfully in thin films. TPA material testing was performed using an ultra fast titan – sapphire laser system (Mai Tai, pulse duration: 120 fs, repetition rate: 1 kHz) at a wavelength of 600 nm. Material testing was performed on thin films, to determine firstly, the fabrication window which can be used to structure. High laser powers can lead to a burning or ablation of the material, and too low, and waveguides of very low contrast will be structured. Adjusting the optics of the laser can be performed to alter the shape of the cross section of the waveguide structures, which can be observed using optical microscopy. The cross sections of the written waveguides are observed only when the material can be effectively cut, enabling the in-coupling of light into the waveguide. Phase contrast microscopy can be used to characterise the waveguide structures, as areas of different refractive index can be visualised. During such material testing, the laser system needs to be fully optimised, in order to obtain the best performance from the optical material. Two-photon processing can then be used to fabricate waveguides using only our optical polymeric material. The laser is focused into the material, usually scraped onto glass slides

or rigid-breakable FR-4 substrates, with a layer thickness of between 300 and 500 μm. The absorption of the material at the laser wavelength is low, which enables the fabrication of the waveguides with high precision between 80 and 250 μm below the surface. The photon density in the focal volume is sufficient to initiate the cross linking of the methacrylate monomers, forming a solid structure embedded in the non-exposed surrounding cladding material.

The method of TPA material testing described here is the same used for all three optical materials described in this work, with only minor changes to the laser system which will be mentioned. The results of the material testing obtained using this material are described in detail elsewhere, along with the results of the fabrication of demonstrators[56]. This section is therefore used to describe how the processes were performed, with more detailed results using the newly developed epoxy / diamine and silanol terminated optical materials in sections 8 and 9.
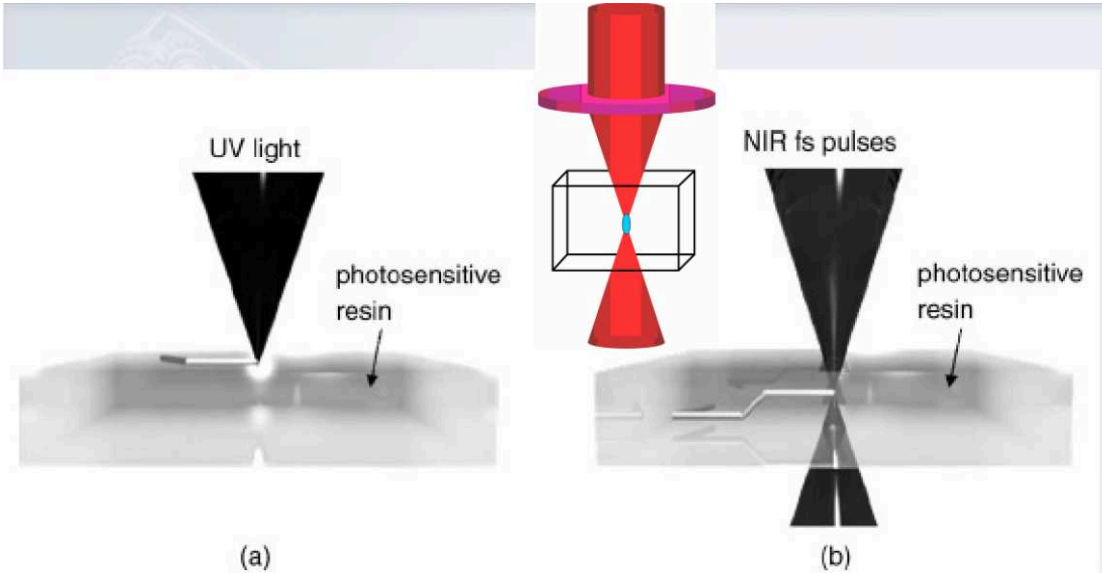

Figure 71: Representation of one-photon and two-photon absorption

7.3.2 Results

The polysiloxane material was coated on glass slides or rigid-breakable FR-4 substrates to perform TPA material testing. To determine the fabrication window of the material, structures were inscribed using different laser powers between 550-800 µW. Phase contrast was then used to observe the waveguides, using an Olympus BX 51 microscope. An example of the phase contrast images are seen in Figure 72 and Figure 73. The first aspect to be noted when observing the waveguide structures is the contrast, with a higher contrast produced when the difference in refractive index is greater. The second point to note is that non interrupted structures are produced, which do not include burns or defects. This can occur when the laser power is too high, as well as when particles and impurities are present in the material

The cross section of the waveguides is related to the laser power, the adjustment of the optics and the reactivity of the monomers. Using this material, the cross sections of the waveguides were between 25 and 35 µm. An example of the cross sections is shown in Figure 74. Short waveguide structures were written on rigid-breakable substrates, which enabled the material to be cut, using a rotary cutter. Optical microscopy was then used to characterise the cross sections, enabling the shape, size and depth of the structures to be optimised. The correct laser power and optical beam quality can then be decided, as different optical materials behave differently during the TPA process. Prior to the fabrication of demonstrators this process is carried out, as any change in the composition of the material, as well as slight changes in the laser system, can lead to differences in the performance of the fabrication.
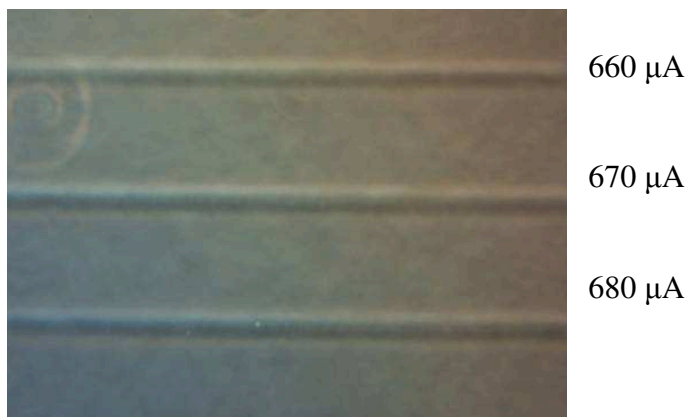

660 µA

670 µA

680 µA

Figure 72: Waveguides structured using different laser powers, observed using phase contrast microscopy. Siloxane matrix material containing 8 wt. % monomers
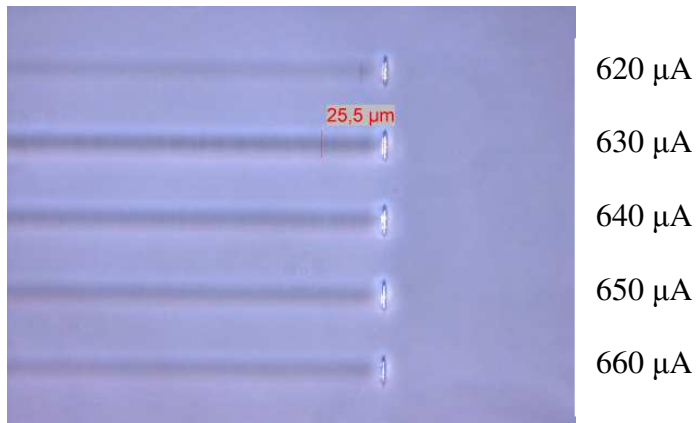
620 µA

25,5 µm

630 µA

640 µA

650 µA

660 µA

Figure 73: Waveguides structured using different laser powers, observed using phase contrast microscopy Siloxane matrix material containing 10 wt. % monomers
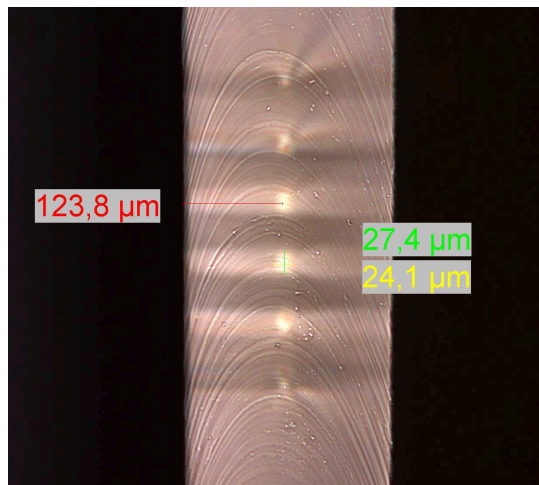

123,8 µm

27,4 µm

24,1 µm

Figure 74: Waveguide cross sections structured using different laser powers, observed by optical microscopy

7.4 Fabrication of Optical Interconnects

7.4.1 Introduction

Once initial TPA material testing has been performed, optoelectronic printed circuit boards can be fabricated. Figure 75 shows a schematic representation of such a board. During this work, all materials were used for the production of experimental rigid and rigid-flex boards, shown in Figure 76. The integrated optical connections include a vertical-cavity surface-emitting laser (VCSEL), which is mounted upright, emitting light at a wavelength of 850 nm, parallel to the surface of the substrate, shown in Figure 77. On the opposite side, a photodiode is mounted, facing the VCSEL. The components are completely embedded in a

layer of the optical material, between 300 and 500 µm thick. The TPA written waveguide then connects the optical components.
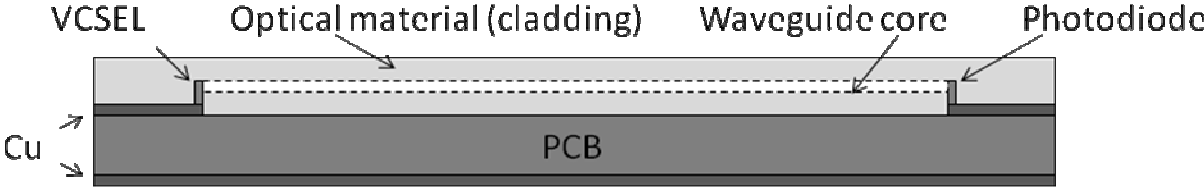

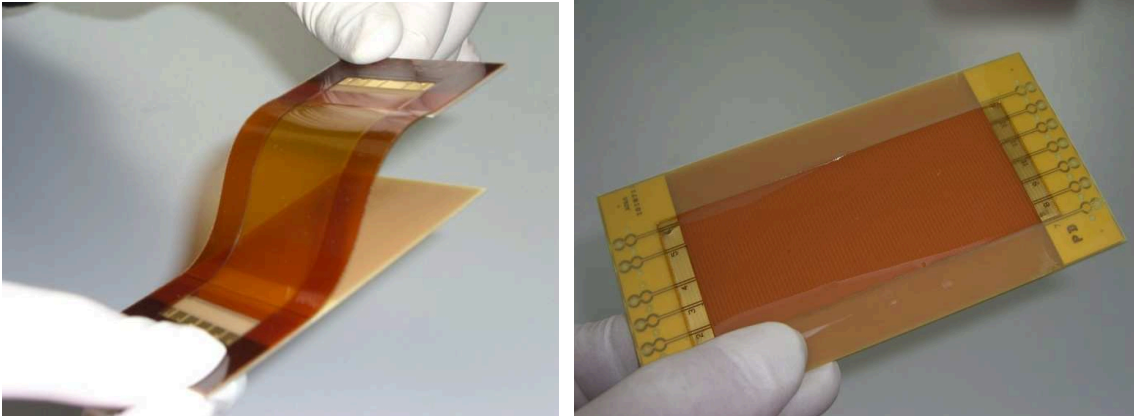**Figure 75: Schematic representation of an optoelectronic PCB**

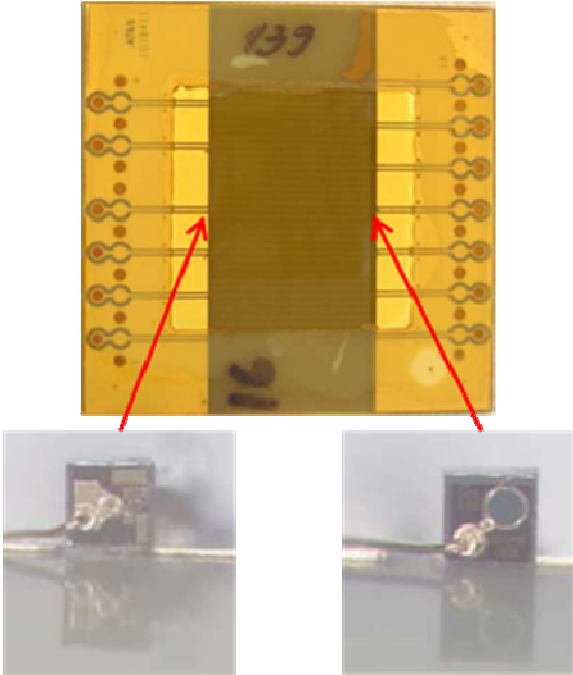**Figure 76: Printed circuit board with mounted laser and photo diodes. Rigid-flex (left) and rigid board**

Figure 77: Printed circuit board with optical components. Mounted on the left side is

the laser diode, and on the right side the photodiode

The waveguide fabrication process is performed by collecting an accurate 3D representation of the sample, which is required to correctly align the waveguide on the active areas of the optoelectronic components[74]. The x-y position of the components is determined using a CCD camera. The surface of the optical material as well as the z position of the components is determined by monitoring the intensity of the back-reflected light of a He-He laser with a photodiode using a confocal setup. Once the start point, end point and waveguide path are defined, a correctly aligned waveguide can be structured. Misalignment of the waveguide with the optoelectronic components can result in loss of light during in and out coupling. Using this method, waveguides can be structured at different depths, allowing more than one waveguide to be written. During our demonstrator processing, the usual method was to write a waveguide bundle, consisting of a mother waveguide surrounded by six further waveguides. The photocurrent was measured before, during and after the TPA structuring. The photocurrents of the demonstrators before and after the TPA structuring of waveguides were recorded using a Keithley 6485 Picoampermeter and the laser diode is driven with 6 mA by a Newport 505B Laser Diode Driver.

7.4.2 Results

This material was the first to be used to develop optical interconnects. The material has a high enough viscosity to be applied onto the demonstrators using a specially designed scraper, producing a layer thickness of 500 or 300 µm. Rigid substrates were investigated first, with a length of 7 cm between the optical interconnections. Table 23 includes the photocurrents of the fabricated rigid demonstrators, recorded before, after and following a few days storage. The photocurrent was always taken during these times, to firstly calculate the photofactor, (f), which is defined as the ratio Φ_s/Φ_0 where Φ_0 is the photocurrent prior to the structuring of the waveguides and Φ_s the photocurrent recorded following TPA structuring. Following TPA structuring, the photocurrent also increases slightly, due to photoinitiator radicals still be present in the material, leading to a post polymerisation, which is believed to further improve the interconnecting cross linking inside the waveguide core. Although the photocurrents obtained following TPA structuring were quite low, photocurrent did show an increase in all demonstrators which were fabricated by correctly connecting the laser and photo diodes. With each demonstrator, waveguide bundles were structured, with the mother waveguide being structured at an average depth of 125 µm below the surface. A feed rate of 20 mm/minute was used, with laser powers of between 700 and 800 µW.

Table 23: Photocurrent measurements of rigid demonstrators, pre and post TPA and after a few days storage

Photocurrent pre TPA [μA]	Photocurrent post TPA [μA]	Photocurrent post storage [μA]
1.3	107	83.1
1.4	49	47.5
0.3	22	16
1.4	88	81
0.45	34	32
0.8	70	87.8

Following the TPA structuring, an average photofactor of 80 was achieved. The increase in the photocurrent is believed to arise from the whole waveguide bundle, with each separate waveguide participating. As more waveguides are structured, there is a general increase in the photocurrent, however if the written waveguides are structured too high or too deep into the material it is possible to burn the substrate, as well as the material. A chart of the obtained photocurrents is included in Figure 78.
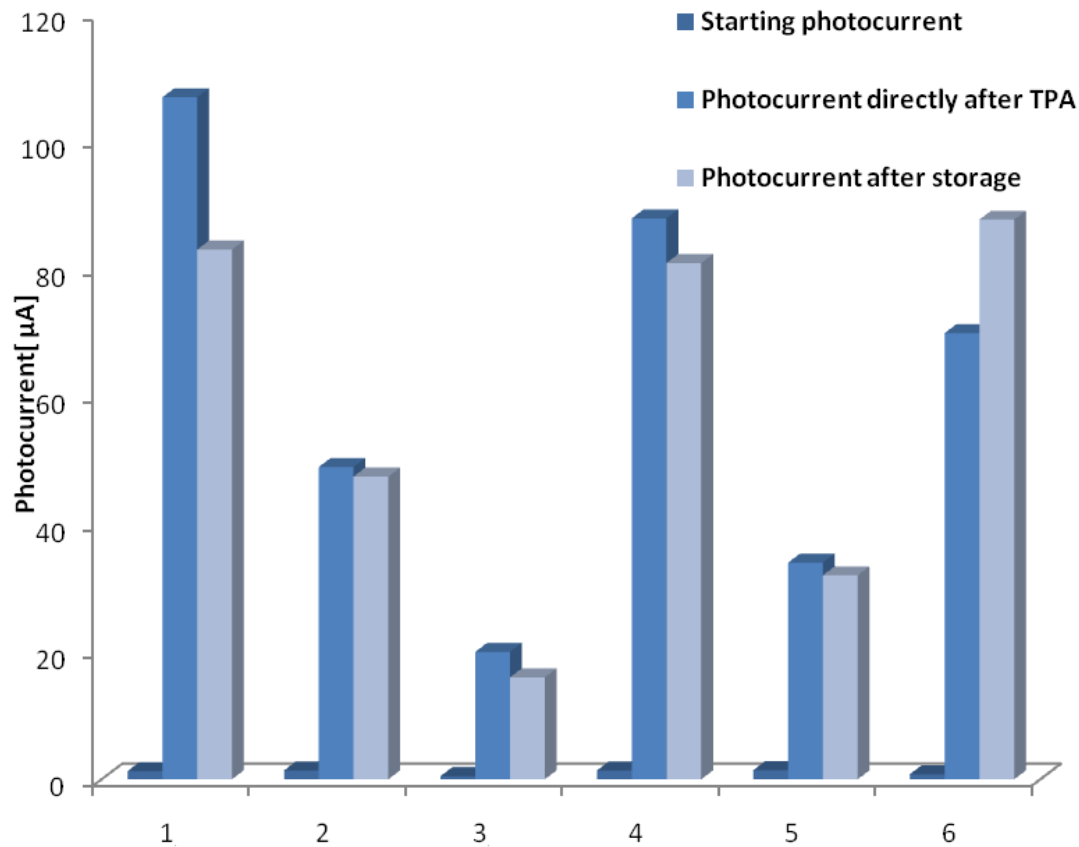
Figure 78: Results of the detected photocurrents before TPA, after and after a few days storage of a number of optical PBCs

Using this material to produce rigid-flex demonstrators was more of a challenge, due to a "step" present just before the diodes. This step is the area where the substrates can be disassembled, allowing the removal of the polyimide foil from the FR-4 substrate. During the structuring, the photocurrent goes down, due to a loss of light, attributed to scattering in this area. For this reason, lower photocurrents were achieved using such substrates. Successful structuring was however performed, with an increase in the photocurrent recorded for all correctly aligned waveguides. Table 24 includes the resulting photocurrents achieved before, after TPA structuring and following a few days storage. The material performed well, with no burns or ablation occurring during the TPA fabrication. Scattering centres were however visible over the area of the step, indicating higher photocurrents are possible using differently designed substrates. The results are also presented in Figure 79.

Table 24: Photocurrent measurements of rigid-flex demonstrators, pre TPA structuring, post TPA and after a few days storage

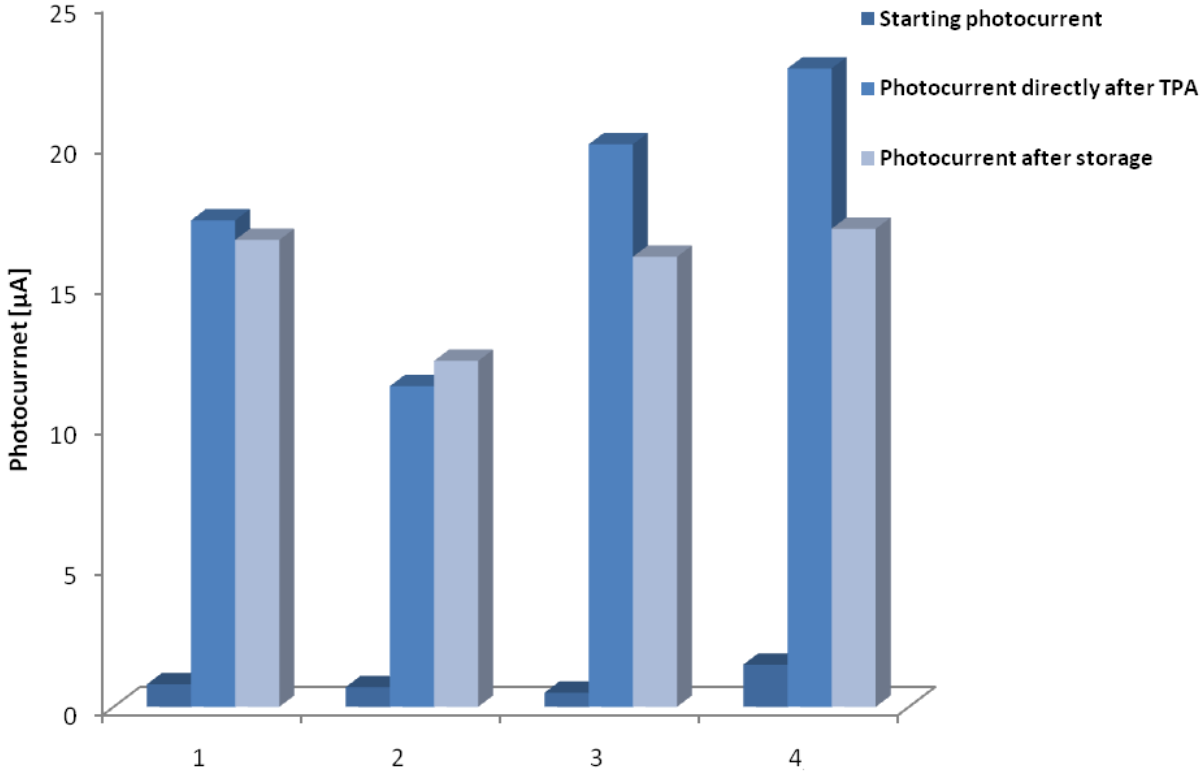| Photocurrent pre TPA [µA]	Photocurrent post TPA [µA]	Photocurrent post storage [µA]
0.8	17.3	16.6
0.7	11.4	12.3
0.5	20	16
1.5	22.7	17

Figure 79: Results of the detected photocurrents before, after and after a few days storage of a number of flexible optical PBCs

Following TPA structuring, a post thermal step needs to be performed on the demonstrators, in order to remove the remaining methacrylate monomers. This not only stabilises the material by producing a fully cross linked network, but also the refractive index difference between the waveguide core and cladding is increased. A 100 °C baking step, for 20 hours

(40 mbar) was carried out, and the photocurrents were measured. This step has been found to have a detrimental effect on the written waveguides, leading to an average decrease in the photocurrent of 30 %. It is clear that the waveguides were not destroyed, as photocurrents of an acceptable level were detected, however it is believed that a shrinkage occurs, causing the coupling of light into the waveguide to be altered. The correct alignment of the waveguide between the optical components results in the highest photocurrents, due to the fact that the light is effectively in-coupled. All demonstrators fabricated using this material, following the post thermal treatment showed a decrease in photocurrent, which cannot be explained. It is also possible methacrylate monomers, present in the waveguide core are removed during the thermal treatment, leading to defects in the interface between the core and cladding.

7.5 Conclusion

This polysiloxane matrix material is well suited for the use in TPA applications. The processing and characteristics of the material were optimised, leading to a suitable ratio of high refractive index methacrylate monomers to be included in the material, thus forming a tight network of polymethacrylate waveguide core via photopolymerisation. Optical losses of the waveguides were found to be low, and cut back measurements, including light extraction tests were performed, proving the effective functioning of the waveguides. A high enough difference in the refractive index is achieved between the waveguide core and cladding, determined by spectroscopic ellipsometry, with a difference of ~ 0.02 in the telecom and datacom regions achieved. This is the first material used to fabricate fully operating demonstrators, on rigid and rigid-flex substrates. Waveguides were correctly aligned between optical components, leading to an increase in the photocurrent, which remained stable for over one year, when stored under temperatures of 80 and 10 °C. Following post thermal treatment of the demonstrators, the decrease in photocurrent led to the conclusion that a material needs to be developed which has a higher thermal stability, and can be used in combination with acrylate monomers, which are more reactive, and likely to enable the fabrication of waveguides with larger cross sections. Continuing with a polysiloxane backbone, a new material was therefore developed which had a higher stability and could be used with more reactive acrylate monomers. This material (System B) is described in section 5 and results of optical characterisation are presented in Section 8.

Optical Characterisation

System B

8 Optical Characterisation of a Material developed from Epoxy Terminated Polysiloxane Cross linked with a Diamine (System B)

8.1 Introduction

An epoxy terminated polysiloxane, cross linked with 1,3-bis(3-aminopropyl)tetramethyl-disiloxane, described in section 5, was optimised and used as an optical material for TPA fabrication of optical waveguides. STA experiments reveal the material has a high thermal stability, as well as the acrylate monomers being removed straightforwardly during a post thermal treatment, producing a stable matrix following TPA. Once the development and processing the material were optimised, a series of optical characterisation experiments was performed, to firstly, establish whether the material was optically transparent on the telecom and datacom regions of the NIR spectrum, and to ascertain the difference in refractive index between the cladding and waveguide core. All waveguiding materials need to have low optical losses in such wavelengths. Optical losses can arise from absorption, scattering, polarization dependence, reflectance, radiation and coupling[75]. C-H and O-H overtones can be absorptive in the telecommunication window, and so using a polymer such as ours, containing diphenyl substitutions, should have no electronic absorptions which contribute significantly to optical losses.

Ellipsometric spectroscopy was performed on thin layers of System B, using UV illuminated and non illuminated samples, however bad adhesion to the silicon chips, even after a surface modification, made the measurements extremely difficult. Simple investigations using an Abbe refractometer, enabled the refractive index difference to be determined between the samples, at a wavelength of 589 nm. The change in refractive index was measured as the sample was cured and then UV illuminated on the Abbe prism, giving us an indication of how the refractive index changes during these conditions.

8.2 NIR spectroscopy

8.2.1 Sample preparation

Optical waveguides need to have low optical losses, particularly at the major telecommunication wavelengths, which are 1310, 1550 and 840 nm. To determine whether absorbance's in these regions are causing optical losses, NIR spectroscopy was performed.

System B was prepared in the same way as described in section 5.5. The material was then placed in plastic cuvettes and left to cure at room temperature for ~ 20 hours. Following an initial spectrum of the matrix material, the sample was illuminated for 15 seconds on each

face of the cuvette, using a UV lamp. This was carried out to determine differences in the optical losses of the cladding and core of the written waveguides. In order to determine whether the absorbance at certain wavelengths causes optical losses, the results were compared with that of System A which showed good structuring behaviour, with high photocurrents achieved when demonstrators were fabricated.

8.2.2 Results

The analysis of System B is presented, with the spectra of the irradiated and non-irradiated samples displayed. The transmission is firstly displayed in Figure 80 followed by the damping in Figure 81 Two tables, displaying the results firstly from the hydride / vinyl terminated polysiloxane matrix as a comparison are presented in Table 25 and Table 26.
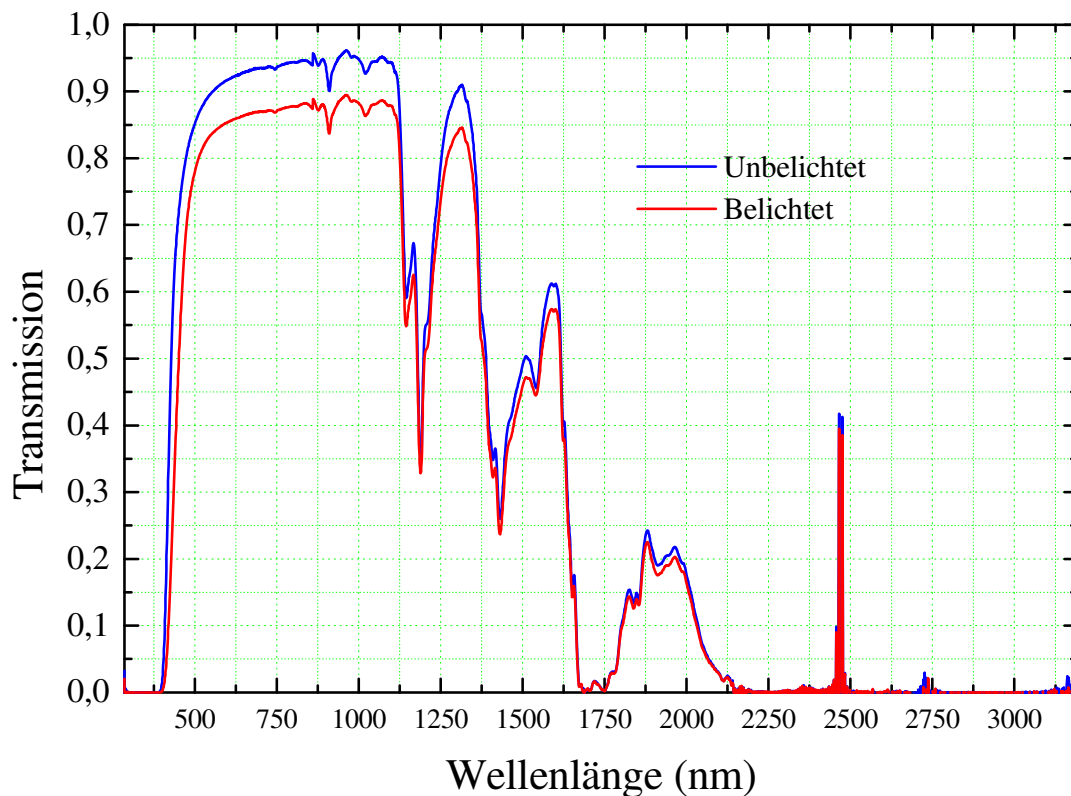

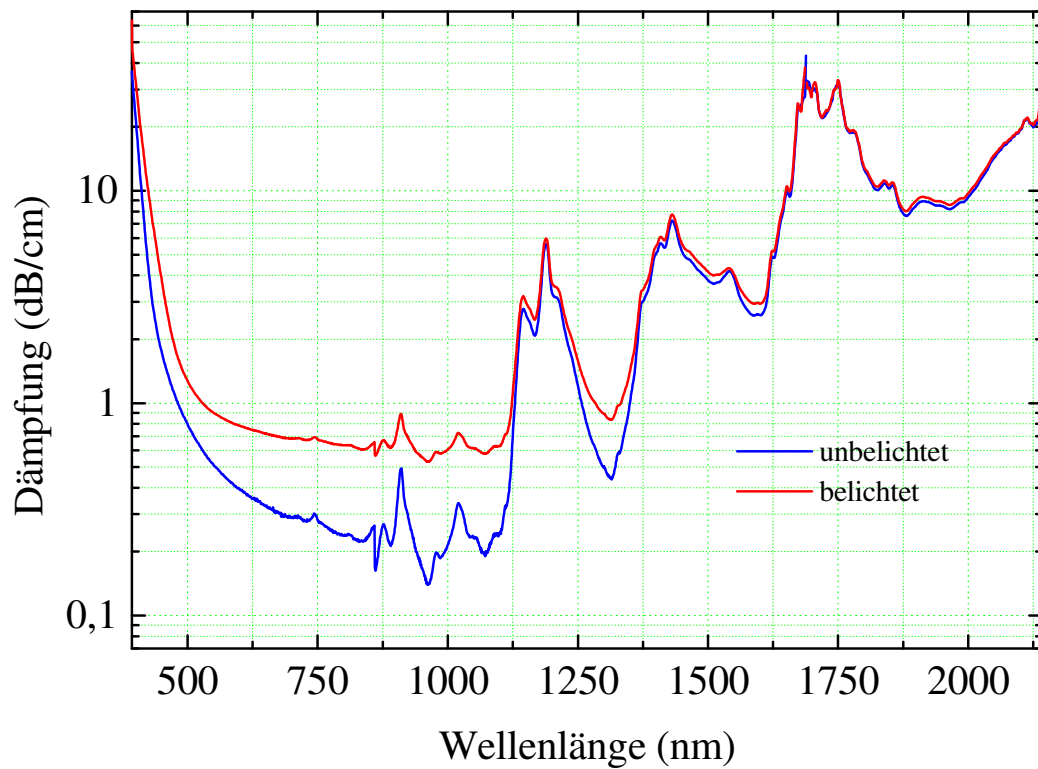**Figure 80: NIR spectra of the epoxy / diamine matrix material, pre and post UV illumination**

Figure 81: NIR spectra of System B, pre and post UV illumination, displaying the wavelength against damping (dB/cm)

Table 25: Table displaying transmission results from System A (description of samples is shown below)

Band	Sample1	Sample 2	Sample 3	Sample 4	Sample 5	Sample 6
850 nm	0.83312	0,85510	0,84581	0,89019	0,90227	0,90822
1310 nm	0,88288	0,86047	0,86506	0,89019	0,89074	0,89668
1550 nm	0,65815	0,65792	0,65857	0,67408	0,66968	0,67266

141

Sample 1:
Polysiloxane matrix – thermally cured
Sample 2:
Polysiloxane matrix including 10 wt. % monomers – no thermal treatment
Sample 3:
Polysiloxane matrix including 10 wt. % monomers – thermally cured
Sample 4
 Polysiloxane matrix including 10 wt. % monomers + Irgacure. 379 – no thermal treatment
Sample 5
Polysiloxane matrix including 10 wt. % monomers + Irgacure. 379 – thermally cured
Sample 6
Polysiloxane matrix including 10 wt. % monomers + Irgacure. 379 – thermally cured and UV illuminated

Table 26: Table displaying transmission results from System B

Band	Transmission (non illuminated)	Transmission (illuminated)	Optical loss non illuminated in dB/cm	Optical loss illuminated in dB/cm
850 nm	0,94369	0,87944	0,23934	0,62399
1310 nm	0,90432	0,84237	0,47069	0,86027
1550 nm	0,46144	0,45107	4,12325	4,24669

To compare the two materials optical properties, one can observe the results obtained from sample 5, consisting of System A and the unexposed sample from the epoxy /diamine material. The results suggest the transmission in the vinyl/ hydride terminated matrix were worse than that of the epoxy matrix, with the transmission being lower. However when comparing the illuminated samples, the transmissions of the epoxy / diamine matrix are lower, suggesting that the core material is absorbing in the NIR region to a greater extent, which can lead the optical losses from the waveguide core. Following UV exposure, the material becomes visibly more yellow, which may contribute to the optical losses during the guiding of the light. The results suggest that there should be no major optical losses using this material for wave guiding purposes, however optical losses may be reduced if the OH groups present in this material, formed from the ring opening of the epoxy are kept to a minimum.

8.3 Refractive Index Measurements

To carry out the analysis, the epoxy resin matrix was prepared by including 12 wt.% of the acrylate monomers, 1,3 butanediol diacrylate, benzyl acrylate and phenyl acrylate. The material was pre cured at 70 ºC for 2 hours, and applied to optical glass slides with a thickness of 500 μm.. The samples were then cured at 50 ºC for 24 hours in a desiccator containing a stock solution of acrylate monomers, in order to avoid the loss by evaporation.

Due to the tackiness of the material it was possible to measure the refractive index with ease using the refractometer. Samples were placed onto the prism, and refractive indices were recorded. Each sample was then left on the instrument, and then UV irradiated using a spot cure lamp. The recorded refractive index was recorded at 10 second intervals during the irradiation. Irradiation was continued until no difference in the refractive index was observed. The results of the change in the refractive indices are depicted in Figure 82.

The samples following 100 s of irradiation, showed a change in the refractive index of ~ 0.003, which is lower than for the previous polysiloxane material. The difference is enough to form waveguides for our purposes, however a higher refractive index is likely to be achieved during the two-photon polymerisation, using N-DPD as photoinitiator.
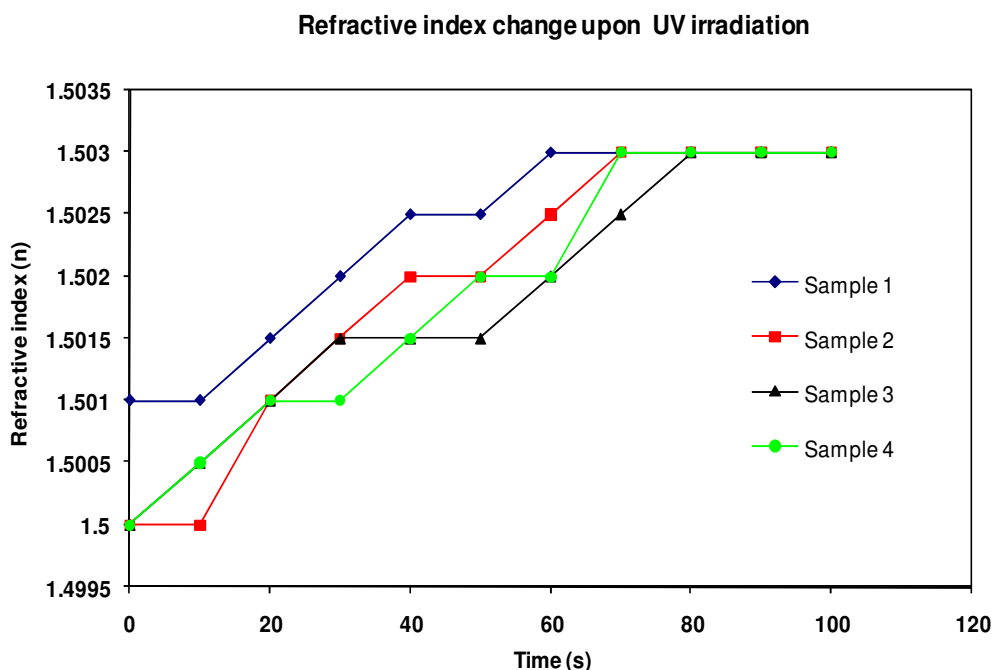

Figure 82: Refractive index change following UV irradiation of epoxy terminated polysiloxane containing 10 wt. % acrylate monomers – perfroemd using an Abbe refractometer

143

8.4 TPA Structuring

8.4.1 TPA Material Testing

In this section, we investigated the performance of the developed epoxy terminated polysiloxane, cross linked with a diamine, using N-DPD as photoinitiator, under two-photon conditions. Samples were prepared on glass slides or rigid breakable FR-4 substrates, with layer thicknesses of between 300 and 500 µm. Preliminary experiments were performed with samples containing either 0.025 wt%. or 0.05 wt.% of the non modified, or dibutyl-N-DPD. The material tests were performed at a laser wavelength of 400 / 800 nm and with a laser power in the range from 300 µW to 150 µW (Feed rate: 20 mm/min). A detailed description of the laser setup is included in section 7.3.1.

Following the laser writing of the waveguides, phase contrast microscopy was used to characterise the structures. Comparing the two photoinitiators, the non modified N-DPD performed better, with the waveguide structures having a higher contrast, and the material having a larger fabrication window with these samples. Non interrupted waveguides were obtained, displaying a larger contrast observed between cladding and waveguide core. An average diameter of 30 µm was achieved. Due to the fact that structuring experiments carried out using the non modified N-DPD were better, it was decided to use this photoinitiator for all further TPA investigations using this material. Butyl-N-DPD also has a darker orange colour than the non modified structure, suggesting there may be more absorption and subsequiently optical losses when the matrix is brightly coloured. Phase contrast images are displayed in Figure 83 and Figure 84.
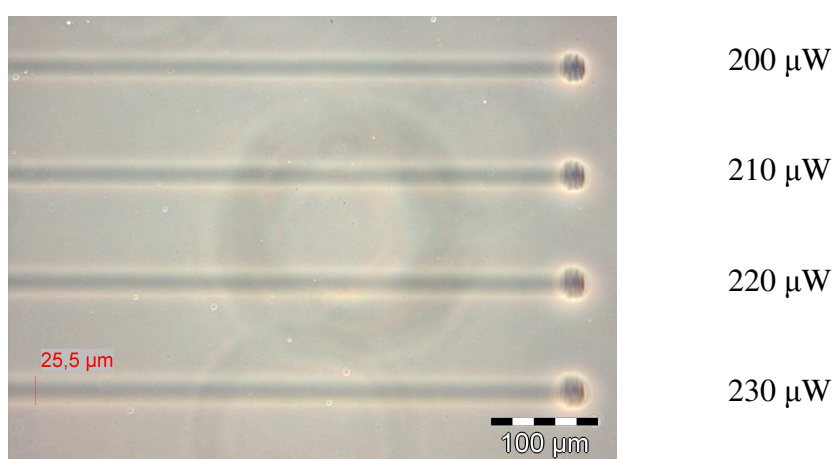

Figure 83: Detection of written waveguides by phase contrast microscopy, structured using different laser powers (epoxy resin containing 10 wt.% acrylates (1:1:1=BA:PA:BDA) and 0.025 wt.% photoinitiator N-DPD)
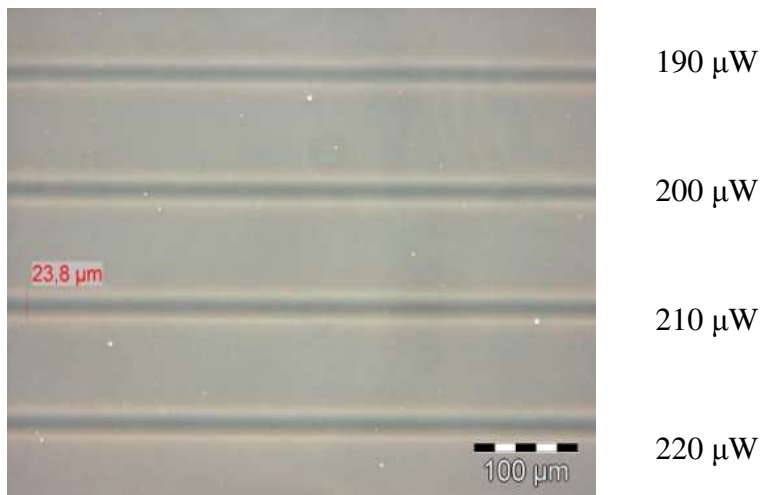
144

Figure 84: Detection of written waveguides by phase contrast microscopy, structured using different laser powers (epoxy resin containing 10 wt. % acrylates (1:1:1=BA:PA:BDA) and 0.05 wt.% photoinitiator butyl-N-DPD)

Further TPA material tests using samples consisting of 0.025 wt.% N-DPD. Well defined, non-interrupted waveguides with a diameter of 40-60 μm were observed, displaying the effective structuring behaviour of the developed optical material. A contrast between the illuminated core and the non-illuminated cladding material was detectable; suggesting a refractive index change obtained by the photo-induced polymerisation of the acrylates had occurred. It appeared however, that although during the material testing larger cross sections were achieved on some occasions, the contrast observed between the cladding and core was quite low, questioning whether the concentration of the acrylate monomers had decreased during the processing and structuring. Figure 85 below depicts a number of waveguide structures written using different laser powers, displaying large cross sections but weak contrasts.
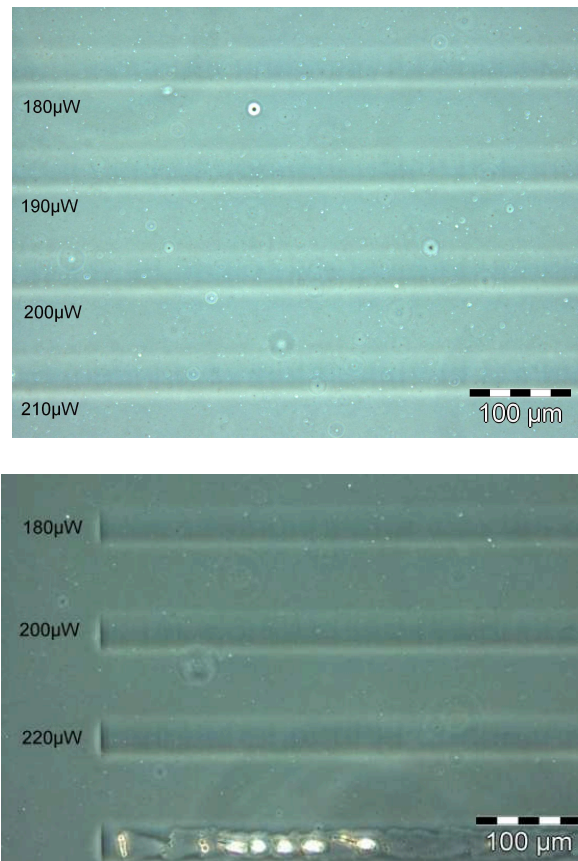
Figure 85: Detection of written waveguides by phase contrast microscopy (epoxy resin containing 10 wt. % acrylates and 0.025 wt. % photoinitiator N-DPD; laser power: 180 – 210 µW)

In further experiments waveguide bundles consisting of 7 waveguides were inscribed into the optical material either at a laser power of 200 µW or 190 µW. Waveguide bundles are normally structured on demonstrators, so it was important to establish which laser power and structuring depth should be used, to produce the best performing waveguides. Following TPA structuring the fabricated waveguides were investigated by phase contrast microscopy. As can be seen in Figure 86, the inscribed bundles were clearly detectable, displaying no areas of burning or ablation.
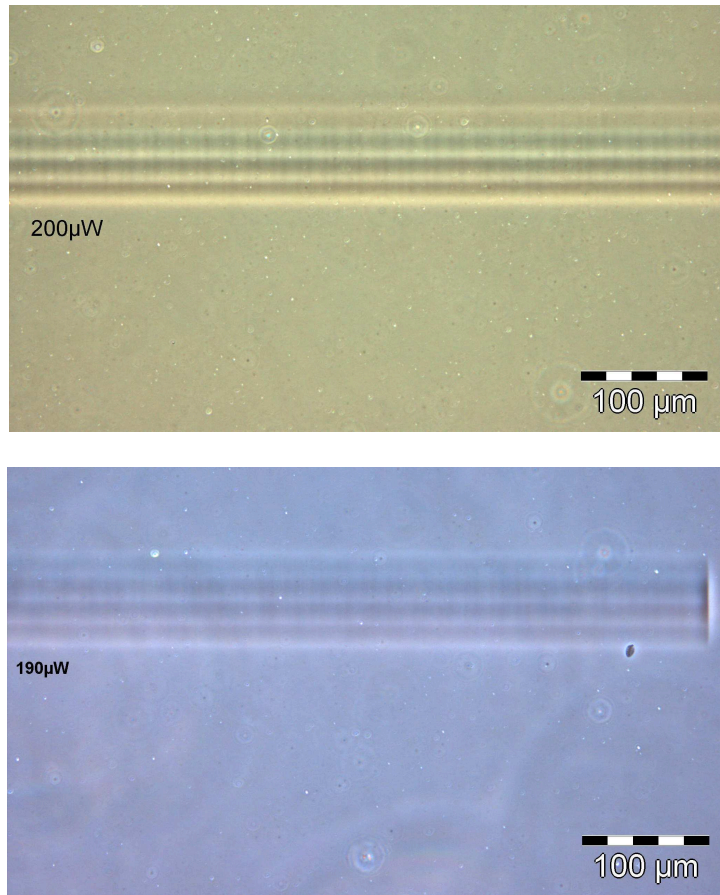
Figure 86: Detection of inscribed waveguide bundles by phase contrast microscopy (epoxy resin containing 10 wt. % acrylates and 0.025 wt.% photoinitiator N-DPD; laser power 175 and 200 µW)

After a series of attempts, it was discovered that a sharp rotary cutter could be used to achieve good clean cross sections, in order to observe the cross sections of the waveguides, structured at different laser powers. Following cutting of the optical material, the cross sections of written waveguides and waveguide bundles were observed using optical microscopy. The inscribed structures were clearly detectable by light guiding in the formed waveguide core. Being able to observe the waveguides meant the focus and optics of the laser could be adjusted so that more circular cross sections could be achieved. An almost circular shape of the embedded waveguides without any scattering of the in-coupled light into the surrounding cladding material was observed. It was also possible to observe the cross section of a bundle of seven waveguides, by accurately cutting the material on a rigid-breakable substrate. The diameter of the waveguide bundles was found to be nearly 80 µm, larger than the previous polysiloxane material. This is likely to be attributed to the use of acrylate monomers, which are more reactive than the previous methacrylate monomers. N-

147

DPD also performs better than Irgacure 379 under two-photon conditions. Images of the observed cross sections are presented in Figure 87 and Figure 88.

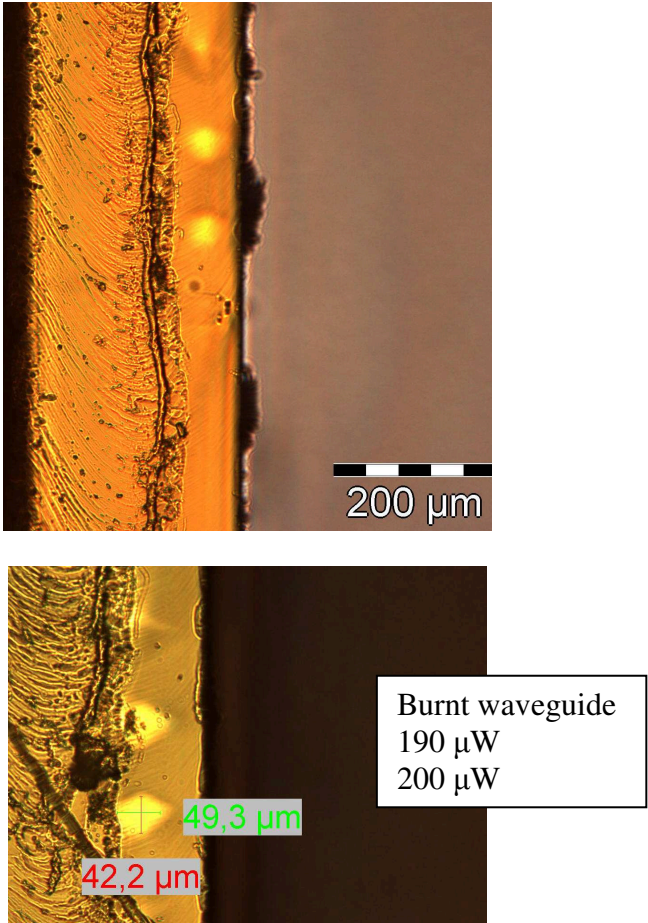49,3 µm

42,2 µm

Burnt waveguide
190 µW
200 µW

Figure 87: Cross sections of inscribed waveguides structured using different laser powers (epoxy resin containing 10 wt. % acrylates and 0.025 wt. % photoinitiator N-DPD)
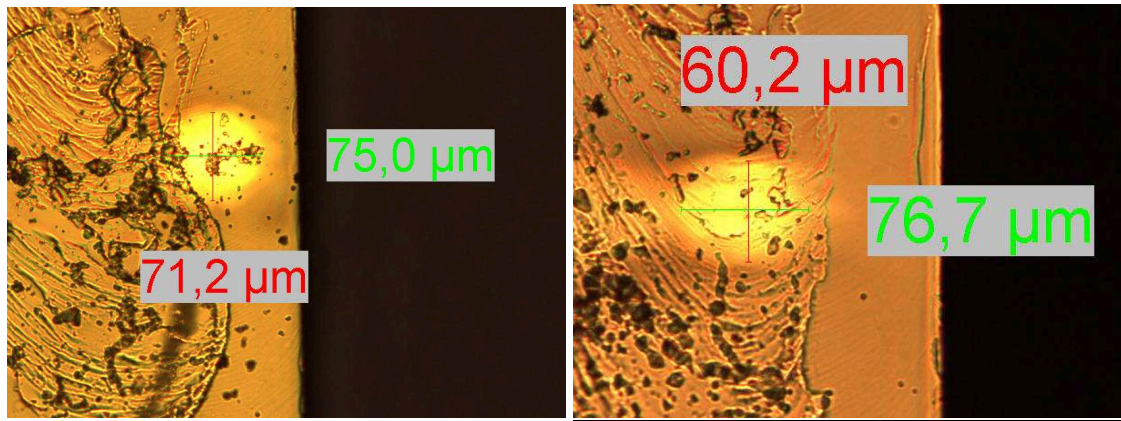
Figure 88: Cross sections of inscribed waveguide bundles (epoxy resin containing 10 wt. % acrylates and 0.025 wt. % photoinitiator N-DPD)

All TPA material results using this material suggest that effective waveguides and waveguide bundles can be used to form optical connections on PBCs. The high contrast observed using phase contrast microscopy provide evidence that a large difference in refractive index is achieved through TPA, and a relatively large fabrication window can be used. Almost circular waveguide structures were observed, leading to the next stage of material investigations. The viscosity of the material as well as the high quality thin films produced, led to the development of demonstrators, prepared usin rigid and rigid breakable substrates.

8.5   Fabrication of Optical Interconnections

A detailed description of the design and preparation of demonstrators prepared on rigid and rigid-flex substrates is explained in section 7.4. Due to the viscosity of the epoxy material following the pre curing step, the substrates could be prepared once again by scraping the material, providing a smooth, even surface, which completely covered the mounted diodes. The prototypes developed were 2 cm and 7 cm rigid substrates, as well as 7 cm rigid-flex substrates. Using an optimised laser system, demonstrators were structured, by writing waveguide bundles between the embedded diodes. The increasing photocurrent was monitored by on line photocurrent measurements. Some demonstrators, following the inscription of one bundle, showed only a minor increase in the photocurrent, so further bundles were structured above or below the previously structured waveguides with a number of demonstrators. Using this material, relatively low photocurrents were achieved. The results of the three types of demonstrators produced are presented in Table 27 and Figure 89. Due to the low photocurrents achieved, not all demonstrators were given a post thermal treatment. The post thermal treatment of 100 ° C for ~ 20 hours was performed to remove any remaining acrylate monomers, in order to stabilise the material, as well as increase the difference in refractive index between the cladding and waveguide core. The post thermal

treatment was found to lead to a decrease in the photocurrent, once again by around 50 %, suggesting either the waveguides are not stable enough to survive the high temperatures, or the material undergoes a shrinkage, leading to a misalignment of the waveguides with the active faces on the mounted diodes.

Table 27: Detected photocurrents before and after the TPA structuring (samples using rigid boards (WL=2 cm)

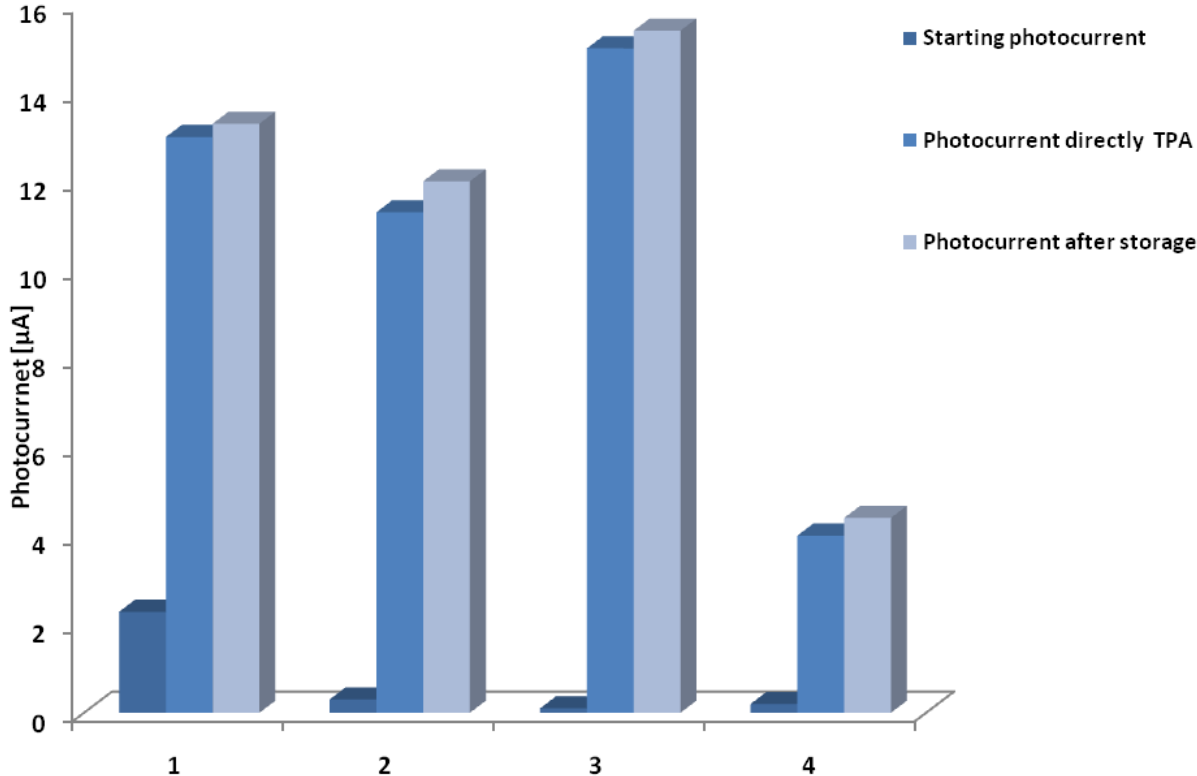| photocurrent pre TPA [µA]	photocurrent post TPA [µA]	photocurrent post storage [µA]	photocurrent post thermal treatment [µA]
2.28	13	13	19
0.3	11.3	12	5.3
0.1	15	15.4	6.8

Figure 89: Detected photocurrents before and after the TPA structuring (Samples using rigid boards (length of waveguide=2 cm))

A second set of demonstrators were fabricated using 7 cm rigid substrates. Using this material, TPA structuring prior to the fabrication of demonstrators produced good contrasted, non interrupted waveguides and waveguide bundles, with the cross sections clearly visible using optical microscopy. The demonstrators did not perform as well as expected, with relatively low photocurrents detected following the TPA structuring of a bundle of waveguides (Figure 90). One demonstrator was selected to perform a post thermal treatment, which resulted once again in a loss of around 50 % of the detected photocurrent.
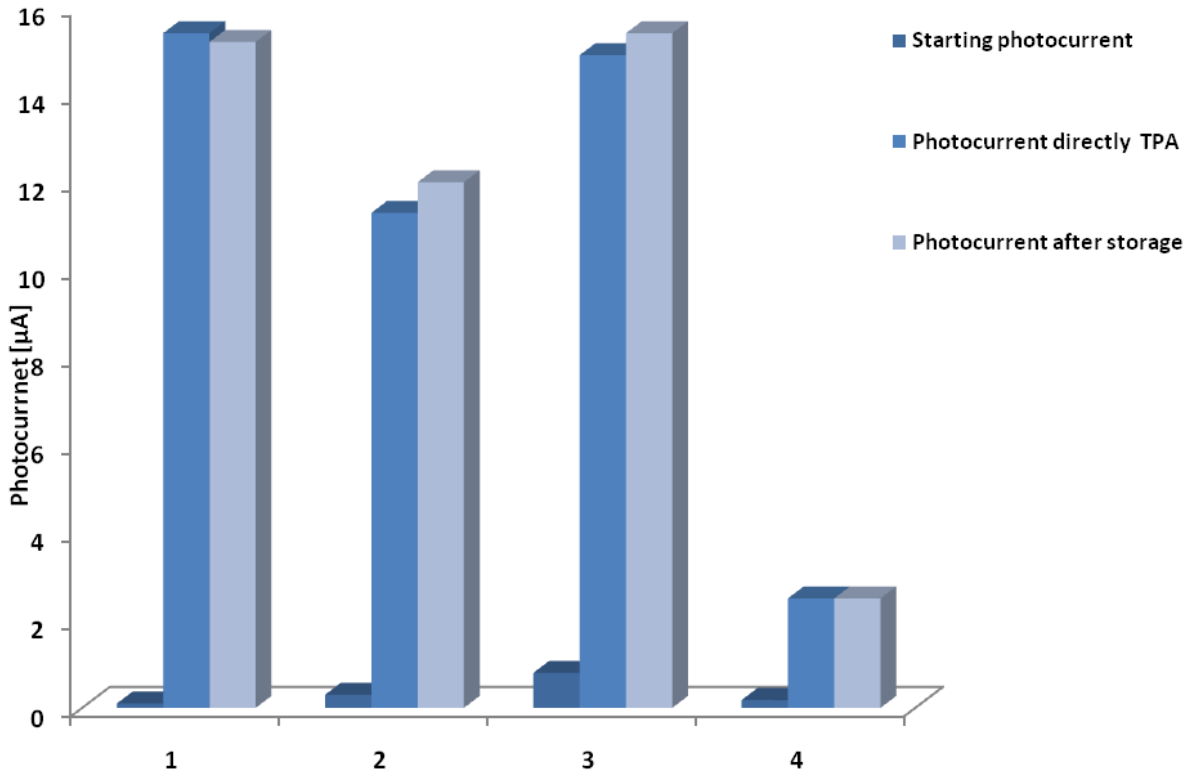

Figure 90: Detected photocurrents before and after the TPA structuring (Samples using rigid boards (length of waveguide=7 cm))

8.6   Conclusion

Due to the low photocurrents achieved when fabricating demonstrators using the epoxy terminated polysiloxane, cross linked with a 1,3-bis(3-aminopropyl)tetramethyl-disiloxane, it was decided not to continue further with this material. One explanation for the low photocurrents is that the refractive index difference between the epoxy cladding and core is too low. The uncured epoxy polysiloxane has a refractive index of 1.475, and it appears the refractive index of the waveguide core is not high enough to function efficiently. A series of cut back measurements and light extractions investigations were performed, to determine why the waveguides gave low photocurrents. The material was cut and cross sections were observed using an optical microscope. The waveguides were detectable, as shown in Figure 91, however in a further set of experiments, light at a wavelength of 633 nm was in-coupled into the waveguides to investigate the light field at the out-coupling face. The waveguide core was not visible, and an area of illuminated material was observed through the bulk of the layer. It appeared that the waveguides could be observed only when the illumination of the in coupled light was significantly adjusted; suggesting the numerical aperture of the waveguides is small. This also indicates the increase in the refractive index of the waveguide by TPA is low. Figure 92 gives an example of the light field distribution of the in coupled light. An illuminated area through the whole material is clearly visible, likely to be near the focus of the laser above and below the embedded waveguide. Acrylate monomers are known to self polymerise[76], and it is possible the acrylate monomers undergo a thermal or UV induced polymerisation in the area of the laser beam, resulting in the observed illuminated strip through the material.

During the post thermal treatment, it is likely a shrinking of the matrix material occurs. The coupling of the waveguides with the diodes is then altered, resulting in the decrease of the detected photocurrent. Acrylate monomers, trapped in the waveguide core may also be evaporated during the thermal treatment, leading to defects and scattering centres in the waveguide, all leading to loss of light.

The epoxy material showed extremely high thermal stability, performed well in TPA material testing, and is compatible with high refractive index acrylate monomers, as well as the two-photon photoinitiator N-DPD. Due to the low photocurrents detected following the fabrication of demonstrators, along with the loss of around 50 % of the photocurrent following the post thermal treatment, further experiments need to be performed, in order to determine the exact refractive index difference which is achievable using such a system. The acrylate monomers are relatively volatile, and in some TPA investigations, it was apparent that the concentration of the monomers was quite low. A polysiloxane material, where high refractive index functional groups are attached to the polymer backbone may be a new approach, so as to

avoid the loss of monomers, as well as avoiding the need to perform thermal post stabilising steps.
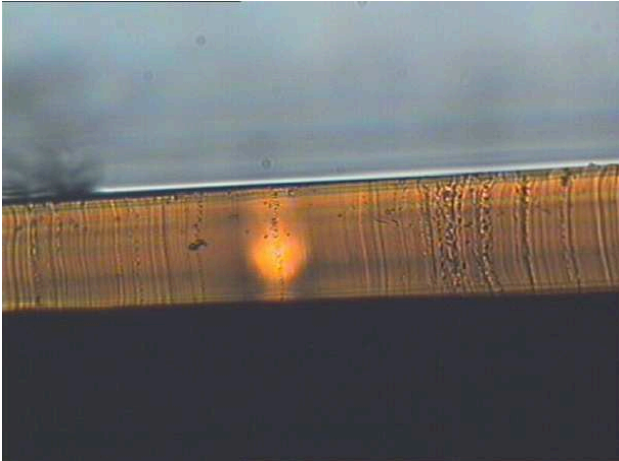

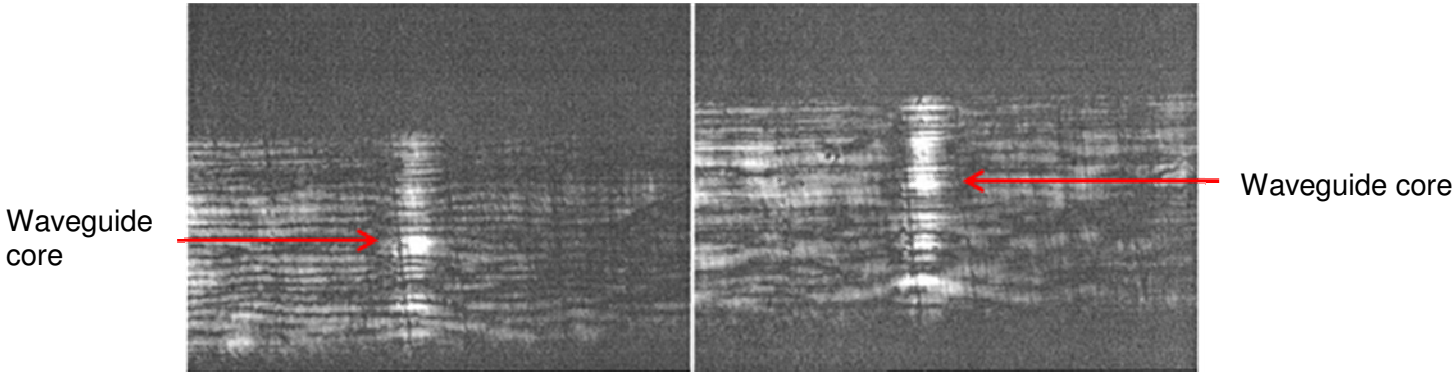**Figure 91: Detection of the inscribed waveguide structures by optical microscopy**

Waveguide core

Waveguide core

Figure 92: Detection of the light field distribution of the in-coupled light at the cut face

Optical Characterisation

System C

9 Optical Characterisation of a Silanol Terminated Polysiloxane Cross linked with an Acryloxy Silane (System C)

9.1 Introduction

A silanol terminated diphenyl dimethyl polysiloxane, cross linked with an acryloxy silane, described (System C) described in section 6.2 was optically characterised, including cut back and light extraction testing, NIR spectroscopy and spectroscopic ellipsometry. This newly developed material has a high thermal stability, is processed in under an hour and forms thin flexible films. The material was therefore used in TPA experiments, performing material testing and finally fabricating demonstrators on specially designed 7 and 15 cm rigid substrates containing mounted optical components. The material is suited for optical applications, as a high refractive index acrylate functional group is attached to the polymer backbone, which is polymerised by TPA to form the waveguide core. Following the TPA, previous materials were thermally treated, to stabilise the matrix by removing non reacted monomers. Using this material however, no post thermal treatment is performed, due to the fact that the acrylate functional groups are stable in the cladding material, attached to the polysiloxane backbone. The photoinitiator N-DPD is extremely stable under one-photon conditions, and no polymerisation in the cladding material occurs, even when exposed to light. A thermal post treatment was carried out on a number of demonstrators, which improved the functioning of the waveguides. One noticeable change was the appearance of the waveguide structures, which appeared darker, and were visible by eye in the matrix material. Secondly the photocurrent of the thermally treated demonstrators increased in nearly every case, signifying the stability of the written waveguides.

9.2 Refractive Index Measurements - Ellipsometry

It was important to determine the difference in refractive index achieved upon the photopolymerisation of the acrylate functional groups, so ellipsometry measurements were performed. Using spectroscopic ellipsometry, the refractive index of the thin films could be measured at different wavelengths, including the telecom and datacom wavelengths. Samples containing the silanol polymer cross linked with 10 wt. % acryloxymethyl trimethoxy silane were prepared. The samples were prepared in duplicate, so that one sample could be exposed to UV light using a spot cure lamp. The samples were spin coated onto silicon slides to produce a thin homogeneous film. The samples exposed to UV light represent the core of the waveguide. Using the photoinitiator Irgacure 379 can lead to particles in the very thin layers required which leads to problems with the analysis. Therefore N-DPD was used

and samples were illuminated for a longer period of time. The illumination time was monitored by FT-IR spectroscopy to achieve a high double bond conversion of the acrylate functional group. A Cauchy fit displaying the increase of refractive index at different wavelengths is presented in Figure 93, with the difference in refractive indices at telecom and datacom wavelengths included in Table 28. The results showed that at the three telecommunication wavelengths, the refractive index difference between the illuminated and non-illuminated material was 0.01. It is likely that a silanol terminated matrix material cross-linked with 20 wt. % acryloxy crosslinker would show a bigger increase in the refractive index upon illumination. Samples prepared using 20 wt. % of the acryloxy cross linker, used in TPA experiments, showed a very high contrast when viewed using phase contrast microscopy, suggesting a higher refractive index difference is achieved using higher amounts of cross linker.

Table 28: Description of refractive indices at different wavelengths, of the cladding and core material

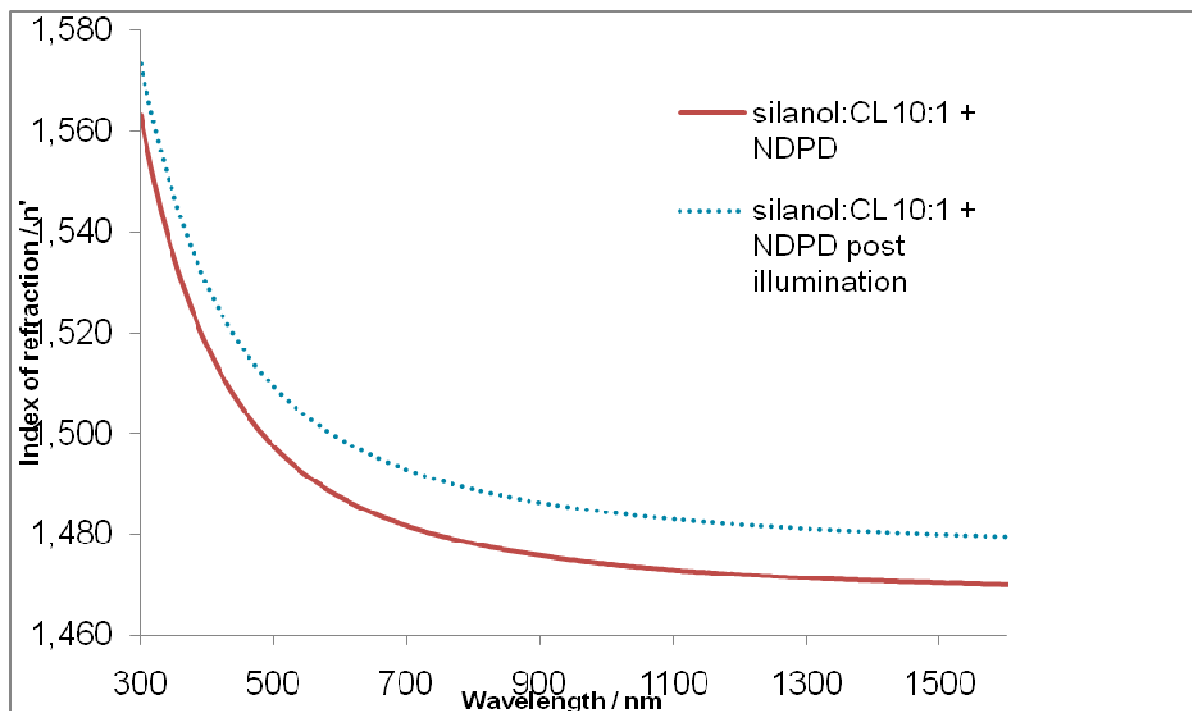| Wavelength (nm)	Refractive index (cladding)	Refractive index (core)	Δn
840	1.477	1.488	0.011
1310	1.471	1.481	0.01
1550	1.470	1.480	0.01

Figure 93: Cauchy fit of the refractive index of the illuminated and non-illuminated silanol terminated polysiloxane cross linked with 10 wt. % acryloxymethyl trimethoxy silane using N-DPD as photoinitiator

9.3   NIR Spectroscopy

Optical waveguides need to have low optical losses, particularly at the major telecommunication wavelengths, which are 1310, 1550 and 840 nm. To determine whether absorbance's in these regions are causing optical losses, and deem the silanol matrix material unsuitable for waveguide structuring, near infrared spectroscopy was carried out. Samples were prepared in plastic cuvettes, which could then be broken open to form free standing cubes of material. This avoided problems with the interfaces between air and plastic when measuring the blank sample. Samples were prepared consisting of the silanol terminated polymer, cross linked with 20 wt. % acryloxymethyl trimethoxy silane, with 0.1 wt. % Sn catalyst. Samples also contained 0.025 wt. % N-DPD. One sample was left non illuminated, to represent the cladding material surrounding the waveguides, and the second sample was illuminated on each face of the cube for 20 seconds using a spot cure lamp (light intensity of 1.4 W/cm^2. Following UV exposure, the photoinitiator N-DPD tends to turn a deeper yellow colour, so it was important to compare the optical losses of the "core" material against the cladding material. Spectra were recorded of both materials in the NIR region, from 200 nm to 2500 nm.

The spectra are presented in Figure 94. The results show the transmission at the telecommunication wavelengths are 90 % at 840 nm, 86 at 1310 nm and 64 % at 1550 nm

157

for the non illuminated sample, and 91 % at 840 nm, 87 at 1310 nm and 65 % at 1550 nm for the illuminated sample. The spectra of the illuminated and non-illuminated samples revealed no major optical losses, due to the fact that the OH groups, which are known to be highly absorptive in the 1550 nm region, as well as aliphatic C-H groups[77], are only present on the terminal polymer chains, and the methyl groups on the polymer chain were partly substituted with phenyl groups. The optical losses in dB were calculated for the telecom and datacom wavelengths, for the UV illuminated and non illuminated samples (Table 29). As expected, the calculated losses in dB/cm were low, with no functional groups contributing to optical losses.
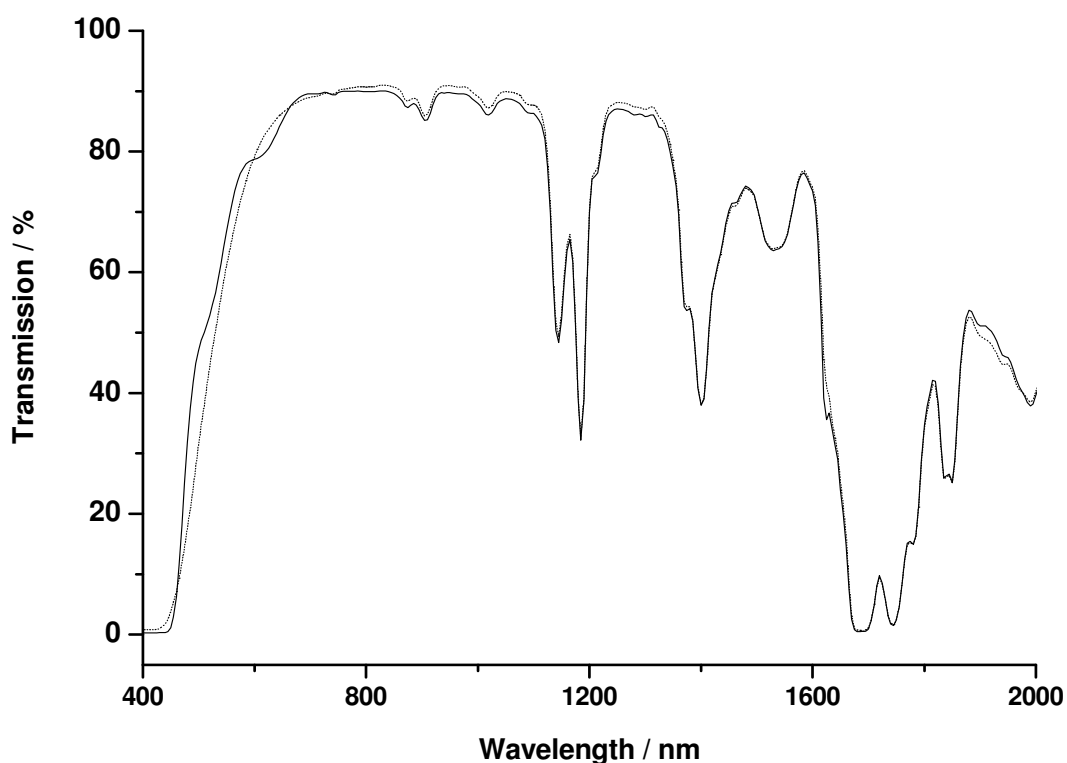
Figure 94: NIR spectra of non-illuminated (dashed line) representing the cladding material, and illuminated (solid line) representing the waveguide core material of silanol terminated polysiloxane cross linked with acryloxymethyl trimethoxy silane

158

Table 29: Optical losses calculated in dB/cm from the NIR spectra, for illuminated and non illuminated samples

Wavelength (nm)	dB/cm (non illuminated sample)	dB/cm (illuminated sample)
840	0.41	0.46
1310	0.59	0.65
1550	1.85	1.87

9.4   TPA Material Tests

9.4.1   TPA Material Tests using N-DPD

For All TPA material tests, mixtures based on the silanol terminated polysiloxane, cross linked with 20 wt. % acryloxymethyl trimethoxy silane were used, as described in Section 6.2. Once a pre curing step had been performed, the material had a high enough viscosity and was scraped onto optical glass slides and rigid breakable FR-4 substrates. TPA material testing was then carried out to determine whether this material was suitable to be used as a matrix material to structure optical waveguides. To carry out TPA material testing, thin films of material (400-500 µm) were used to determine which laser power was most suitable to fabricate non-interrupted waveguides with a high contrast. A detailed description of the laser set up, and conditions are included in section 7.3. To observe the waveguide structures after the TPA structuring, phase contrast microscopy was used. The waveguides, structured using different laser powers were observed, and any burns or interruptions in the structures were indentified. Further samples were prepared on rigid breakable substrates, used to structure shorter waveguides, which could be cut, in order to observe the cross sections of the waveguides. Optical microscopy was used to observe the shape, and diameter of single waveguides and bundles of seven waveguides. Laser powers of between 160 and 260 µW were used. Phase contrast microscopy images of the inscribed waveguide structures are presented below in Figure 95, Figure 96 and Figure 97. The phase contrast images revealed high contrast waveguide structures, with cross sections of up to 40 µm achieved. Higher laser powers had to be used to achieve the clear waveguide structures; however, observing the image in Figure 95, it was possible to use a large fabrication window to structure. A laser power of 260 µW was used to effectively burn the material, in order to locate the waveguide structures more easily using the optical microscope; however laser powers of between 180 to 220 µW produced non interrupted, high contrast waveguides with large cross sections. The

material, under the microscope appeared to be homogenous, with no phase separation visible, or any trace crystals of photoinitiator. The material was also fully flexible and using a rotary cutter, samples prepared on rigid breakable substrates were able to be structured, and clean cuts prepared to reveal well defined cross sections of single waveguides, structured at different laser powers, and also waveguide bundles, depicted in Figure 98 and Figure 99. Waveguide bundles were also structured successfully and characterised with phase contrast microscopy. The bundles were structured with a distance of 20 μm between the 7 bundles, and it was discovered a laser power of 210-220 μW produced the best waveguide structures, with no interruptions or burns. Once waveguide bundles had been successfully structured, it was decided, following successful cut back measurements, where the optical waveguides were characterised and optical losses were calculated; that the structuring of demonstrators would be carried out, using rigid and rigid flex mounted substrates. The results of the structuring can be found in the following sections.
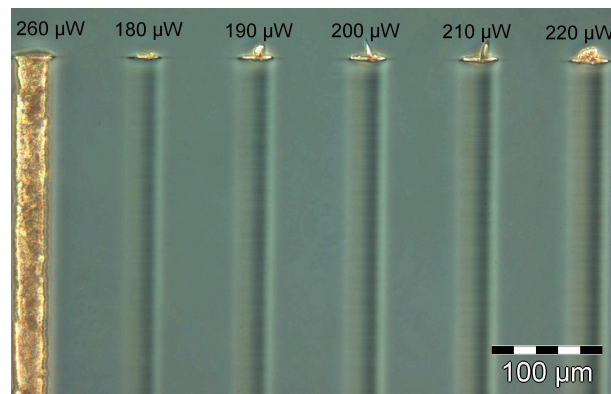

Figure 95: Phase contrast microscopy image of written waveguide structures written using different laser powers, using silanol terminated polysiloxane cross-linked with 20 wt. % acryloxymethyl trimethoxy silane, and 0.025 wt. % N-DPD
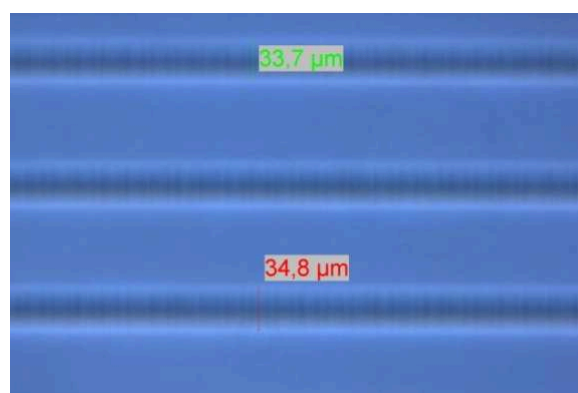

Figure 96: Phase contrast microscopy image of written waveguide structures using silanol terminated polysiloxane cross-linked with 20 wt. % acryloxymethyl trimethoxy silane and 0.025 wt. % N-DPD
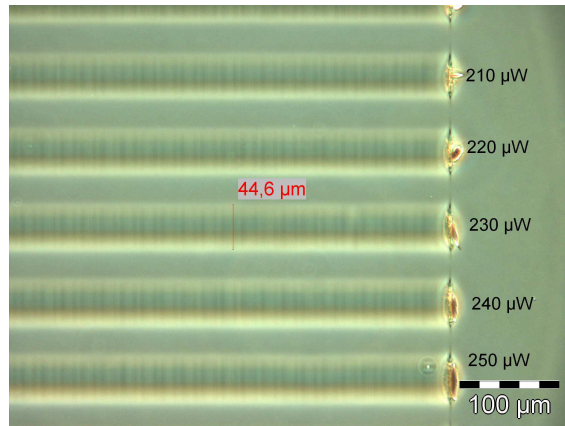
160

Figure 97: Phase contrast microscopy image of written waveguide structures using silanol terminated polysiloxane cross-linked with 20 wt. % acryloxymethyl trimethoxy silane and 0.025 wt. % N-DPD
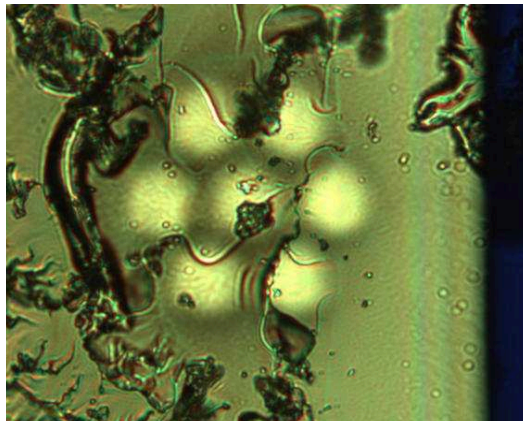

Figure 98: Optical microscopy image of written waveguide bundle using silanol terminated polysiloxane cross-linked with 20 wt. % acryloxymethyl trimethoxy silane and 0.025 wt. % N-DPD
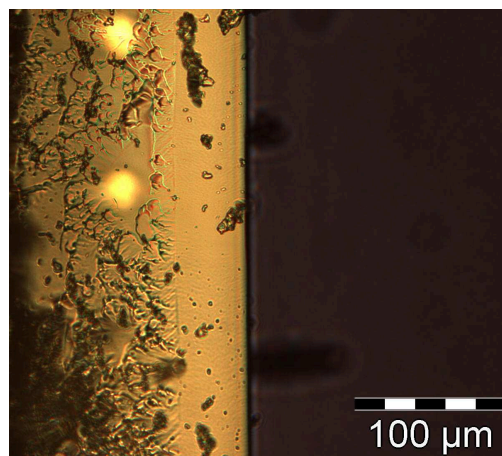

Figure 99: Optical microscopy image of written waveguide cross sections using silanol terminated polysiloxane cross-linked with 20 wt. % acryloxymethyl trimethoxy silane and 0.025 wt. % N-DPD
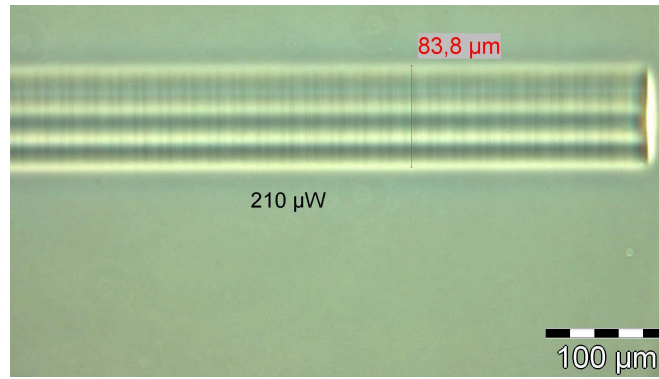
161

Figure 100: Phase contrast microscopy image of written waveguide bundle using silanol terminated polysiloxane cross-linked with 20 wt. % acryloxymethyl trimethoxy silane and 0.025 wt. % N-DPD – laser power 210 µW

To show that TPA structuring could also be carried out in not only thin films but 3D samples, a solid cube of the silanol terminated material was prepared, and a field of waveguides were structured, as well as a bundle. Optical microscopy was used to in couple light into the structures, revealing the waveguide cross sections in the cube, shown in Figure 101.
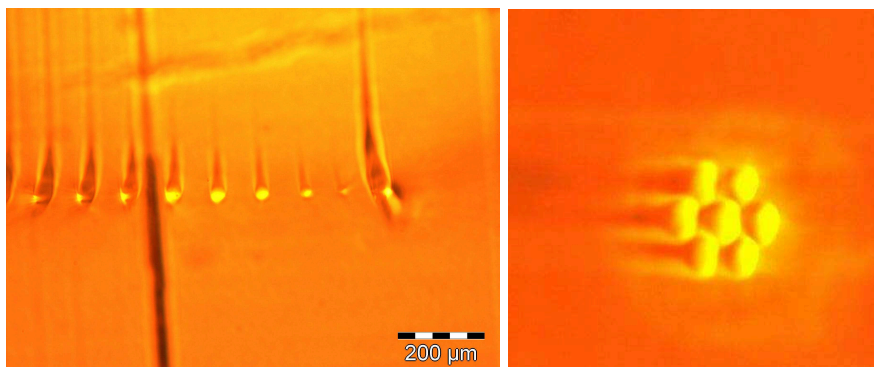

Figure 101: Optical microscopy image of written waveguide field as well as bundle, structured using different laser powers in a 3D sample of silanol terminated polysiloxane cross-linked with acryloxymethyl trimethoxy silane – 0.025 wt. % N-DPD

9.4.2 TPA Material Tests using Butyl-N-DPD

A series of TPA material tests were performed using butyl-N-DPD, in a concentration of 0.05 wt. %. The samples appeared red in appearance when prepared and it is likely a lower concentration can be used to perform TPA. The waveguide cross sections were very difficult to discern, an example of which is shown in Figure 103. However using phase contrast microscopy, waveguide structures with extremely high contrast were written, along with a very large cross section. This modified N-DPD displays excellent TPA properties, however

for wave guiding it is possible that the brightly coloured matrix and waveguides will result in optical losses of the material, with the guiding of the light affected. It was not possible using the optical microscope, to in couple light into the waveguides to be able to observe the cross sections clearly.
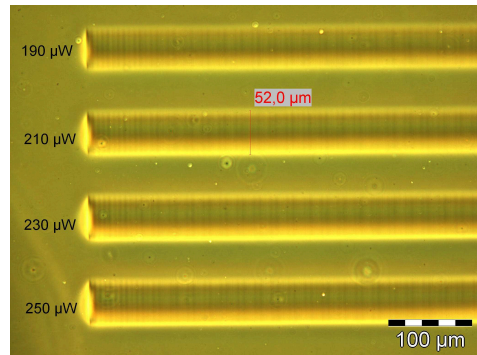

Figure 102: Phase contrast microscopy image of inscribed waveguide structures in silanol terminated polysiloxane cross-linked with 20 wt. % acryloxymethyl trimethoxy silane and 0.05 wt. % butyl-N-DPD

Figure 103: Microscopy image of written waveguide cross sections in silanol terminated polysiloxane cross-linked with 20 wt. % acryloxymethyl trimethoxy silane, 0.05 wt. % butyl-N-DPD

9.5   Determination of the Optical Losses of TPA Written Waveguides – Light Extraction and Cut Back Measurements

9.5.1   Introduction

Following successful TPA material tests, measurements were performed to determine how well the waveguide structures function, and to check the optical losses. Cut back techniques are common, in measuring the transmission, attenuation and bandwidth of optical fibres and waveguides[78]. A detailed description of the experimental technique and sample preparation is included in section 10.4. These experiments were performed by Dr. Nicole Galler, at the University of Graz.

9.5.2 Results

Using a rotary cutter, a clean cross section of the material was possible, enabling the in coupling of light and light extraction tests to be performed. The cross section of the material achieved using a rotary cutter is shown in Figure 104, with the cross sections of the waveguides, structured using different laser powers clearly visible. Using optical microscopy, it was also possible to characterise the cross sections of the written waveguides, by adjusting the focus of the light. Following the successful cutting of the material, it was possible to in couple the light into all six inscribed waveguides with the optical fibre. Four out of the six waveguides tested appeared to be clear, circular and functioned well, shown in Figure 105. The results are presented for two waveguides, given as WL2 and WL3 in graphs showing the optical losses at different path lengths in Figure 106 and Figure 107. The optical losses measured for the two waveguides, structured with laser powers of 210 and 190 µW were measured to be 2.21-2.65 dB/cm and 1.4-2.3 dB/cm. These results were the first to be carried out on System C and the low optical losses, as well as the successful light extraction investigations on all the written waveguides, suggest the waveguides function exceptionally well. Further cut back measurements were performed on waveguides which received a post thermal treatment, leading to even lower optical losses being measured.
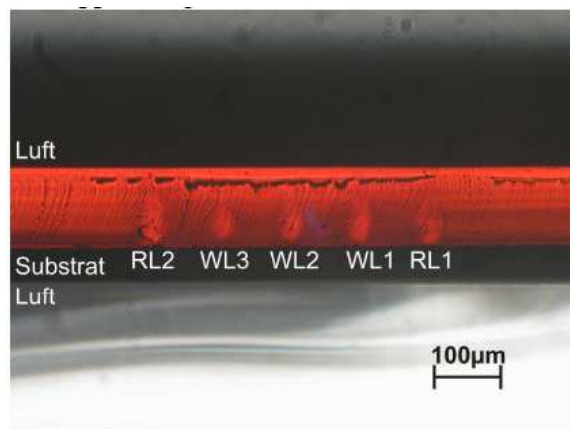

Figure 104: Waveguide cross sections observed by optical microscopy, inscribed using silanol matrix cross linked with 20 wt. % acryloxymethyl trimethoxy silane
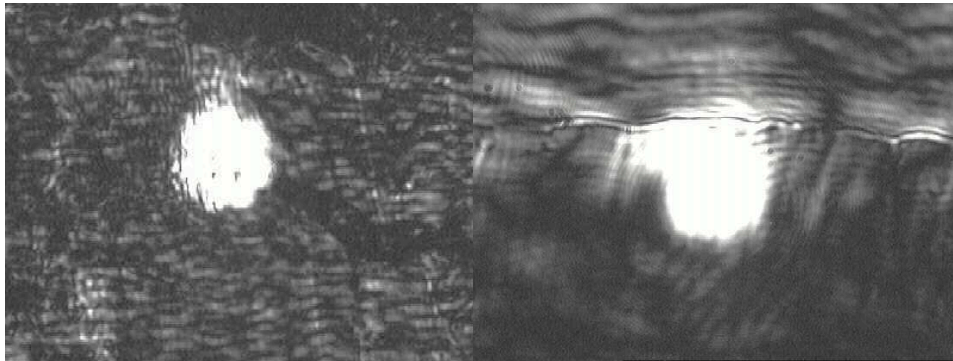
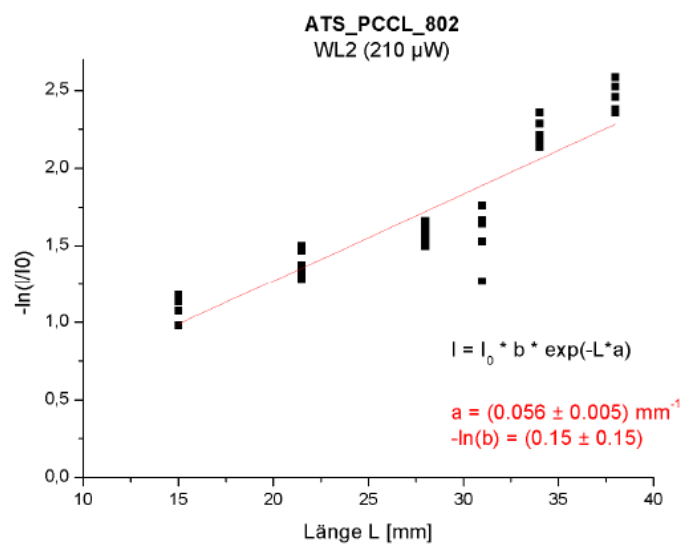**Figure 105: Out coupled light from TPA structured waveguides using laser powers of 200 and 210 µW**

Figure 106: Cut back results - determination of optical loss at different path lengths of the in coupled light (WL2 (210µW): dampening (2.43 ± 0.22) dB/cm
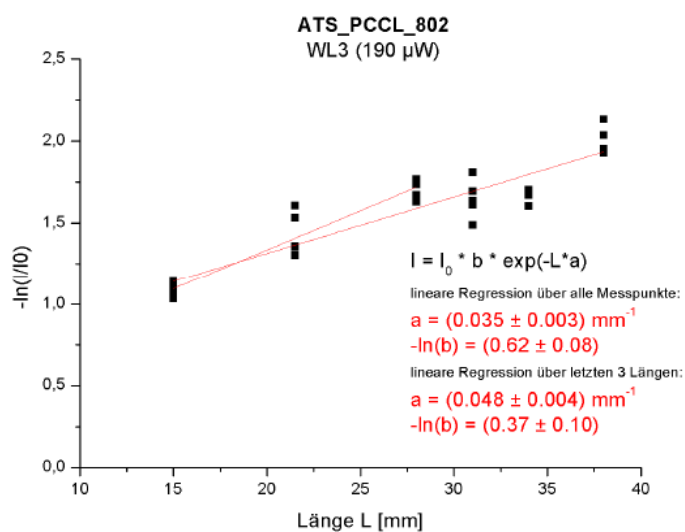

Figure 107: Cut back results - determination of optical loss at different path lengths of the in coupled light (WL3 (190µW): dampening (1.39 ± 2.26) dB/cm

A further sample was thermally treated at 150 °C for 1 hour, to determine whether the optical losses decrease when the material is stabilised. Once again in all attempts at in coupling of the light was successful.

The results of the thermally treated sample revealed the waveguides functioned remarkably well. A good cross section of the material was prepared, with all waveguides being observed. Light could be in coupled into the waveguides, with an example of WL3, structured with a laser power of 210 µW, presented in Figure 108. Cut back measurements performed on this sample gave an optical damping of 0.59 dB/cm, when RL1 was tested, and 0.81 dB/cm when WL1 was tested, which was structured using a laser power of 230 µW. A higher optical loss of 1.26 dB/cm was measured from using the waveguide structured with a lower laser power of 210 µW.

A second sample, prepared in the same way; but omitting the thermal post treatment, was compared to the thermally treated sample. Once again all waveguides could be observed, and light could be in coupled. Cut back measurements were performed on 2 waveguides, WL1 and WL3, structured using laser powers of 230 and 210 µW respectively. The results gave an optical loss of 0.43 ± 0.30 dB/cm for WL1 and 0.22 ± 0.57 dB/cm for WL2. Images of the written waveguides and bundles are seen in Figure 109, Figure 110 and Figure 111. This suggests that although the thermal treatment improves the appearance of the waveguides, the optical loss measured is not affected considerably. Low optical losses were measured for all the samples investigated proving the waveguides structured in this material function well, with the optical losses considerably lower than previous optical materials.
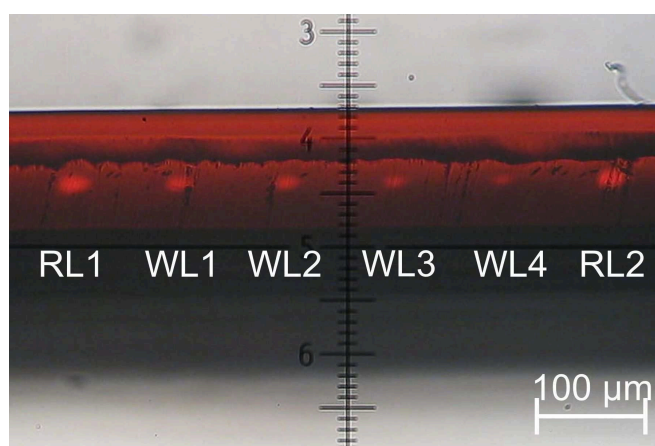

Figure 108: Test cut of silanol matrix cross linked with 20 wt. % acryloxymethyl trimethoxy silane – cut achieved with rotary cutter
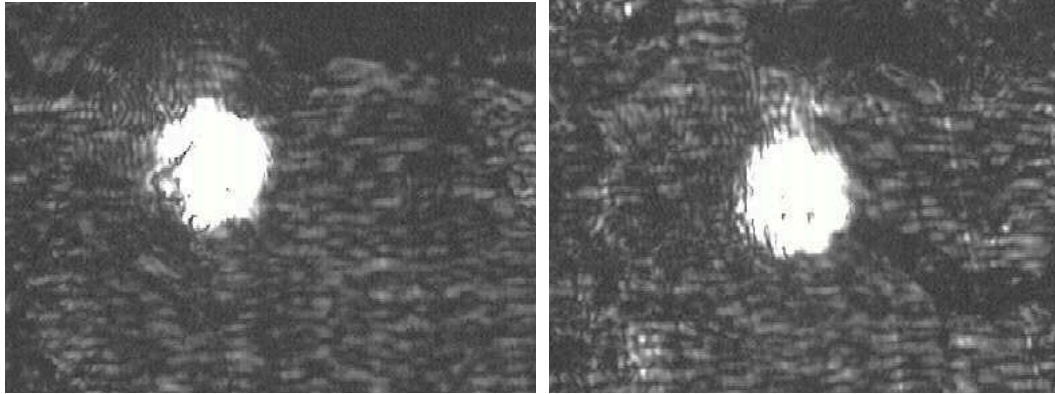
Figure 109: Out coupled light from waveguide structured with a laser power of 210 and 230 µW
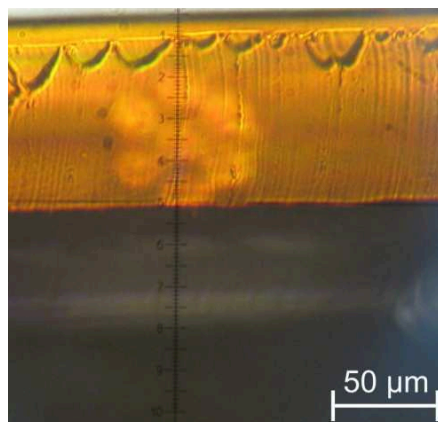

Figure 110: Waveguide bundle cross section observed by optical microscopy, inscribed using a laser power of 220 µW
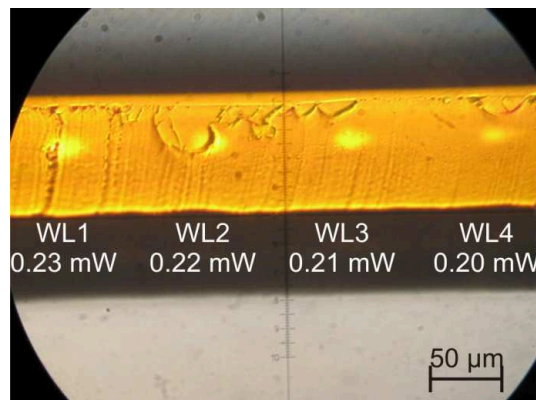

Figure 111: Waveguide cross sections observed by optical microscopy, inscribed with different laser powers

9.6 Fabrication of Optical Interconnects

9.6.1 Fabrication of 7 cm Rigid Boards

The description and design of the PBCs used for the fabrication of the demonstrators are included in Section 7.4. This section describes three different types of demonstrators, which are separated into three sections. Rigid and rigid-flex substrates, 7 cm in length, used with previous optical materials, as well as 15 cm rigid substrates were used to study the wave guiding capabilities of the silanol polysiloxane. 7 cm rigid substrates were the first to be fabricated, with waveguide bundles aligned between the mounted diodes. First attempts showed the material performed remarkably well, with a number of demonstrators containing only a few waveguides. Following the structuring of only one waveguide, the photocurrent increased substantially, displaying the high quality of the single waveguides. All demonstrators performed well, with a continuation in the increase in the photocurrent observed after a few days storage. Laser powers of 190 μW were used to structure the waveguide bundles, with depths of between 200 and 300 μm.

A noticeable difference when using this material to fabricate demonstrators was the increase in photocurrent following the TPA structuring. With previous materials, there was a tendency of the photocurrent to decrease in the days after the waveguides were structured. Using the silanol terminated polysiloxane; the photocurrents detected remained stable during the two day storage period, and increased in nearly all cases. A chart including the detected photocurrents is presented in Figure 112.
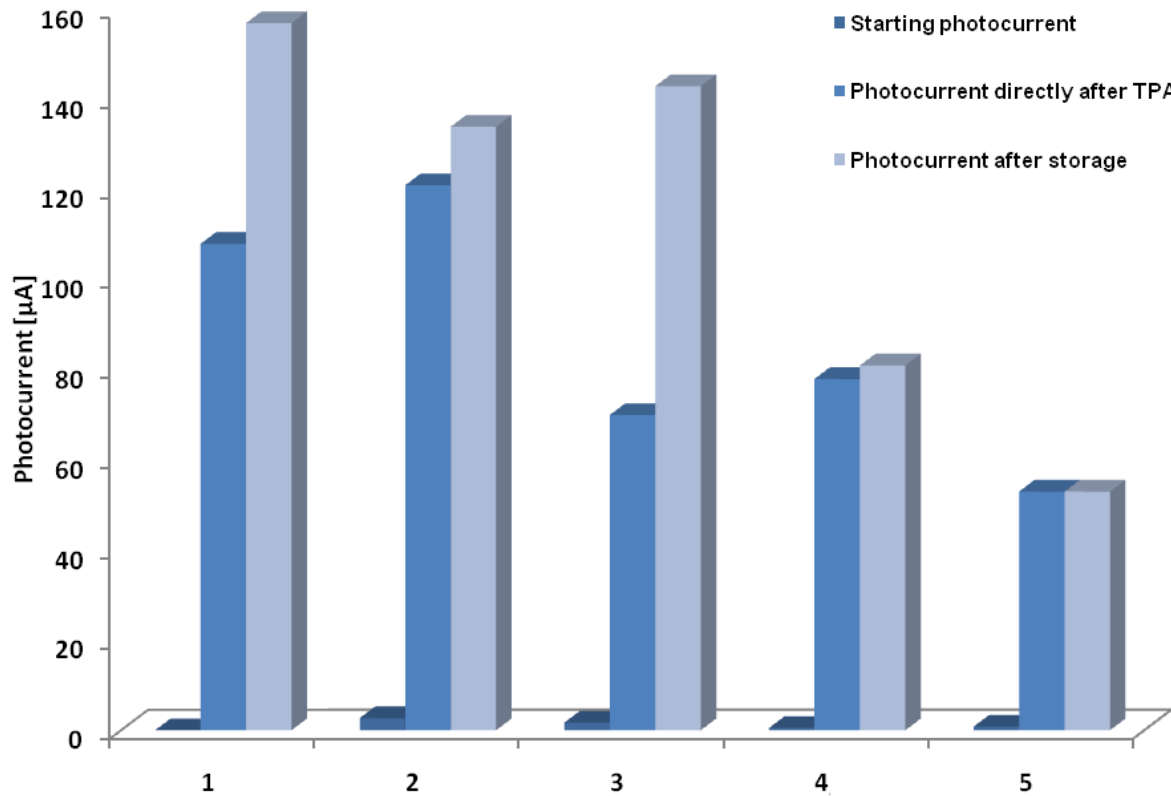
Figure 112: Detected photocurrents before, after and after storage of demonstrators structured using rigid boards

9.6.2 Fabrication of 7 cm Rigid-flex Boards

With previous materials, structuring of demonstrators using rig-flex demonstrators was more of a challenge, as due to the design, the waveguides need to be written over a small step, where the polyimide foil is attached to the FR-4 substrate. In contrast, using this material, extremely high photocurrents were achieved, with no scattering centres observed over the step. Waveguide bundles with a laser power of 220 µW were structured correctly between the mounted diodes. An average photocurrent of over 250 µA was achieved, with once again, a large increase in the photocurrent observed after only the first waveguide was written. In all tests, the material was prepared in the same way, using only 0.025 wt. % of the photoinitiator N-DPD. Preparing the layers to produce a smooth, even surface was found to be the best way to achieve high photocurrents, as it was easier to determine the correct positions of the active areas on the mounted diodes. This was the case with most of the rigid-flex substrates, prepared by either scraping the material across the substrate, or drop casting the material, to enable the frame around the substrate to be completely filled. A table including the photocurrents before and after structuring are included in Figure 113.
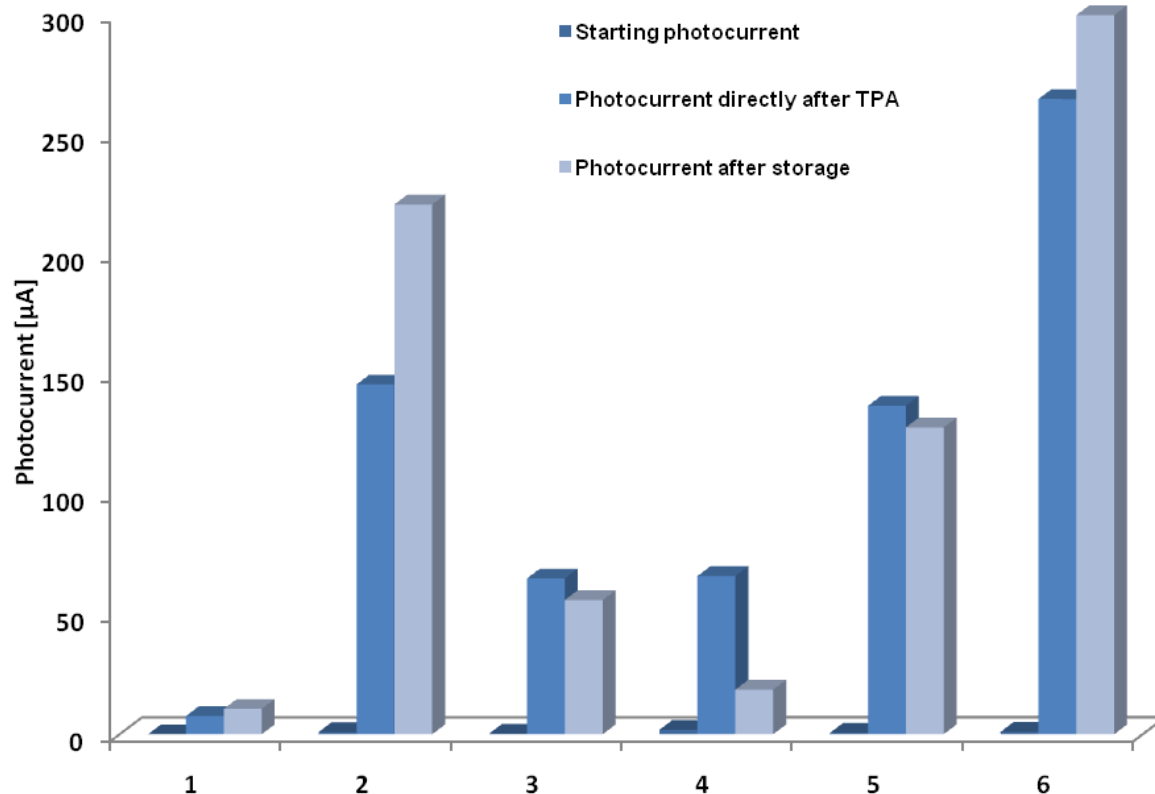
169

Figure 113: Detected photocurrents before, after and after storage of demonstrators structured using rigid-flex boards

9.6.3   Fabrication of 15 cm Rigid Boards

Due to the successful fabrication of demonstrators using 7 cm rigid and rigid-flex substrates, longer rigid boards were investigated. To achieve high photocurrents was more of a challenge using such substrates, as during the TPA structuring, there was more of a chance of structuring through air bubbles, dust particles, or inhomogeneous sections in the material. Waveguide bundles were structured in the same way as previously described, with two demonstrators fabricated. Once again a high photocurrent was detected following the structuring of a single waveguide, with the final photocurrent following the TPA structuring of the whole bundle being over 100 µA for both demonstrators. A photofactor of over 6000 was achieved for both demonstrators, signifying that good quality waveguides were structured, with low optical losses. The photocurrents of the demonstrators were monitored for a few weeks after TPA structuring, revealing a substantial increase in the photocurrent, shown in Figure 114.
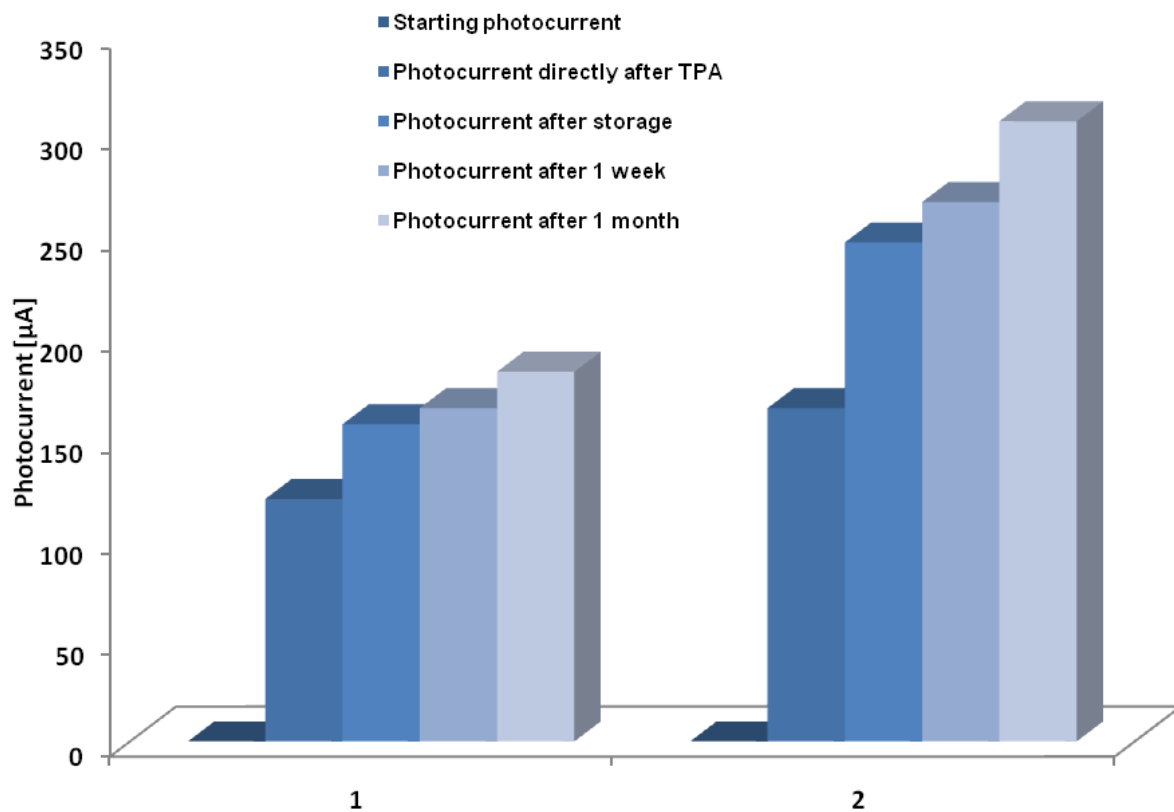
Figure 114: Detected photocurrents before, after and after storage of demonstrators structured using 15 cm rigid boards

9.7   Long Term Stability Monitoring of Demonstrators

Following the fabrication of the demonstrators, all successful boards were stored in the dark, and their photocurrent was monitored regularly. What was found for almost all demonstrators was that following the first week after structuring, a considerable increase in the photocurrent was observed. Over the next few weeks, a slower increase in the photocurrent was observed, with stable photocurrents being detected after one month. For 8 months, a number of demonstrators were monitored, with the photocurrents presented in Figure 115. To demonstrate the stability of the written waveguides, boards with low photocurrents achieved are also included, as these also demonstrated an increase, followed by stable photocurrents over an 8 month period. The exact reason for the increase in photocurrent is unknown, however phase contrast microscopy, as well as visual inspection reveals the appearance of the waveguides changes. Usually, following the TPA, the waveguides can only be seen very faintly by eye; however following storage of the demonstrators, as well as thermal treatments of 100 °C enables the waveguides to be observed more clearly. The waveguides possibly increase in size following the TPA process, which would certainly explain the increase in photocurrent, as more light is in coupled into the waveguides. The refractive index difference between the waveguide and cladding may also increase, due to water and methanol,

products from the curing process, evaporating from the cladding. The interconnected network of the polyacrylate waveguide core seems to improve following the TPA, attributed to a post polymerisation, improving the core structure and increasing the light guiding capabilities.

A thermal treatment was carried out on a number of demonstrators following TPA. Due to the unexplained increase in the photocurrent in the weeks following TPA, it was believed removing any curing by-products, and stabilising the matrix led to the increase. It is also important that the waveguides survive the harsh PCB processing steps, including temperatures of over 200 °C. Demonstrator 1 in Figure 115 is an example of a rigid board, which was used to determine the thermal stability. Following a thermal step of 150 °C for 30 minutes, the photocurrent was unaffected, however after 1 hour, the photocurrent doubled. A stable photocurrent was also recorded after a 200 °C thermal treatment for 7 minutes. Over the next 5 months, the photocurrent continued to increase, remaining stable for over 8 months. It is clear that stabilising the matrix led to higher detected photocurrents. The demonstrators were also unaffected by 200 °C thermal steps, proving this material outperforms previous optical materials investigated. All demonstrators have maintained stable photocurrents since production, displaying the exceptional stability of the waveguides and cladding. No evidence of localised polymerisation occurring in the cladding material, even under UV conditions, has been observed.
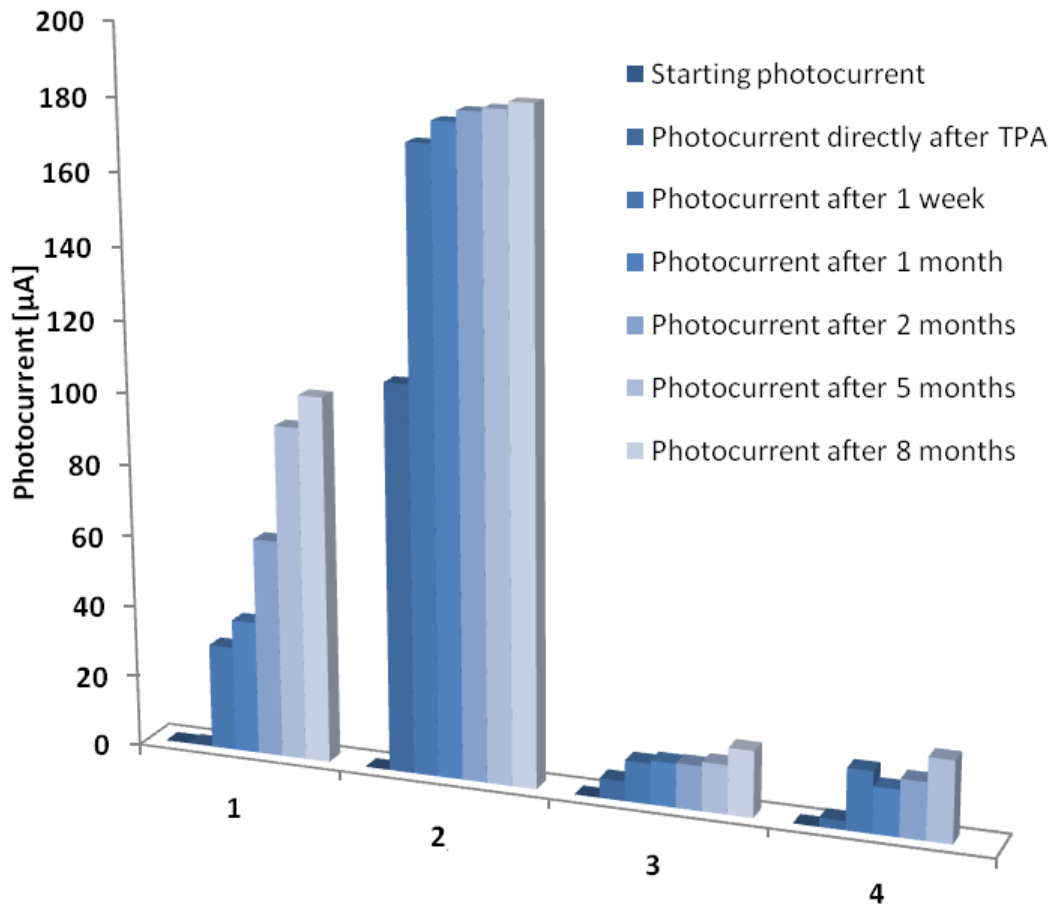
Figure 115: Detected photocurrents before, after and after 8 months storage of demonstrators structured - rigid and rigid-flex substrates

9.8 Data Transfer Properties of Demonstrators

9.8.1 Introduction

The next sections describe a number of investigations carried out by Prof. W. Leeb and G. Schmid at Vienna University of Technology, Institute of Telecommunications. A summary of some of the experiments and results of the tests are included here.

The bit rate is the number of bits conveyed or processed per unit of time. In our investigations the data rates achieved are over 1 Gbit/s (1000000000-bit/s).

The bit error ratio (BER) is the number of bit errors divided by the total number of transferred bits in a specific time interval. It is unitless, but can be expressed as a percentage.

Two 7 cm rigid demonstrators were investigated for their data transmission capability. A transmitter laser was used (VCSEL diode, type ULM850-05-TN-U0101U emitting at a wavelength of λ = 850 nm) with an output of around 2 mW at room temperature. Figure 116 depicts one of the rigid boards investigated. The multimode VCSEL and a GaAs pin photodiode, type ULMPIN-04-TN-U0101U, both from ULM Photonics were grounded by

coplanar lines to connect them electrically to the interfaces. The measurements were performed to estimate the optical losses as well as the data transmission. The photocurrent vs. the laser current was established, as well as the bit error ratio vs. the data rate.
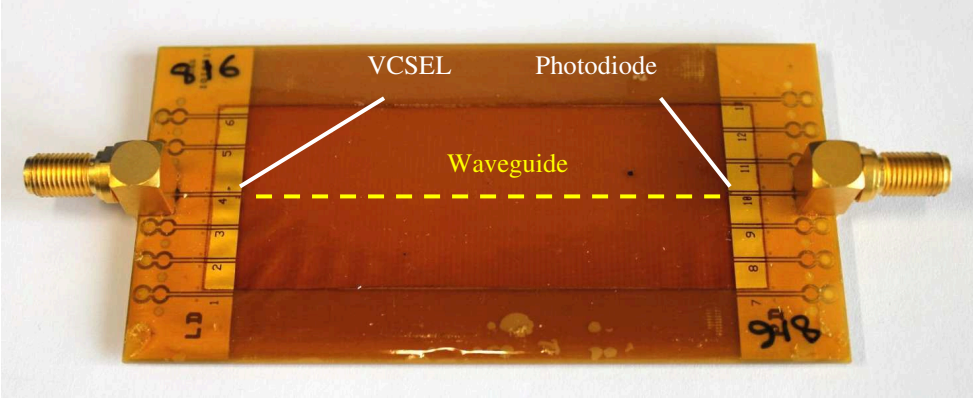

Figure 116: Photograph of the rigid board used to measure data transmission

9.8.2 Determination of Photocurrent vs. Laser Current

To determine the photocurrent at different laser currents, a set up shown in Figure 117 was used. The laser diode controller drove the laser whilst simultaneously measuring the photocurrent. The programme used allowed an increase in the laser current in small increments from $I° = 0$ up to 12 mA, to determine the photocurrent (I_d). The results are shown in Figure 118. The solid and dashed lines correspond to the I_d-I characteristics. At the normal operating photocurrent of $I° = 6$ mA, the two boards maintained photocurrents of 182 and 169 µA. The optical power at a laser current of $I° = 6$ mA of the multimode VCSEL used on the demonstrators was $P_{I°} = 2$ mW in air[79]. Using this value and the measured photocurrents of the demonstrators, the approximate value of the entire optical loss (A) in dB can be calculated using the equation:

$$A = 10 \cdot \log_{10}\left(\frac{P_l}{P_d}\right) = 10 \cdot \log_{10}\left(\frac{S \cdot P_l}{I_d}\right)$$

The photodiodes used on the demonstrators had a sensitivity of $S° = 0.6$ A/W[80][81]: This is the absolute spectral sensitivity and is expressed in amperes per watt. For example the radiant power at a specific wavelength λ falls on the active area of the photodiode, and generates a photocurrent is the ratio between the generated photocurrent and the radiant power which falls on the detector.

P_d is designated as the optical power detected by the photodiode. The optical losses were calculated as (A) = 8.2 and 8.5 dB for the two rigid boards investigated.
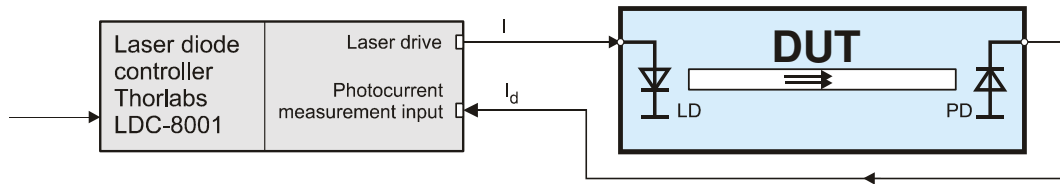
174

Figure 117: Setup for measuring the photocurrent I$_d$ vs. laser current I
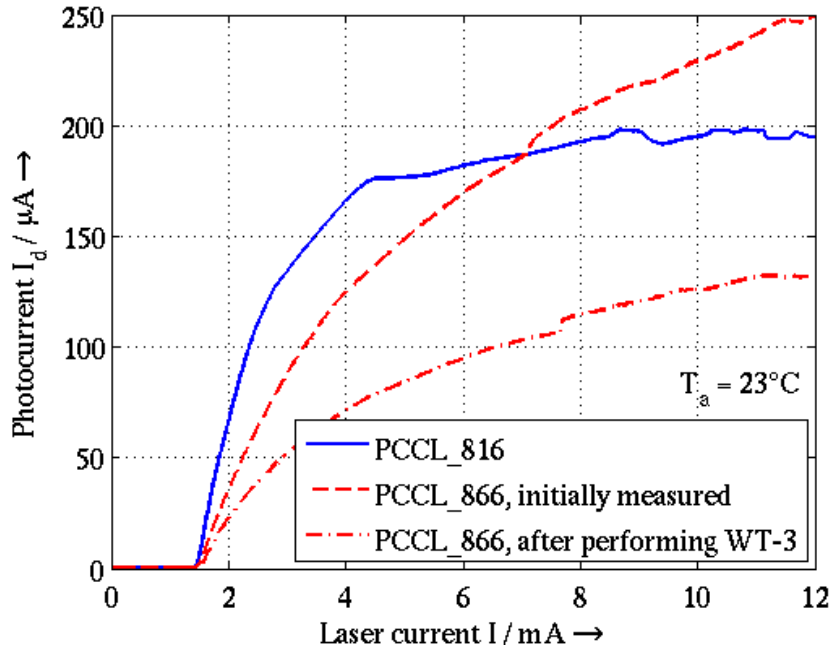

Figure 118: Photocurrent I$_d$ vs. laser current I of both measured rigid boards (WT-3 denotes the temperature dependent data transmission measurements performed on the boards)

9.8.3 Determination of Bit Error Ratio (BER) vs. Data Rate

The second part of the measurement was carried out using the set up shown in Figure 119. The laser diode controller provided the DC laser bias of I° = 6 mA, and the bit error ratio tester (BERT) created a test pattern with a modulation voltage of V$_{pp}$ = 385 mV, consisting of a pseudo random bit sequence length of 2^{31}-1. The BERT is the electronic test equipment used to test the quality of the signal transmission. Bias tees, which are used to inject DC currents or voltages into RF circuits, added the DC bias voltage for the photodiode (U = 2V), along with the laser bias current (I). Both boards showed the lowest BER when only the amplifier shown in the set up was used for conditioning the signal to the data input of the BERT.

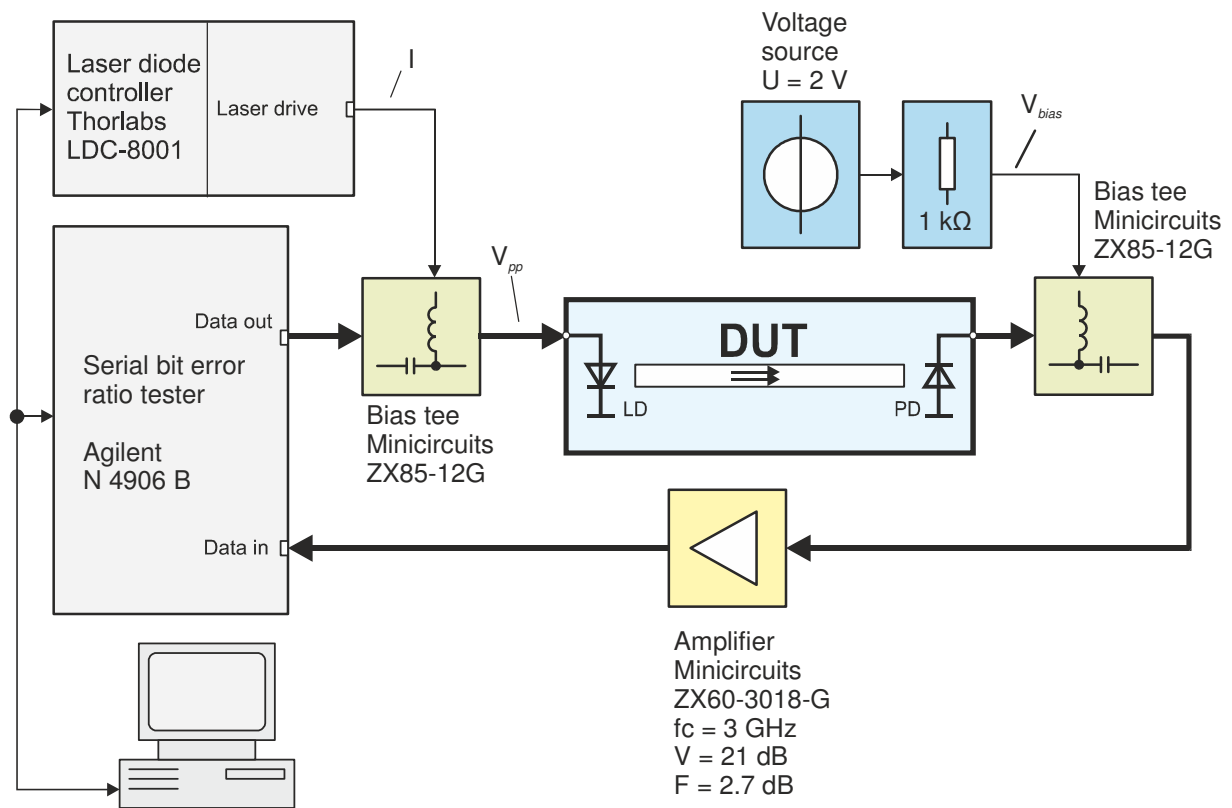**Figure 119: Setup for measuring the bit error ratio BER vs. data rate (fc = frequency, V = gain over frequency, and F = noise figure)**

As shown in Figure 120, it was possible to transmit signals with a rate of nearly R = 4.5 Gbit/s with BER ≤ 10^{-9} via board PCCL_816. Board PCCL_866, where slightly higher optical losses were determined, allowed data transmission of up to R = 6.5 Gbit/s.
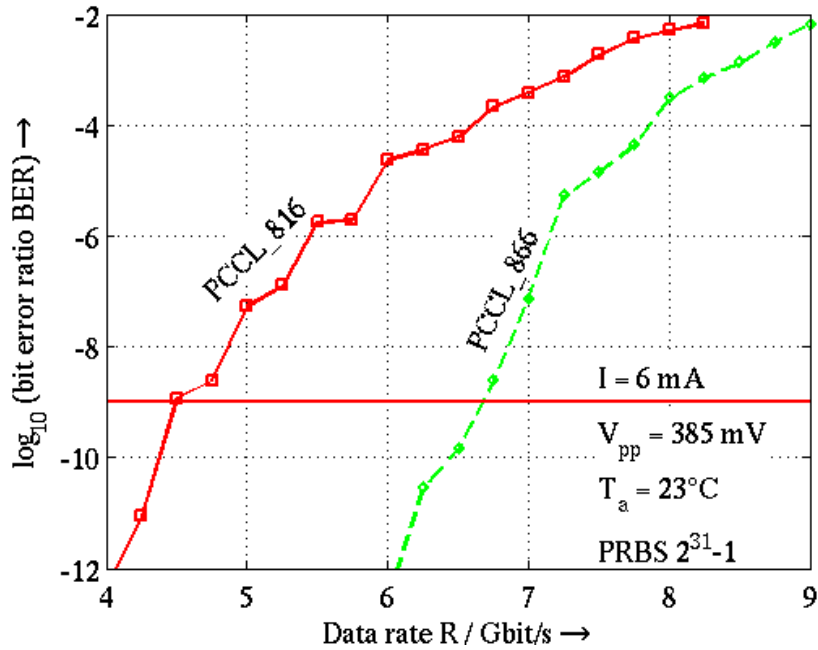
Figure 120: Bit error ratio (BER) vs. data rate R of both tested boards

Boards PCCL_816 and PCCL_866 were the first boards used for such tests, with both boards showing acceptable entire optical losses. Both boards allowed transmission of high data rates, as summarised in Table 30.

Table 30: Summary of the measurement results using boards 816 and 866

Demonstrator	Measured photocurrent I_d/µA	Calculated optical losses A / dB	Maximum data rate with BER ≤ 10^{-9}/ Gbit/s
PCCL_816	182	8.2	4.25
PCCL_866	169	8.5	6.5

9.8.4 Temperature Dependent Data Transmission Properties of Demonstrators

This section describes measurements carried out to test the data transmission properties of the opto-electronic circuit boards at various ambient temperatures. The optical losses of both tested boards, PCCL_816 and PCCL_866, showed only low temperature dependence, with a general tendency to decrease with increasing temperature. For board PCCL_816 the entire

calculated losses decreased from 8.9 dB at −20 ℃ to 7.2 dB at +80 ℃. Board PCCL_866 showed a similar behaviour within the same temperature range, with the losses decreasing from 11.7 dB to 10 dB. A description of the boards and an image are presented in section 9.8.1. For the measurements, the following were performed. Firstly the photocurrent vs. the ambient temperature for both boards was measured. Secondly, eye diagrams at four different discrete temperatures were then performed for board PCCL_866, as this board showed better data transfer properties.

The photocurrent (I_d) at a given ambient temperature (T_a) was recorded and the board was placed in a temperature controlled chamber. The laser diode controller drove the laser diode with a constant current of if I = 6 mA. The temperature was increased linearly inside the chamber, with a gradient of 1 ℃/min from T_a = −20 ℃ to +80 ℃.
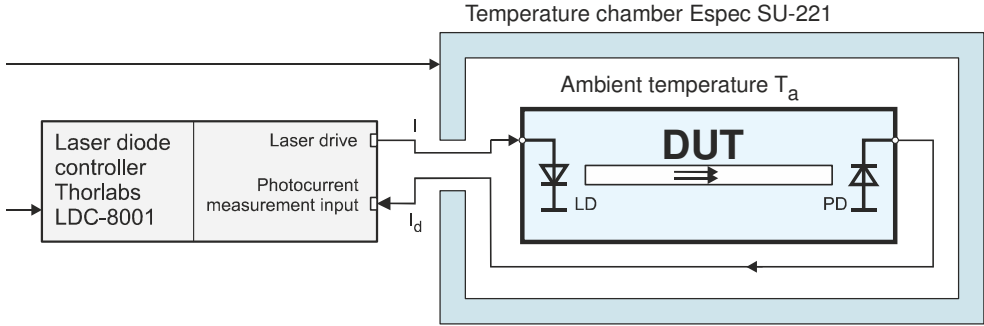
Figure 121: Setup for measuring the photocurrent I_d vs. ambient temperature T_a.

Figure 122 shows the I_d- T_a characteristics of the boards in the temperature range from −20 ℃ ≤ T_a ≤ +80 ℃ when the laser was driven at the usual DC operating current. Both boards showed a low temperature dependence of the photocurrent, with the maximum photocurrent recorded at ambient temperatures.

178

Figure 122: Optical loss *A* vs. ambient temperature *T*ₐ of two PCBs. (*I* designates the laser current).

.

9.9 Eye Diagrams

An eye diagram is used in telecommunications to form an oscilloscope display, by which a digital data signal from a receiver is sampled and applied to a vertical input, while the data rate is used to trigger the horizontal sweep. The pattern is viewed like a series of "eyes". When the signals are too long, too short or noisy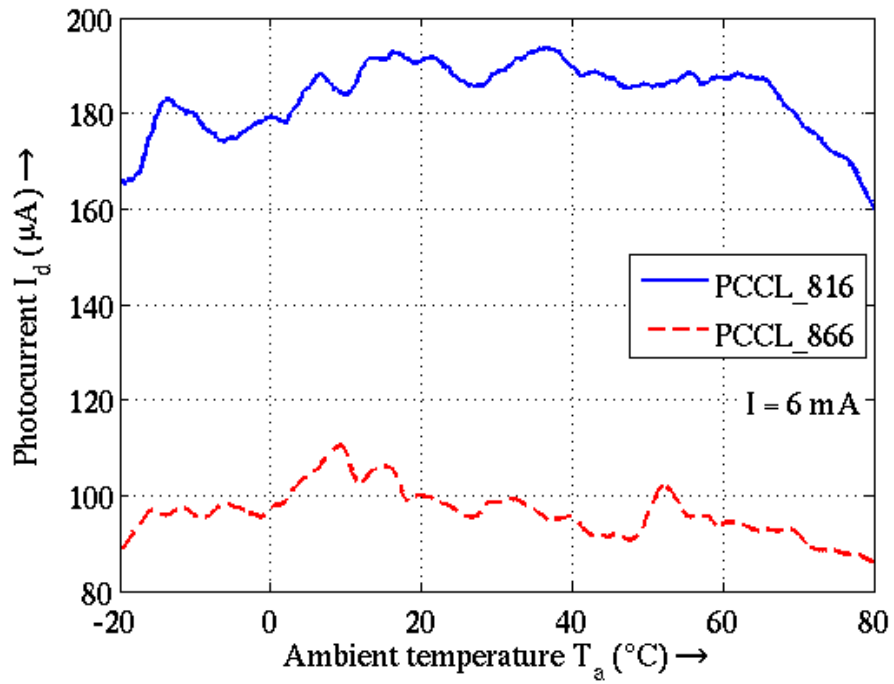, this can be determined by examining the eye diagram. An open eye represents minimum signal distortion, and a closed eye signifies a distorted signal, due to inter-symbol interference and noise[82].

So-called eye diagrams obtained by properly synchronising an oscilloscope display of the digital signal received were recorded to assess the transmission quality at a range of ambient temperature Ta, After placing the PCB into a temperature chamber eye diagrams at Ta = -20°C, +20°C, +40°C and +80°C were taken at a data rate of 4 Gbit/s. Best results were observed at Ta = +40 °C and +80 °C, with the eye diagram recorded at +40°C.The wide vertical opening of the eye indicates a low bit error ratio.

Figure 123 depicts the set up for the recording of the eye diagrams at given temperatures. The laser diode provided the DC bias current of I = 6 mA. The bit error ratio tester (BERT) created a test pattern with a modulation voltage V_{pp} = 385 mV, consisting of a pseudo-random bit sequence of length 2^7-1 with a data rate of R = 4 Gbit/s. Bias tees added the DC bias voltage for the photodiode (U = 2 V) as well as the laser bias current I. An amplifier was used to condition the signal before feeding it to the oscilloscope.

Figure 124, Figure 125, Figure 126 and Figure 127 display the eye diagrams at ambient temperatures of T_a = –20°C, T_a = +20°C, T_a = +40°C and T_a = +80°C. Only at the lowest temperatures of -20 °C did the eye opening drop slightly, indicating a near constant data transmission quality over a wide temperature range.

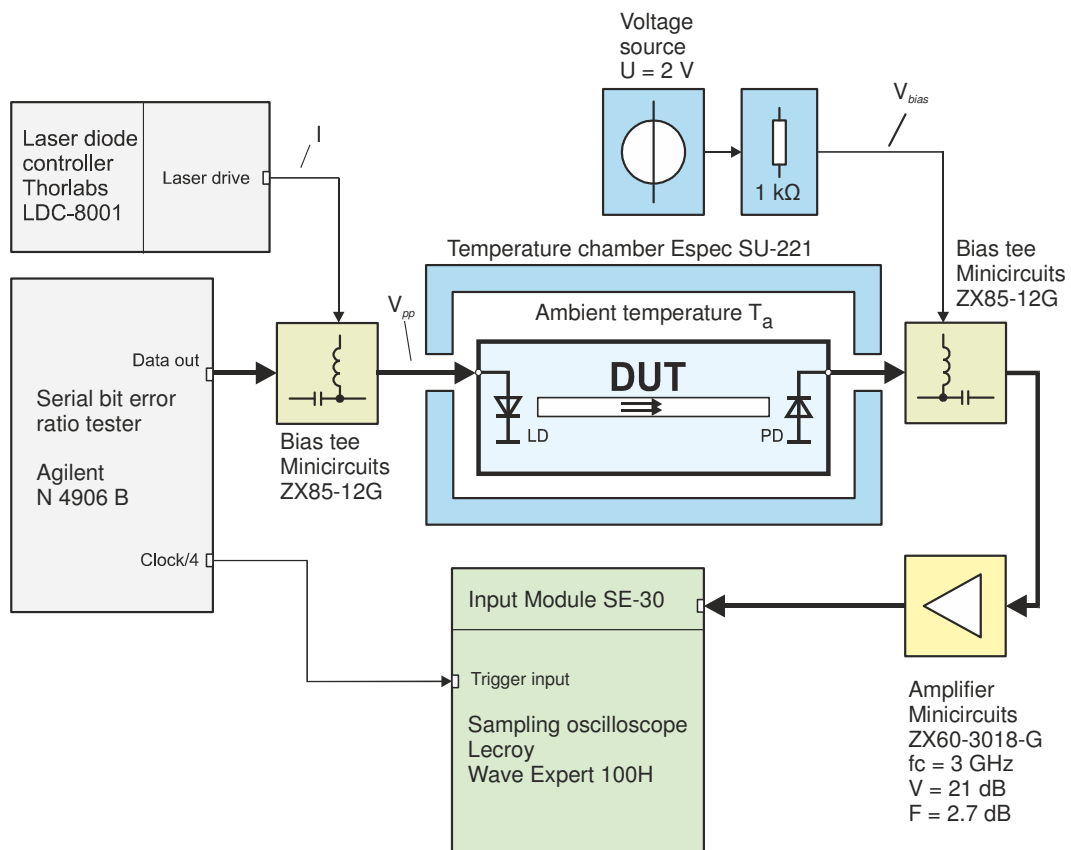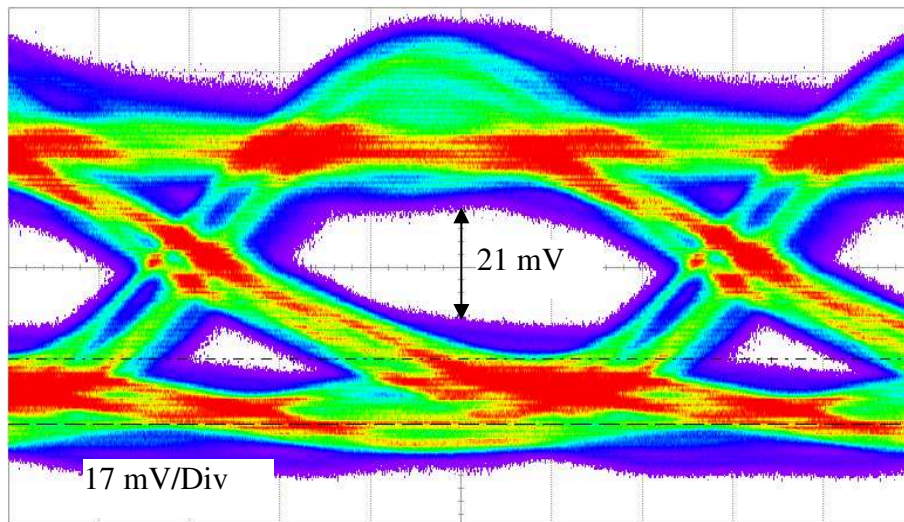**Figure 123: Setup for recording eye diagrams at various temperatures**

Figure 124: Eye diagram at an ambient temperature of $T_a = -20\,°C$ at a data rate of $R = 4$ Gbit/s
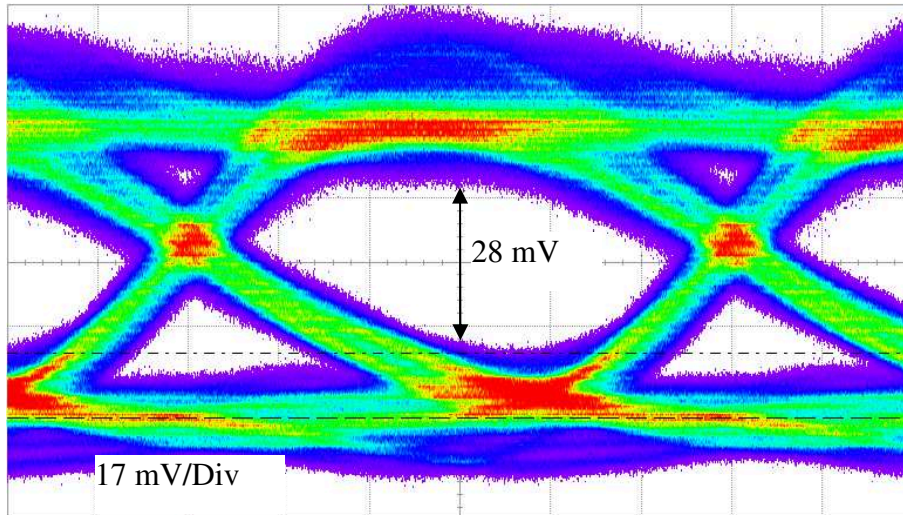
Figure 125: Eye diagram at an ambient temperature of T$_a$ = +20°C at a data rate of R = 4 Gbit/s
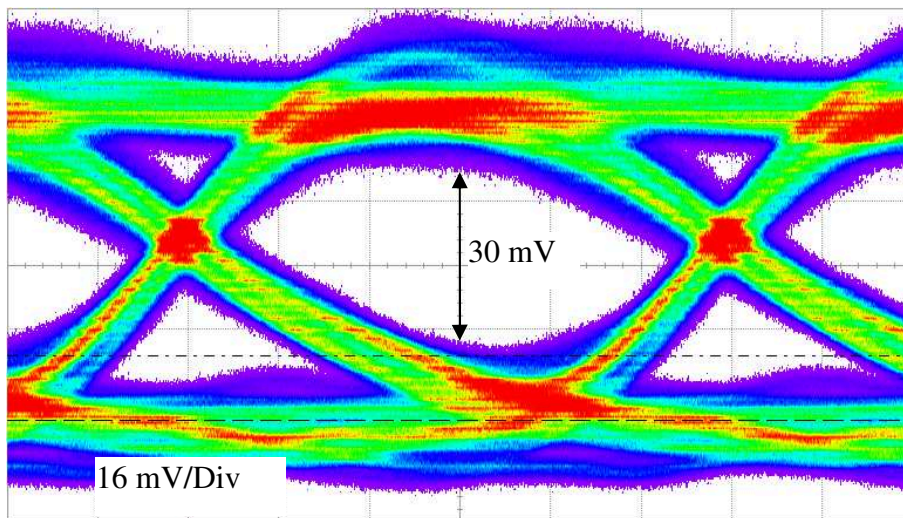
Figure 126: Eye diagram at an ambient temperature of T$_a$ = +40°C at a data rate of R = 4 Gbit/s.

182
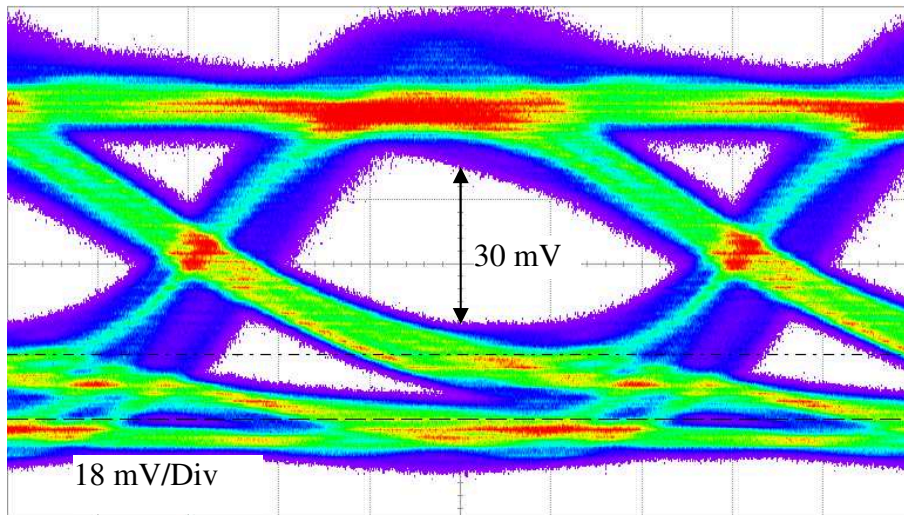
Figure 127: Eye diagram at an ambient temperature of T_a = +80°C at a data rate of R = 4 Gbit/s

9.10 Thermal Cycle Testing

A final set of measurements were carried out on a rigid-flex board to determine the changes in the photocurrent at different temperatures. In this test, the photocurrent was measured online whilst the ambient temperature was altered. The temperature profile used was 25 °C for 30 minutes, 25-75 °C for 30 minutes, 75 °C for 30 minutes and 75-25 °C for 30 minutes. The board was measured alongside a board made with another optical material, Ormocer, which has been used previously as a wave-guiding material, yielding high photocurrents and low optical losses[83]. Board number PCCL_865 was measured against ATS_TPA2_90 (Ormocer). The results are presented in Figure 128. It can clearly be seen that our optical material shows much lower temperature dependence, with around a 50 % change of the photocurrent. The results showed that the photocurrent was stable also on the rigid-flex boards. The board showed a very low temperature dependency and a high photocurrent was recorded throughout, displaying the suitability of this material for such applications.

Figure 128: Online photocurrent measurements of PCCL_ 865 and ATS_TPA2_90 (Ormocer) at different temperature cycles

184

9.11 Conclusion

Comparing the three optical materials developed and characterised, System C proved to be the most promising. The material was found to be thermally stable, non-toxic, and easily processed. A number of optoelectronic PBCs were fabricated, including 7 cm and 15 cm rigid substrates and 7 cm rigid-flex substrates. When the demonstrators were prepared with a flat, homogeneous layer of material and the waveguides were correctly aligned, extremely high photo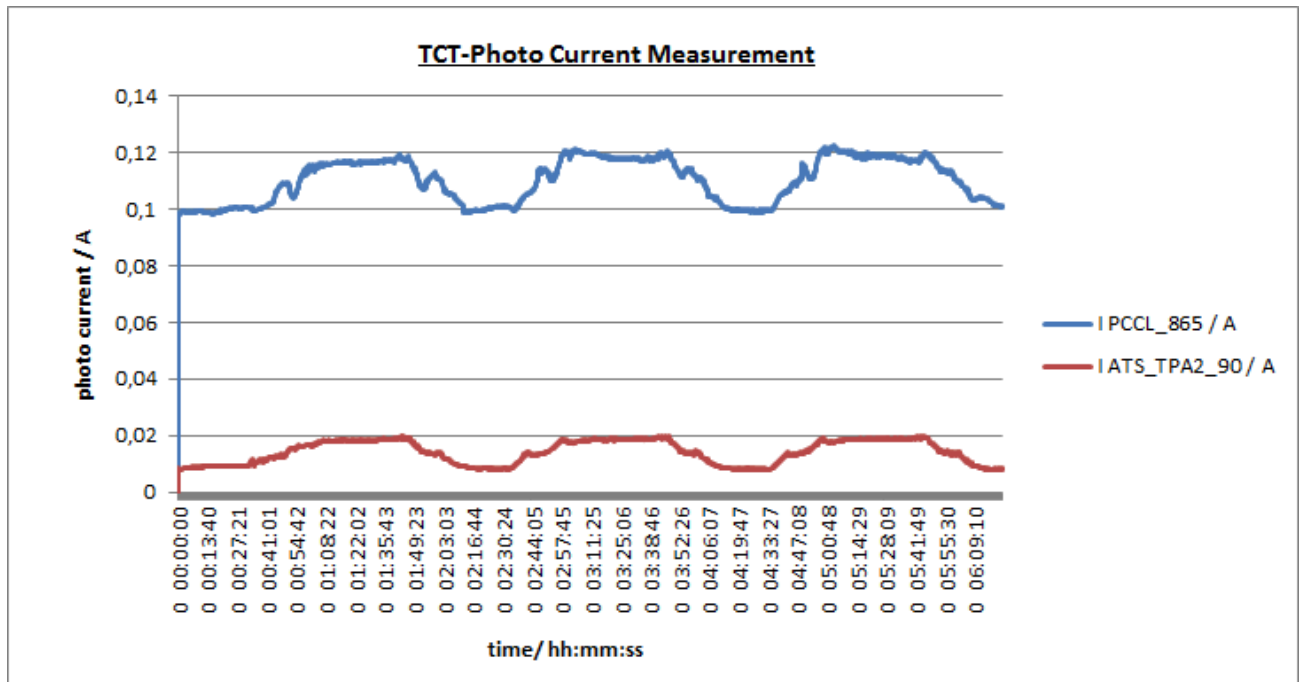currents were achieved. Light extraction tests and cut-back measurements revealed the optical losses of the waveguides were lower than the two previous materials, and the size and shape of the waveguides were also better. The detected photocurrents of the demonstrators remained stable following TPA structuring, with nearly all demonstrators showing a rapid increase in the photocurrent over a period of weeks. This was not observed with System A and B, whose photocurrents decreased following structuring. What seems to be a great advantage with this material is that there is no need to carry out a post baking step to remove any remaining monomers. The monomers are attached to the polymer backbone, and are stable, so no post treatment is required. Post thermal treatments carried out on Systems A and B led to decreases in the photocurrent, due to either damage to the waveguides or shrinkage of the material. Fully functioning optoelectronic PBCs were developed, and have remained stable for over nine months. A number of demonstrators including rigid-flex boards and 15 cm rigid boards were used to investigate the data transmission properties. The results from all data transmission testing revealed the optical waveguides displayed satisfactorily transmission rates at varying temperatures, along with entire optical losses in the range suitable for our requirements.

10 Experimental

10.1 Gas Chromatography

Gas Chromatography was performed on samples of System A, to determine the amount of methacrylate monomers remaining following thermal curing. Preparation of System A is described in Section 4. Samples of the polysiloxane matrix were prepared on glass slides with a layer thickness of 500 μm. A thermal treatment of 80 °C for 25 minutes was performed on one sample, with the other sample also treated at 100 °C for 20 hours (40 mbar). Following an extraction technique using CH_2Cl_2 to swell the matrix, the samples were analysed by GC. 0.9 g of material was scraped off the slides and an extraction was carried out for 24 hours. A small amount of BHT was added to the samples to avoid polymerisation after the extraction. A quantitative study was carried out by using a calibration method. The column used was HP-5 5% phenyl methyl siloxane. The inlet heater was set to 120 °C, with a pressure of 0.817 bar. A total flow of 17.5 ml/min was used, with a split ratio of 5.0. Standard solutions were made up of the three monomers in CH_2Cl_2, which were then diluted to gain a calibration curve ranging from 0.1 -0.02 wt. %. The internal standard used was heptane-(density 0.684, b.p 98.4 °C); 1 μL was added to the samples using a micro syringe. Following the measurements, the corresponding peaks were integrated to gain a true area. The calibration curves obtained are shown in Figure 129, Figure 130 and Figure 131. An external calibration method was also carried out to compare the results.
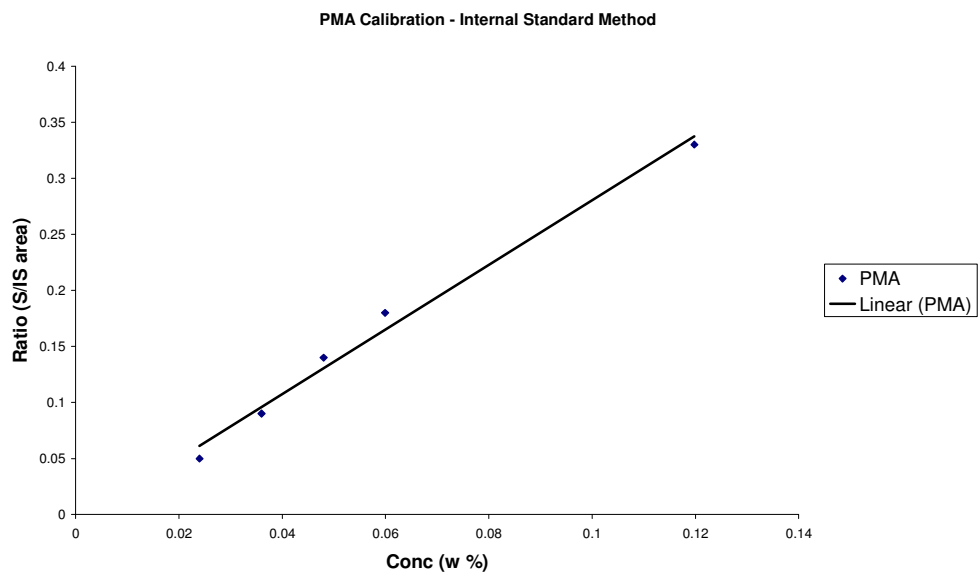
Figure 129: PMA calibration using Internal method - normalised GC peak area vs. concentration
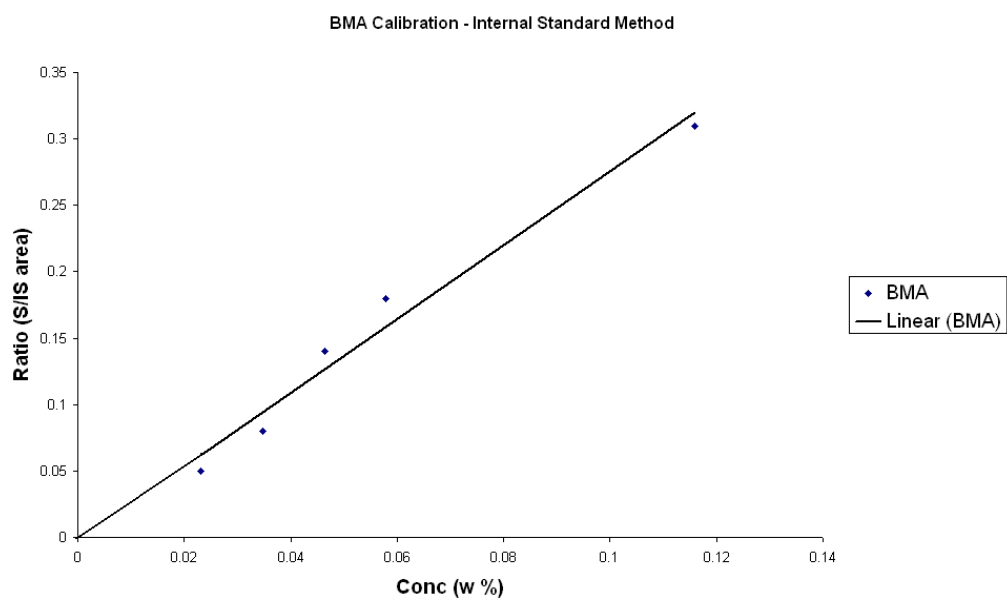
Figure 130: BMA calibration using Internal method – normalised GC peak area vs. concentration

187
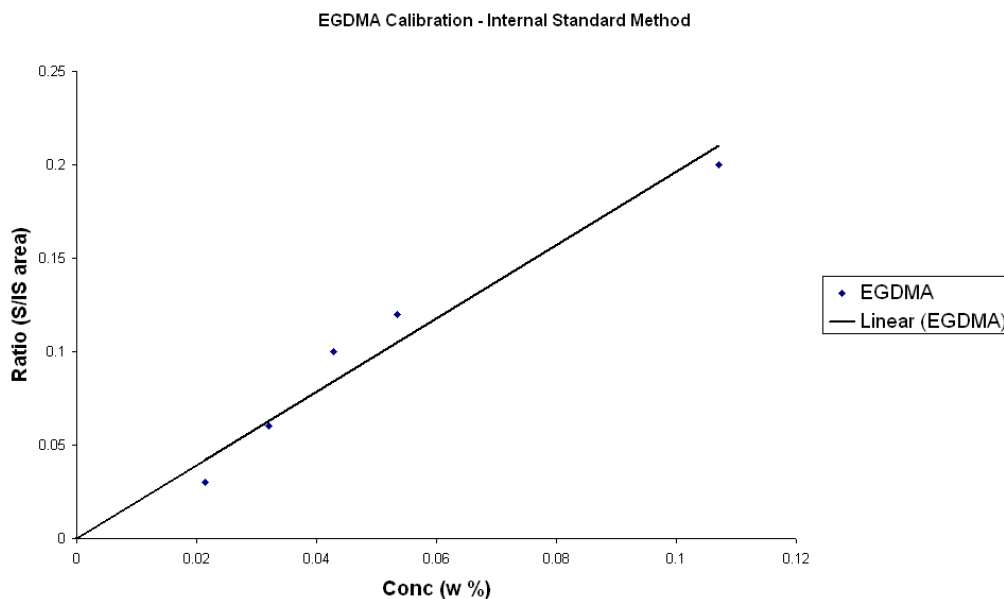
Figure 131: EGDMA calibration using Internal method – normalised GC peak area vs. concentration

10.2 High Performance Liquid Chromatography (HPLC) – Determination of the Amount of Photoinitiator Remaining Following Thermal Treatments (System A)

HPLC was performed on samples of System A to determine the concentration of Irgacure 379 remaining following thermal curing and thermal finishing treatments. The polysiloxane matrix was prepared as described in section 4.2 and containing 1.8 wt. % Irgacure 379. The material was scraped onto glass slides, with a thickness of 300 µm. A thermal step of 80 °C for 25 minutes was performed on all samples, followed by a thermal step of 100 °C for 20 hours (40 mbar) on half the samples. A final thermal step of 170 °C for 18 hours was then performed on one sample. Each sample was removed from the glass slides, weighed and placed in a sealed glass flask, with 10 mL $CHCl_2$, and stirred for 24 hours at room temperature. Following the extraction, the remaining residue was dissolved in 10 mL CH_3CN.

After constructing a calibration curve using different concentrations of Irgacure 379 (Figure 132) the concentrations and percentage of the photoinitiator remaining in the matrix material was calculated. The results are presented in section 4.2.5.

188
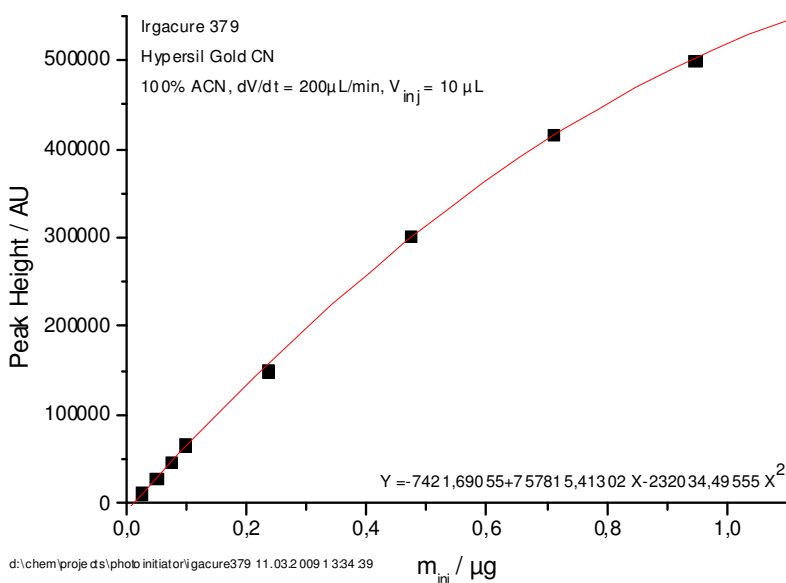
Figure 132: HPLC calibration curve constructed using different concentrations of Irgacure 379 – concentration vs. peak height

10.3 Synthesis of 2-methyl-1-naphthyl-methacrylate

To improve the refractive index difference between the cladding and waveguide core in System A, a number of naphthyl derivatives were investigated. A naphthyl methacrylate monomer, 2-methyl-1 naphthyl-methacrylate was synthesised to determine whether it could be incorporated into System A. Naphthyl derivatives have high refractive indices but the monomer is more difficult to remove from the system following TPA structuring.

The following materials were obtained from Sigma Aldrich, and used as received. 2-methyl-1 naphthyl methacrylate was synthesised by adding 1-methyl-2 naphthol (500 mg, 0.0042 mol) to CH_2Cl_2 (12.5 mL) and triethylamine (0.57 mL). The components were placed in a 2 necked flask, placed in an ice bath and stirred. Methacryloyl chloride (0.41 mL) was dissolved in 1 mL CH_2Cl_2, and added dropwise under constant stirring. Following the addition, the reaction mixture was allowed to stir for 2 hours, and then at room temperature for 1 hour. The precipitated triethylammonium chloride was filtered off, and excess solvent removed by rotary evaporation. The residue was dissolved in ether, and washed twice with 0.1 % NaOH solution. The residue was purified on a silica gel column with 5:1 cyclohexane:ethyl acetate as eluent. 0.55 g of an off white solid was obtained (78 % yield). The reaction is presented in Figure 133.

^{1}H (500MHz, 20℃, CDCl$_3$): δ =□2.10 (1H, s), δ =2.40 (3H, s), δ =5.92 (1H, s), δ =6.59 (1H, s), δ =7.22 (1H, d) δ =7.38 (1H, dd), δ =7. 42 (1H, d), δ =7.50 (1H dd), δ =7.60 (1H, d), δ =7.80 (1H, d)
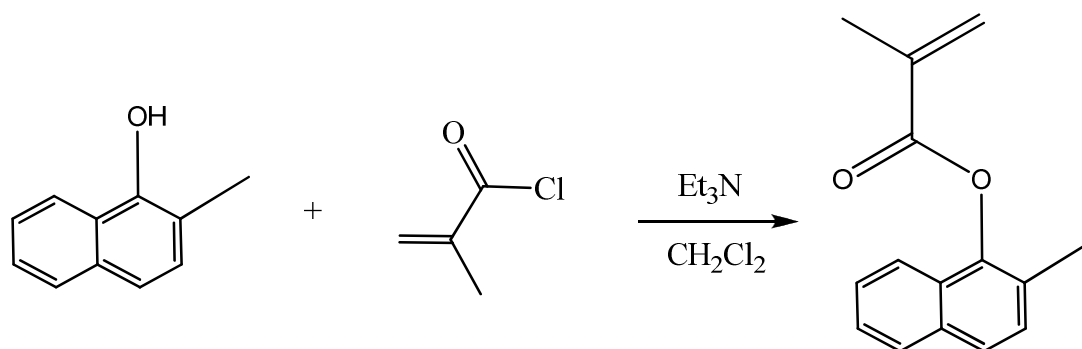
Figure 133: Synthesis of 2 methyl -1 naphthyl-methacrylate

10.4   Head Space Gas Chromatography

10.4.1 Sample Preparation – Calibration

In System B, high refractive index acrylate monomers are incorporated into the matrix to form the waveguide core. The remaining monomers need to be completely removed from the material following TPA structuring. To determine whether the parameters currently used during the thermal steps remove the monomers, Head space GC was performed. Poly diphenyl dimethyl siloxane, epoxy propoxy terminated was hardened with 1,3 bis(3-aminopropyl) tetramethyl siloxane in a 1:1 ratio of active hydrogen equivalent weight and epoxy equivalent weight. The sample was first pre cured at 80 ℃ for one hour to increase the viscosity of the material. Acrylate monomers, (benzyl acrylate, ethylene glycol phenyl ether acrylate and 1, 3 butanediol diacrylate), were added in different weight percentages to each sample. Samples containing 0.5, 1, 2, 3, 4 and 5 weight percent of the acrylate monomers in total, were made up and mechanically stirred for 20 minutes. Each sample was then scraped onto optical glass substrates with a layer thickness of 300 µm. The samples were then cured in a saturated acrylate atmosphere to avoid volatilization during curing, for 20 hours at 50 ° C. Each of the thin layers was then scraped off the glass slides, and 50 mg was accurately weighed into tall glass vials. The samples were analysed in duplicate, and measured at the same time as the unknown samples.

Three samples were prepared to determine the weight percent of acrylate monomers remaining in the matrix following different thermal treatments. All three samples were prepared with the same starting materials as the calibration films. Each sample contained 3.3

wt. % of each of the three selected monomers, so 10 wt. % total monomers in the films. The film thickness was no more than 300 μm thick. Sample 1 was then left for one week, in ambient conditions, by placing it in a non air-tight petri dish, to determine how stable the acrylate monomers were in System B. It is desirable to determine what percentage of monomers are present in the matrix when structuring is carried out, as well as whether the monomers diffuse out from the matrix if not stored in closed conditions. Sample 2 was given a thermal treatment of 80 °C for 20 hours, 40 mbar. Sample 3 was given a thermal treatment of 100 °C for 20 hours, 40 mbar. All samples were analysed in duplicate. The weight of the sample films analysed are presented in Table 31 along with the weights of the three acrylate monomers present in the matrix. Samples 1, 2 and 3 are described in Table 32.

Table 31: Calibration sample weights

Sample description	Weight (mg)	Weight benzyl acrylate (mg)	Weight 1,3 butanediol diacrylate (mg)	Weight ethylene glycol phenyl ether acrylate (mg)
0.5 wt.% (1)	54.60	0.091	0.091	0.091
0.5 wt.% (2)	52.41	0.087	0.087	0.087
1 wt.% (1)	51.01	0.17	0.17	0.17
1 wt.% (2)	51.61	0.17	0.17	0.17
2 wt.% (1)	53.50	0.36	0.36	0.36
2 wt.% (2)	50.95	0.34	0.34	0.34
3 wt.% (1)	50.16	0.5	0.5	0.5
3 wt.% (2)	52.30	0.52	0.52	0.52
4 wt.% (1)	52.28	0.7	0.7	0.7
4 wt.% (2)	50.22	0.67	0.67	0.67
5 wt. % (1)	50.29	0.84	0.84	0.84
5 wt % (2)	51.35	0.86	0.86	0.86
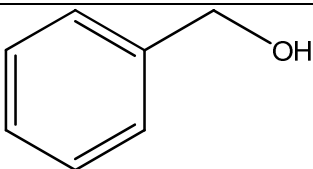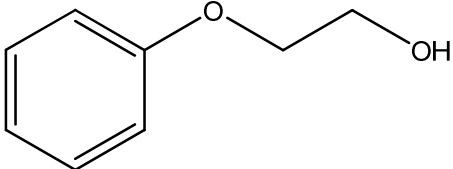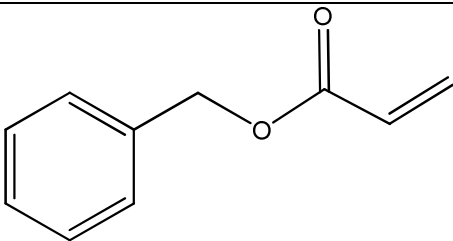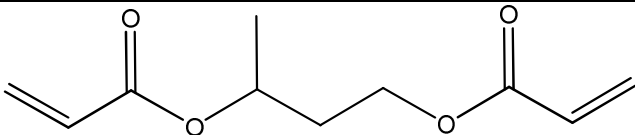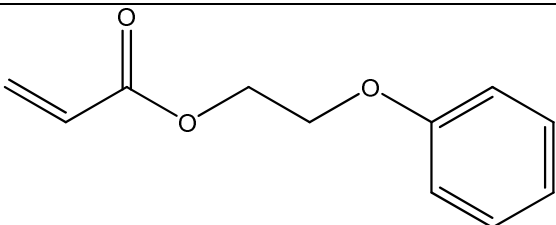
Table 32: Unknown sample weights – starting weight of 10 wt. % total monomer

Sample description	Weight (mg)
Sample 1 – 50 °C curing, 20 hours, Stored in ambient conditions (1)	51.56
Sample 1 – 50 °C curing, 20 hours, stored in ambient conditions (2)	52.02
Sample 2 – 80 °C, 40 mbar	50.34
Sample 2 (orange, thicker) – 80 ° C, 40 mbar	52.86
Sample 3 (thin layer) - 100 °C 40 mbar	50.97
Sample 3 (thicker layer) - 100 °C, 40 mbar	50.35
Sample 3 (thick layer) - 100 °C, 40 mbar	52.03

10.4.2 Analysis Conditions

The 50 mg thin film samples were placed in tall glass vials and sealed tightly, making sure the films were broken into small pieces. A blank sample of air was first analysed, followed by a second blank, epoxy amine resin containing no acrylate monomers. This sample revealed no peaks which would interrupt the interpretation of the three peaks corresponding to the acrylate monomers. The procedure carried out, included each sample being heated to 150 °C for 150 minutes to volatise the acrylate monomers in the samples. A full scan MS was carried out, from 15 to 550 amu. After all samples were run, five peaks could be clearly identified. The three peaks corresponding to the acrylate monomers were present, along with two other compounds, discovered to be benzyl alcohol and phenoxyethanol. These two compounds were not present in the epoxy-amine resin only samples, so are likely to be degradation products from the acrylate monomers. The five monomers are described in Table 33.

Table 33: Description of detected monomers

Monomer	Structure	Retention time (minutes)	Boiling point (°C)
benzyl alcohol		6.18	205
phenoxyethanol		8.42	247
benzyl acrylate		8.74	110-111 (8 mm Hg)
1,3 butanediol diacrylate		9.11	
ethylene glycol phenyl ether acrylate		10.90	111 (2.7 mm Hg)

The calibration curves were first constructed with each separate sample, and then with an average of the two peak areas. Benzyl acrylate and 1,3 butanediol diacrylate gave reasonable calibration curves, however phenyl acrylate showed a lower concentration than expected, which is likely to be due to either the 150 °C heating step of the samples not being sufficient enough to volatise all the monomer, or the degradation product phenoxy ethanol playing a bigger part in the percentage of the overall acrylate monomer. Therefore a calibration curve was also constructed including the peak area of the phenoxy ethanol, to determine the amount of ethylene glycol phenyl ether acrylate that degrades. The calibration curve for each monomer is presented below. The peak areas for the unknown samples are presented in Table 34.
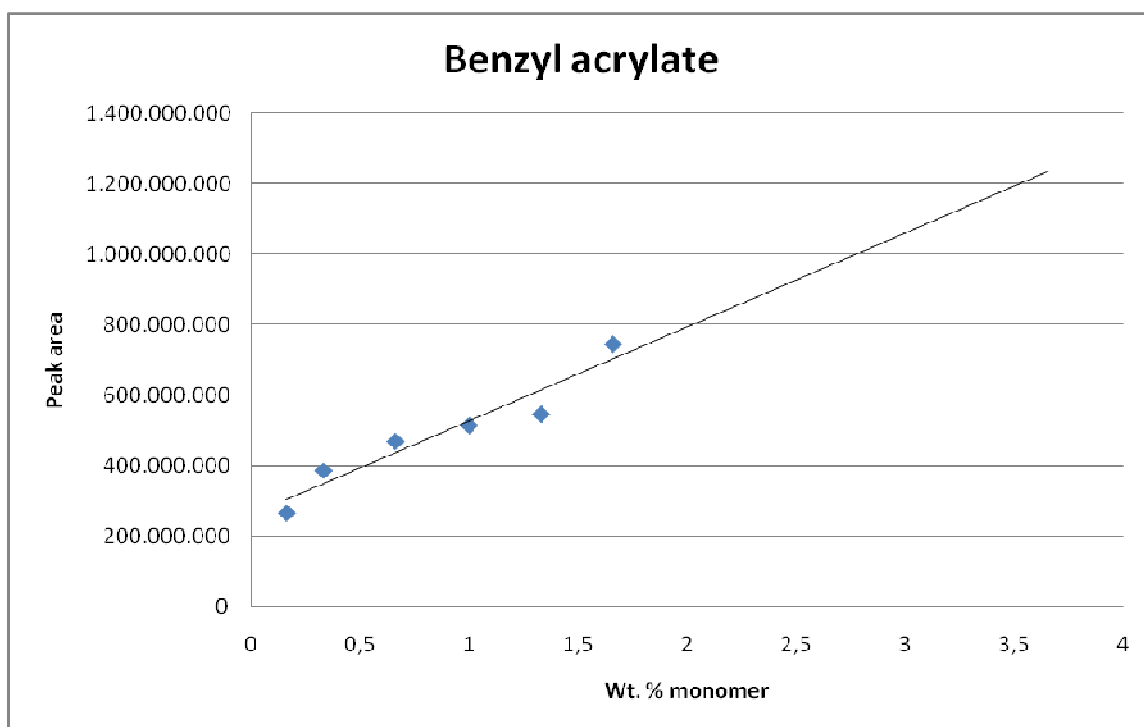
Figure 134: Calibration curve, Benzyl acrylate – average of two analysed sample films
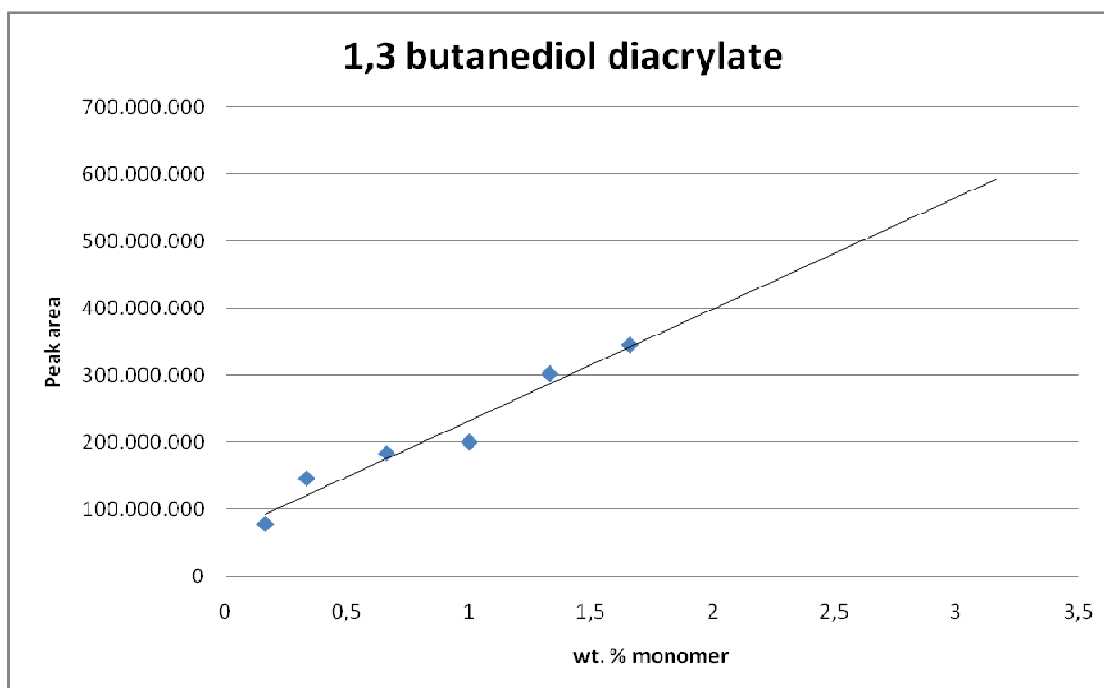
Figure 135: Calibration curve, 1,3 butanediol diacrylate – average of two analysed sample films

194
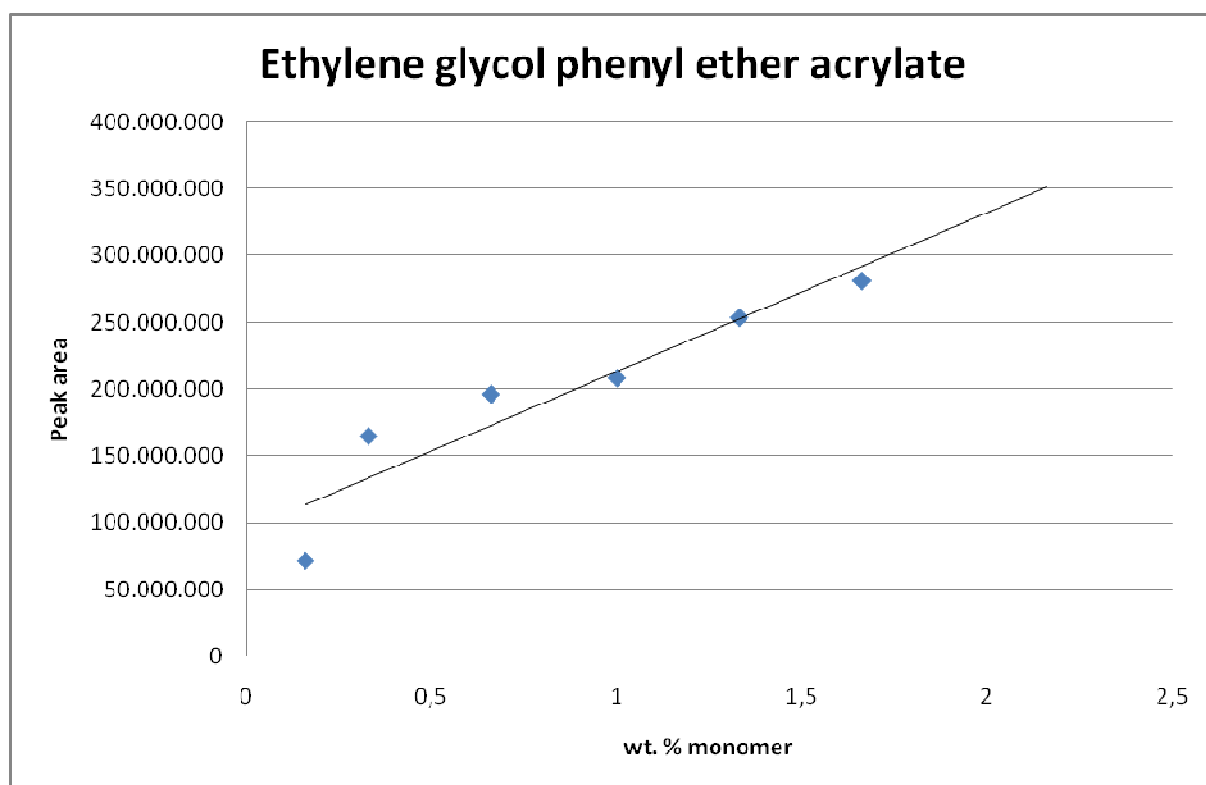
Figure 136: Calibration curve, ethylene glycol phenyl ether acrylate – average of two analysed sample films

Table 34: Peak areas and calculated weight percent of each selected monomer (starting wt. % 3.3 of each monomer)

Sample 1 (no thermal treatment – 1 wk ambient conditions)	Peak area (average)	wt. % monomer remaining in matrix (starting wt. % 3.3)	Fraction of monomer remaining in matrix (%)	Fraction of monomer removed from matrix (%)
Benzyl acrylate	1.07×10^9	2.8	85	15
1,3 Butanediol diacrylate	6.50×10^8	3.3	100	0
Ethylene glycol phenyl ether acrylate	3.07×10^8	1.8	54	46
Ethylene glycol phenyl ether acrylate + phenoxy ethanol	5.09×10^8	1.8	54	46

Sample 2 (80 °C thermal treatment, 40 mbar)				
Benzyl acrylate	2.28×10^8	0.2	6	94
1,3 Butanediol diacrylate	2.47×10^8	1.1	34	66
Ethylene glycol phenyl ether acrylate	6.12×10^7	> 0.16	>5	< 95
Ethylene glycol phenyl ether acrylate + phenoxy ethanol	2.80×10^8	> 0.16	>5	<95
Sample 3 (100 °C thermal treatment, 40 mbar) Benzyl acrylate	8.65×10^7	>>0.16 (3)	>>5	< 95 91
1,3 Butanediol diacrylate	1.25×10^8	0.3	9	
Ethylene glycol phenyl ether acrylate	1.58×10^7	>>> 0.16 (5)	>>>5	< 95

10.5 Determination of the Optical Losses of TPA Written Waveguides – Cut Back Measurements

Light extraction tests and cut –back measurements were performed on System C, in order to determine the optical losses. The optical fibre set-up is shown in Figure 137. In this type of experiment, the waveguide is cut into different known lengths, and the optical power through the waveguide is measured compared to the output. Both ends of the waveguide need to be accessible for in coupling and out coupling of light. This makes measurements difficult to perform if bad cross sections are produced or the material is too soft to prepare smooth surfaces.
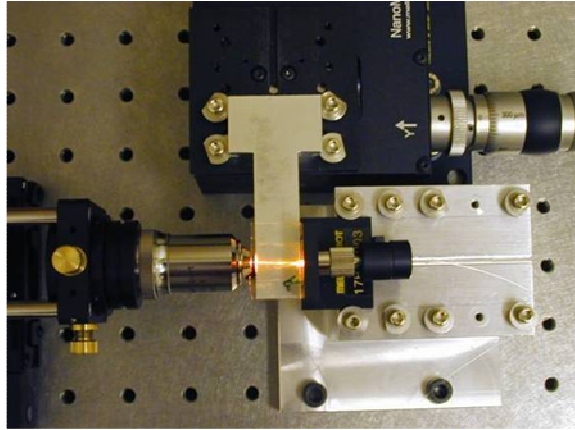
Figure 137: Optical fibre set up used to perform cut back measurements

Three samples were prepared on 7 cm rigid-flex substrates to perform light extraction and cut back measurements. The samples contained 0.025 wt. % N-DPD, and had layer thicknesses of ~ 300 μm. The samples were prepared by structuring a field of waveguides with laser powers of 190-250 μW in 20 μW intervals. Two waveguide fields were structured consisting of 6 waveguides, 20 μm apart, with laser powers of 260, 230, 220, 210, 200, and 260 μW. The waveguides structured with 260 μW were used as markers for the waveguides, as at this laser power, the material burns, thus making the other four waveguides easy to locate. A bundle of seven waveguides was also structured in each sample. One sample was given a thermal treatment of 150 ºC for 1 hour, to determine whether the optical losses decrease. To carry out the measurements, the samples were first cut with a rotary cutter, and the waveguide cross sections were observed in the optical microscope. In coupling of light was then carried out using an optical fibre (λ_0 = 850 nm). It was possible to then observe each of the 4 waveguides using the monomode fibre when the light was in coupled. The cut-back measurements were then carried out by cutting the waveguides into different lengths, (38, 34, 33, 28, 24, 20 and 15 mm. The optical loss for each waveguide length was then measured, using a Monomode fibre (Butt-Coupling, Faser FS-SN-4224). It was possible to achieve an effective cut for each sample, so each sample was able to be measured. Results of these measurements are presented in section 9.5.

11 Methodology

The following section outlines all instrumental techniques used during this project, outlining some of the general methods and a description of the apparatus used.

11.1 STA-MS

To determine the thermal stability of the developed materials, along with the analysis of compounds being removed during thermal steps, Simultaneous Thermal Analysis (STA) coupled with Mass Spectrometry (MS) was performed. The model of the instrument was a Netzsch STA 449 C coupled with an Aeolos 32 MS.

11.2 Ellipsometery

To determine the refractive index of a number of illuminated and non illuminated samples of the developed materials, spectroscopic ellipsometry was performed A Woollam VASE spectroscopic ellipsometer was employed (Xenon short arc lamp, wavelength range 240 nm-1100 nm, spectral bandwidth 5 nm). The implemented software uses the Levenberg-Marquardt fit algorithm. Using the ellipsometric data, the dispersion of the refractive index (Cauchy fit) was able to be obtained.

Ellipsometry is the primary method by which the optical constants of thin films can be determined. Ellipsometry measures the change in the polarization state of light which is reflected from the surface of a sample. By preparing thin films of our material, elipsometric spectroscopy could be performed on UV illuminated and non-illuminated samples, to determine the increase in refractive index upon polymerisation. The refractive index difference between the core and cladding for waveguides is dependent on the dimensions and wavelength of the light source, however for our applications, a difference of between 0.003 and 0.1 is required

11.3 FT-IR Spectroscopy

To characterise all components used in the development of the optical materials, FT-IR spectroscopy was performed. Time-base FT-IR spectroscopy was also carried out on a number of samples, to monitor the double bond conversion of monomers used to form the optical waveguides. To perform the measurements, a Perkin Elmer Spectrum One, with pyroelectric DTGS-detector (Deuterated triglycine sulphate) and a classic KBr optic were used.

Time-based FT-IR spectra were recorded with an FT-IR spectrometer (Spectrum One, Perkin Elmer). Samples were spin coated onto gold coated silica plates to obtain thin films. Samples were placed inside a wide angle reflection cell, which was purged with nitrogen.

11.4   Spot Cure Lamp – Illumination Experiments

For single-photon irradiation experiments, an Omicure s1000 spot cure lamp was used, with a standard 320-500 nm filter. Illuminations were carried out under nitrogen atmosphere, with the light guide 7 cm above the thin films of the optical material. The lamp used had an output of 18 W / cm^2.

11.5   Near Infrared Spectroscopy

Near infrared spectroscopy was carried out on an NIR spectrophotometer with integrating sphere. (PerkinElmer Lambda 950). The silanol material was cured in plastic optical cuvettes, which were broken open to produce free standing samples. One sample was irradiated using an omicure spot cure lamp, to induce polymerisation.

11.6   Microscopy

The microscope used to record images of the waveguides was an Olympus BX 51. The microscope can be used in light field, dark field and phase contrast modes, and images can be captured using analysis Five software from Soft Imaging System.

11.7   High Performance Liquid Chromatography (HPLC) coupled with Mass Spectroscopy (MS)

To perform HPLC, an LCQ Advantage MAX Ultra Sensitive LC-MS/MS Ion Trap System (Thermo Electron) was used, containing the following: Surveyor MS Pump Plus, Surveyor Autosampler Plus, Surveyor PDA Detector and an ESI Probe. The settings of the MS included:

    Sheath Gas Flow Rate: 20 a.u

    Spray Voltage: 6.5 kV

    Capillary Temperature: 200 °C

    Capillary Voltage: 3 V

Tube Lens Offset: 10 V

The LC settings included:

Hypersil Gold CN Column, 150 m x 2.1 mm, 3 μm + Guard column (Thermo Electron)

Flow Rate: 200 μL/min

Injected Volume: 10 μL

11.8   Headspace Gas Chromatography

The instrument used was a Perkin Elmer, headspace sampler HS 40, coupled to a 5890 series gas chromatograph. The column had a length of 30 m, and a diameter of 0.25 m, with helium as the carrier gas. The injection temperature of the sample was 270 °C and the oven temperature was set at 325 °C.

11.9   Rheology

11.9.1 Rheometer

To determine the viscosity of some of the materials investigated, rheology was used.The instrument utilised was an Anton Paar Physica cone-plate rheometer, which allows thermostatted operation.

11.9.2 Principles of Rheology

Viscosity is a property of liquids which indicates the resistance to flow. Displacement (deformation) occurs when force is applied to a volume of material. If two plates with an area A, (depicted in Figure 138) are separated by a fluid of distance H and are moved at velocity V, by a force F, relative to each other, then Newton's law states that the shear stress, which is the force divided by the area parallel to the force, F/A, will be proportional to the shear strain rate (V/H). This is known as the dynamic viscosity, (η). The *shear strain* is quantified by the displacement per unit height (D/H) and the rate of this effect or the *strain rate* is the velocity per unit height (V/H). The viscosity is therefore the tendency of the fluid to resist flow and is defined as:

$$\eta = \frac{\text{Shear stress}}{\text{Strain rate}} \quad \text{(Pa s)}$$
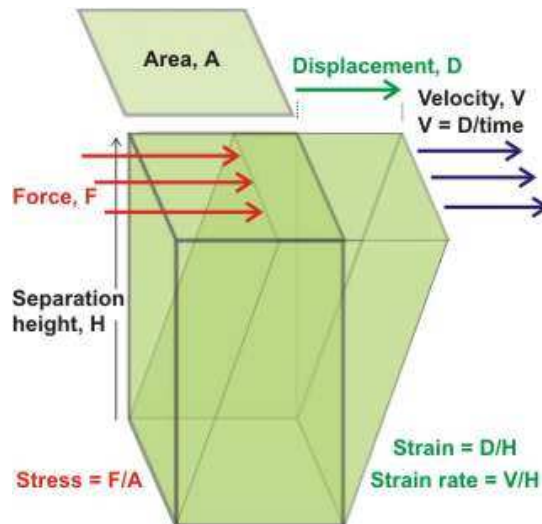
Figure 138: Laminar shear of fluid between two plates. Friction between the fluid and the moving boundaries causes the fluid to shear. The force required for this action is a measure of the fluid's viscosity.

Parameters

Storage modulus (G`): This can be defined as the ratio of shear stress to strain or deformation, when dynamic deformation is applied when using a cone and plate rheometer. This represents the elastic portion. It relates to the elasticity of the polymer, the **loss modulus (G``)** and in dynamic measurements, relates to the viscous behavior. G, together with G``, give an idea of the dual nature of the polymer melt, which is a partly elastic and partly viscous fluid. These measurements, which were performed together, provided information on the curing behaviour.

Complex modulus: Sometimes stated as dynamic modulus, is the ratio of stress to strain under vibratory conditions.

Complex viscosity: Complex Modulus divided by Angular Frequency.

11.10 Abbe Refractometer

To determine the change in the refractive index between the cladding and core of the epoxy polysiloxane material following UV irradiation, an Abbe refractometer was utilised. This devise is used to measure the refractive index of solid samples such as glass, plastics and polymer films. A schematic description of the refractometer is depicted in Figure 139.

Figure 139: Schematic representation of the Abbe refractometer

12 Summary and Outlook

This work describes three different optical materials, to be used as matrix materials on PBCs. The first material, developed from hydride and vinyl terminated polysiloxanes and containing methacrylate monomers, was thermally cured via a hydrosilylation reaction. The material was fully characterised via FT-IR and ST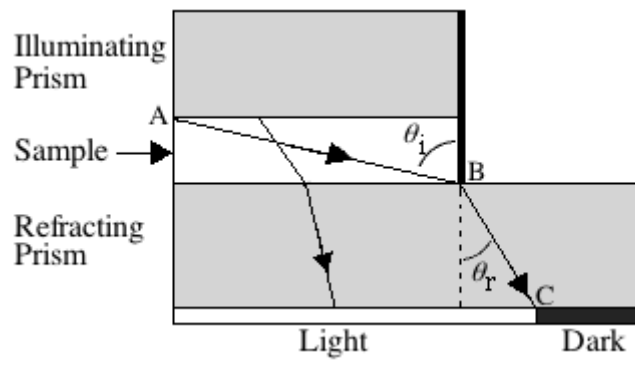A analyses. Optimisation of the material was performed by changing the monomers and investigating different thermal steps to remove all monomers following TPA in order to stabilise the material. Optical characterisation was performed by means of determining the refractive index change between the cladding and waveguide core, performing cut back investigations and conducting a number of TPA material testing, where optical waveguide structures were inscribed into the material. The structures were characterised by optical and phase contrast microscopy. Finally optoelectronic printed circuit boards were developed, which could then be used to monitor the increase in photocurrent arising from the connection of mounted optical components. An increase in the photocurrent was observed following TPA structuring, and a number of demonstrators maintained a stable photocurrent for over a year. Although the material has a high thermal stability, essential post thermal treatments performed on the demonstrators led to a decrease of the photocurrent. The chosen photoinitiator, Irgacure 379 was also found to be unstable in the matrix material, leading to "out blooming" of breakdown products following exposure to light. It was discovered that the out blooming was detrimental to the waveguides when they were exposed to light, leading to a decrease in the photocurrent.

In order to be able to carry out TPA testing with the specific two-photon photoinitiator N-DPD, a new matrix material was developed, in which the hydrosilylation reaction was not used as a curing method. N-DPD contains triple bonds, which are likely to take part in the Pt catalysed hydrosilylation reaction, leading to a breakdown of the π-conjugated system. The matrix material, based on an epoxy propoxy terminated polysiloxane cross linked with a diamine, was used in conjunction with more reactive acrylate monomers, and cured at room temperature. The material had a higher thermal stability than System A, and the incorporated acrylate monomers were removed from the matrix following TPA more easily. TPA material testing revealed high contrast, non interrupted waveguide structures which could be structured with a large fabrication window. Using acrylate monomers in combination with N-DPD led to waveguides being structured with larger cross sections compared to methacrylate monomers. Optoelectronic printed circuit boards were fabricated on rigid and rigid-flex boards; however the post thermal treatment, performed to remove the remaining acrylate monomers once again led to a decrease in the photocurrent. Using N-DPD as photoinitiator led to better TPA structuring, and only very low concentrations were needed, however the

acrylate monomers were still difficult to remove completely from the material, meaning high thermal post treatments were performed.

To overcome the problems associated with post thermal treatments, it was decided that if the high refractive index functional group could be attached to a polymer backbone, no removal of monomers would be necessary. A third material was therefore developed, consisting of a silanol terminated polysiloxane, cross linked with an acryloxy methyl siloxane. The material was fully characterised by FT-IR spectroscopy, STA and Ellipsometry. Optical characterisation revealed the material considerably outperformed Systems A and B, with exceptional TPA material testing results. Processing of the material consisted of simple mixing and room temperature curing, with no additional monomers added. N-DPD was soluble in the material, with no "out blooming" or crystals observed. Waveguide structures with large cross sections were fabricated, using a wide laser power fabrication window. A number of thermal steps up to 150 °C revealed that the waveguides and optical material were stable. In most cases thermally treating the waveguides led to an improvement in the contrast between the waveguide core and cladding. A number of successful fully functioning optoelectronic printed circuit boards were fabricated on rigid and rigid-flex substrates, with extremely high photocurrents achieved. The refractive index difference between the waveguide core and cladding material, determined by ellipsometry, was found to be 0.01 when 20 wt. % cross linker was added. This is likely to increase following post thermal steps, as the contrast between the waveguide and cladding visually improves. For the first time, System C was used on optoelectronic printed circuit boards for characterisation with respect to data transmission properties. High data transmissions of up to 6 Gbit/s at a bit error rate of 10^{-9} were demonstrated, with the material showing low temperature dependence with respect to the photocurrent as well as the total optical losses. Bend tests conducted using rigid-flex demonstrators revealed photocurrents and the rate of data transfer only slightly decreased when deforming the boards.

System C is clearly applicable in the manufacture of optical interconnects, which was the object of this work. With respect to thermal stability, the material performed extremely well with respect to STA measurements and post thermal treatments. Systems A and B both suffered from a loss of photocurrent when thermal treatments were performed, however when System C was used for demonstrator fabrication, the photocurrent increased following thermal steps. With respect to optical losses, the fabrication of demonstrators and data transmission experiments, System C outperformed the other two systems, with work being continued to optimise the material to be used in the manufacture of optical interconnects.

From the obtained results future work will be based on further optimisation of System C to develop optical connections on printed circuit boards. Processing of the material is relatively

simple, concerning the mixing of two components and room temperature curing. Applying the material to the substrates however, needs to be optimised, as achieving homogenous, smooth thin films leads to the best possible chance of producing a successful alignment of the waveguide between the mounted diodes. The nature of the curing of the material means layers thinner than 400 μm lead to an uneven surface, as the top layer cures at a faster rate. If the layer is too thin, the mounted diodes are not correctly covered, making the exact position of the active area difficult to locate. Optimum results are obtained when the active areas on the mounted laser and photo diodes can be determined, which is only possible when the material layer has a perfectly smooth surface, free of inhomogeneities and foreign particles.

Further investigations need to be carried out in order to determine exactly why the photocurrent of demonstrators produced using System C increeaseed following TPA structuring. It is not uncommon for post TPA processes to occur, however demonstrators monitored for over 6 months revealed a continuing increase of the photocurrent, suggesting other factors are involved. Optical microscopy can be performed on cross sections of the waveguides, in order to observe any changes to the size and shape. Another method would be to perform long term ellipsometry investigations, to establish whether the refractive index difference between the cladding and waveguide core changes over a period of months. Preliminary tests on demonstrators which were given thermal treatments between 100 and 150 °C for periods of up to an hour led to an increase in the photocurrent, suggesting either a change in the waveguide network, or the cladding material was more stabilised due to removal of any by-products from curing.

Using N-DPD as photoinitiator led to high quality TPA structured waveguides; however the yellow colour of the photoinitiator leads to a substantial yellowing of the matrix material. Although NIR spectroscopy revealed no significant absorbance of the material in the wavelengths of interest, a specific TPA photoinitiator with such a bright colour may lead to long term stability problems. Other acryloxy functional cross linkers were investigated in System C, however longer chain cross linkers, leading to promising TPA structuring results, took much longer to cure, and produced waveguide structures with smaller cross sections. An acryloxy functional silane bearing phenyl groups is one cross linker which should be investigated, due to the possibility of achieving a higher refractive index contrast.

System C is suitable to be produced on a larger scale, and once sealed and protected from moisture, can be stored over a period of months, making the material applicable to be used as an optical matrix material for flexible printed circuit boards. Transmission of signals with a rate of up to 6.5 Gbit/s were achieved with the demonstrators produced, with rigid-flexible boards also performing well in all experiments.

References

[1] D.R. Selviah, *J. Inst. Circ. Technol*.1 **2008** 3.

[2] J-P. Fouassier. *Photoinitiation, Photopolymerisation, and Photocuring: Fundamentals and Applications* Hanser Gardner Publications **1995**

[3] H-B. Sun, S. Kawata. *APS* 170 **2004** 169

[4] V. Schmidt, *Mikro- und Nanostrukturierung von Polymeren mit Femtosekunden Laserpulsen (Zwei-Photonen-3D-Laserlithographie)*

[5] M.Zhou, H.F. Yang, J.J. Kong, F. Yan, L. Cai. *J. Mater. Process. Technol*. 200 **2008** 158

[6] J.F. Rabek. *Mechanisms of photophysical processes and photochemical reactions in polymers* Wiley **1987**

[7] K-S. Lee,R.H. Kim, D-Y. Yang, S.H. Park, *Prog. Polym. Sci.* 33 **2008** 631

[88] T.C. Lin, S.J. Chung, K.S. Kim, X.P. Wang, G.S. He, J. Swiatkiewicz, H.E. Pudavar, P.N. Prasad, *Adv. Polym. Sci*. 161 **2003** 157

[9] H. Ma, A. K-Y. Jen, L. R. *Dalton. Adv. Mater*. 14 **2002**

[10] K.D. Dorkenoo,O,. Cregut, L. Mager,F. Gillot,C. Carré,A. Fort, *Opt. Lett*. 27 **2002** 1782

[11] S. Klein, A. Barsella, G. Taupier, V. Stortz, A.Fort,K.D. Dorkenoo, *App. Surf. Sci*. 252 **2005** 4919

[12] M.P. Joshi,H.E. Pudivar,J. Swiatkiewicz,P.N. Prasad, B.A. Reianhardt, *App. Phys. Let*. 74 **1999** 170

[13]K. Kaneko, H.B. Sun, X.M. Duan, S. Kawata, *App. Phys. Lett*. 83 **2003** 2091

[14] W.H. Zhou, S.M. Kuebler, K.L. Braun, T.Y. Yu, J.K. Cammack, C.K. Ober, J.W. Perry, S.R. Marder, *Sci*. 296 **2002** 1106

[15] K.D. Belfield, K.J. Schafer, Y.U. Liu,J. Lui, X.B. Ren, E.W. Van Stryland, *J. Phys. Org. Chem* 13 **2000** 837

[16] K.D. Belfield, K.J. Schafer, K.J. *Polym.* 43 **2002** 405

[17] I. Wang, M. Bouriau, P.L. Baldeck,C. Martineau, C. Andraud, *Opt. Lett.* 27 **2002** 1348

[18] Y.M.. Lu, F. Hasegawa, Y. Kawazu, K. Totani, T. Yamashita, W. Toshiyuki, *Seni-Gakkai-shi* 60 **2004** 165

[19]Y.M. Lu, F. Hasegawa, S. Ohkuma, T. Goto, S. Fukuhara, Y. Kawazu, K. Totani, T. Yamashita, T. Watanbe, *J. Mater. Chem* 14 **2004** 75

[20] K.J. Schafer, J.M. Hales, M. Balu, K.D. Belfield, K.D., E.W. Van Stryland, D.J. Hagan, D.J. *J. Photochem. Photobiol.* 162 **2004** 497

[21] Wu, S., Serbin, J., Gu, M. *J. Photochem. Photobiol.- A:* 181 **2006** 1

[22] S. Maruo,S, O.Nakamura,S. Kawata, *Opt. Lett.* 78 **1997** 13

[23] C. Martineau, R. Anémian, C. Andraud, I. Wang, M. Bouriau, P.L. Balkeck, *Chem. Phys. Lett.* 362 **2002** 291

[24] B.H. Cumpston, S.P. Aanathavel, S.Barlow, D.L. Dyer, J.E. Ehrlich, L.L Erskine, A.A. Heikal, S.M. Kuebler, I.Y.S. Lee, D. McCord-Maughhon, J. Qin, H. Röckel, M. Rumi, X.L. Wu, S.R. Marder, J.W. Perry, *Nat.* 398 **1999** 51

[25] B. Siedl,K. Kalinyaprak-icten, N. Fuß, M. Hoefer, R. Liska, *J. Polym. Sci* 46 **2007** 289

[26] N. Arsu, M. Aydin,Y. Yaqci, S. Jockusch, N. Turro, *J.P.Ed; Photochem. Photobiol. Research Signpost* 3 **2006** 17

[27] K.S. Lee, R.H. Kim, D-Y. Yang., S.H. Park, *Prog. Polym. Sci.* 33 **2008** 631

[28] B.A. Reinhardt, L.L. Brott, S.J. Clarson, A.G. Dillard, J.C. Bhatt. R. Kannan. *Chem. Mater.* 10 **1998** 1863

[29] B. Strehmel, A.M. Sarker, H. Detert, *Chem. Phys.* 4 **2003** 249

[30] L. Beverina, J. Fu, A. Leclercq, E. Zojer, P. Pacher, S. Barlow, *J. Am. Chem. Soc.* 127 **2005** 7282

[31] M. Albota, D. Beljonne, J-L. Bredas, J.E. Ehrlich, J-Y. Fu, A. A. Heikal, *Sci.* 281 **1998** 1653

[32] S.M. Kuebler, B.H. Cumpston, S. Aanathavel, S. Barlow, J.E. Ehrlich, L.L. Erskine, A.A Heikal, D. McCord-Maughon, J. Qin, H. Rockel, M. Rumi, S.R. Marder, J.R. Perry, *Proc. SPIE* 3937 **2000** 97

[33] Y. Boiko, J.M. Costa, M. Wang, S. Esener, *Opt. Express* 8 **2001** 571

[34] T. Baldacchini, C.N. LaFratta. R.A. Farra, M.C. Teich, M.J. Naughton, J.T. Fourkas, *J. Appl. Phys.* 95 **2004** 11

[35] S. Wu, M.G. Straub, *Polym.* 46 **2005** 10246

[36] R. Copperwhite, M. Oubaha, D. Versace, C. Croutxè-Barghorn, B.D. MacCraith, *J. Non-Cryst. Solids.* **2008**

[37] R. Infuehr, N. Pucher, C. Heller, H. Lichtenegger, R. Liska, V. Schmidt, L. Kuna, A. Haase, J. Stampfl, *Appl. Surf. Sci.* 254 **2007** 836

[38] H.B. Sun, S. Kawata, *Adv. Polym. Sci.* 170 **2004** 169

[39] M. Joshi, H.E. Pudavar, J. Swiatkiewicz, P.N. Prasad, *Appl. Phys. Lett.* 74 **1999** 170

[40] K. Miura, J. Qui, H. Inouye, I. Mitsuyu, K. Hirao, *Appl. Phys. Let.* 71 **1997** 3329

[41] C.A. Coenjarts, C.K. Ober, *Chem. Mater* 16. **2004**, 5556

[42] M. Oubaha, R. Copperwhite, B. Murphy, B. Kolodziejczyk, H. Barry, K. O'Dwyer, B.D. MacCraith, *Thin Solid Films* 510 **2005** 334

[43] M. Oubaha, P. Etienne, S. Calas, P. Coudray, J.M. Nedelec, Y. Moreau, *Sol-Gel Sci. Technol.* 33 **2005** 241

[44] D. Bosc, A. Maalouf, F. Henrio, S. Haesaert, *Opt. Mater.* **2007**

[45] S.K. Sharma, S.C.K. Misra, K.N. Tripathi, *Int. J. Light Electron Optics* 114 **2003** 106

[46] T.C. Sum, A.A. Bettiol, S. Venugopal Rao, J.A. Van Kan, A. Ramam, F. Watt, *Proc. Of SPIE* 5347 **2004**

[47] T.J. Bunning, S.M. Kirkpatrick, L.V. Natarajan, V.P. Tondiglia, D.W. Tomlin, *Chem. Mater.* 12 **2000** 2842

[48] X. Yu,X. Zhang, K. Wong, G. Xu, X. Xu, Y. Ren, W. He, X. Xu, Z. Shao, X. Tao, M. Jiang, *Mater. Lett.* 58 **2004** 3879

[49] Z. Zhang, G. Yao, P. Zhao, *Appl. Opt.* 44 **2005** 2402

[50] Z. Zhang, P. Zhao P. Lin, F. Sun, *Polym.* 47 **2006** 4893

[51] W. Haske, V.W. Chen, J.M. Hales, W. Dong, S. Barlow, S. Marder, .J.W. Perry, *Opt. Express* 15 **2007** 3426

[52] T.J. Bunning, P.J. Campagnola, S.L. Goodman, *Macromol.* 33 **2000** 1514

[53] M. Albota, D. Beljonne, J.W. Perry, *Sci.* 281 **1998** 1653

[54]B.Marciniec, J.Gulinski, W. Urbaniak, Z.W. Kornetka, *Comprehensive Handbook on Hydrosilylation*; Pergamon Press: Oxford

[55] S. Pichler, PhD Thesis, TU Graz **2007**

[56] S. Bichler, PhD Thesis, TU Graz **2010**

[57] G. Langer, I. Muehlbacher, S Pichler, H. Stahr, F. Stelzer, J. Sassmannshausen, PCT Int. Appl. WO 2009021256 A1 20090219 **2009**

[58] L.H. Nguyen, L. H., Straub, M. and Gu, M., *Adv. Funct. Mater*. 15 **2005** 209

[59] Straub, M., Nguyen, L. H., Fazlic, A, Gu, M., *Opt. Mater.* 27 **2004** 359

[60] S. Wu, M. Straub, M. Gu, *Polym*. 46 **2005** 10246

[61] J.V. Crivello, K. Dietliker, *Photoinitiators for free radical cationic & anionic photopolymerisation* 2nd edition Vol III **1998** 159

[62] S. Ananda Kumar, Z. Denchev, M. Alagar, *Eur. Polym. J*. 42 **2006** 2419

[63] T. Satoshi, S. Wataru, Y. Tetsuzo, *Appl. Phys. Lett*. 60 **1992** 1158

[64] C. A. Leatherdale R. J. DeVoe, *Proc. of SPIE* Vol. 5211 123

[65] .C. Heller, N. Pucher, B. Seidl, K. Kalinyaprak-Icten, G. Ullrich, L. Kuna, V. Satzinger, V. Schmidt, H. Lichtenegger, J. Stampfl, R. Liska *J. Polym. Sci* 45 **2007** 3280

[66] N. Pucher, A. Rosspeintner, V. Satzinger, V. Schmidt, G. Gescheidt, J. Stampfl, R. Liska, *Macromol*. 42 **2009** 6519

[68] Z. Zhang, S. Fang, *Chin. J. Polym. Sci.* 17 **1999** 537

[69] S. J. Clarson, J.A. Semlyen (eds) **1993**, Siloxane Polymers, P T R Prentice Hall, New Jersey

[70] F. de Buyl , *Int. J. Adhes. Adhes.* 21 **2001** 411

[71] D. Zidar, Bachelor Thesis, Montanuniversität Leoben **2011**

[72] C. Heller, N. Pucher, B. Seidl, K. Kalinyaprak-Icten, G. Ullrich, L. Kuna, V. Satzinger, V. Schmidt, H. C. Lichtenegger, J. Stampfl, R. Liska, *J. Polym Sci*. 45 **2007** 3280

[73] S. Bichler, PhD Thesis, TU Graz **2009**

[74] V. Schmidt, L. Kuna, V. Satzinger, R. Houbertz, G. Jakopic, G. Leising, SPIE Proceeding 6002 **2007**

[75] R.A Norwood, R.Y. Gao, J. Sharma, C.C Teng. SPIE 4439 **2001** 19

[76] T. Scherzer, W. Knolle, S. Naumov, C. Elsner, M. R. Buchmeiser. *J. Polym Sci.: Part A*:. 46 **2008** 4905

[77] C. Dreyer, M. Bauer, J. Bauer, N. Keil, H. Yao, C. Zawadzki, *Microsyst. Technol*. 7 **2002** 229

[78] S. Chen, Q. Yan, Q. Xu, Z. Fan, J. Liu, *Opt. Commun*. 256 **2005** 68

[79] G. Schmid, J. Reitterer, W. Leeb, Report on WP4-24, "*Characterization of a board with a single-core waveguide* (ATS_TPA2_074)" **2008**

[81] http://www.ulm-photonics.com/new/index.php

[82] G. Breed *Analyzing Signals using the Eye Digram.* High Frequency Electronics **2005**

[83] R. Houbertz, V. Satzinger, V. Schmid, W. Leeb, G. Langer, *Organic 3D photonic materials and devices II* **2008**

Appendix

Publications

S. Bicher, S. Feldbacher, **R. Woods**, V. Satzinger, V. Schmidt, G. Jakopic, W. Kern."*Two photon patterning of optical waveguides in flexible polymers*". Linear and Nonlinear Optics of Organic Materials IX Proc. Of SPIE Vol. 7413. **2009**

R Woods, S. Feldbacher, G. Langer, V. Satzinger, V. Schmidt V., W. Kern "*Epoxy silicone based matrix materials for two-photon patterning of optical waveguides*", Polym 52 **2011** 3031-3037

S. Bicher, S. Feldbacher, **R. Woods**, V. Satzinger, V. Schmidt, G. Jakopic, G. Langer W. Kern "*Functional silicon based flexible polymer for two photon patterning of optical waveguides*", Opt. Mater. In press, available on line Nov **2011**

R. Woods, S. Feldbacher, D. Zidar, G. Langer, V. Satzinger, V. Schmidt, N. Pucher, R. Liska, W. Kern "*3D Optical waveguides produced by two photon photopolymerisation of a flexible silanol terminated polysiloxane containing acrylate functional groups*", Submitted to "Polymers for Advanced Technologies" **2012**

R. Woods, S. Feldbacher, D. Zidar, G. Langer, V. Satzinger, G. Schmid, W. Leeb, W. Kern "*Development and characterisation of opto-electronic circuit boards produced by two photon polymerisation using a polysiloxane containing acrylate functional groups*", Submitted to Optical Materials **2012**

Presentations

R. Woods, S. Feldbacher, G. Langer, V. Satzinger, W. Kern, „*Waveguide structures in polymers by two photon patterning*", ISOTEC meeting, Austria **2010**

R. Woods, S. Feldbacher, G. Langer, V. Satzinger, W. Kern " *Two photon patterning of optical waveguides in silicone based flexible polymers*" 10th Austrian-Slovenian polymer meeting, Leoben, Austria **2010**

R. Woods, S. Fedbacher, D. Zidar, G. Langer, V. Satzinger, W. Kern, *"Waveguide structures in polymers by to photon pattering"* Zing Polymer Conference, Puerto Morelos, Mexico **2010**

R. Woods, S. Fedbacher, D. Zidar, G. Langer, V. Satzinger, W. Kern, *"Two photon structuring of 3D optical waveguides in flexible polysiloxane materials"* 27th World Congress of the Polymer Processing Society (PPS), Marrakech, Morocco **2011**

R. Woods, S. Fedbacher, D. Zidar, G. Langer, V. Satzinger, W. Kern, "*3D optical waveguides produced by two photon photopolymerisation of a flexible silanol terminatedpolysiloxane containing acrylate functional groups* (European Polymer Federation) *EPF) Granada, Spain* **2011**

R. Woods, S. Feldbacher, D. Zidar, G. Langer, V. Satzinger, W. Kern, *"Fabrication of 3D optical waveguides in a flexible polysiloxane material via two photon photopolymerisation"* (Advances in Polymer Science and Technology (APST) 2) Linz, Austria **2011**

Patents

W. Kern, S. Feldbacher, R. Woods, **Patent** "*Schicht mit einem Lichtwellenleiter und Verfahren zu deren Herstellung"* **A1376/2011**

Posters

R. Woods, S. Bichler, G. Langer, V. Satzinger, V. Schmidt, W. Kern. "*Two-photon photopolymerisation of selected monomers in an inert silicone matrix*" E-MRS, Strasbourg, France **2009**

R. Woods, S. Bichler, G. Langer, V. Satzinger, V. Schmidt, W. Kern. "*Silicon based matrix materials for two-photon patterning of waveguides*" European Polymer Congress (EPF), Graz, Austria **2009**

R. Woods., S. Feldbacher, D. Zidar, G. Langer, V. Satzinger, W. Kern, *"Waveguide structures in polymers by to photon pattering"* Zing Polymer Conference, Puerto Morelos, Mexico **2010**

Curriculum Vitae

Rachel Woods 28:10:82
rajwoods@hotmail.com

Education

Ph.D., Chemistry of Polymeric Materials, May 2008 - Dec 2011
Institute of Chemistry of Polymeric Materials (University of Leoben)

Research Masters: Sep 2006-Sep 2007 "*Investigation and Development of Cuprosolvency Testing Methods using a Simple Pipe Test Rig*"
Institute of Environmental Engineering (University of Wales, Swansea)

MChem.: "*Synthesis, Characterization and Photophysical Properties of some Metallated Meso-Tetrakis (Pentafluorophenyl) and Metalloporphyrins Bound to Long Chain Alcohols*"
Institute of Chemistry (University of Wales, Swansea)